ΠΑΝΕΠΙΣΤΗΜΙΟ ΚΡΗΤΗΣ

ΣΧΟΛΗ ΕΠΙΣΤΗΜΩΝ ΥΓΕΙΑΣ-ΤΜΗΜΑ ΙΑΤΡΙΚΗΣ

ΤΟΜΕΑΣ ΒΑΣΙΚΩΝ ΕΠΙΣΤΗΜΩΝ

ΕΡΓΑΣΤΗΡΙΟ ΒΙΟΧΗΜΕΙΑΣ

Διδακτορική διατριβή

ΑΝΑΛΥΣΗ ΤΟΥ ΜΟΝΟΠΑΤΙΟΥ ΒΙΟΓΕΝΕΣΗΣ ΤΗΣ HDL ΜΕ ΜΕΤΑΛΛΑΞΙΟΓΕΝΕΣΗ ΤΗΣ ΑΠΟΛΙΠΟΠΡΩΤΕΙΝΗΣ Α-Ι

Ανδρέας Κατεϊφίδης

Επιβλέπων Καθηγητής: Δ. Καρδάσης

Ιούλιος 2011

UNIVERSITY OF CRETE

SCHOOL HEALTH SCIENCES-DEPARTMENT OF MEDICINE

BASIC SCIENCES-BIOCHEMISTRY

Ph.D. thesis

ANALYSIS OF THE PATHWAY OF BIOGENESIS OF HDL BY MUTATIONS OF APOLIPOPROTEIN A-I

Andreas Kateifides

Supervisor: Prof. D. Kardasis

Submitted in fulfillment of the requirements for the

PhD degree in the graduate programme

"Molecular basis of human disease"

July 2011

To my parents for their

continuous support

ACKNOWLEDGMENTS

With the completion of my PhD thesis I would like to truthfully thank my advisor Professor Vassilis I. Zannis for all his support and guidance through the last eight years of my life. With his encouragement it became possible for me to start and complete this chapter of my life. His help made it also possible to continue pursuing my dreams and start the new chapter of my life.

I would also like to thank Professor Dimitris Kardassis, my "official" advisor for providing me the chance to work in his lab during my first rotation which was the start of this trip. Though I was in Boston, Dimitris was always by my side providing help, new techniques and suggestions how to optimize my results and work. I also want to thank him for the financial support. I would also like to thank the members of my committee Dr. Eliopoulos, Dr. Thermos, Dr. Boumpas, Dr. Papadaki and Dr. Sourvinos.

I would also like to thank my biggest collaborator Irina Gorshkova. It was not just her contribution to my work but all the discussions we had about biophysics, a field beyond my knowledge that always fascinated me. My thanks also go to Angelika Chroni and George Daniil. They helped me during my stay at Demokritos and made sure that my stay in Athens was as productive as possible. I would also like to thank all my other collaborators, Christiane, Ioanna and Dimitra. Their contribution made it possible for this work to become more complete and provide more information for apolipoprotein A-I.

I would also like to thank George Koukos for all the help that he provided me during my first year in Dr. Zannis lab. My thanks also go to the wonderful people in Dr.

Zannis lab, including Dr. Kyriakos Kypreos, Dr. Costas Drosatos, Adelina Duka and Gayle Forbes. I also thank Dr. Alex Vezeridis, it was really nice to interact with him in the lab and a reason for me to work more so I would leave from the lab later than him. I am also thankful to Panagiotis Fotakis, the new lab member. The interaction with him was very fruitful and gave me the opportunity to become a teacher myself and realize how much I have learned during my tenure at the Molecular Genetics lab.

I am also very thankful to Mary Adamaki, she has been always there to help me whenever I had a problem and without her help I would not have been able to complete my commitments to the program.

This work was financially supported by ΠΕΝΕΔ03 ΕΔ 780

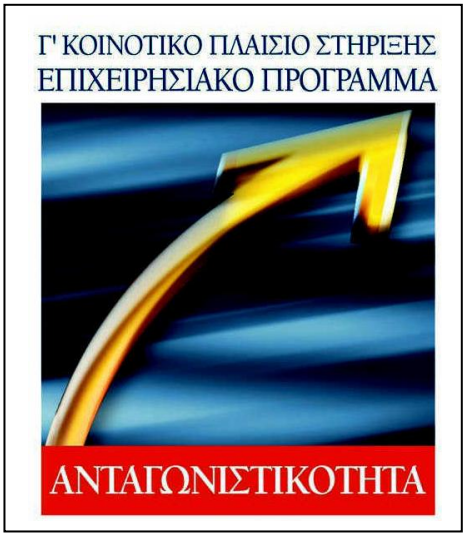

TABLE OF CONTENTS

ABSTRACT

Apolipoprotein A-I is a key protein for the biogenesis of High Density Lipoproteins and protects from atherosclerosis. Mutations in apoA-I gene are associated with low HDL levels and predisposition to atherosclerosis. The purpose of the present thesis was to explore the structure-function relationship in human apoA-I and the role of specific amino acid residues in HDL biogenesis and maturation. The thesis is organized in two parts.

Part I: Alteration of Negatively Charged Residues in the 89 to 99 Domain of ApoA-I Affects Lipid Homeostasis and the Maturation of HDL (J Lipid Res. 2011 Jul;52(7):1363-72). Adenovirus-mediated gene transfer in apoA-I$^{-/-}$ mice showed that an apoA-I[D89A/E91A/E92A] mutant increased plasma cholesterol and caused severe hypertriglyceridemia. HDL levels were reduced and approximately 40% of the apoA-I was distributed in VLDL/IDL. The HDL consisted of mostly spherical and few discoidal particles and contained preβ1 and α4-HDL subpopulations. The mutant protein had increased affinity for triglyceride-rich emulsions. The lipid, lipoprotein and HDL profiles of the apoA-I[K94A/K96A] mutant were similar, but not identical, to those of wild type apoA-I. Co-expression of apoA-I[D89A/E91A/E92A] and human lipoprotein lipase abolished hypertriglyceridemia, restored in part the α1,2,3,4 HDL subpopulations, redistributed apoA-I in the HDL2/HDL3 regions, but did not prevent the formation of discoidal HDL particles. We conclude that residues D89, E91 and E92 of apoA-I are important for plasma cholesterol and triglyceride homeostasis as well as for the maturation of HDL. The present and two previous studies raise the possibility that

mutations in apoA-I in the general population may alter the functions of apoA-I and HDL and contribute to hypertriglyceridemia.

Part II: Contribution of the residues 218 to 226 of apoA-I in the biogenesis of HDL. Adenovirus mediated gene transfer of an apoA-I [L218A/L219A/V221A/L222A] mutant in apoA-I$^{-/-}$ mice resulted in decreased plasma cholesterol and apoA-I levels to approximately 10 % as compared to WT control and generated preβ and α4-HDL particles. The HDL cholesterol peak of the mutant protein was greatly diminished. When expressed in double deficient mice for apoA-I and apoE the apoA-I[L218A/L219A/V221A/L222A] mutant failed to form HDL particles as determined by 2D gel electrophoresis and electron microscopy. The apoA-I[E223A/K226A] mutant had similar plasma apoA-I levels and similar but not identical lipid and lipoprotein profiles with WT apoA-I. Overall the findings suggest that crucial changes in the C-terminal 218-222 hydrophobic residues of apoA-I impair seriously the functional interactions of apoA-I with ABCA1 and/or LCAT and inhibit biogenesis of HDL.

In the context of this thesis we also investigated, in collaboration with other groups, the role of apoA-I C-terminus in endothelial transcytosis of HDL (*J Biol Chem. 2011 Mar 11;286(10):7744-54*), the bactericidal activity of apoA-I against *Yersinia enterocolitica* serotypre O:3 (*manuscript in preparation*) and apoA-I mutations in patients with increased risk of ischaemic heart disease and total mortality in the population of Copenhagen (*J Intern Med. 2011 Mar 28. doi: 10.1111 in press*)

ΠΕΡΙΛΗΨΗ

Η απολιποπρωτεΐνη A-I είναι σημαντική για την βιογένεση της λιποπρωτεΐνης υψηλής πυκνότητας (HDL) και προστατεύει από την αθηροσκλήρωση. Μεταλλάξεις στην αποA-I σχετίζονται με χαμηλά επίπεδα HDL στο πλάσμα και προδιάθεση για αθηροσκλήρωση. Ο σκοπός της παρούσας διατριβής ήταν να διερευνηθεί η σχέση δομής-λειτουργίας της αποA-I του ανθρώπου και ο ρόλος συγκεκριμένων αμινοξέων της αποA-I στην βιογένεση και την ωρίμανση της HDL. Η διατριβή χωρίζεται σε δυο μέρη.

Μέρος Ι: Μεταλλαξιογένεση των αρνητικά φορτισμένων αμινοξέων στην περιοχή 89 με 99 της απολιποπρωτεΐνης A-I επηρεάζει την ομοιόσταση των λιπιδίων και την ωρίμανση της HDL. (J Lipid Res. 2011 Jul;52(7):1363-72). Γονιδιακή μεταφορά σε ποντίκια με ανεπάρκεια της αποA-I (αποA-$I^{-/-}$) έδειξε ότι η μετάλλαξη αποA-I[D89A/E91A/E92A] αύξησε τα επίπεδα χοληστερόλης του πλάσματος και προκάλεσε σοβαρή υπερτριγλυκεριδεμία. Τα επίπεδα της HDL μειώθηκαν και περίπου 40% της αποA-I μετατοπίστηκε στη περιοχή της VLDL/IDL. Το κλάσμα της HDL περιείχε ως επί το πλείστον σφαιρικά σωματιδία καθώς και μερικά δισκοϊδή και το πλάσμα περιείχε preβ1 και α4 υποπληθυσμούς της HDL. Η μεταλλαγμένη πρωτεΐνη είχε αυξημένη συγγένεια σε γαλακτώματα πλούσια σε τριγλυκερίδια. Τα επίπεδα λιπιδίων και λιποπρωτεϊνών καθώς και το προφίλ της HDL της αποA-I[K94A/K96A] ήταν παρόμοια αλλά όχι ίδια με αυτά της αποA-I αγρίου τύπου. Ταυτόχρονη έκφραση αποA-I[D89A/E91A/E92A] και ανθρώπινης λιποπροτεϊνικής λιπάσης διόρθωσε την υπερτριγλυκεριδαιμία, διόρθωσε εν μέρει τους α1,2,3,4 υποπληθυσμούς της HDL, επανέφερε την αποA-I στις HDL2/HDL3 περιοχές, αλλά δεν απέτρεψε τον σχηματισμό

δισκοϊδών σωματιδίων. Συμπερασματικά, τα αμινοξέα D89, E91 και E92 της αποA-I είναι σημαντικά για τα επίπεδα της χοληστερόλης στο πλασμα και την ομοιόσταση των τριγλυκεριδίων καθώς και για την ωρίμανση της HDL.

Μέρος ΙΙ: Συμβολή των αμινοξέων 218 εώς 226 του γονιδίου της απολιποπροτεϊνης Α-Ι στη βιογένεση της HDL. Γονιδιακή μεταφορά με χρήση αδενοϊών της αποA-I[L218A/L219A/V221A/L222A] σε αποA-$I^{-/-}$ ποντίκια οδήγησε σε σχεδόν αξαφάνιση της HDL, μείωση κατά περίπου 90% στα επίπεδα της χοληστερόλης και της αποA-I στο πλάσμα συγκριτικά με τα ποντίκια που εκφράζουν την αποA-I αγρίου τύπου καθώς και στο σχηματισμό preβ και α4-HDL σωματιδίων. Ανάλυση με ηλεκτροφόρηση δύο διαστάσεων και με ηλεκτρονική μικροσκοπία έδειξαν ότι η μεταλλαγμένη αποA-I[L218A/L219A/ V221A/L222A] μορφή δεν μπορεί να σχηματίσει HDL σωματίδια όταν εκφραστεί σε αποA-$I^{-/-}$ x αποE$^{-/-}$ ποντίκια.

Η μεταλλαγμένη αποA-I[E223A/K226A] μορφή είχε παρόμοια επίπεδα αποA-I στο πλάσμα και είχε παρόμοια αλλά όχι ταυτόσημα προφίλ λιπιδίων και λιποπρωτεϊνών με την αποA-I αγρίου τύπου. Συμπεραίνουμε ότι κρίσιμες αλλαγές στα υδρόφοβα αμινοξέα 218-222 του C-τερματικού άκρου της αποA-I επηρεάζουν σημαντικά τις αλληλεπιδράσεις της αποA-I με την ABCA1 ή/και την LCAT και αναστέλουν την βιογένεση της HDL.

Στα πλαίσια της παρούσης διατριβής, μελετήσαμε σε συνεργασία με άλλες ερευνητικές ομάδες τον ρόλο του καρβοξυτερματικού άκρου της αποA-I στην τρανσ-ενδοκύττωση της HDL από ενδοθηλιακά κύτταρα (*J Biol Chem. 2011 Mar 11;286(10):7744-54*), την αντιβακτηριδιακή δράση της αποA-I απέναντι στο βακτήριο

the *Yersinia enterocolitica* ορότυπος O:3 (*manuscript in preparation*) και ο ρόλος μεταλλάξεων στην αποA-I σε ασθενείς με αυξημένο κίνδυνο για καρδιοπάθεια στον πληθυσμό της Κοπεγχάγης (*J Intern Med. 2011 Mar 28. doi: 10.1111 in press*)

1. INTRODUCTION

1.1. Apolipoprotein A-I

1.1.1. ApoA-I Synthesis and Importance

Human apolipoprotein A-I (apoA-I) is a 243-aa plasma protein (1) that is derived from a 249-aa precursor. It is synthesized and secreted predominantly by the liver and the intestine (2) and is incorporated into high-density lipoprotein (HDL) particles (*3;4*). ApoA-1 constitutes ~70% of the apolipoprotein content of HDL particles and apoA-I deficiency prevents the formation of HDL (5).

Elevated levels of HDL in apoA-I transgenic mice are correlated with protection against atherosclerosis (6), proving in principle that apoA-I overexpression can positively influence both plasma HDL concentrations as well as atherosclerosis progression (7). Epidemiological and genetic data have shown that low (*8;9*) or high (*10;11*) levels of HDL or apoA-I are associated with increased or decreased risk of developing coronary artery disease respectively.

1.1.2. Genetics and naturally occurring mutations

The apoA-I gene is a 3kb gene that is located on chromosome 11q23 (12). The apoA-I gene is closely linked to the apoCIII gene. The genes have opposite orientation (13).

Several apoA-I mutations have been described in the general population. From a total of 46 natural apoA-I mutations that have been reported, 25 are associated with low plasma HDL levels (14). Most of the mutations that affect the interaction of apoA-I with LCAT occur around helix 6. Eight more mutations, seven between residues 26 and 107

and one on residue 173, have been associated with amyloidosis and low HDL levels (*14;15*).

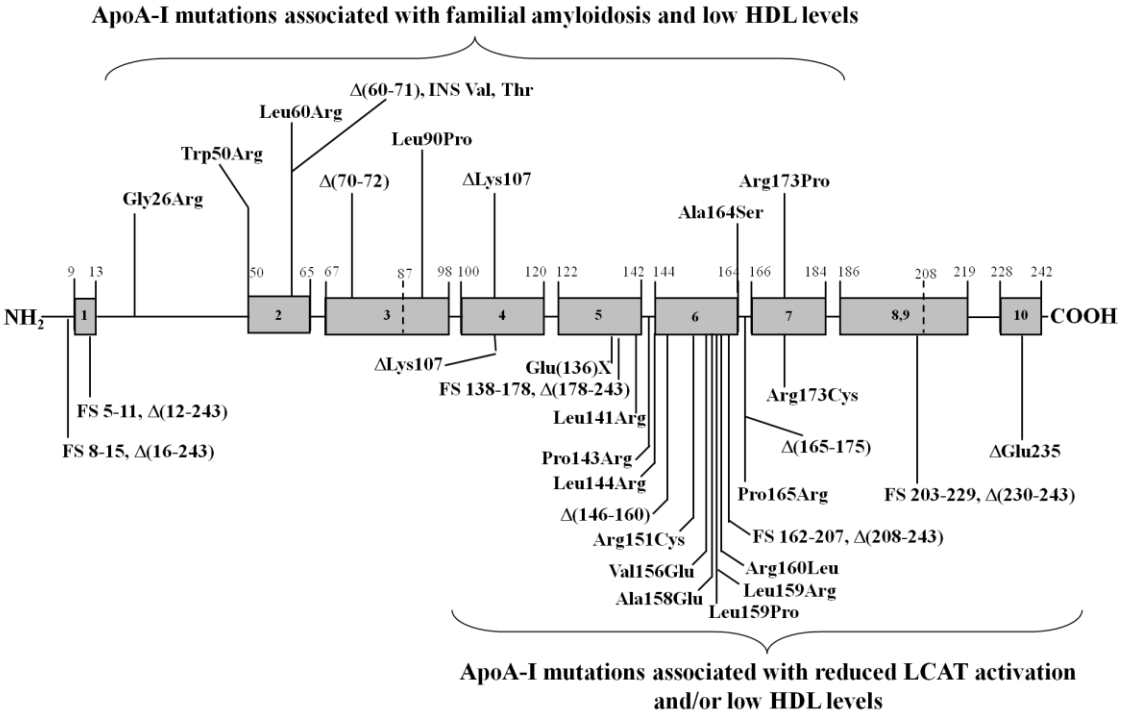

Figure 1.1. Schematic representation of the human apoA-I gene and various apoA-I mutations associated with defective LCAT activation familiar amyloidosis or impairment in the synthesis and various functions of HDL. * The apoA-I[Ala164Ser] mutation is associated with increased risk for ischemic heart disease although carriers have normal apoA-I and HDL cholesterol plasma levels.

1.1.3. Gene regulation

Studies in transgenic mice that carry the apoA-I gene along with the regulatory sequence of the apoA-I/apoCIII gene cluster have shown that hormone nuclear receptors and

specificity protein 1 (SP1) family are important for the transcription of the apoA-I gene (16).

Regulation of the apoA-I gene occurs primarily at the transcriptional level and is mediated by the *cis*-acting sequences present in the proximal apoA-I promoter and the apoCIII enhancer (16). Post-transcriptional regulation has been also reported that is caused by increasing the stability of the partially spliced and unspliced nuclear apoA-I mRNA (17). Dietary fat, alcohol, estrogen, androgens, thyroid hormone, retinoids, glucocorticoids, fibrates, niacin, and HMG-CoA reductase inhibitors are some of the many nutritional, hormonal, and pharmacological factors known to influence transcriptional induction of the apoA-I gene (*17;18*). Based on animal studies, upregulation of apoA-I expression in humans would be expected to raise HDLc concentrations and provide protection against atherosclerosis (19).

1.1.4. Structure of apoA-I in solution and on discoidal and spherical HDL Particles

ApoA-I contains 22 or 11 amino acid repeats which, according to the models of Nolte & Atkinson (20), are organized in amphipathic a-helices (21) (Fig. 1.2A). Monomeric apoA-I in solution is loosely folded (*22;23*), and probably exists as a helical bundle that is ellipsoidal in shape and may assume different configurations in solution (22-24). The N-terminal deletion mutant of apoA-I, apoA-I[Δ(1-43)], was crystallized and its structure was determined at 4 Å resolution. In this low resolution structure apoA-I appears to have a continuous amphipathic α-helical sequence that is punctuated by small or pronounced

kinks. Overall the apoA-I molecule appears to adopt a horseshoe shape with dimensions of 125x80x40 Å (25-30). In the unit cell, four apolipoprotein A-I monomers form two antiparallel dimers that are associated via hydrophobic faces (31). The dimers form central helix 5-5 and terminal helix 10-10 overlaps (Fig. 1.2B). Based on the crystal structure of apoA-I in solution a belt model was proposed to explain the structure of apoA-I on discoidal HDL particles. In this model, two antiparallel molecules of apoA-I consisting of continuous amphipathic a helices with 3.67 residues per turn, designated 11/3 helix, are parallel to the plane of the disc (*25-28;32*). The apoA-I dimer is wrapped belt wise around a discoidal bilayer containing 160 phospholipid molecules and shields the hydrophobic fatty acid chains of the phospholipids (Fig. 1.2C). It has been proposed that the optimal arrangements of the dimers are those that maximize intermolecular salt bridge interactions (*26;27*). This alignment of the two anti-parallel apoA-I molecules creates overlays of the central helixes 5-5 and terminal helixes 10-10 that match the overlap pattern of the crystal structure of lipid-free apolipoprotein A-I (31). However, it is also possible that mutations in apoA-I may affect the 5-5 overlapping arrangement of the apoA-I dimers and thus affect the functions of HDL. It was proposed earlier that esterification of the cholesterol of the discoidal HDL converts the 3.67 residues per turn helices to an idealized 3.6 residues per turn helix and changes the discoidal into spheroidal particles (31).

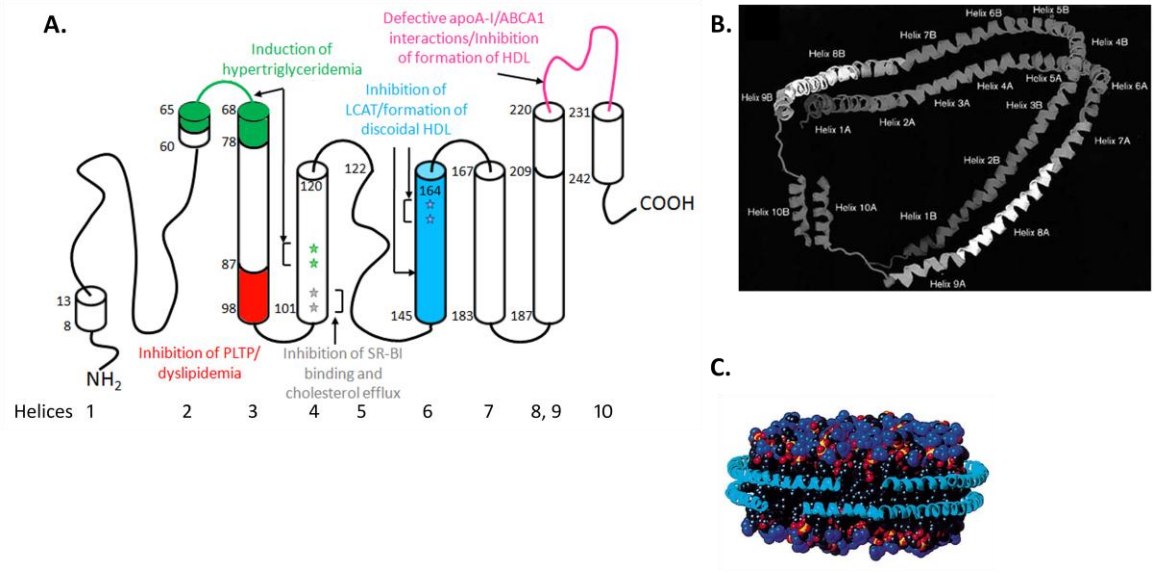

Figure 1.2. Summary of structure of apoA-I. (A) Secondary structure of apoA-I [adapted from (*20;31;33*)]. Cylinders represent amphipathic α-helices. Predicted amphipathic α-helices are shown in white and additional α-helical regions that were observed by X-ray crystallography are shown in black or pink. Asterisks on helices 4, 6 and colored regions (62-78), (89-99), (145-164) and (220-232) indicate informative mutations in apoA-I as described on the figure. (B) Model of the crystal structure of apoA-I [Δ(1-43)]. The figure is based on the protein Databank 1AVI.PDB and (9,14). (C) "Belt" model of apoA-I on discoidal HDL particles adapted from (27).

Analysis of the 93 Å spherical HDL in solution by small angle neutron scattering (SANS) showed that apoA-I folds around a central lipid core that has 88.4 Å x 62.8 Å dimensions to form a spheroidal HDL (sHDL) particle (Fig. 1.3). The following three possible arrangements of apoA-I on the sHDL particle were considered: a model designated HdHp (heterodimer and a hairpin) where two apoA-I molecules were arranged

in anti-parallel planar orientation and a third molecule assumed a hairpin structure; a model designated 3Hp (3 hairpins) where three apoA-I molecules were folded as hairpins; a model designated integrated trimer (iT) where three apoA-I molecules interact with each other on the HDL surface (34). Negative staining electron microscopy showed contiguous high densities originating from the protein moieties near the centers and the edges of the HDL particles (35).

Cross-linking data provided information on the relative proximity and orientation of the K residues of the apoA-I molecules arranged in anti-parallel or hairpin orientations. The cross-links can occur in residues of the same helix (intra) or among the anti-parallel helices (inter).

Based on cross-linking of the K residues with a cross-linker (bisulfosuccinimidyl suberate, BS3) that has 11.4 Å spacer arm and mass spectrometry analyses from this as well as previous studies (36-40) Wu *et al.* suggested that spherical HDL may be compatible with the HdHp model (34). This model retains the predominant anti-parallel orientation of the two apoA-I molecules and a 5-5 helix registry proposed for the crystal structure of apoA-I for the two molecules (31).

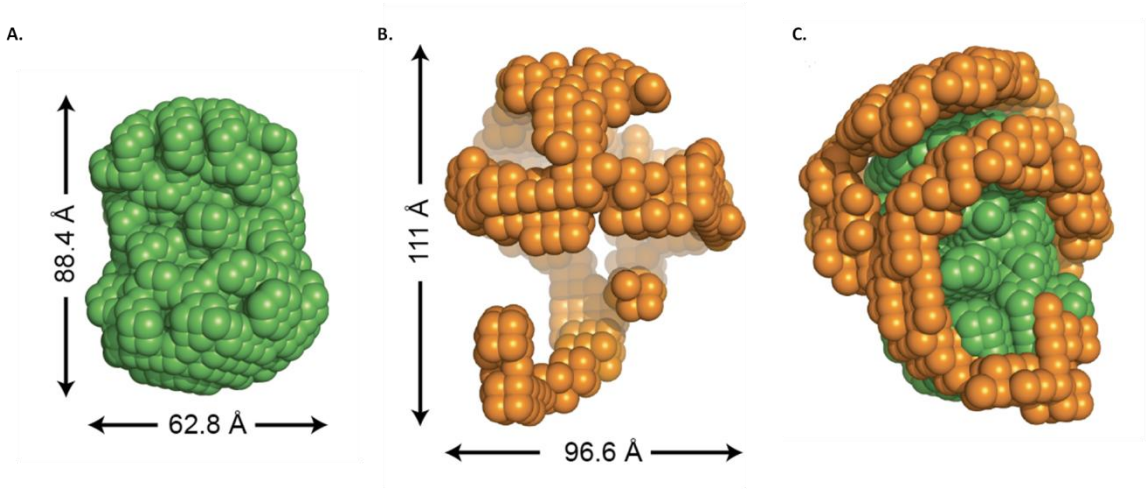

Figure 1.3. (A) Low resolution structure of the lipid component of sHDL obtained by *p*(R) value based on small neutron scattering results for sHDL in 42% D_2O. (B) Low resolution structure of the protein component of sHDL obtained by *p*(R) value based on small neutron scattering results in 12% D_2O. (C) Overlap of the low resolutions of structures for the 42% D2O (green) and 12% D2O (orange). Obtained from (34).

In a different cross-linking study Silva *et al.* (39) identified 23 cross-links in reconstituted spherical 93 Å particles; fourteen of them were intra-chain and seven inter-chain cross-links. Silva *et al.* (39) considered three models: a) a planar circular belt containing three apoA-I molecules in anti-parallel orientation; b) two apoA-I molecules arranged in planar circular anti-parallel double belt and a third molecule in the form of hairpin; c) a "trefoil" model where the right hand half of two anti-parallel apoA-I molecules of the double belt model were displaced by 60^o out of their planar position of the disc and were aligned in anti-parallel orientation with a third molecule bent at 60^o angle (39) (Fig. 1.4).

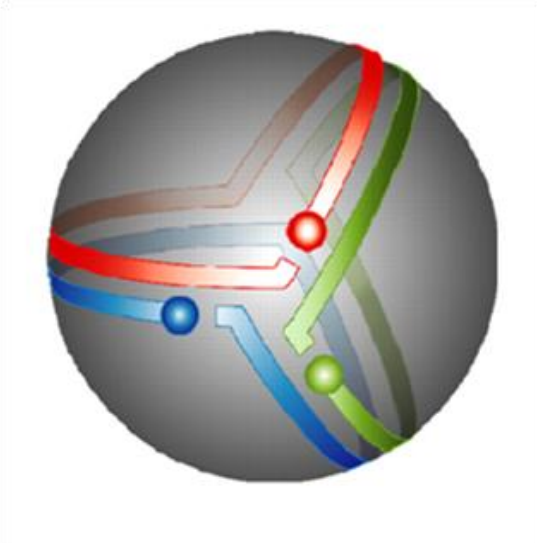

Figure 1.4. The trefoil model is generated by displacing the right hand half of two anti-parallel apoA-I molecules of the double belt model by 60^{o} out of their planar position of the disc and then aligned in anti-parallel orientation with a third molecule bent at 60^{o} angle. Obtained from (39)

Several of the cross-links observed in the reconstituted spherical HDL were also found in the reconstituted discoidal HDL and 7 new cross-links were only observed on spherical HDL (39). A summary of the cross-linking studies is shown in Fig. 1.5. Some of the cross-links, indicated by the green lines, are common in the two studies, other cross-links indicated by blue lines (K118-N_T, K118-K133, K182-K239, K182-238) are unique to the model proposed by Wu *et al.* and those indicated by red lines (K40-K45, K59-K208, K88-K94, K94-K96, K96-K106, K118-K133, K133-K140, K182-K238, K238-K239) are unique to the model proposed by Silva *et al.* In addition, it was suggested that the HdHp N_T-K118 and K182-K239 might represent either intra or inter-chain cross-links (34).

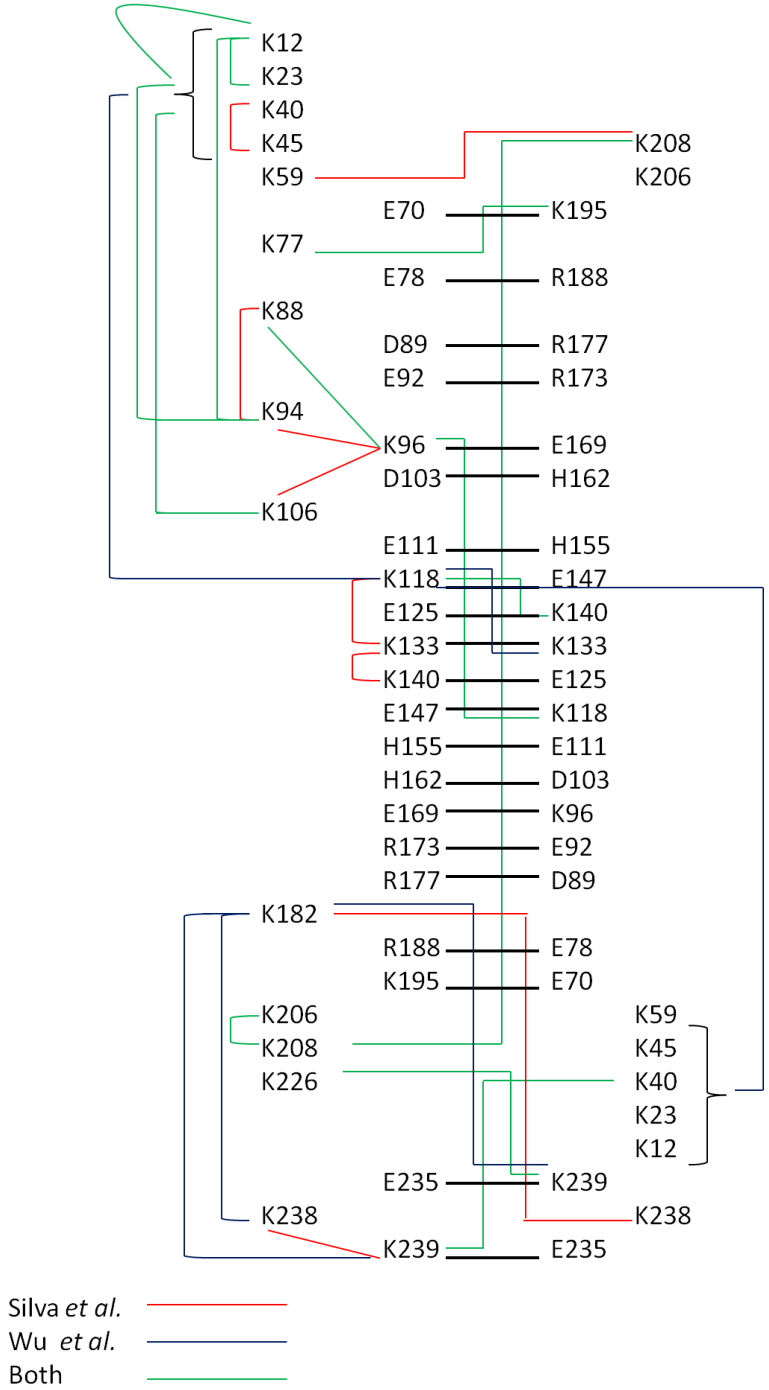

Figure 1.5. Inter and intra-chain K residues cross-links with BS3 and potential salt bridges based on the antiparallel double belt model.

The HdHp, the 3Hp and the iT models satisfy 23, 19, and 21 cross-links respectively. Some of the cross-links do not fit the proposed models and it has been suggested that cross-links K182-K238, K208-K208, K96-K118, K182-K238 may represent anti-parallel orientation of the apoA-I molecules in a 5/2 registry. It has been suggested (34) that all three models proposed by Wu *et al.* might coexist and that by transient rearrangements of the HdHp, 3Hp and iT models they may facilitate exchange of apoA-I (*41;42*) or conversion of lipid-poor to lipid-rich particles (*43;44*).

Several cross-linking studies also indicate that the N terminal regions of apoA-I may fold back and come in closer proximity to the central regions (*34;45-47*). It was shown earlier that human apoA-I and mouse apoA-I have 70% and 46% similarity in the N- and C-terminal domains respectively (48). The N-terminal domain of human and mouse apoA-I adopts a helical bundle structure and the C-terminal forms a separate domain (48). These two domains appear to have different functionalities. The mouse N-terminal domain can bind lipids but the human N-terminal domain cannot bind lipids efficiently. Hybrid molecules, where the mouse N-terminal domain was exchanged with the human domain and vice versa, functioned efficiently in lipid binding indicating that the two domains in the intact apoA-I molecule have preserved their functions (48). A recent study used electron paramagnetic resonance spectroscopy to assess the conformation of the N-terminal region (residues 6-98) of apoA-I on 93 Å reconstituted HDL particles. It was found that residues 6-34 and 50-98 form α-helices, residues 35-39 are unstructured and residues 40-49 form β-strands. There were only modest changes in the conformation of apoA-I when the size of the rHDL increased from 93 Å to 96 Å and

it was suggested that the 35-49 region of apoA-I may contribute to the adaptation of apoA-I in HDL particles of different size (45).

Three molecular dynamics simulation models of spherical HDL containing two apoA-I chains in a belt model have been reported (49-51). According to these models the planar arrangement of apoA-I is distorted in and out of the plane during the simulation. It has been suggested that the N- and C-terminal helices of apoA-I are more flexible and mobile during the simulation as compared to the central region (50). In addition, temperature jump molecular dynamic simulation (*52;53*) indicated that the D89-R177 and E111-H155 are more stable than the E78-R188 salt bridge.

1.1.5. Role of apoA-I in the biogenesis of HDL

HDL is synthesized through a complex pathway (54). The first step involves an ABCA1 mediated transfer of cellular phospholipids and cholesterol to lipid poor apoA-I extracellularly. The lipidated apoA-I is gradually converted to discoidal particles that are remodelled in the plasma compartment by the esterification of cholesterol by the enzyme lecithin: cholesterol acyl transferase (LCAT) (4) and are converted to spherical HDL particles. The cholesteryl esters formed are transferred to VLDL/IDL by the cholesteryl ester transfer protein (CETP) (55). Additional remodelling of HDL involves transfer of phospholipids from VLDL/LDL to HDL by the phospholipid transfer protein (PLTP) (56), cholesterol efflux from cells or delivery of cholesteryl esters to cells mediated by the scavenger receptor class B, type I (SR-BI) (57) as well as cholesterol efflux mediated by the cell surface transporter ABCG1 (58). Finally hydrolysis of lipids of HDL is

mediated by various lipases [lipoprotein lipase (LpL), hepatic lipase (HL), endothelial lipase (EL)] (59-62). Mutations in any of these proteins may affect the biogenesis, maturation and the functions of HDL. The functional interactions of apoA-I with ABCA1, LCAT, ABCG1 and SR-BI appear to have great physiological significance for the biogenesis and/or the functions of HDL and are analyzed in detail below (Fig. 1.6).

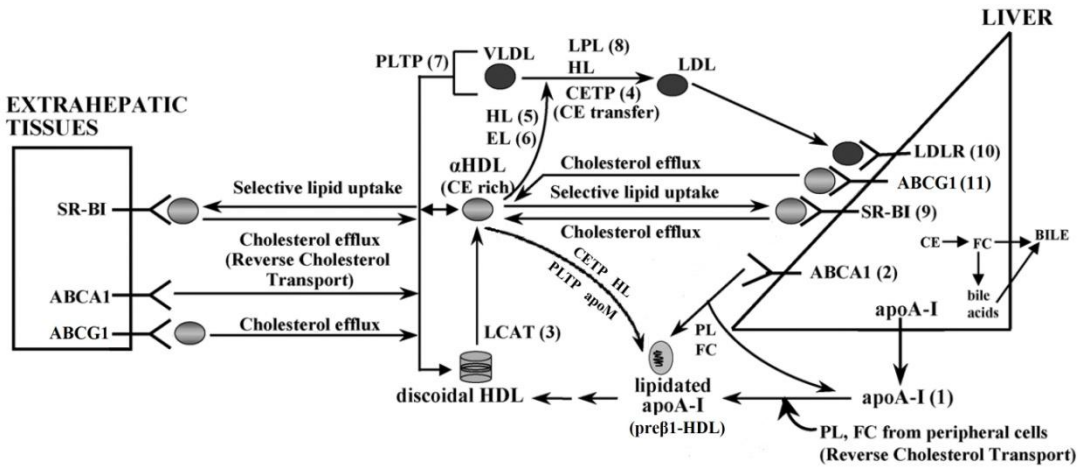

Figure 1.6. Schematic representation of the biogenesis and functions of HDL. Adapted from (63).

1.2. Interactions of ApoA-I with ABCA1

1.2.1. Properties of ABCA1

ABCA1 is a ubiquitous protein that belongs to the ABC family of transporters and is expressed abundantly in the liver, macrophages, brain and various other tissues (*64;65*). ABCA1 is localized only on the basolateral surface of the hepatocytes (*66*), it is also found on endocytic vesicles and was shown to travel between late endocytic vesicles and the cell surface (*67*). ABCA1 was shown to promote the efflux of cellular phospholipids

and cholesterol to lipid free apoA-I and other apolipoproteins and amphipathic peptides, but it does not promote efflux to spherical HDL particles (*68-71*). Lipid poor apoA-I particles containing one apoA-I molecule and three to four phospholipid molecules can promote ABCA1-mediated efflux of phospholipid and cholesterol similarly to lipid free apoA-I (*72*). Inactivating mutations in ABCA1 are present in patients with Tangier disease (*73*) (Fig. 1.7). The deficiency is associated with very low levels of total plasma and HDL cholesterol and abnormal lipid deposition in various tissues (*74-78*).

Fluorescence microscopy of HeLa cells that expressed an ABCA1 green fluorescence fusion protein has shown the intracellular trafficking of apoA-I/ABCA1 complexes (*66;67*). It has been reported that in macrophages apoA-I binds to ABCA1 in the coated pits, it is internalized and following interaction with intracellular lipid pools it is re-secreted as a lipidated particle (*79;80*). A similar pathway that leads to transcytosis has been observed in endothelial cells (*81;82*). Calmodulin in the presence of Ca^{2+} binds and stabilizes ABCA1 and protects it from calpain mediated degradation thus leading to increased HDL formation (*83*).

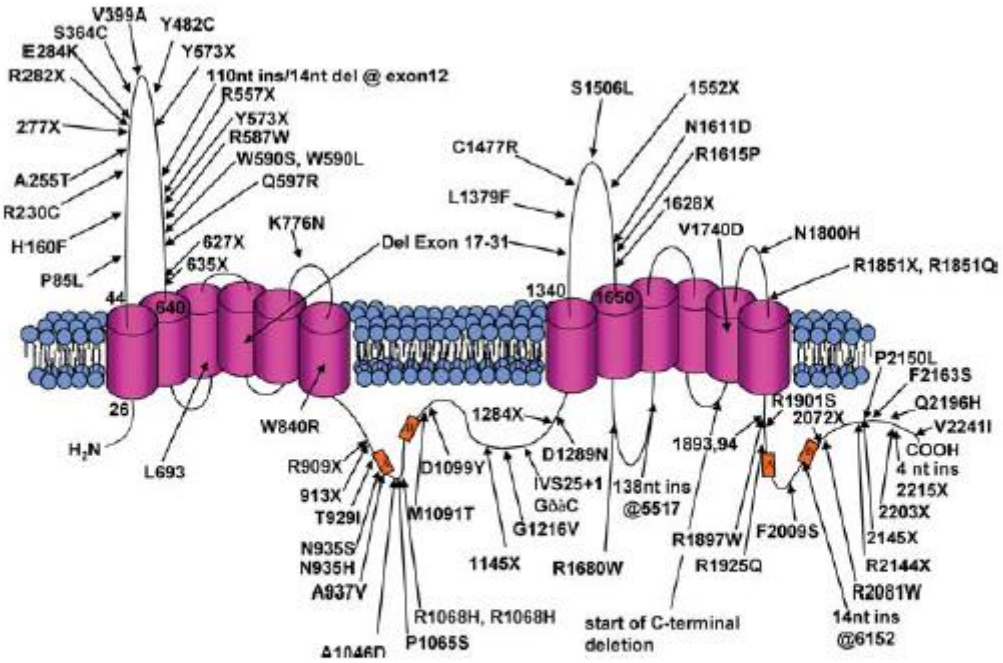

Figure 1.7. Schematic representation of ABCA1. All known ABCA1 mutations are indicated by arrows. Obtained from (*73*).

1.2.2. Interactions of apoA-I with ABCA1 in cell cultures

Tangier patients carrying the mutations in figure 1.7 and ABCA1$^{-/-}$ mice do not form discoidal or spherical HDL, but form preβ1 HDL particles (*84;85*). Skin fibroblasts obtained from Tangier patients or ABCA1$^{-/-}$ mice have diminished ability to promote cellular cholesterol efflux (*74;75;86-90*).

A series of cell culture and in vitro experiments investigated the ability of apoA-I mutants to promote ABCA1 mediated efflux of cholesterol and phospholipids and to crosslink ABCA1. A set of apoA-I mutants was generated. These mutants had amino terminal deletions, carboxy terminal deletions that removed the 220-231 region, carboxy terminal deletions apoA-I[Δ(232-243)] that left the 220-231 region and double deletions of the amino- and carboxy- terminal region (*91*).

For the efflux studies two types of cell cultures were used. The one was J774 macrophages in which expression of ABCA1 can be induced by cAMP analogues. The other was Human Embryonic Kidney (HEK) 293 EBNA cells transfected with an ABCA1-expressing plasmid. These studies showed that WT ABCA1-mediated cholesterol and phospholipid efflux was not affected by amino-terminal deletions, it was diminished by carboxy-terminal deletions in which residues 220-231 were removed, it was not affected by deletion of the C-terminal 232-243 region and it was restored to 80% of WT control by double deletions of both the amino and carboxy termini (*4;54;91;92*). These findings are consistent with direct ABCA1/apoA-I interactions that involve the central helices of apoA-I. Lipid efflux was either unaffected or moderately reduced by a variety of point mutations or deletions of internal helices 2-7 and indicated that different

combinations of central helices can promote lipid efflux (*93;94*). Chemical cross-linking/ immunoprecipitation studies showed that the ability of apoA-I mutants to promote ABCA1 depended lipid efflux is correlated with the ability of these mutants to be cross-linked efficiently to ABCA1 (*94*). Other studies showed that synthetic peptides of L or D configuration can also promote ABCA1-mediated cholesterol efflux in vitro (*91*). These properties of the synthetic peptides however do not necessarily imply that following efflux in vivo they can proceed to form HDL type particles (*69;94-96*).

Cross-linking between apoA-I and ABCA1 and cholesterol efflux may be affected by mutations in ABCA1 that are found in patients with Tangier disease. The majority of the ABCA1 mutations cross link poorly with WT apoA-I and have diminished capacity to promote cholesterol efflux (*87;97;98*). In vitro studies showed that in some cases apoA-I and ABCA1 bound efficiently but this interaction did not lead to the synthesis of HDL particles. In this case the binding was characterized as "non-productive" binding (*96*). A notable example is the ABCA1[W590S] mutant which can cross-link stronger to apoA-I than the WT ABCA1 but has diminished capacity to promote cholesterol efflux and to promote formation of HDL (*87;97;98*). When the cross-linking properties of several apoA-I mutants to cells that expressed either the WT ABCA1 or the ABCA1[W590S] were compared, significant differences in binding were observed. It was proposed that this might have happened because this mutation may have altered the environment of the binding site of ABCA1 in such a way that the binding is strong but not productive and prevents efficient lipid efflux (*94*).

1.2.3. Interactions of apoA-I with ABCA1 in vivo are the first step in the biogenesis of HDL

The in vivo interactions of apoA-I with ABCA1 were studied by adenovirus mediated gene transfer. In these experiments, apoA-I deficient mice were infected with 1 to $2x10^9$ plaque forming units (pfu) of an adenovirus expressing WT apoA-I or the apoA-I mutants that were previously studied by in vitro experiments. Four to five days post infection plasma was collected and analyzed for plasma lipids and lipoproteins by two-dimensional gel electrophoresis. The plasma was fractionated by density gradient ultracentrifugation and fast protein liquid chromatography (FPLC) and the HDL fraction was analysed by electron microscopy (EM) (*91;92*). Also the hepatic mRNA levels of apoA-I were determined to ensure that there was comparable expression of the WT and the mutant apoA-I forms. These experiments showed that the WT apoA-I and amino terminal deletion mutants generated HDL in vivo. The two-dimensional gel electrophoresis showed that most of WT apoA-I had particles with α electrophoretic mobility and a small fraction had β electrophoretic mobility (*54;84;91;92*). A double deletion mutant (of the amino and the C-terminal combined) formed discoidal HDL particles (*91*). The mutants with the C-terminal deletion generated very little HDL, that consisted of preβ1-HDL particles (*84*). Some spherical particles were observed in the C-terminal apoA-I deletion mutants but these particles were enriched in apoE. These experiments showed that the first step of biogenesis of HDL can be blocked by C-terminal deletions in the apoA-I gene (*84;91*). The preβ-migrating particles that were found in the C-terminal deletion mutants can be also found in the plasma of $ABCA1^{-/-}$ mice and in the plasma of Tangier

disease patients (*85;94;96*). This shows that these particles are created by mechanisms that may not involve the ABCA1/apoA-I interaction.

Based on the in vitro and in vivo studies a two step model of lipid efflux was suggested. In the first step the formation of a tight complex between ABCA1 and apoA-I takes place (*94;96*). This step seems to be necessary but not sufficient for lipid efflux and requires that the complex formed is productive to allow lipid efflux (*96;97*). In the second step the ABCA1-mediated transfer of lipids from the cell to apoA-I takes place.

Several studies indicated that there are two sites of interaction of apoA-I on the cell membrane (*99;100*). The first site is a low capacity apoA-I binding site on the ABCA1 molecule. This interaction appears to stabilize ABCA1 on the cell membrane and to protect it from proteolytic degradation (*101-103*). The second site is a high capacity apoA-I binding site and may be created by the phospholipid translocase activity of ABCA1 (*100*). It has been proposed that following the initial transient interaction of apoA-I with ABCA1, apoA-I is inserted in the high capacity binding site, and thus extract PL and FC from cells. The lipidated apoA-I can then be released in the form of nascent HDL particles (*96;104*).

It has been reported that intestinal ABCA1 mediated production of HDL accounts for the 30% of HDL in mice (*105*). When the liver and intestinal ABCA1 genes were inactivated there was no production of HDL indicating that the liver and the intestine are the only sites that contribute to the production of HDL cholesterol. HDL produced in the intestine is secreted directly into the plasma, whereas the HDL found in the lymph originates from pre-existing plasma HDL. Thus in mice that do not express intestinal

ABCA1 there was no transport of intestinal HDL cholesterol to the plasma, whereas the cholesterol concentration of lymph was not affected. In contrast in mice that do not express hepatic ABCA1 the HDL concentration in the lymph was nearly abolished (*105*).

It has been reported that the interactions of ABCA1/apoA-I in the liver are essential for the initial lipidation of apoA-I and also determine the subsequent maturation of nascent preβ-HDL to spherical αHDL particles (*78;106*). When ABCA1 is inactivated in the liver, lipidated apoA-I particles or preβ HDL generated in the peripheral tissues fail to mature and are catabolized rapidly by the kidney (*78;106*).

Various studies have shown that macrophages can bind HDL and apoA-I in a specific manner (*68;71;107-109*). HDL can compete for apoA-I binding to macrophages whereas apoA-I cannot compete for binding to HDL indicating that apoA-I and HDL have a minimum of two different binding sites on macrophages (*110*). The same study has shown that lipid free apoA-I can be endocytosed into macrophages in a saturable specific way. These findings are consistent with the prevailing concept that lipid-free apoA-I can interact with ABCA1 to promote cholesterol efflux and form HDL which in turn interacts with either SR-BI or ABCG1 to promote efflux of additional cholesterol from macrophages (*110*).

1.2.4. Other physiological functions of ABCA1 and its role in atheroprotection and other diseases

The ABCA1 deficiency in humans or experimental animals is also associated with accelerated atherosclerosis (*111*). Overexpression of ABCA1 in the liver of C57BL/6

mice protected the mice from diet induced atherosclerosis. The ABCA1 transgenic mice displayed antiatherogenic phenotype with decreased plasma cholesterol and apoB levels and more than two fold increase in apoA-I and HDL levels (*112*). Unexpectedly hepatic overexpression of ABCA1 in apoE$^{-/-}$ mice did not affect the plasma lipid profiles but increased 2 to 6 fold atherosclerosis in the aortas (*112*).

ABCA1$^{-/-}$ mice are characterized by low total serum cholesterol levels, lipid deposition in various tissues, impaired growth and neuronal development and mimic the phenotype described for patients with Tangier disease (*74*). In addition ABCA1$^{-/-}$ mice exhibited moderate increase in cholesterol absorption in response to high cholesterol diet (*76;113*).

Inactivation of the ABCA1 gene in macrophages increases the susceptibility to atherosclerosis. Transplantation of normal bone marrow in ABCA1$^{-/-}$ mice affected minimally the plasma HDL levels (*114*). Bone marrow transplantation of ABCA1$^{-/-}$ leukocytes in LDLr$^{-/-}$ or apoE$^{-/-}$ mice increased the number of macrophages in the peripheral blood leukocytes, the spleen and the liver and increased atherosclerosis (*115;116*), thus suggesting an important role of ABCA1 in the control of macrophage recruitment to tissues and development of atherosclerosis.

The role of ABCA1 on the lipid content of bile salts and cholesterol secretion is not clear. One study indicates that the cholesterol and phospholipid concentration in the bile increased 1.8 fold in ABCA1 transgenic mice (*117*) whereas another indicated that ABCA1 deficiency in mice did not affect the bile acid content and the secretion rates of biliary cholesterol, bile acids and phospholipids (*118*).

The combined results of three population studies of white subjects from Copenhagen, Denmark showed that decreased HDL levels resulting from heterozygosity for the ABCA1 mutations P1065S, G1216V, N1800H and R2144X were not a risk factor for developing ischemic hard disease (IHD) (*119*). However, a study following 9259 individuals from the Danish general population showed that five ABCA1 SNPs regardless of their association with high (V771M, V825I), normal (I883M, E1172D) or low (R1587K) HDL levels, were predictors for IHD. The R219K SNP (normal HDL) was not associated with IHD. Additionally it was shown that the V771M, I883M and E1172D mutations were the most important predictors and pairs of the V771M/I883M and I883M/E1172D mutations led to additive effects on the risk for IHD (*120*).

An ABCA1 variant (R230C) has been identified exclusively and in high frequency in subjects with Native American descent that was associated with lower HDL cholesterol levels and higher body mass index and may be related to positive selection in the Native American population (*121*).

1.3. Interactions of lipid-bound apoA-I with LCAT

Plasma LCAT is a 416 amino acid long protein that is synthesized and secreted by the liver. LCAT interacts with discoidal and spherical HDL by transferring the 2-acyl group of lecithin or phosphatidylethanolamine to the free hydroxyl residue of cholesterol to form cholesteryl esters (Fig. 1.8). Following esterification, cholesteryl esters become part of the HDL particle (*122*).

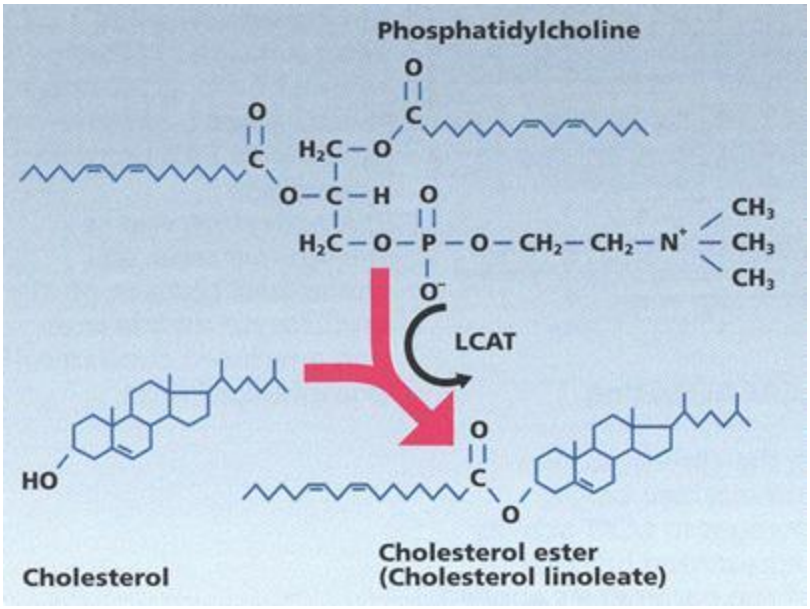

Figure 1.8. Schematic representation of LCAT-catalyzed esterification of cholesterol.

ApoA-I in nascent discoidal HDL is the most potent apolipoprotein activator of plasma enzyme LCAT. Esterification of free cholesterol of HDL in vivo converts the discoidal to mature spherical HDL (*123;124*).

Mutations in the enzyme LCAT are associated with two phenotypes. The familiar LCAT deficiency (FLD) is characterized by the inability of the mutant LCAT to esterify cholesterol on HDL and LDL and the accumulation of discoidal HDL in the plasma. The fish eye disease (FED) is characterized by the inability of mutant LCAT to esterify cholesterol on HDL only. Both diseases are characterized by low HDL levels (*125*) (Table I).

Studies using apoA-I mutants (that will be discussed later), synthetic peptides, and monoclonal antibodies, have indicated that residues in the 143–166 region of apoA-I

play an important role for the activation of LCAT. Most of these residues are in helix 6 (residues 145–164 of apoA-I) (Fig. 1.1). Oxidation of M148 reduced the ability of apoA-I to activate LCAT. Reduction of the oxidized methionine sulphoxide reductase restored the ability of HDL to activate LCAT. The LCAT activation ability of apoA-I was inhibited following treatment with MPO. However, an apoA-I [M148L] mutant retained its ability to activate LCAT, suggesting the specific change of M148 to methionine sulfoxide is important for LCAT activation (*126*).

Heterozygosity for LCAT mutations in the Italian population was not associated with increased preclinical atherosclerosis (*127*). Sera obtained from LCAT heterozygote subjects had increased capacity to promote ABCA1 mediated cholesterol efflux and decreased capacity to promote ABCG1 and SR-BI mediated cholesterol efflux from macrophages as compared with sera obtained from normal subjects. These properties were attributed to the increased preβ and decreased α HDL subpopulations in the sera of the LCAT heterozygotes (*128*).

Residues A130 and K133 of apoA-I are well conserved in mammals and are basic and acidic respectively in fish. It has been proposed that these residues play an important role in the formation of an amphipathic presentation tunnel located between helices 5-5 in the double belt model (Fig. 1.2B). Such a tunnel could allow migration of the hydrophobic acyl chains of phospholipids and the ampipathic unesterified cholesterol from the bilayer to the active site of LCAT that contains sites for phospholipase activity and esterification activity (*129*).

Table I. List of LCAT mutations that underlie LCAT deficiency syndromes.

Adapted from (*130*)

Defect			Exon	Clinical Phenotype FLD	FED
Homozygous mutations					
1.	C-insertion (codons 9, 10)		1	X	
2.	P10L		1		X
3.	G30S		2	X	
4.	Y83-stop		3	X	
5.	A93T[a]		3	X	
6.	T123I		4		X
7.	N131D		4		X
8.	R140H		4	X	
9.	G141-insertion		4	X	
10.	L209P		5	X	
11.	N228K		6	X	
12.	R244G		6	X	
13.	M252K		6	X	
14.	M293I		6	X	
15.	L300-deletion		6	X	
16.	T321M		6	X	
17.	G344S		6	X	
18.	G-deletion (codon 264)		6	X	
Heterozygous mutations					
1.	P10Q	R135Q	1, 4		X
2.	L32P	T321M	2, 6	X	
3.	G33R	30 bp Insertion (codon 4)	1, 2	X	
4.	Y83-stop	Y156N	3, 5	X	
5.	T123I	Y144C	4, 4		X
6.	T123I	Intron 4 defect (IVS4:T-22C)	4, intron 4		X
7.	T123I	T347M	4, 6		X
8.	T123I	Unknown	4, ?		X
9.	R135W	A-insertion (codon 376)[b]	4, 6	X	
10.	R147W	Unknown	4, ?	X	
11.	G183S	A–T substitution/C–deletion (codon 120)[c]	4, 5	X	
12.	M252K	N391S	6, 6		X
13.	T321M	C-deletion (codon 168)[d]	5, 6	X	
14.	R399C	C-insertion (codons 9, 10)[e]	6, 1	X	

FLD: Total loss of catalytic activity

FED: Partial loss of activity against HDL only

1.3.1. Effect of apoA-I mutations on the activation of LCAT

The in vivo interactions of apoA-I mutants with LCAT were studied by adenovirus-mediated gene transfer in apoA-I deficient mice. These studies investigated

the ability of the naturally occurring mutants apoA-I(Leu141Arg)$_{Pisa}$, apoA-I(Leu159Arg)$_{FIN}$, apoA-I[Arg151Cys]$_{Paris}$, apoA-I[Arg160Leu]$_{Oslo,}$ apoA-I[Leu144Arg] as well as the apoA-I[Arg149Ala] mutant that was generated by in vitro mutagenesis to promote biogenesis of HDL. The first two mutants are associated with very low HDL and apoA-I levels in humans (*131-134*) and premature atherosclerosis (*131;135*) and the other three are associated with low HDL but milder phenotype in humans (*136-139*). In vitro studies showed that all six mutants had reduced capacity to activate LCAT (*139-141*). The gene transfer studies showed that all the mutants generated aberrant HDL phenotypes (*139-141*). The mutants apoA-I[Leu141Arg]$_{Pisa}$ and apoA-I[Leu159Arg]$_{FIN}$ produced only small amounts of HDL that formed mostly preβ1 HDL particles. The apoA-I[Arg151Cys]$_{Paris}$ and apoA-I[Arg160Leu]$_{Oslo}$ mutants formed discoidal HDL particles. These studies indicated that apoA-I[Leu141Arg]$_{Pisa}$ and apoA-I[Leu159Arg]$_{FIN}$ mutation may inhibit an early step in the biogenesis of HDL due to insufficient esterification of the cholesterol of the preβ1-HDL particles by the endogenous LCAT. The LCAT insufficiency appears to result for depletion of the plasma LCAT mass (*141*). It was suggested that the mutations in apoA-I promote rapid catabolism of the newly lipidated apoA-I as well as the LCAT that is associated with these particles (Fig. 1.9). The resulting depletion of LCAT prevents the formation of either discoidal or spherical HDL particles (*141*). Mice expressing the apoA-I[Leu144Arg] mutant had low total plasma cholesterol, HDL cholesterol and apoA-I levels and decreased cholesteryl ester to total cholesterol ratio (CE/TC). ApoA-I was distributed mainly in the HDL3 region. The apoA-I[Leu144Arg] mutant promoted the formation of lipid-poor preβ and α4-HDL

particles (*139*). The mutants apoA-I[Arg151Cys]$_{Paris}$, apoA-I[Arg160Leu]$_{Oslo}$, apoA-I[Leu144Arg]

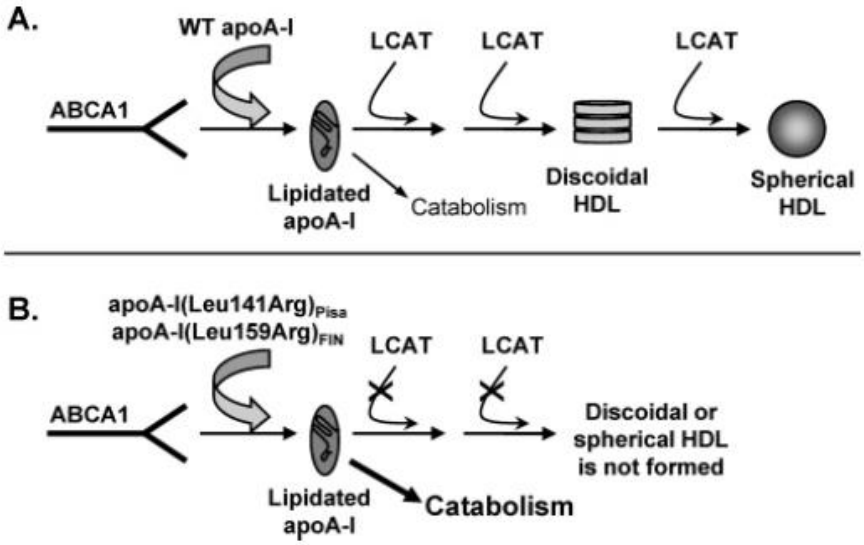

Figure 1.9. Schematic representation showing the pathway of biogenesis of HDL and how the mutations apoA-I(Leu141Arg)$_{Pisa}$ and apoA-I(Leu159Arg)$_{FIN}$ affect the esterification of cholesterol of the initially lipidated particles and prevent their conversion to discoidal and spherical HDL, thus promoting their catabolism. Obtained from (*141*).

and apoA-I[Arg149Ala] formed mixture of discoidal and spherical particles and this also suggests insufficiency of the endogenous LCAT, which resulted in slow conversion of discoidal HDL to spherical HDL (*139;140*). A remarkable finding was that all the aberrant phenotypes were corrected by treatment with exogenous LCAT. This indicates that LCAT administration could be a potential therapeutic intervention to correct low-HDL conditions in humans that are caused by these and other unidentified mutations. Recently it was shown that adenovirus mediated gene transfer of human LCAT in

squirrel monkeys increased 2 fold HDL levels without affecting apoA-I levels, increased the size of HDL and decreased apoB levels (*142*).

1.4. Interactions of lipid-bound apoA-I with SR-BI

SR-BI is an 82 kDa membrane glycoprotein. The protein has a large extracellular domain, two transmembrane domains and two cytoplasmic amino and carboxy terminal domains (*143*). SR-BI is primarily expressed in the liver and steroidogenic tissues but is also found in other tissues (*144*). SR-BI binds a variety of ligands including HDL, LDL and VLDL (*57;143-146*). However the most important property of SR-BI is considered its ability to act as the HDL receptor. There is evidence that the interaction of SR-BI with apoA-I and apoE is important for the maturation of HDL and the generation of HDL particles (*57;147-151*).

It has been shown that SR-BI binds to HDL and discoidal reconstituted HDL, through its apoprotein moiety (apoA-I or apoE) (*57;151-153*). When it is bound to lipoproteins, SR-BI mediates both selective uptake of cholesteryl ester (*144;154-156*) as well as uptake of triglycerides, phospholipids and vitamin E (*144;154-156*) from HDL (*144;157*) to cells (*144;158;159*). It also promotes bidirectional movement of unesterified cholesterol (*160;161*). Interactions of rHDL with SR-BI are responsible for mobilization of free cholesterol from the whole body (*162*). SR-BI mutants which display altered biological functions were generated by in vitro mutagenesis. A SR-BI[Met158Arg] mutant does not bind HDL (*161*). A SR-BI[Gln402Arg/Gln418Arg] mutant also does not bind HDL but in contrast with the first mutant it binds LDL

(*158;161*). A SR-BI(Gly420His) mutant has normal selective cholesteryl ester uptake but reduced cholesterol efflux to HDL and reduced hydrolysis of internalized cholesteryl esters (*163*). Cell culture cholesterol efflux studies using rHDL containing mutated apoA-I and these SR-BI mutants, showed that the greater reduction of cholesterol efflux in cells expressing WT SR-BI was with mutants apoA-I(Asp102Ala/Asp103Ala) and apoA-I(Arg160Val/His162Ala) (21% and 49% respectively) (*164*). When the mutant SR-BI were examined all the apoA-I mutants had reduced efflux and bound less tightly compared to WT apoA-I with the exception of rHDL that contained the mutant apoA-I(Arg160Val/His162Ala). The binding of this mutant was almost as tight to the cells that expressed SR-BI(Met158Arg) mutant as it was for the cells that expressed WT SR-BI (*164*). Based on these data the authors suggested that efficient SR-BI mediated cholesterol efflux requires not only direct binding (*161*) but also the formation of a productive complex between SR-BI and the rHDL particle (*164*).

1.4.1. In vivo functions of SR-BI

A variety of studies have established that the in vivo interactions of SR-BI with its ligand HDL are physiologically important (*57;143;165;166*). Transgenic mice expressing SR-BI in the liver had decreased apoA-I and HDL levels and increased clearance of VLDL and LDL (*147;148*). SR-BI deficient mice had decreased HDL cholesterol clearance (*167*), two fold increased plasma cholesterol and presence of large size abnormal apoE enriched particles that were distributed in the HDL/IDL/LDL region (*149*). The in vivo phenotypes generated by overexpression or deficiency of SR-BI are consistent with its in vitro

functions to promote selectively lipid transport from HDL to cells and efflux of free cholesterol from cells.

SR-BI has also been shown to affect chylomicron metabolism in vivo and bind non-HDL lipoproteins in vitro (*168;169*). Deficiency of SR-BI in mice reduced greatly the cholesteryl ester stores of steroidogenic tissues and decreased the secretion of biliary cholesterol by approximately 50%. However, the SR-BI deficiency did not affect the secretion of the pool size of bile acids or the fecal secretion of bile acids and the intestinal cholesterol absorption (*149;170*). These findings established that two important functions of HDL are the transfer of HDL cholesterol to the bile for excretion (*149;170*) and the delivery of cholesterol esters to the steroidogenic tissues where it is utilized for synthesis of steroid hormones (*171*). Furthermore SR-BI controls the concentrations and composition of plasma HDL (*57;147-150*) and protects mice from atherosclerosis. SR-BI deficiency also caused defective maturation of oocytes and red blood cells due to accumulation of cholesterol in the plasma membrane of progenitor cells (*172;173*) and caused infertility in the female but not the male mice (*172;174*). The infertility could be corrected by restoration of SR-BI gene by adenovirus mediated gene transfer (*175*). Subsequent experiments showed a negative correlation of follicular HDL cholesterol levels in women and embryo fragmentation during in vitro fertilization (*176*). Taken together these data suggest a role of HDL in oocyte development and embryogenesis.

Interactions of HDL with SR-BI in endothelial cells triggers signaling mechanisms, that will be discussed later, that involve activation of eNOS and release of nitric oxide that causes vasodilation (*177-182*).

Overexpression of SR-BI in the liver of transgenic mice decreased dramatically the plasma HDL levels and protected the mice from atherosclerosis (*183-185*). In contrast SR-BI deficiency in the background of LDLr deficient or apoE deficient mice accelerated dramatically the development of atherosclerosis (*172;186*). The double deficient mice for apoE and SR-BI developed occlusive coronary atherosclerosis, cardiac hypertrophy, myocardial infarctions, cardiac dysfunction and died prematurely (mean age of death ~6 weeks) (*172;187-190*). An unexpected finding was that treatment of the double deficient mice for apoE and SR-BI with probucol reversed most of the cardiac and red blood cell abnormalities, corrected the lipid and lipoprotein profiles and extended the life of the mice up to 60 weeks (*188*).

Expression of CETP in SR-BI deficient mice (SR-BI$^{-/-}$ x CETP Tg) decreased plasma cholesterol levels and normalized partially the size of the large HDL particles found in SR-BI$^{-/-}$ mice. However similarly to SR-BI$^{-/-}$, the SR-BI$^{-/-}$ x CETP Tg mice, developed atherosclerosis, had female infertility, reticulocytosis, impaired platelet aggregation, thrombocytopenia and were characterized by high VLDL levels and high free cholesterol/total cholesterol ratio (*191*).

A model of diet induced atherosclerosis was generated by crossing SR-BI deficient mice with apoE(T61R) transgenic mice that express low levels of the mutant mouse apoE gene (*192*). These mice are resistant to atherosclerosis on chow diet but develop occlusive atherosclerosis, myocardial infarction and cardiac dysfunction when they are placed on high fat diet (*192*).

Human subjects have been identified with a P297S substitution in SR-BI. Heterozygote carriers for this mutation had increased HDL levels, decreased adrenal stereidogenesis and dysfunctional platelets but did not develop atherosclerosis. HDL derived from these subjects had decreased ability to promote cholesterol efflux from macrophages (*165*).

A recent study has shown the impact SR-BI SNPs on female fertility. Carriers of a minor SNP polymorphic A allele (rs4238001) that causes a non-synonymous change at amino acid 2 of SR-BI (glycine to serine) had decreased follicular progesterone levels in Caucasians and was associated with non viable fetuses on Day 42 following embryo transfer. Another SNP (rs10846744) was associated with gestational sacs and fetal heart beats and was associated with poor fetal viability in African-Americans (*166*).

1.5. Remodeling of HDL by the action of ABCG1

HDL can be remodeled following interactions with ABCG1 a 67 kDa protein which is a member of ABC family of half transporters. ABCG1 is expressed in the spleen, thymus, lung and brain (*193-195*) and is localized on plasma membrane the Golgi and recycling endosomes. The expression of ABCG1 is induced by LXR agonists or by cholesterol loading in macrophages and in the liver (*196-198*). Overexpression of ABCG1 promotes cholesterol efflux from cells to HDL but not to lipid free apoA-I (*58;195;198;199*). ABCG1 mediated cholesterol efflux to HDL is abolished by mutations in the ATP binding motif (*199*). It was suggested that cholesterol efflux does not require direct binding of HDL to ABCG1 (*199*). ABCG1 accounts for 50% of cholesterol efflux by

bone marrow-derived macrophages to rHDL (*162*). In macrophages it has been suggested that ABCG1 plays an important role for cholesterol export from cells (*198*). It has also been shown that HDL_2 can be formed by the action of lipid free apoA-I, ABCA1 and ABCG1 (58). First ABCA1 forms the nascent or preβ-HDL and then ABCG1 mediates the export of lipids to the nascent particles to form HDL (*200*). It is still not known how HDL interacts with ABCG1 to promote the efflux (*201*). The absence of ABCG1 in mice causes cholesterol accumulation in various tissues (*201*) and selective deletion of both ABCA1 and ABCG1 genes in macrophages further increases cholesterol accumulation and results in severe atherosclerosis (*202;203*).

The ability of various lipid transporters to promote cholesterol efflux was tested in human placenta endothelial cells (HPEC) and HUVECs. The ABCA1-mediated efflux to lipid free apoA-I was 2.5 fold increased in HPEC as compared to HUVEC whereas efflux to HDL3 was similar in both cell types. Cholesterol efflux in HPECs to apoE-enriched HDL3 was slightly increased as compared to HDL3. Both ABCA1 and ABCG1 were visualized predominantly in the apical side of the cells. LXR activators and 24-hydroxy cholesterol increased ABCA1 and ABCG1 expression in HPEC and enhanced the ABCA1 and ABCG1 mediated cholesterol efflux to their cholesterol acceptors. Down-regulation of ABCA1 and ABCG1 expression by siRNA in HPEC decreased the ABCA1 and ABCG1 mediated cholesterol efflux to their cholesterol acceptors. The ability of HPEC to promote ABCA1 and ABCG1 mediated efflux may facilitate the transfer of maternal cholesterol to the fetus (*204*).

The contribution of ABCA1, SR-BI and ABCG1 to promote cholesterol efflux to apoA-I or HDL in vitro and in vivo was tested in adipocytes obtained from mice deficient for ABCA1, SR-BI or ABCG1. Efflux to apoA-I was impaired in ABCA1 deficient adipocytes and efflux to HDL was impaired in SR-BI but not in ABCG1 deficient adipocytes. TNF-α reduced ABCA-1 and SR-BI expression and dimished cholesterol efflux from partially differentiated adipocytes. In vivo experiments showed that intra-peritoneal injection of ^{3}H-cholesterol loaded adipocytes obtained from ABCA1$^{-/-}$ or SR-BI$^{-/-}$ mice had reduced efflux of ^{3}H-cholesterol into the plasma as compared to wild type adipocytes. ApoA-I deficiency decreased the release of ^{3}H-cholesterol from cholesterol loaded 3T3L1 adipocytes to the plasma of apoA-I deficient mice (*205*). Cholesterol efflux from adipocytes mediated by ABCA1 or SR-BI may be relevant to inflammatory diseases such as type 2 diabetes mellitus. Small POPC/apoA-I rHDL particles of 7.8 nm nm of diameter can efficiently promote cholesterol efflux via ABCG1 and ABCA1whereas SR-BI can only mediate efflux to rHDL particles with diameter over 9.6 nm (*206*).

1.6. Transcytosis of apoA-I and HDL

It has been shown that endothelial cells have the ability to bind and transcytose lipid-free apoA-I in a specific manner. This process depends on ABCA1 and leads to the generation of a lipidated apoA-I particle that is secreted (*81;207*). Endothelial cells can also transcytose HDL and this process required the functions of SR-BI and ABCG1 (*208*). ApoA-I mutants with defective C-terminal apoA-I[Δ(185-243)] and apoA-

I[L218A/L219A/V221A/L222A]) had 80% decreased specific binding and 90% decreased specific transport by aortic endothelial cells. Following lipidation of these mutants the rHDL particles formed were transported through endothelial cells by an ABCG1 and SR-BI dependent process. Amino and combined amino and carboxy terminal apoA-I deletion mutants displayed increased non-specific binding but the specific binding or transport remained absent (*82*). These data support the model in which apoA-I is initially lipidated by ABCA1 and subsequently processed by ABCA1 independent mechanisms. Transcytosis of apoA-I and HDL may provide a mechanism for transfer of HDL in the sub-endothelial space.

1.7. Interactions of apoA-I with F1-ATPase

The β-chain subunit of F1-ATPase has been identified as a high affinity receptor for lipid-free apoA-I in HepG2 cells (*209*). Subsequent studies have shown that this receptor is also present on the surface of endothelial cells and binds angiostatin (*210;211*). F1-ATPase contributes to the regulation of HDL uptake by hepatocytes as well as to cell proliferation and inhibition of endothelial cell apoptosis (*211*). Binding of lipid-free apoA-I to F1-ATPase activated endocytosis of the lipidated HDL particle by low affinity binding site (*212*).

1.8. HDL subpopulations

As a consequence of the pathway of biogenesis and remodeling of HDL that has been described in figure 1.6 and the preceding sections several HDL subpopulations have

been described previously based on different fractionation procedures (*213-215*). The HDL subpopulations can be easily separated by two-dimensional electrophoresis which involves in the first dimension agarose gel electrophoresis and in the second dimension non-denaturing polyacrylamide gradient gel electrophoresis (*124;216-218*). This analysis reveals the presence of preβ-HDL and the α-HDL subpopulations (Fig. 1.10). It has been reported earlier that preβ HDL is approximately 5% of plasma HDL, it is heterogeneous and has a size is 5-6 nm in diameter (*219;220*). The subpopulation of preβ1 is increased in large lymph vessels (*221;222*) and in aortic intima (*223;224*). The cholesterol of the preβ particles can be esterified by LCAT (*225*). The origin of preβ particles and their functions is still unclear. There is no precursor-product relationship between preβ and α-HDL particles. There are two potential pathways that can lead to the formation of preβ-HDL particles in plasma. The first is de novo synthesis (*226-228*) and the second is formation by remodeling of αHDL particles (*229-231*).

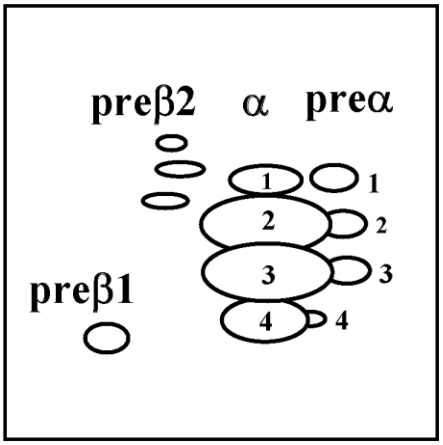

Figure 1.10. HDL subpopulations as revealed following analysis by two-dimensional non-denaturing electrophoresis.

1.9. Clinical phenotypes of humans carrying naturally occurring apoA-I mutations

The first described structural mutation of apoA-I, found in Italy, has been called apoA-I_{MILANO} and results from R173C substitution (*232-234*). Subjects heterozygous for apoA-I_{MILANO} have low HDL cholesterol and apoA-I levels, but do not appear to suffer from premature atherosclerotic disease (*233;235*). Subsequently, other heterozygote apoA-I variants designated apoA-$I_{Giessen}$ (R143P substitution) and apoA-$I_{Marburg}$ (ΔK107) have been described (*236-238*). The subjects with apoA-$I_{Marburg}$ had hypertriglyceridemia and reduced HDL cholesterol levels (*237*). Subjects with apoA-$I_{Giessen}$ had low apoA-I levels (*238*). Both mutant apoA-I forms have 40-70% ability to activate LCAT as compared to wild type apoA-I (*236;238*). Another apoA-I mutation which is associated with HDL deficiency, partial LCAT deficiency and corneal opacities results from a frameshift starting at residue 202 which causes incorporation of 27 random carboxy-terminal residues, including 3 cysteins (*239*). The G26R substitution is associated with familiar amyloidotic polyneuropathy III and is inherited as an autosomal dominant trait (*240;241*). The amyloid fibrils formed in this condition consist of the 83 amino-terminal residues of apoA-I. Two human conditions characterized by severe deficiencies of plasma apoCIII and HDL are associated with premature atherosclerosis. One condition has resulted from deletion of the apoA-I/apoCIII/apoA-IV locus (*242;242*) and the other from an inversion of the apoA-I/apoCIII locus. A homozygous nonsense mutation at the codon specifying residue 84 of apoA-I prevents synthesis of apoA-I and is associated with premature atherosclerosis (*243*). The rather moderate clinical phenotype observed in this and other

apoA-I mutants suggest that some of the functions of apoA-I may be assumed by other apolipoproteins , perhaps apoE or apoA-IV.

A missense mutation has been identified in a kindred in Spain. This mutation is in exon 4 of the apoA-I gene and is responsible for the substitution of leucine 144 with arginine (L144R). Heterozygotes carrying this mutation have decreased HDL cholesterol levels, increased triglyceride levels and a decrease in the cholesteryl esters to free cholesterol ratio, the latter indicating LCAT insufficiency. Humans carrying this mutation had reduced apoA-I, apoA-II and HDL-C levels. In addition, the HDL particles of these subjects have different composition compared to HDL particles obtained from control subjects (*244*). The fractional catabolic rate of apoA-I and apoA-II of the carriers of apoA-I[Leu144Arg] was increased and while the apoA-I secretion rate was also increased, the apoA-II secretion rate was normal (*244*).

A substitution, Leu159Arg, was found in a kindred in Finland (*134;135;245*). Heterozygous carriers of this mutation had lower HDL cholesterol and apoA-I plasma levels (20% and 25% respectively compared to unaffected family members) and the mutation was characterized as dominant negative (14).

A mutant apoA-I, designated as apoA-$I_{Tomioka}$, has a deletion of two A nucleotides at codon 138 of the apoA-I gene. This generated a frameshift mutation that led to the incorporation of 41 new amino acids between residues 138-178. Two homozygote carriers of this mutation had HDL and apoA-I deficiency while heterozygotes had 50% of normal plasma HDL but their large α1 and small preβ1 subpopulations were significantly decreased (*246*).

An insertion of one nucleotide in the codon corresponding to amino acid 17 of pro-apoA-I results in a frameshift that causes premature chain termination at codon 26 and complete apoA-I deficiency (*247*).

A nonsense mutation (GAA to CAA) at the codon for amino acid 136 has been identified in French Canadians and is characterized by low HDL cholesterol levels (< 5th percentile for age and gender matched controls) and is associated with CAD. This mutation is dominant negative (*248*).

A novel apoA-I mutation characterized by a A164S substitution has been identified by the Copenhagen City Heart Study. The mutation was present in one out of 500 of the general population. The heterozygosity for this mutation predicted increased risk for IHD and a mean reduction of lifespan by 10 years. Interestingly heterozygote carriers for this mutant had normal plasma lipid and apoA-I levels a finding that was confirmed by adenovirus mediated gene transfer of the apoA-I[A164S] mutant in apoA-I$^{-/-}$ mice (*139*).

Earlier studies indicated that the ability of mouse and human sera containing the apoA-I_{MILANO} to promote cholesterol efflux from hepatoma Fu5AH cells follows the order apoA-I_{MILANO} obtained from transgenic mice > apoA-I_{MILANO} from heterozygotes > apoA-I from normal subjects (*249;250*). Similar observations were reported for ABCA1-mediated cholesterol efflux from J774 macrophages and human fibroblasts. The authors suggested that the increased capacity of apoA-I_{MILANO} to promote cholesterol efflux was due to the presence of an HDL particle containing an apoA-I dimer that was sensitive to chymase digestion (*249*). Another study however showed that rHDL containing WT

apoA-I or apoA-I_{MILANO} have similar capacity to promote ABCA1 and SR-BI mediated cholesterol efflux. Furthermore, when adjusted for HDL cholesterol levels the sera of mice expressing apoA-I_{MILANO} or WT apoA-I had similar ability to promote cholesterol efflux from macrophages (*251*).

1.10. Bioengineered mutations in apoA-I that cause dyslipidemia

Three mutations in apoA-I have been described which affect the overall cholesterol and triglyceride levels. Two mutants, apoA-I[Δ(62-78)] and apoA-I [Glu110Ala/Glu111Ala], caused combined hyperlipidemia, characterized by high plasma cholesterol and severe hypertriglyceridemia (*93;252*). All the triglycerides and the majority of the excess cholesterol were distributed in the apoA-I-enriched VLDL/IDL-sized lipoproteins. The findings indicate that the apoA-I mutants had increased affinity for lower density lipoprotein fractions. In addition, the VLDL/IDL fractions of mice expressing these mutants had decreased levels of apoE and apoCII and increased level of apoB-48 which in combination with the increased apoA-I levels in these fractions might have inhibited lipolysis in vivo. When the mice were infected with two adenoviruses, the one expressing the mutant apoA-I and the other expressing human lipoprotein lipase, VLDL triglycerides were reduced (*252*). These studies showed for the first time that apoA-I mutations may induce hypertriglyceridemia or combined dyslipidemia. Similar studies showed that the apoA-I[Δ(89-99)] deletion mutant induced hypercholesterolemia that was characterized by increased cholesterol and phospholipids in the VLDL/IDL/LDL size lipoproteins. There was also substantial decrease of the CE/TC ratio in HDL and LDL whereas the

triglycerides remained normal. This apoA-I deletion also increased apoA-I levels in the LDL-sized particles, generated discoidal HDL particles and had increased level of preβ1 relative to the αHDL subpopulation (*252*).

The expression of the apoA-I[Δ(89-99)] mutant reduced the plasma PLTP activity to 32% of that of mice that expressed the WT apoA-I. PLTP interacts physically with apoA-I (*253*) and its function is to link the donor and acceptor lipoprotein particles in order to facilitate the net transfer of phospholipids to HDL (*254*). It has been shown that PLTP remodels the HDL and promotes the generation of preβ-HDL particles (*255-257*). High fat diet increased the concentration of phospholipids and cholesterol in the VLDL and LDL of $PLTP^{-/-}$ mice and promoted the formation of discoidal particles (*258*). The phenotype of these mice was similar to that of mice expressing the apoA-I[Δ(89-99)] mutant.

The systematic study of the functions of apoA-I by adenovirus mediated gene transfer as well as the phenotypes of naturally occurring apoA-I mutants identified five steps where this pathway of biogenesis and/or catabolism of HDL can be disrupted and lead to dyslipidemia (Fig. 1.11):

1) Lack of synthesis of HDL due to mutations in ABCA1 or mutations in apoA-I that affect the ABCA1/apoA-I interaction, 2) Failure to synthesize discoidal or spherical HDL. This defect most likely results from fast catabolism of apoA-I following its lipidation by ABCA1, 3) Accumulation of discoidal HDL associated with inhibition of PLTP and induction of hypercholesterolemia. This condition has been observed in the case of the apoA-I[Δ(89-99)] mutant, 4) Accumulation of discoidal HDL. This phenotype

has been generated by the mutations in the 149-160 region of apoA-I or other mutations that inhibit LCAT activation 5) Induction of hypertriglyceridemia. This defect has been observed in the case of apoA-I[Δ(62-78)] and apoA-I[Glu110Ala/Glu111Ala] mutants.

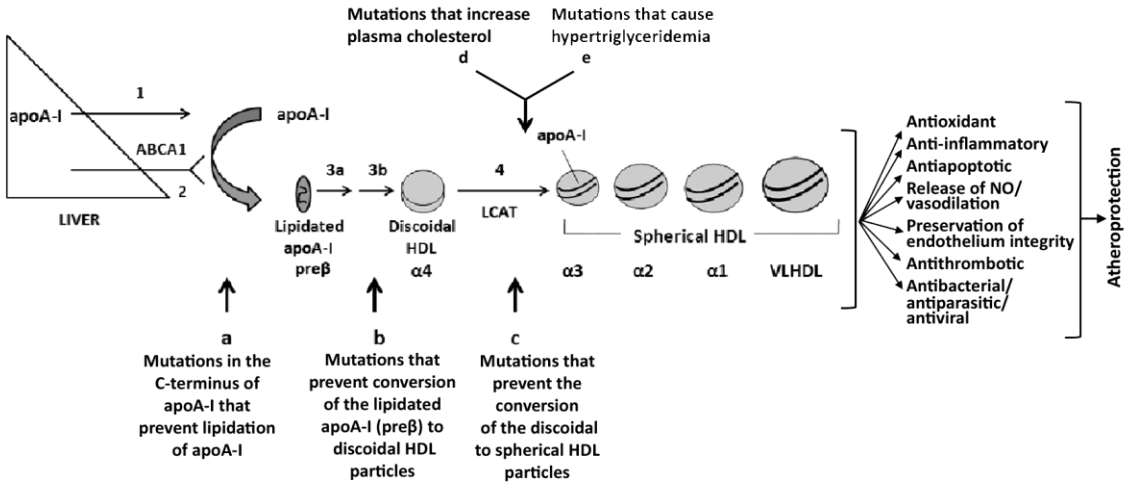

Figure 1.11. The pathway of HDL biogenesis. Superimposed on the pathway are defects that inhibit different steps of this pathway. Different subpopulations of HDL may have different functions.

1.11. Physiological functions of ApoA-I and HDL that may be relevant to its atheroprotective properties

1.11.1. Cell signaling pathways mediated by HDL and apoA-I

Various studies have shown that increased HDL levels are associated with greater vasodilator effects in humans and this effect is impaired in patients with CHD (*259-261*). Treatment with HDL increased eNOS protein levels in cultured human aortic endothelial

cells (HAECs) by increasing its half life without affecting steady state eNOS mRNA levels (*262;263*).

Earlier studies in endothelial cells and Chinese hamster ovary (CHO) cells that express SR-BI showed that SR-BI is involved in the activation of eNOS by HDL (*179*). The HDL-induced eNOS activation occurs in the caveolae (*179*). The HDL-mediated NO-dependent relaxation is lost in aortic rings of SR-BI$^{-/-}$ mice (*179*). Experiments in cultures of endothelial cells and COS M6 cells transfected with eNOS and SR-BI showed that interaction of HDL with SR-BI triggered signalling mechanisms which led to phosphorylation of eNOS at Ser1179 and increased its activity. On the other hand phosphorylation of Thr 497 of eNOS attenuated its activity. The signalling cascade initially involves the nonreceptor tyrosine kinase Src which phosphorylated PI3 kinase. Inhibition of Src by specific inhibitors prevented eNOS phosphorylation. PI3K activation led to phosphorylation of Akt and MAPK kinase which independently phosphorylated eNOS. Inhibitors of MAPK did not affect HDL-mediated Akt activation and a dominant negative Akt did not affect HDL-mediated MAPK activation and eNOS phosphorylation (*177*). (Fig. 1.12)

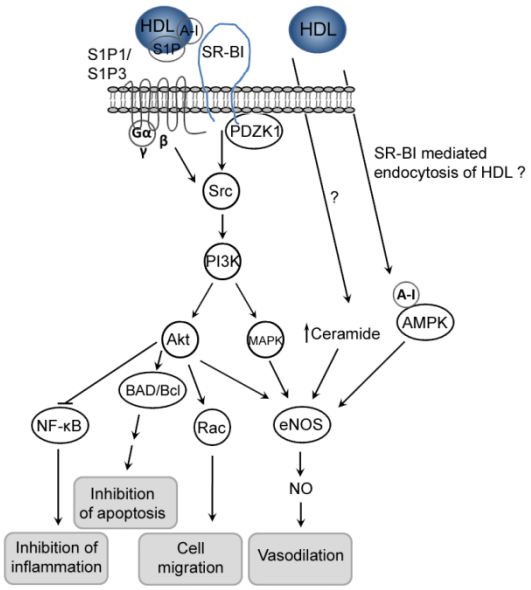

Figure 1.12. Schematic representation of SR-BI signalling that can lead to vasodilation, cell migration and inhibition of inflammation and apoptosis.

The mechanism of the SR-BI mediated activation of eNOS was studied in detail (*264*). HDL and cholesterol-free rHDL particles containing apoA-I and phosphatidylocholine (Lp2A-I) as well as cyclodextrin stimulated eNOS activity whereas rHDL particles that contain cholesterol did not. Blocking of cholesterol efflux with a monoclonal antibody to SR-BI abolished the activation of eNOS. Experiments using SR-BII, a SR-BI mutant that lacks the C-terminal amino acid 509 [SR-BI(Δ509)] and chimeric receptors where the transmembrane domain of SR-BI was replaced by the corresponding domain of CD36 established that the C-terminal cytoplasmic PDZ-interacting domain and the transmembrane domain of SR-BI were both required for HDL-mediated signaling that leads to eNOS activation (*264*). The cytoplasmic PDZ interacting domain of SR-BI binds adaptor proteins such as PDZK1 that may participate

in cell signalling (*265;266*). A photoactive derivative of cholesterol was shown to bind to the transmembrane region of SR-BI indicating that this region serves as a cholesterol sensor on the plasma membrane (*264*).

ApoA-I and lysophospholipids that are components of HDL including sphingosylphosphorylcholine (SPC), sphingosine-1-phospate (S1P) and lysosulphatide cause eNOS dependent relaxation of mouse aortic rings via intracellular Ca^{2+} mobilization and eNOS phosphorylation mediated by Akt (*267*). Another study however, indicated that interactions of HDL with SR-BI stimulate eNOS by increasing intracellular ceramide levels without affecting intracellular calcium levels and Akt phosphorylation (*180*). The proposed role of HDL-associated estradiol in the stimulation of eNOS activity is unclear (*181;268*).

AMPK may also play a role in the HDL-mediated phosphorylation of eNOS at multiple sites (Ser116, Ser635, and Ser1179) (*269*). It was suggested that activation by AMPK may involve physical interactions between the apoA-I component of HDL and eNOS; such interactions may be accomplished following SR-BI mediated endocytosis of HDL (*270*).

HDL also affected the signaling in endothelial cells by the bone morphogenetic protein-4 (BMP-4) and increased expression of the activin-like kinase receptor 1 and 2 (*271*). This resulted in increased expression of VEGF and matrix gla protein (MGP). VEGF promotes endothelial cell survival and MGP prevents vascular calcification and thus contribute to the maintenance, the integrity and the preservation of the functions of the endothelium (*271*) (Fig. 1.13).

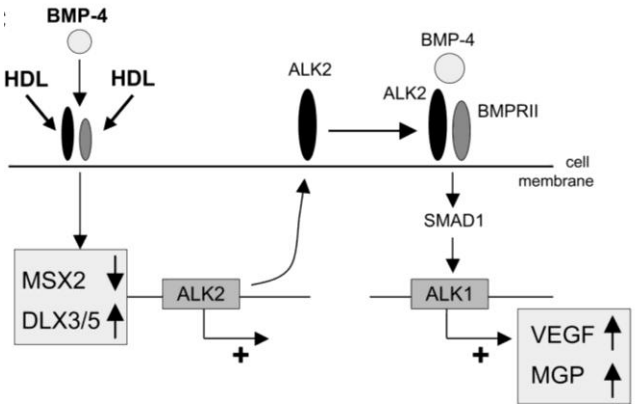

Figure 1.13. Schematic representation of BMP-4 mediated signaling in endothelial cells showing the involvement of HDL in the initiation of the cascade. The increased VEGF and MGP expression lead to endothelial cell survival and prevention of vascular calcification. Obtained from (*271*). BMP-4: Bone morphogenetic protein-4; ALK: Activin like kinase receptor; VEGF: Vascular endothelial growth factor; MGP: Matrix gla protein; MSX2: MSH homeodomain 2; DLX3/5: distal-less homeodomains 3 and 5.

Cell signaling cascades may also originate from interactions of apoA-I with ABCA1. Studies in human fibroblasts showed that binding of lipid free apoA-I to ABCA1 in human fibroblasts initiates signaling events that include the activation of Cdc42 and subsequently the phosphorylation of PAK-1 and (p54)JNK that leads to the polymerization of actin (*272*) (Fig. 1.14). Binding of apoA-I to ABCA1 amplifies the interaction between ABCA1 and Cdc42 (*272*). ABCA1 co-immunoprecipitates with Cdc42 in cells expressing the WT but not the mutant ABCA1 forms and confocal microscopy showed that ABCA1 colocalizes with Cdc42 intracellularly (*273*). However, it is unclear whether the signaling events are initiated through the ABCA1/Cdc42

interactions. Mutations in ABCA1 or inhibition of ABCA1 with glyburide, abrogate this signaling pathway (*272*).

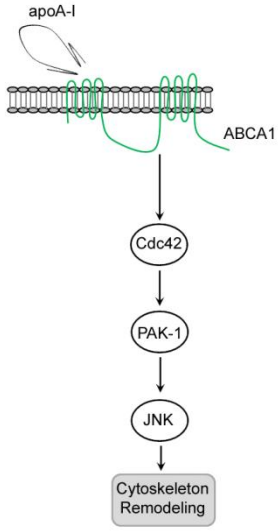

Figure 1.14. Schematic representation of ABCA1 mediated signaling in human fibroblasts showing the involvement of apoA-I in the initiation of the cascade that led to phosphorylation of (p54)JNK and actin polymerization.

1.11.2. Effect of HDL and apoA-I on inflammation

An initial step in the atherosclerotic process is the association of the monocytes to adhesion molecules of the endothelial cells that facilitates their entry in the subendothelial space (*274*). Induction of adhesion molecules is promoted by pro-inflammatory stimuli (*275*). Recruitment and migration of monocytes into subendothelial space is promoted by monocyte chemoattractant factor (MCP-1) as well as by oxidized LDL (*276*). HDL has anti-oxidant properties and can prevent the oxidation of LDL (*277;278*). Interactions of HDL or apoA-I with cells of the vascular wall were shown to

prevent the expression of pro-inflammatory cytokines and chemokines that induce the expression of adhesion molecules (*279-281*). The anti-inflammatory functions of HDL were manifested in several ways.

HDL binds via its apoA-I moiety to progranulin produced by macrophages. This prevents conversion of progranulin to inflammatory granulins which were shown to induce expression of TNFα and IL-β in monocyte macrophages (*282*). HDL and rHDL were shown to inhibit the cytokine induced expression of vascular cell adhesion molecule-1 (VCAM-1) and inter-cellular adhesion molecule-1 (ICAM-1) by endothelial cells (*279*). In addition HDL promoted expression of anti-inflammatory cytokines in endothelial cells. Thus treatment of endothelial cells (HUVEC) with HDL and lysosphingolipids present in HDL increased the expression of TGF-β_2 through mechanisms that involve the activation of Akt and ERK1/2. Consistently with the cell culture studies, the expression of TGF-β_2 and the phosphorylation of ERK1/2, Akt and Smad2/3 were increased in apoA-I transgenic mice and diminished in apoA-I deficient mice (*283*). In vivo studies also showed that infusion of rHDL inhibited the pro-oxidant and pro-inflammatory events that occurred following implantation of non occlusive periarteral collars in rabbits that induce acute arterial inflammation. In these studies the rHDL inhibited neutrofil infiltration, ROS production and VCAM-1, ICAM-1, monocyte chemoattractant protein-1 (MCP-1) and E-selectin expression (*284*). The carotid vascular inflammation and neutrofil infiltration could be inhibited by rHDL containing normal apoA-I but not by apoA-I obtained from diabetic patients (*281*).

The beneficial effects of rHDL containing apoA-I in vivo and in cell cultures could be duplicated using synthetic apoA-I mimetics such as 5A, L37pA and D37pA (*285;286*). The 5A/PLPC complexes reduced the vascular inflammation that is associated with collar insertion in a rabbit model by reducing the ICAM-1 and VCAM-1 expression, the infiltration of neutrofils and the Nox4 activity. In cultures of human carotid endothelial cells (HCEC) 5A/PLPC and rHDL containing apoA-I inhibited the TNF-α induced VCAM-1 and ICAM-1 expression as well as the activation of NF-κB pathway and these effects were abolished by ABCA1 silencing (*285*). Complexes of L37pA or D37pA with POPC reduced the post-ischemic cardiac contractile dysfunction in a rat heart model of ischemia/reperfusion. They also reduced TNF-α levels and increased prostacyclin levels in the perfusate and inhibited the TNF-α mediated VCAM-1 expression in endothelial cell cultures (*286*).

In monocyte and endothelial cell cultures HDL also suppressed expression of chemokines CCL2, CCL5 and CX3CL1 and chemokine receptors CCR2, CCR5 and CX3CR1 (*280;287*). This effect was mediated by inhibition of Iκ-Bα phosphorylation and NF-κB(p65) expression and in some cases by PPARγ activation. Consistently with the cell culture studies in vivo infusion of apoA-I in cholesterol fed apoE deficient mice reduced expression of chemokines and chemokine receptors (*280*).

In cultures of smooth muscle cells HDL downregulated the NADPH-oxidase mediated generation of ROS and inhibited production of MCP-1. The inhibitory effect was attenuated by antagonists of $S1P_1$ and $S1P_3$ receptors. The data showed that free S1P or S3P alone or as components of HDL could attenuate production of MCP-1.

Consistently with these findings MCP-1 production and ROS generation in the aortas of $S1P_3$ receptor and SR-BI$^{-/-}$ mice were not affected by treatment with HDL, S1P and sphingosylphosphorylcholine (SPC) (*287*).

HDL and its protein moiety apoA-I have been shown to inhibit the expression of CD11b of human monocytes that is induced by PMA and promote cell adhesion. Inhibition of the ABCA1-mediated and to a lesser extent SR-BI mediated cholesterol efflux by monoclonal antibodies attenuated the inhibitory effect of apoA-I and HDL respectively. Expression of CD11b was also affected by depletion of the membrane cholesterol by treatment of the cells with cyclodextrin (*288*), pointing out to a potential role of cholesterol efflux in the inhibition of inflammation. Consistently with the ex vivo results, infusion of rHDL in patients with type 2 diabetes mellitus reduced the expression of CD11b of the peripheral monocytes and reduced the adhesion of the patients' neutrophils to a fibrinogen matrix. Plasma HDL isolated 4 to 72 hours post rHDL infusion suppressed the expression of VCAM-1 in cultures of HAECs and had increased ability to promote cholesterol efflux from THP-1 macrophages (*289*).

ApoA-I induced the expression of the adhesion molecule CD31, and changed the morphology and size distribution of lineage negative bone marrow cells. The treatment also increased the ability of the cells to bind to fibronectin and to cultured endothelial cells. Deletion of the C-terminal helix 10 of apoA-I abolished the effects of apoA-I on bone marrow cells (*290*).

ApoA-I/ABCA1 interactions trigger signaling mechanisms that involve JAK2 and STAT3 and result in phosphorylation and translocation of STAT3 to the nucleus and activation of expression of anti-inflammatory genes in endothelial cells (*291;292*).

1.11.3. Effect of HDL and apoA-I on endothelial cell apoptosis

Exposure of endothelial cells to inflammatory stimuli may disturb the endothelial monolayer integrity (*293*). Numerous factors that promote endothelial apoptosis have been described and include OxLDL (*294;295*), TNF-a (*295;296*), homocysteine (*297*), and angiotensin II (*298*). HDL also can reverse the TNF-a induced and growth deprivation induced endothelial cell apoptosis (*299;300*). OxLDL increased intracellular calcium and apoptosis that can be inhibited by HDL (*301*). ApoA-I and HDL inhibit apoptosis and promote proliferation in endothelial cells. ApoA-I interacts with ABCA1 and F1-ATPase (*91;302*), whereas HDL interacts with SR-BI and ABCG1 (*58;152*) and the sphingolipid components of HDL interact with the S1P receptors (*303;304*). These interactions have been implicated in the inhibition of endothelial cell apoptosis.

HDL protected endothelial cells from apoptosis induced by oxLDL by preventing the generation of intracellular ROS. The anti-apoptotic activity was highest for HDL_3 and diminished as the size of HDL increased. It was suggested that approximately 70% of the anti-apoptotic activity of HDL was attributed to apoA-I which has the capacity to accept through its methionine residues the phospholipid hydroperoxides (PLOOH) of oxLDL (*305;306*). The anti-apoptotic functions of small size HDL_3 was reduced by 35% in subjects with metabolic syndrome and this reduction was correlated with the clinical

phenotype of the human subjects. Compared to normal HDL the HDL_3 fractions of the diabetic subjects had increased total triglyceride levels and decreased CE/TG ratio suggesting that the lipid core of HDL_3 was enriched with triglycerides (*307*). HDL_3 also inhibited apoptotic cell death induced by oxLDL and preserved lysosomal integrity of an osteoblastic cell line. The anti-apoptotic effects were attributed to the increased expression of SR-BI that is mediated by HDL_3, combined with the ability of HDL to compete for the binding of oxLDL to osteoblasts as well as increased selective uptake of the cholesterol of the oxLDL by the cells (*308*).

Interaction of apoA-I with cell surface F1-ATPase showed that apoA-I inhibited apoptosis of human umbilical vein endothelial cells (HUVEC) and stimulated cell proliferation (*210;211*). In the absence of apoA-I, specific inhibitors for F1-ATPase (IF_1-H49K) and angiostatin or specific antibodies promoted apoptosis and inhibited cell proliferation. In the presence of apoA-I, the F1-ATPase inhibitors and antibodies diminished its anti-apoptotic and anti-proliferative effects. Down-regulation of the ABCA1 by siRNA did not affect the anti-apoptotic and proliferative functions of apoA-I whereas inhibition of SR-BI by a specific antibody diminished the anti-apoptotic and proliferative functions of HDL_3 (*211*). The findings suggest that interactions of lipid free apoA-I with F1-ATPase and of HDL with SR-BI contribute to their anti-apoptotic and anti-proliferative effects on endothelial cells. The antiapoptotic effects of HDL on endothelial cells could be mimicked by the lysosphingolipid components of HDL (*300*).

SR-BI mediated signaling led to activation of eNOS, promoted cell growth and migration and protected cells from apoptosis (*309;310*). Activation of eNOS required its

localization in the caveolae, where caveolin, SR-BI and CD36 are also found (*311*). It has been proposed that oxLDL acting through CD36 (*312*) depletes the cholesterol content of caveolae and leads to eNOS redistribution to intracellular sites and decrease eNOS activity (*311;312*). HDL acting through SR-BI maintains the concentration of caveolae-associated cholesterol, inhibits the actions of oxLDL and maintains eNOS in the caveolae (*311*). This interpretation implies that strong interactions between eNOS and Cav-1 stimulate eNOS activity.

Other studies provided the opposite mechanism of modulation of eNOS activity by interactions with caveolin (*313*). It was shown that these interactions were enhanced by loading cells with cholesterol or oxysterols and decreased by cholesterol depletion in endothelial cells. HDL diminished the interactions of eNOS with Cav-1 that are caused by cholesterol loading in an ABCG1 depended manner. Studies in murine lung endothelial cells (MLEC) also showed that HDL could reverse the inhibition of eNOS activity caused by cholesterol loading in the normal but not the Cav-1 deficient cells (*313*). It was proposed that diminished interactions between eNOS and Cav-1 caused by ABCG1-mediated efflux stimulated eNOS activity.

It has been shown that oxidized phospholipids uncoupled eNOS activity and led to the generation of $O_2^{\cdot -}$ which activated and induced the expression of sterol regulatory element binding protein (SREBP) and interleukin (IL)-8 (*314;315*). Expression of SR-BI in endothelial cells induced by apoA-I mimetic peptides reverses the impact of OxLDL on the localization and function of eNOS (*179*). It has also been shown that apoA-I

mimetic peptides prevent LDL from uncoupling eNOS activity to favour $O_2^{\cdot -}$ anion production as opposed to normal production of NO (*316-318*).

Finally it has been shown that SR-BI via a highly conserved redox motif CXXS between residues 323-326 can promote a ligand-independed apoptosis via a caspase 8 pathway and this effect could be reversed by HDL and eNOS (*182*). It was proposed that at low HDL levels oxitative stress causes relocation of eNOS away from the caveolae and this results in SR-BI induced apoptosis (*182*).

The picture that emerges from these studies is that HDL promotes survival and migration of endothelial cells by signalling mechanisms that originate from interactions of HDL with SR-BI as well as of interactions of S1P with S1P1 and S1P3 receptors as well as interactions of lipid-free apoA-I with F1-ATPase.

1.11.4. Effect of HDL on endothelial cell proliferation and migration

Damage of the endothelium is associated with vascular disease (*319*) which can be blunted by re-endothelialization (*320;321*). HDL promoted proliferation of human aortic endothelial cells (HUVEC) via mechanisms that increased intracellular Ca^{2+} and upregulated the production of prostacyclin (*322*). HDL also promoted endothelial cell migration (*323*). Migration was promoted by signalling cascades mediated by interaction of S1P with S1P1 and S1P3 receptors that led to the activation of PI3 kinase, p38MAP kinase and Rho kinases (*303*). Another beneficial effect of HDL is its capacity to promote capillary tube formation in vitro. This function is pertussis toxin sensitive and requires p44/42MAP kinase which is downstream of Ras (*324*).

Other studies showed that interaction of SR-BI with HDL or rHDL activated Src kinases and Rac GTPases and stimulated endothelial cell migration in a NO independent fashion (*325*). In vivo experiments have also shown that re-endothelialization of carotid artery following injury is promoted by apoA-I expression and is inhibited by apoA-I deficiency in mice (*325*).

1.11.5. Effect of HDL on thrombosis

Increased HDL cholesterol levels are associated with decreased risk of venous thrombosis (*326*). In contrast low HDL levels are associated with increased risk of venous thrombosis (*327;328*). The ability of HDL to inhibit endothelial cell apoptosis (*293;329*) prevents vessel denudation and formation of microparticles that may contribute to thrombosis (*330-332*). It has been shown that thrombogenic membrane microparticles that may originate from apoptotic endothelial cells are increased in the plasma of patients with acute coronary syndrome (ACS) (*333;334*). Infusion of rHDL in volunteers that received low levels of endotoxin limited the prothrombotic and procoagulant effect of endotoxin (*335*). Furthermore infusion of apoA-I_{MILANO} in a rat model of acute arterial thrombosis increased the time of thrombus formation and decreased the weight of the thrombus (*336*).

HDL may affect thrombosis via a variety of mechanisms. Early studies showed that HDL causes increased synthesis of prostacyclin in cultured endothelial cells (*322;337*). Prostacyclin in combination with NO promote smooth muscle cells relaxation, inhibit platelet activation and local smooth muscle cell proliferation (*338*). The HDL

mediated release of prostacyclin may contribute to the antithrombotic properties of HDL. It has been reported that HDL_3 induced expression of Cox-2 by smooth muscle cells and promoted release of prostacyclin (PGI2) via a signalling pathway that involves p38MAP kinase and N terminal kinase c-Jun (JNK-1) (*339-341*). PGI2 synthesis was enhanced by HMGCoA reduactase inhibitors (*341*).

It has been reported that the oxidized phospholipid components of HDL downregulate the expression of adhesion molecules that are induced by CRP in endothelial cells (*342*). It has been shown that there is a positive correlation between plasma HDL levels and anticoagulant response to activated protein C (APC)/protein S in vitro (*343*) and negative correlation with the plasma thrombin activation markers such as prothrombin fragments F1.2 and D-dimer (*344*). APC inactivates, by proteolysis, factors Va and VIIIa in plasma and thus it can downregulate thrombin formation (*345*). Administration of HDL to cholesterol-fed rabbits increased endothelial cell thrombomodulin levels, promoted generation of APC and inhibited formation of thrombin (*346*). Due to the antiinflammatory properties of thrombomodulin (*347*), the HDL mediated increase in its expression may have important implications for vascular disorders.

It has been shown that glucosylceramide and glycosphingolipids which are present in HDL are lipid cofactors for the anticoagulant activity of APC and in a significant number of patients with venous thrombosis the levels of glucosylceramides are low (*348;349*). Shpingosine, another molecule present in HDL, has been shown to

inhibit prothrombin activation on platelets' surface by disrupting procoagulant interactions between factors Xa and Va (*350*).

HDL can activate the MAPK pathway either through processes that involve PKC, Raf-1, MEK and ERK1/2 or PKC independent pathways that lead to the activation of Ras. These pathways can be inhibited by pertussis toxin and neutralizing antibodies against SR-BI (*351*). The data suggest that interactions of HDL with SR-BI activate Ras in a PKC independent manner and this leads to subsequent activation of MAPK signalling cascade (*351*) (Fig. 1.15).

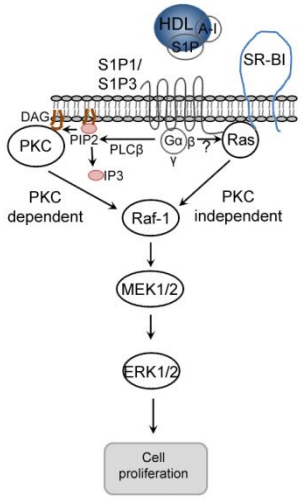

Figure 1.15. Schematic representation of PKC-dependant and SR-BI-dependant signalling pathways that promote cell proliferation.

HDL also downregulated expression of plasminogen activator inhibitor-I (PAI-1) and upregulated tissue plasminogen activator (t-PA) in endothelial cell cultures (*352;353*). In contrast oxidized HDL3 induces the expression of PAI-I in endothelial cells

through signalling mechanisms that involve activation of extracellular signal activated kinases (ERK1/2) and p38MAPK and mRNA stabilization (*354*). It has been shown that transgenic mice expressing the human PAI-1 developed age-dependent coronary arterial thrombosis, demonstrating the involvement of PAI-1 in the pathogenesis of arterial thrombosis (*353*).

1.11.6. Interactions of HDL with platelets

Several pieces of evidence link HDL and proteins related to the HDL pathway with the platelets' functions. Elevated HDL cholesterol inhibited platelet dependent thrombus formation ex vivo (*355*). It has been shown that infusion of rHDL in human subjects suppressed the activation of platelets ex vivo (*356*). HDL may also modify platelet functions indirectly through its actions on endothelial cells. HDL can downregurale the release of platelet activating factor and can also upregulate the synthesis and release of NO from endothelial cells (*177;352*). It has been shown that HDL can limit the generation of thromboxane A2 (TxA2) and can increase the production of prostacyclin (*352*). HDL2 can promote more effectively these antithrombotic effects compared to HDL3 that involve the balance of TxA2/Prostacyclin (*357*).

It has been shown that SR-BI$^{-/-}$ mice are characterized by thrombocytopenia and platelet abnormalities that include high clearance rates, abnormal morphologies and cholesterol content, as well as blunted aggregation response to the ADP agonist but not to protease-activated receptor 4 (PAR4) (thrombin receptor) agonist. When platelets obtained from normal mice were infused into SR-BI$^{-/-}$ mice acquired the characteristics of

the recipient mice 24 hours post infusion (*358*). It was proposed that the structural and functional abnormalities of platelets are a consequence of the increased ratio of unesterified to total cholesterol that exists in the SR-BI$^{-/-}$ mice. These lipid and lipoprotein abnormalities appear to be also responsible for the defective erythrocyte maturation of SR-BI$^{-/-}$ mice (*173*).

A recent study showed that binding of HDL_3 to platelet SR-BI inhibited thrombin-induced platelet aggregation, fibrinogen binding, P-selectin expression as well as mobilization of intracellular Ca^{2+}. Further experiments showed that the interaction involved signaling cascades that led to diacylglycerol production and protein kinase C activation. The involvement of HDL in the activation of PKC was also reported in a previous study (*351*). The responses of platelets to HDL_3 were correlated with the phospatidylserine and phospatidylinositol content of HDL. Platelets lacking SR-BI were not responsive to HDL_3 or phospatidylserine (*359*) (Fig. 1.15).

Patients with type 2 diabetes are characterized by increased platelet aggregation (*360-363*). Infusion of rHDL in diabetic patients reduced the platelet aggregation and response to agonists and resulted in attenuation of platelet function and thrombus formation. The effects could be accounted for by the phospholipid components of rHDL that reduced the cholesterol content of the platelet membranes (*364*).

1.11.7. Effect of HDL on diabetes

In vivo and in vitro studies have provided evidence that HDL may have beneficial effects on glucose metabolism (*365*).

Oral glucose tolerance test in a limited number of patients with Tangier disease (that lack or have dysfunctional ABCA1) showed that they had glucose intolerance as compared to controls (*366*), thus implicating ABCA1, apoA-I and HDL in glucose metabolism.

Cell culture studies using primary pancreatic islets cells and a pancreatic β-cell line (Min6), showed that lipid free apoA-I or apoA-II or reconstituted HDL increased insulin secretion up to 5-fold in a Ca^{2+} dependent manner (*367*). The free apoproteins also increased insulin mRNA levels. HDL mediated secretion in culture has also been observed in cultures of mouse pancreatic β-cells (MIN6N8) (*368*). The increase in insulin secretion mediated by lipid-free apoproteins and rHDL required the functions of ABCA1 and SRBI or ABCG1 respectively. These functions may be different from those involved in cholesterol efflux. For high but not low glucose concentrations enhanced insulin secretion required the action of K_{ATP} channel and glucose catabolism in the pancreatic cell (*367*).

Further insight on the role of ABCA1 in diabetes was obtained by studies in mice with selective deficiency of abca1 in pancreas ($ABCA1^{-P/-P}$). These mice accumulated cholesterol in their islets and were characterized by impaired acute phase insulin secretion and glucose intolerance. The $ABCA1^{-P/-P}$ mice exhibited normal insulin sensitivity indicating normal response of the peripheral tissues to insulin. The impairment in insulin secretion was verified in cell culture experiments using islets isolated from the $ABCA1^{-P/-P}$ mice. In contrast, whole ABCA1 deficient mice had normal glucose

tolerance, displayed only small impairment in the islet function and did not accumulate significant amount of cholesterol in the islets (*369*).

Pancreatic islets isolated from apoE deficient mice also had increased cholesterol content and reduced insulin secretion as compared to islets obtained from WT mice. The reduced insulin secretion in the pancreatic islets or cultures of β-cells could be restored by depletion of the cellular cholesterol using mevastatin or methyl-β-cyclodextrin (MβCD) (*370*). Experiments in cell lines of pancreatic β-cell origin indicated that cholesterol loading or cholesterol depletion affect the activity of glucokinase which is known to regulate insulin secretion (*371*). The experiments showed that under normal cholesterol levels glucokinase is associated with a dimeric form of nNOS on insulin containing granules in the cytoplasm and is inactive (*371*). Increase in plasma cholesterol increased dimerization of nNOS and enhanced its association with GK whereas reduction in the cholesterol levels or increase in the extracellular glucose levels promoted monomerization of nNOS and release of active GK in the cytoplasm (*370*).

The role of the increase in the cholesterol content of β-cells in insulin secretion was tested in transgenic mice expressing SREBP-2 in β-cells under the control of insulin promoter. These mice had normal plasma cholesterol levels but developed severe diabetes characterized by 5-fold increase in gluco-hemoglobin and defects in glucose and potassium-stimulated insulin secretion and were characterized by glucose intolerance. The islets were fewer, smaller and deformed and had increased levels of total and esterified cholesterol (*372*). It was proposed that the loss of β-cell mass could be related

to the down regulation of genes such as PDX-1 and BETA2 that are involved in β-cell differentiation.

Another clinical study showed that the protective functions of HDL can be compromised in type 2 diabetes mellitus and inflammatory diseases and this negative effect can be reversed by appropriate HDL-based therapies. A recent comprehensive study has measured the properties of HDL isolated from patients with type 2 diabetes mellitus and their functions on endothelial cells in vitro and in vivo. HDL isolated from patients with low HDL and type 2 diabetes mellitus contained increased levels of lipid peroxides and increased myeloperoxidase activity. In endothelial cell cultures diabetic HDL had reduced production of NO and increased NADPH oxidase activity that resulted in increased oxidant stress. Diabetic HDL had diminished endothelium dependent relaxation of aortic rings and endothelial progenitor cells obtained from diabetic subjects had diminished capacity to promote reendothelialization in vivo. A remarkable finding in this study was that extended release niacin treatment of the diabetic patients restored the properties and functions of HDL. The HDL obtained after treatment had normal levels of peroxides and normal MPO activity. Studies with endothelial cultures showed that following treatment of the diabetic patients their HDL could induce normal NO production and NADPH oxidase activity and promoted normal relaxation of aortic rings. Progenitor cells obtained from diabetic patients following niacin treatment had normal ability to promote reendothelialization in vivo (*373*).

Intravenous infusion of rHDL (80 mg/kg over 4 hours) in type 2 diabetic human subjects decreased plasma glucose level, increased plasma insulin level and increased β-

cell functions as compared to patients receiving placebo (*368*). HDL and apoA-I increased glucose uptake of primary human skeletal muscle cultures established from patients with type 2 diabetes mellitus. HDL induced glucose uptake and fatty acid oxidation and increased AMPKα2 activity and phosphorylation. These effects were modulated through a Ca^{2+} depended pathway. Subsequent in vitro and in vivo studies showed that rHDL inhibited lipolysis in 3T3-L1 adipocytes partially via activation of AMPK pathway. Infusion of rHDL also inhibited fasting induced lipolysis and fatty acid oxidation but increased the circulating non essential fatty acids possibly due to the action of phospholipase on the rHDL phospholipids (*374*). The HDL depended glucose uptake by the skeletal muscle cells was abrogated by inhibition of ABCA1 with a blocking antibody suggesting that ABCA1 functions not related to cholesterol efflux may contribute to the increased glucose uptake and β-oxidation by skeletal muscle cells obtained from patients with type 2 diabetic mellitus (*374*).

The effect of apoA-I on glucose metabolism was also studied in C2C12 myocytes and apoA-I deficient mice. Consistent with the studies with primary human skeletal muscle cultures, apoA-I stimulated AMPK and Acetyl-CoA carboxylase (ACC) phosphorylation and glucose uptake and endocytosis into C2C12 cells. The apoA-I deficient mice had increased fat content decreased glucose tolerance and increased expression of gluconeogenic enzymes in the liver and decreased AMPK-depended phosphorylation in skeletal muscle and the liver (*375*).

Ex vivo studies showed that HDL and delipidated apoA-I or S1P decreased IL-1β and glucose-mediated apoptosis and thus increased the survival of human and murine

islets. HDL treatment down-regulated the expression of iNOS and its downstream target Fas which is pro-apoptotic and up-regulated the expression of FLIP which is anti-apoptotic (*365*).

HDL can reverse the toxic effects of oxidized LDL on beta cells that are associated with apoptosis and transcriptional repression of the insulin gene and is mediated by c-Jun N-terminal kinase (JNK) (*376*). ApoA-I has been implicated in the control of obesity by controlling energy expenditure and improving insulin sensitivity in apoA-I transgenic mice. In cultures of brown adipocytes apoA-I increased UCP-1 mRNA and protein levels and stimulated AMPK phosphorylation (*377*).

1.11.8. Effect HDL and apoA-I on endothelial progenitor cells

The term endothelial progenitor cells (EPC) applies to a subset of bone marrow derived cells. The identification and characterization of the EPC based on unique surface markers as well as their functions is incomplete (*378*). The lack of strict definition of the EPC requires that these studies are interpreted with caution.

Earlier studies have suggested that important beneficial properties of HDL may be related to its ability to increase the number and improve the functions of endothelial progenitor cells (EPC) (*379;380*). It has been reported that HDL and apoA-I promote the recruitment of endothelial progenitor cells (EPC) to the site of vascular injury and contribute to reendothelialization (*381;382*).

Studies with human subjects showed that increased levels of $CD34^+$ kinase insert domain receptor $(KDR)^+$ in endothelial progenitor cells were predictors of decreased risk

for cardiovascular events and death (*383*). The number of circulating EPC is decreased and their functions are impaired in patients with type 2 diabetes mellitus (*384*). Infusion of rHDL in type 2 diabetic patients increased the number of $CD34^{+}VEGFR\text{-}2^{+}$ EPCs 7 days post-infusion pointing to the possibility of decreasing the cardiovascular risk in these patients with effective HDL raising therapies (*385*).

Injection of rHDL also increased blood flow and capillary density and promoted the incorporation of bone marrow derived cells in the newly-formed capillaries in the ischemic muscle of a murine model of ischemia. The rHDL mediated increase in blood flow recovery was severely impaired in $eNOS^{-/-}$ mice. HDL promoted differentiation of human peripheral mononuclear cells to EPC via a PI3/Akt depended pathway that activates eNOS (*386*) (Fig.1.12) suggesting that eNOS promotes the formation of the new vessels after the hind-limp ischemia.

ApoA-I gene transfer in mice transplanted with $SR\text{-}BI^{+/+}$ bone marrow attenuated graft vasculopathy following paratopic artery transplantation. The beneficial effects of apoA-I gene transfer that increased plasma HDL levels were attributed to the 2-fold increased expression of endothelial progenitor cells that accelerated endothelial regeneration. This effect was abolished in mice that were transplanted with $SR\text{-}BI^{-/-}$ bone marrow (*387*).

1.11.9. Effect of HDL on hematopoietic stem and progenitor cells (HSPCs)

HDL was shown to suppress the proliferation of hematopoietic stem and progenitor cells (HSPCs). It was found that mice double deficient for ABCA1 and ABCG1, fail to

synthesize HDL, develop severe atherosclerosis (*202*). The ABCA1$^{-/-}$ x ABCG1$^{-/-}$ have five-fold increase of HSPC population containing Lin^{-}Sca-1^{+}Kit^{+} (LSK) in the bone marrow and this leads to the development of leukocytosis (*388*). The leukocytosis and myeloproliferative disorder as well as the atherosclerosis were suppressed by transplantation of ABCA1$^{-/-}$ x ABCG1$^{-/-}$ bone marrow in apoA-I transgenic mice that overexpress the human apoA-I. Experiments in cultures of bone marrow LSK cells obtained from mice transplanted with either WT or ABCA1$^{-/-}$ x ABCG1$^{-/-}$ bone marrow showed increased cell proliferation and ERK1/2 phosphorylation in response to IL-3 and GM-CSF treatment. IL-3 or HDL treatment of bone marrow obtained from WT and the Abca1$^{-/-}$ x ABCG1$^{-/-}$ mice showed that IL-3 stimulates and HDL suppresses Ras expression. The expression of IL-3Rβ receptor was attenuated in the bone marrow of apoA-I transgenic mice transplanted with the ABCA1$^{-/-}$ x ABCG1$^{-/-}$ bone marrow as compared to WT recipient mice (*388*). The data are consistent with inhibition by HDL of the cell signaling cascade that originates from interaction of IL-3 receptor with IL-3 and GM-CSF that controls ERK1/2 phosphorylation, Ras expression and cell proliferation. In the absence of HDL the signaling pathway is activated and cell proliferation ensues leading to leukocytosis and atherosclerosis (*388*).

1.11.10. Antibacterial, anti-parasitic and antiviral activity of HDL and apoA-I

ApoA-I has anti-microbial activity against gram positive and gram negative bacteria including fish pathogens (*389;390*).

A collaborative study under review by Dr. Jauhiainen laboratory showed that apoA-I can act as a host defense molecule and contributes to the killing of *Yersinia enterocolitica* (Serotype O:3) by the complement pathway. Moreover, it was shown that the C-terminal domain is the mediator of this effect and specifically an apoA-I mutant carrying the [L218A/L219A/V221A/L222A] mutation was shown to have abolished bactericidal activity. Another C-terminal mutant (E223A/K226A) was able to partially retain its bactericidal activity. It was shown that both HDL associated and lipid-free apoA-I have bactericidal activity. In addition, it was shown that apoA-I did not interact directly with the bacteria surface, instead the association of apoA-I with the bacteria required the exposure of the bacteria to the serum proteins.

ApoA-I neutralizes bacterial toxins such as enterohemolysin (*391*), lipopolysaccharide (LPS), and lipoteichoic acid (*392-396*). These toxins promote inflammatory responses in cell cultures and animal models of inflammation. The human antibacterial and lipopolysaccharide binding protein cathelicidin, hCAP-18, exerts its function by binding to HDL and LDL lipoproteins through its carboxyterminal domain (*397*).

HDL has been shown to suppress expression of genes induced by lipo-polysaccharites in macrophages which regulate type 1 interferon response pathway including interferon-β. This response is controlled by Toll-like receptor 4 and the TRAM/TRIF signaling pathway. Consistently with the cell culture studies infection of apoA-I deficient mice with *Salmonella typhinurium* increased 6-fold the plasma levels of interferon-β (*398*).

The inhibition of anti-inflammatory activity of HDL following streptococcal infections has been attributed to the serum opacity factor, a protein secreted by group A streptococci. Serum opacity factor can bind with high affinity to the protein moieties of HDL (apoA-I, apoA-II). The K(d) for interaction for apo A-I and apoA-II is 6 and 30nm nm respectively. Binding of serum opacity factor removes apoA-I and apoA-II from HDL. This results in the formation of the lipid free apoA-I small discoidal HDL-like particles and the release of CE-rich lipid droplets that causes opacification of serum (*399*).

Humans have developed innate immunity against African trypanosomes which is mediated by apolipoprotein L-I and haptoglobin-related protein (Hpr). These proteins form a complex with a minor subfraction of HDL and IgM/apolipoprotein A-I respectively to generate trypanosome lytic factors TLF1 and TLF2. TLF1 forms a complex with Hpr and hemoglobin (Hb) which bind to the trypanosome haptoglobin (Hp)-Hb receptor and is endocytoced. Following endocytosis, TLF1 goes to the lysosomes where apoL-I is released and is inserted into the lysosomal membrane via its bcl-2 related domain. The pore thus generated triggers efflux of chlorine ions and water into the lysosomes and results in the swelling and lysis of the trypanosomes. TLF2 enters trypanosomes through the same pathway but the mechanism of lysis has not been fully elucidated (*400;401*) (Fig. 1.16). TLF formed in transgenic mice that express apoL-I and Hpr can reduce the pathogen burden and ameliorate the infection by Leishmania parasite (*402*).

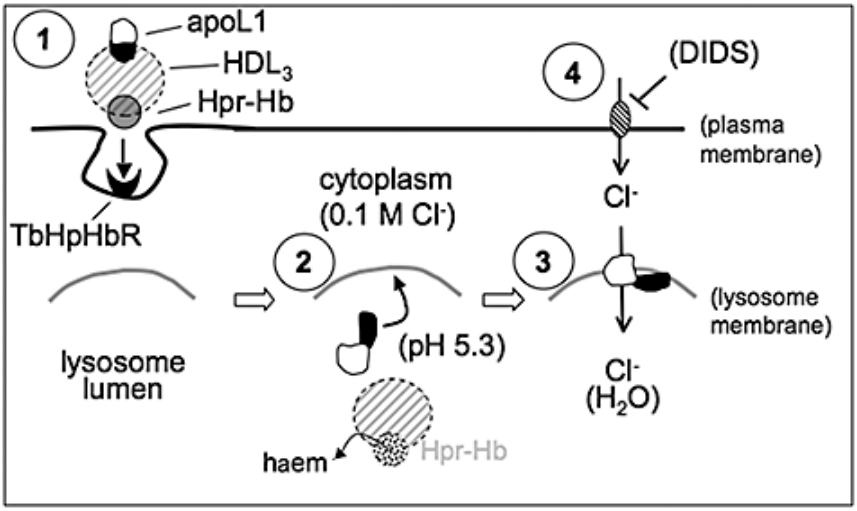

Figure 1.16. Schematic representation of trypanolysis by TLF1. ApoL-I is bound to HDL_3. The HDL_3 particles bind to the TbHpHbR receptors of the trypanosomes. This leads to the uptake of HDL_3 and transfer to lysosome. Upon acidification apoL-I dissociates from HDL and is inserted in the lysosomal membrane. This lead to the formation of pores and the flux of chloride ions and water in the lysosome. As a result the lysosomes undergo uncontrolled osmotic swelling. Obtained from (*401*).

HDL has been also reported to exert antiviral activity through mechanisms that have not been fully elucidated (*403;404*).

1.11.11. Role of HDL-associated proteins in the functions of HDL

Some of the functions of HDL may be mediated by HDL-associated proteins. One of the proteins is paraoxonase-1(PON-1) which is anchored to HDL with its N-terminal Helix H1 and helix H2 (*405;406*). The association of HDL with PON-1 may involve

interactions of π electron rich aromatic residues of PON-1 with K and R residues of apoA-I (*407*). PON-1 deficiency in mice is associated with reduced expression of SR-BI and reduced binding of HDL to mouse peritoneal macrophages (*408*). The expression of SR-BI and the binding to HDL could be corrected by recombinant PON-1 or lysophospatidyl-choline (LPC) through signaling cascades involving ERK1/2 and PI3K (*408*). Deficiency in PON-1 is also associated with reduced serum corticosteroid levels (*409*). A complimentary set of experiments showed that modulation of expression of SR-BI by siRNA in CHO and HepG2 cells decreased the association of PON-1 with HDL and VLDL. Treatment of cells with block lipid transport-1 (BLT-1), which increases the affinity of HDL for SR-BI, increased PON-1 association with HDL and VLDL (*410*). The findings establish a relationship between PON-1 and SR-BI that may contribute to the anti-apoptotic and other functions of HDL (*408-410*).

Platelet-activating factor (PAF) is a lipid mediator produced by endothelial cells in response to injury and induces production of superoxide anions by macrophages (*411;412*). PAF is inactivated by platelet-activating factor acetylhydrolase (PAF-AH) an enzyme that is synthesized by monocytes, macrophages, platelets, spleen and liver cells (*413*) and has anti-inflammatory properties (*414*). In humans PAF-AH is found both in HDL and LDL whereas in mice it is found in HDL only (*415;416*). PAF-AH is thought to contribute to the anti-inflammatory properties of HDL (*414*). Adenovirus mediated gene transfer of PAF-AH reduced by 77% neo-intima formation and by 44% development of atherosclerotic lesions in the aortic root of male but not female mice (*417*).

MPO is a heme protein that is secreted by macrophages (*418*) and uses hydrogen peroxide and chloride to generate hypochlorous acid (*419*). MPO also generates reactive species by catalyzing the reaction of hydrogen peroxide with nitrite (*420;421*). Chlorination but not nitration of apoA-I by MPO inhibits the ABCA-1-apoA-I interaction that leads to cholesterol efflux (*422*).

Myeloperoxidase (MPO) can also bind to HDL in vivo and modify apoA-I by chlorination and nitration of tyrosine residues (*423;424*). MPO-modified HDL or rHDL loses its SR-BI mediated anti-apoptotic and anti-inflammatory properties and gains the ability to bind to a novel unknown receptor. Interaction of MPO-modified HDL with aortic endothelial cells (BAECs) activated NF-κB signaling pathways and led to the expression of pro-inflammatory adhesion molecules (VCAM-1) and reduced eNOS activity. In vitro modifications of all the Met or Tyr or Trp residues of apoA-I did not affect ABCA1 mediated cholesterol efflux from RAW macrophages or VCAM-1 expression in endothelial cells. The properties of MPO-modified mutant apoA-I or rHDL containing these mutants were in general comparable to those of WT apoA-I. These findings suggest that oxidation of these residues does not account for the altered properties of the MPO-oxidized HDL (*425*).

An apoA-I mutant where all tryptophan residues were substituted by phenylalanine retained its ability to promote ABCA1-mediated cholesterol efflux despite modification of apoA-I by MPO at other sites. This finding indicates that MPO modification of tryptophan residues of apoA-I can account for the inhibition of its ability to act as cholesterol acceptor (*426*).

1.12. Genome-wide association studies

Genome wide association (GWA) studies showed that new genes and the corresponding proteins affect plasma HDL levels by unknown mechanisms (*427-435*). In parallel, proteomic analysis showed that a large number of plasma proteins can associate with HDL and this may affect the HDL structure and function. The proteins can be classified in six major categories, and include: proteins involved in lipid, lipoprotein and HDL biogenesis and metabolism, acute phage proteins, protease inhibitors, complement regulatory proteins and few others (albumin, fibrinogen a chain platelet basic protein) (*436;437*). Some representative proteins are shown in Table II.

It has been proposed that the proteinase inhibitors and the acute phase proteins associated with HDL may contribute to its anti-inflammatory properties (*436*) and the complement inhibitors to complement regulation (*438*). Differences were observed in the proteomic composition of HDL subpopulation of different particle size (*439*). Furthermore the HDL proteome could be altered by pharmacological treatments (*440*).

Table II. List of genes identified by GWS that affect HDL plasma levels by unknown mechanisms and HDL related proteins identified by proteomics.

Gene locus	Protein Size (aa)	Function	Effect on HDL level (mg/dL) (*427*)	P-Value (*427*)
MVK	mevalonate kinase 396	Catalyzes an early step in the biosynthesis of cholesterol and isoprenoids. Deficiency causes mevalonic aciduria in humans. Homozygosity for milder MVK mutations causes hyperimmunoglobulinemia syndrome	-0.44	7×10^{-15}
FADS1	fatty acid desaturase 1 501	FADS1 is a rate-limiting enzyme in the synthesis of long chain polyunsaturated fatty acids	-0.73	1.5×10^{-22}
HNF4A	hepatic nuclear factor-4 474	transcription factor member of the orphan nuclear receptor super family	-1.88	1×10^{-15}
ARL15	ADP ribosylation factor like-15 204	member of a family of proteins involved in intracellular vesicle trafficking	-0.49	5×10^{-8}
AMPD3	adenosine monophosphate deaminase 3 767	Converts AMP to IMP	-0.41	5×10^{-8}
LACT B	Lactamase beta 549	A filament-forming protein localized in the mitochondria association with obesity and metabolic disease traits	-0.39	9×10^{-9}
STARD3	StAR-related lipid transfer (START) domain containing 3 445	Endosomal protein involved in lipid trafficking	-0.48	1×10^{-13}
PGS1	phosphatidyl glycerophosphate synthase 1 549	Phospholipid biosynthesis	-0.39	8×10^{-9}
ANGPTL4*	angiopoietin-like 4 406	Serum hormone involved in lipid homeostasis and lipid metabolism. Inhibits apoptosis in vascular endothelial cells	-0.45	3×10^{-8}
GALNT2*	N-acetylgalactosaminyl transferase 2 571	Involved in the O-linked glycosylation of proteins by transferring N-acetylgalactosamine to serine or threonine residues	-0.61	4×10^{-21}
PCYT1A*	Phosphate cytidylyltransferase 1, choline, alpha 367	CTα is the key regulatory enzyme in the CDP-choline pathway for the biosynthesis of phosphatidylcholine	Identified by bioengineered mice	
BMP-1	bone morphogenetic protein 1 202	Bone morphogenetic protein-1 is a protein that converts the 249aa proprotein of apoA-I into the mature apoA-I. It is inhibited by α2-macroglobulin	Identified by cell culture studies	
AAT	alpha-1-antitrypsin 418	Protease inhibitor	Identified by proteomics	
MPO	myeloperoxlase 745	HDL associated protein	Identified by proteomics	
PON1	paraoxonase 355	HDL associated protein	Identified by proteomics	
TTR	transthyretin 127	Serum and cerebrospinal fluid protein that transports holo-retinol-binding protein (RBP; 180250) and thyroxine (summarized by Buxbaum and Reixach, 2009).	Identified by proteomics	

1.13. Role of apoA-I and HDL in atheroprotection

Atherosclerosis is associated with lipid and lipoprotein abnormalities (*274;441*). Patients with coronary heart disease have decreased concentration of the largest size HDL subpopulations (*442-444*). The anti-atherogenic functions of HDL and apoA-I have been partially attributed to their ability to promote efflux from cells (*445*) and promote reverse cholesterol transport via ABCA1, ABCG1 and SR-BI (*200;202*). Hepatic overexpression of the apoA-I gene in the background of apoE or LDL_R deficient mice reduced the atherosclerosis burden of these mice following an atherogenic diet (*446;447*). These findings demonstrate the importance of apoA-I and HDL for atheroprotection. In contrast, double deficient mice for apoA-I and the Ldlr fed an atherogenic diet developed atherosclerosis and had increased concentration of circulating auto-anibodies. The mice were characterized by expanded lymph nodes and increased spleen size and had increased population of T, B, dendritic cells and macrophages, as well as increased T cell proliferation and activation. The abnormal phenotype was corrected by adenovirus mediated gene expression of apoA-I (*448*). Similarly apoA-I transgenic rabbits were resistant to diet induced atherosclerosis (*449*). In contrast, double deficient mice for apoA-I and the Ldlr fed an atherogenic diet developed atherosclerosis and had increased concentration of circulating auto-anibodies. The mice were characterized by expanded lymph nodes and increased spleen size and had increased population of T, B, dendritic cells and macrophages, as well as increased T cell proliferation and activation. The abnormal phenotype was corrected by adenovirus mediated gene expression of apoA-I (*448*). In a clinical trial it was shown that intravenous administration of 15 mg/kg of

apoA-I_{MILANO}/phospholipid complexes in five weekly doses in patients with acute coronary syndrome resulted in significant regression as it was shown by intravascular ultrasound (*450;451*). It was also shown that regression of atherosclerosis was associated with remodelling of the external elastic membrane. As a result the luminal dimensions of the atherosclerotic aortas did not change (*451*). It has been suggested that plasma apoA-I levels should be measured in humans as a component of the assessment of cardiovascular risk (*452*).

High levels of HDL cholesterol are not always correlated with atheroprotection. Human subjects have been identified with high HDL levels and coronary artery disease, thus suggesting that the HDL in these subjects has pro-atherogenic properties (*453*). Also SR-BI-deficient mice have increased levels of HDL but are not protected from diet induced atherosclerosis (*172;186*).

1.14. HDL and apoA-I-based therapies can have beneficial effects in a variety of diseases in humans and experimental animals

1.14.1. Effects of apoA-I in pulmonary fibrosis

Proteomic analysis showed that the apoA-I levels of bronchoalveoral lavage fluids of patients with idiopathic pulmonary fibrosis were significantly lower compared to those obtained from normal control subjects. Further studies in mice with bleomycin-induced fibrosis showed that intranasal treatment with apoA-I reduced the number of inflammatory cells and suppressed fibrosis (*454*), indicating a beneficial effect of apoA-I in pulmonary fibrosis.

1.14.2. Effects of HDL in embolic stroke

HDL was shown to have a neuroprotective effect in rats that underwent embolic occlusion. Intravenous administration of purified HDL immediately or up to 5 hours post embolic stroke reduced cerebral infarct volume and mortality. The beneficial effects of HDL were attributed to the decrease in ICAM-1 positive vessels and reduction in neutrofil recruitment in the infarct area (*455*).

1.14.3. Alteration of HDL properties in renal disease

The anti-oxidant and anti-inflammatory activity of HDL of patients with end-stage renal disease determined by in vitro and cell culture assays is diminished (*456-460*). The properties of HDL obtained from patients with end-stage renal disease can be improved by treatment with the mimetic peptide 4F (*461*).

1.14.4. Effect of HDL and S1P in ischemia/reperfusion injury and endothelial tube formation

HDL and S1P were shown to reduce the damage caused on the myocardium following ischemia/reperfusion injury. Both S1P and HDL reduced apoptosis of the cardiomyocytes in the infract area and in vitro, decreased the number of polymorphonuclear cells in the infarct area and inhibited the adhesion of macrophages to TNF-α activated endothelial cells. The macrophage adhesion and the infract size were depended on the activity of eNOS. The protective effect of HDL and S1P on the infract size was abolished in mice deficient in S1P3R (*462*).

The contribution of S1P in the functions of HDL was also investigated in cell culture experiments. Reconstituted HDL particles containing apoA-I, S1P and POPC as well as HDL, induced proliferation of endothelial cells and promoted cholesterol efflux from RAW264 macrophages. The S1P containing rHDL but not rHDL containing apoA-I and POPC, induced endothelial tube formation through mechanisms that required the phosphorylation of ERK1/2, Akt and the activity of eNOS and $S1P_2$ and $S1P_3$ receptors. In transfected cultures of CHO cells ERK1/2 phosphorylation could be achieved by free S1P and rHDL containing S1P and was also mediated by $S1P_2$ and $S1P_3$ receptors but not by SR-BI (*463*).

1.14.5. Effect of HDL in heart disease

Increase in HDL levels in patients with CAD following a three month niaspan treatment was associated with increased flow mediated dilation of the right brachial artery (*262*). In vivo HDL stimulated myocardial perfusion to similar levels in WT and $S1P_3$ receptor deficient mice indicating the potential involvement of other S1P receptors (*464*).

One study has shown that blood flow responses to endothelium-dependent vasodilators were decreased in patients heterozygous for ABCA1 deficiency and these responses were improved by infusion of rHDL consisting of apoA-I/phosphatidylcholine disks (*465*). Similarly administration of rHDL improved the endothelial functions of hypercholesterolemic men (*466*).

Increase in HDL levels induced by human apoA-I adenovirus-mediated gene transfer in streptozoticin treated rats suppressed the development of diabetic

cardiomyopathy. The increase in plasma apoA-I levels improved left ventricular contractility in vivo and in cardiomyocytes ex vivo. The apoA-I gene transfer reduced oxidative stress as determined by TBARS levels, increased mRNA levels of cardiac and endothelial cell superoxide dismutase (SOD) and increased phosphorylation of p38-MAPK. It also reduced inflammation by reduction of the expression of adhesion molecules ICAM-1, VCAM-1 and of the pro-inflammatory cytokine TNF-α in the left ventricle. Histochemical analyses of the hearts showed reduction of cardiac fibrosis and collagen accumulation that was attributed to the increased phosphorylation of glucogen syntase kinase (GSK). The changes in the caspase 3/7 activity levels and Bcl2/Bax ratio combined with the increased phosphorylation of eNOS indicated reduction in apoptosis and improvement of the endothelial functions in the diabetic rats following gene transfer. The overall findings indicate that increase in HDL levels have beneficial effects and protect from diabetic cardiomyopathy in experimental animal models (*467*).

1.15. Specific aims

ApoA-I is the major protein component of HDL that is required both for the biogenesis, signaling and functions of HDL. ApoA-I also contributes to the overall lipid homeostasis in the circulation and to atheroprotection. Biogenesis and remodeling of HDL are complex pathways that involve apoA-I, ABCA1 and other membrane-bound proteins. Systematic study of naturally occurring and bioengineered apoA-I mutations identified several steps where the pathway of biogenesis and catabolism of HDL is disrupted and may affect HDL synthesis, maturation and stability or may cause dyslipidemia. Despite

the progress that has been made our understanding on the domains and residues of apoA-I that contribute to its numerous important physiological functions remains incomplete.

The broader objectives of my research have been:

1. To determine by gene transfer and in vitro studies crucial domains of apoA-I that may alter the structure and functions of the protein and cause dyslipidemia and correlate of the apoA-I mutants with their physicochemical properties.
2. To determine by gene transfer and in vitro studies crucial domains of apoA-I that may alter its functional interactions with ABCA1 in ways that diminish the biogenesis of HDL and compare the in vivo functions of the apoA-I mutant proteins with their physicochemical properties.

The specific aims of my thesis pertinent to objectives 1 and 2 were:

Specific Aim 1: To investigate the importance of the conserved positively and negatively charged residues present in the 89-99 domain of apoA-I for cholesterol and triglyceride homeostasis and the biogenesis of HDL. The results are presented in Project I.

Specific Aim 2: To investigate the role of four hydrophobic residues (L218, L219, V221, L222) and two charged (E223, K226) on the biogenesis of HDL. The results are presented in Project II

1.16. Significance

Epidemiological and genetic data, combined with transgenic experiments, suggest that increased apoA-I and HDL levels protect from atherosclerosis. In contrast, low apoA-I

and HDL levels predispose humans to CAD, a leading cause for mortality worldwide. In fact, low HDL accounts for 20% of the patients who have suffered from myocardial infarction below the age of 60 years. The studies of this thesis focus on the basic molecular mechanisms which determine the biological functions of apoA-I and HDL that lead to the biogenesis of HDL and are relevant to the development of atherosclerosis.

2. MATERIALS AND METHODS

2.1. Materials

The restriction enzymes, the ligase, the buffers and the DNA polymerases that were used for the construction of plasmids were purchased from New England Biolabs (Ipswich, MA). The dideoxynucleotides (dNTPs) that were used for the polymerase chain reactions (PCR) were purchased from Promega (Madison, WI) and the primers were constructed by Invitrogen (Carlsbad, CA). For the cloning of the mutated forms of apoA-I the plasmid vector pCDNA3.1 from Invitrogen was used. For the apoA-I mutagenesis the QuickChange® II XL Site-Directed Mutagenesis Kit (Agilent Technologies; Santa Clara, CA) was used. The molecular weight marker "1 kb DNA Ladder" for DNA and the Presteained Protein Marker, Broad Range (6-175kDa) for proteins were bought from New England Biolabs; Ipswich, MA. The culture medium Luria Bertani (LB) with or without agar that was used for the solid and liquid cultures of bacteria, respectively, was purchased from American Bioanalytical (Natick, MA). The agarose (Ultrapure Agarose®) was purchased from Invitrogen, also various chemical compounds were bought from Fisher Scientific and Sigma Aldrich. For the DNA isolation in big scale from bacterial culture the High Purity Plasmid Maxiprep System (Origene; Rockville, MD) was used. For the isolation and purification of plasmid DNA fractions up to 10kb from agarose gel I used the Rapid Gel Extraction System bought from Origene. The reagents for reverse transcription and qPCR were purchased from Applied Biosystems (Foster City, CA). The Hybond ECL nitrocellulose membranes were bought from GE Healthcare (Piscataway,

NJ) and the Immobilon™-P polyvinylidene fluoride (PVDF) membranes were bought from Millipore (Billerica, MA). For the detection of proteins by Western I used the enhanced chemiluminescence (ECL) system of GE Healthcare. The materials that were used in the cell cultures and specifically the culture media Dulbecco's Modified Eagles Medium (DMEM), DMEM high glucose and Leibovitz's L-15 (L-15) and HamsF12 medium, the buffer dilution Phosphate Buffered Saline (PBS), the enzyme Trypsin-EDTA as well as the antibiotics Penicillin-Streptomycin 9P/S) were bought from Cellgro (Manassas, VA) whereas the Fetal Bovine Serum (FBS) from Biomeda (Foster City, CA). The acrylamide gels with gradient concentration 4-20% Tris-HCL, IPR COMB were bought from BIO-RAD (Hercules, CA). The column Superose 6 PC 3.2/30 was bought from GE Healthcare. For the Western blotting analyses we used X-Omat LS films (Kodak; Rochester, NY). The [^{3}H]-cholesterol was purchased from Perkin Elmer; Boston, MA. The rest of the chemical compounds that were used were obtained from common commercial sources in the clearest possible form.

2.2. Methods

2.2.1. Generation of mutations on apoA-I gene

The plasmid pCDNA3.1-apoAIg-ΔBglII was used as template for the generation of the mutations on apoA-I gene that we wanted to investigate in this study. For this purpose I used the QuickChange® II XL system that was bought from Agilent Technologies. The template plasmid was generated as it is described in (*140*). Briefly the pUC19-apoAIg plasmid (*468*) was digested with BglII and treated with the Klenow fragment of the DNA

polymerase I to fill the recessed 3′end and ligated in order to eliminate the BglII restricting site. The derivative plasmid, designated pUC19-apoAIg(ΔBglII), was used as a template to amplify by PCR the human apoA-I genomic sequence with two primers carrying the one the XbaI/BglII recognition sites and the EcoRV recognition sites incorporating them to the 5′ and 3′ of the apoA-I genomic sequence, respectively. The product of the PCR was cloned into the pCDNA3.1 vector, resulting in the generation of the vector pCDNA3.1-apoAIg(ΔBglII). The template DNA was incubated with the appropriate primers which are described in Table III. The primers harbor mutations at the center of their sequence and on either side they have the sequence of the nucleotides of the wild type gene. The changes were done in order to obtain the desired amino acid changes in the final protein. The mutagenic primers were constructed according to the guidelines provided by Stratagene.

The mixture of template plasmid and primers was incubated with PfuUltra® polymerase that was provided with the QuickChange®II XL system and dNTPs in a PCR program as described by the manufacturer. After 18 amplification cycles the PCR product was incubated with the restriction enzyme DpnI in order to digest the template plasmid which is methylated or semi-methylated DNA. After the incubation, the newly synthesized DNA which carries the apoA-I mutations was used for the transformation of XL10-Gold® (Agilent Technologies) competent cells (see below). Colonies resistant to ampicillin were selected and grown in mini cultures (see below). DNA was extracted and purified from these cultures, and was sequenced in order to confirm the introduction of the desired mutations. Colonies having the mutation of interest were then used to produce

large quantities of the plasmid (see below). The Maxi Kit manufactured by Origene was used for this plasmid purification. The plasmids that were produced for each mutation were incubated with the restriction enzymes BglII and EcoRV and the generated DNA fragments (2.2 kb) were isolated, following agarose gel electrophoresis (see below), and were ligated (see below) in the corresponding restriction sites, BglII and EcoRV, of the pAdTrack-CMV vector (see below) in order to make the recombinant adenoviruses, according to the AdEasy™ system (Agilent Technologies).

2.2.2. Transformation of bacterial *E.coli* DH5a cells

For the transformation of bacterial cells I transferred 100 μl of DH5a bacterial competent cells and 10 μl of the ligation reaction or 20-100 ng of the plasmid that I wanted to amplify. Cells were incubated on ice for 30 min followed by heat-shock for 45 seconds in a 42^{o}C water bath. The reaction is then placed on ice for 2 minutes. Subsequently, I add 0.9 ml of S.O.C. medium (Invitrogen; Carlsbad, CA) and we incubate in shaker at 225 rpm at 37^{o}C for 1 hour. Then 100 μl of the transformed cells are spread on LB plates with the appropriate antibiotic. The plates are incubated at 37^{o}C for 16-18 hours.

2.2.3. Mini scale preparation (miniprep) for plasmid purification

After bacteria have grown on agar plates overnight, a single colony of bacterial clone is picked and it is transferred in 5 ml of LB broth containing 250 or 500 μg of kanamycin or ampicillin, respectively. The culture is incubated overnight at 37^{o}C in a shaking incubator. The bacteria are centrifuged at 3000 rpm for 10 min. The supernatant is

removed and the pellet is resuspended in 1 ml STE buffer [0.1 M NaCl, 0.01M Tris-HCL pH: 8.0]. The cells are transferred into a 1.5 ml microcentrifuge tube and are centrifuged at 13000 rpm for 30 sec. The supernatant is removed and the cells are resuspended in 200 µl of Cell Suspension Buffer [50 mM Tris-HCl (pH 8.0), 10 mM EDTA, 2 mg RNase A]. Then 400 µl of Cell Lysis Solution [200 mM NaOH, 1% SDS w/v] are added and the cells are incubated on ice for 5 min. The next step is to add the Neutralization Buffer [3.1 M potassium acetate (pH5.5)] and the cells are mixed well. The lysed cells are centrifuged at 13000 rpm for 10 minutes and 500 µl of the supernatant are transferred in to a new tube. Then equal volume of chloroform is added and the contents of the tube are vortexed. The mixture is centrifuged again at 13000 rpm for 5 min and 400 µl of the supernatant are transferred into a new tube. Then 600 µl of isopropanol are added, the contents are mixed well, and the DNA is centrifuged at 13000 rpm for 30 min. The supernatant is then removed and the pellet is left to dry. Finally it is resuspended in 20 µl of ddH_2O.

2.2.4. DNA quantification by UV spectrophotometry

To quantify DNA concentration in solution, ultraviolet spectrophotometry using the Beckman DU530 UV/Vis Spectrophotometer (Beckman; Fullerton, CA) was employed. The following options were selected: nucleic acids, double stranded DNA. A baseline "blank" measurement was made of only water in the quartz optical cuvette of 1 cm path length (Fisher; Agawam, MA) and the program used this value to subtract baseline for further calculations. A known dilution of DNA of unknown concentration was made,

usually 5 µl in 1 ml water, and put in the quartz cuvette and read. The double-stranded DNA program automatically subtracts the baseline value and multiplies by the dilution factor, returning a concentration value. The cuvette was rinsed with water in preparation for the next sample.

2.2.5. Large scale preparation (Maxiprep) for plasmid purification

The "High Purity Plasmid Maxiprep System" produced by Origene was used for the plasmid purification, and the directions provided by the manufacturer were followed. The bacterial cells were pelleted by centrifugation at 4000 rpm for 10 min. The bacterial pellet was resuspended in 10 ml of Cell Suspension Buffer, and lysed by the addition of Cell Lysis Solution. Precipitation of the bacterial proteins was achieved by adding Neutralization Buffer. The mixture was centrifuged at 4000 rpm for 10 minutes and the supernatant was removed and applied on a Marligen column that was previously equilibrated with 30 ml of Equilibration Buffer [600 mM NaCl, 100 mM sodium acetate (pH 5.0), 0.15% Triton® X-100 (v/v)]. The column was washed with 60 ml of Wash Buffer [800 mM NaCl, 100 mM sodium acetate (pH 5.0)], and the DNA was eluted with 15 ml of Elution Buffer [1.25 M NaCl, 100 mM Tris-HCl (pH 8.5)]. The DNA was precipitated by adding 10.5 ml of isopropanol, mixed well and centrifuged at 9000 rpm for 30 minutes. The supernatant was discarded and the DNA was diluted in 300 µl of ddH_2O and transferred to a 1.5 ml microcentrifuge tube. It was finally precipitated with 750 µl of cold (-80°C) ethanol and 30 µl of CH_3COOH 3M (pH 5.5), mixed well and centrifuged at 13000 rpm for 30 minutes. The supernatant was discarded and the pellet

was let to dry. The DNA was then resuspended in 200 μl of TE Buffer [10 mM Tris-HCl (pH 8.0), 0.1 mM EDTA].

2.2.6. Digestion with restriction enzymes

The plasmids and the products of the PCRs that were used for cloning were incubated with restriction enzymes according to the instructions of the manufacturer (New England Biolabs; Ipswich, MA). Most digestions were performed using 15 μg of nucleic acid at 37°C, for 2 hours.

2.2.7. DNA electrophoresis on agarose gel

For the nucleic acid electrophoresis agarose gels of 0.5% to 1% concentration were used. The procedure that was used is the following: In a conical 250 ml flask, 120 ml of TAE 1x (50x TAE; 2M Tris-HCL pH 7.5, 2mM EDTA, acetic acid for pH equilibration) and 1 g agarose are added. The mixture is heated up to boiling point until the agarose is dissolved. When the temperature of the mixture goes down to around 50^{o}C, 7.5 μl of ethidium bromide (10 mg/ml) are added, then the mixture is poured in an appropriate apparatus (cast) and the combs that will form the sample loading wells are placed. When the gel sets it is transferred to a tank that contains 1x TAE buffer. Usually the electrophoresis is performed at 80 Volt (V) and for the isolation of DNA fragments from gel it is performed at 50 V until the samples are efficiently analyzed.

2.2.8. Extraction of DNA from agarose gel

For the extraction of DNA from agarose gel the Gel extraction system (Origene) was used. The band that contained the desired DNA fragment was cut using a clean blade and excised from the agarose gel. The piece of gel was weighted and up to 400 mg were placed in an eppendorf tube. Then for every 10 mg of gel 30 μg of Gel Solubilization Buffer (L1) were added. The gel was solubilized by incubation at 50°C for 15 min. Subsequently the dissolved gel was transferred in a cartilage (provided by the kit) and was centrifuged at 12,000 x g for 1 min. The flowthrough was discarded and the cartilage was washed with an additional 500 μl of L1. The next step was to wash the cartilage with 700 μl of Wash Buffer (L2). The cartilage was further centrifuged an additional minute and then 50 μl of warm TE Buffer were added at the center of the cartilage. It was incubated at RT for 1 min and then collected in a clean eppendorf tube by centrifuging at 12,000 x g for 2 min.

2.2.9. Ligation reaction

The ligation reactions were performed at 16°C, for 16 hours in total volume of 20 μl. The amount of DNA that was used was approximately 200 ng. The reaction had plasmid DNA and DNA of the insert in a ratio of 1:100, T4 DNA ligase and the appropriate buffer according to the manufacturer's (New England Biolabs; Ipswich, MA) instructions.

2.2.10. Transformation of *E.coli* BJ5183-AD1 cells by electroporation

The adenovirus plasmid was generated in BJ-5183-AD1 (Agilent Technologies; Santa Clara, CA) bacterial cells after electroporation in the presence of the pAdTrack-CMV-X vector (where X: the mutated form of apoA-I) that was previously digested with PmeI, according to the instructions of the manufacturer. For the electropotation, 40 μl of BJ-5183-AD1 cells were used for each reaction. These cells have already the pAdEasy-1 plasmid that encodes the genome of adenovirus type 5 except for transcription units E1 and E3 and they also promote the homologous recombination of plasmids. The recombination with the shuttle vector pAdTrack-CMV-X formed finally a plasmid that has the adenoviral genes and the gene that we wanted to study. The electroporation was performed under these conditions: 200 Ω, 2.5 kV, 25 μF using the Bio-Rad Gene Pulser II electroporation machine in 0.2 cm Gene Pulser Cuvettes (Bio-Rad). The cells were plated in agar plates and the correct clones were selected based on their resistance to kanamycin. DNA was purified from the resistant clones and was analyzed on agarose gel. The clones that had the correct recombination gave a 3 or a 4.5 kb band and also had a band at 32 kb after being digested with the restriction enzyme PacI. The positive clones were amplified (DH5a transformation) and were isolated using the High Purity Plasmid Maxiprep System (Origene).

2.2.11. Generation of recombinant adenoviruses

The recombinant vectors for each mutation of apoA-I were incubated with the restriction enzyme PacI in order to get linearized and 10 μg of this DNA were used to transfect 911

cells. For the transfection the Lipofectamin™2000 reagent (Invitrogen; Carlsbad, CA) was used according to the manufacturer's instructions. Ten to twelve days post-transfection the viral particles that were formed caused lysis of the cells and the cell lysate was used for infection of a larger scale culture in a T_{175} flask. The infections were performed in DMEM culture medium with 2% Heat Inactivated Horse Serum (HIHS) and 1% P/S. Two to three days after the new infection the cells were lysed and the new lysate was used for the infection of HEK-293 cells in a larger scale (see below). For this purpose, HEK-293 cells were plated in T_{175} triple flasks and let to grow until the monolayer was confluent. The infection with the previously mentioned lysate was done using L-15 medium with 2% HIHS and 1% P/S. Three days after the infection and before the cells get lysed, large amounts of recombinant viral particles were produced. The cells that carry the produced viral particles were collected with centrifugation at 1000 rpm for 10 minutes. The collected pellet was resuspended in 2 ml of medium and stored at -80^{o}C. Then the suspension was frozen and thawed (-80^{o}C/37^{o}C) three times so the cells would lyse and the viral particles would be released in the medium. The suspension was then centrifuged at 3000 rpm for 10 min. The supernatant that contained the viral particles was subsequently centrifuged in $CsCl_2$ gradient twice in order to isolate the viral particles . For the first centrifugation 2 ml of $CsCl_2$ I (0.619 g/ml in TE) were transferred in a centrifuge tube, they were overlaid with 5 ml of $CsCl_2$ II (0.277 g/ml in TE) and 2-3 ml of the viral particles were placed on top. They were centrifuged at 30,000 rpm for 90 minutes at 4^{o}C. The viral particles were concentrated in a region between the two dilutions. This region was collected with the help of a syringe and was transferred in 12

ml of dilution $CsCl_2$ III (0.450 g/ml in TE). It was centrifuged again at 55,000 rpm at 4^oC for 16-20 hours. The viral particles were concentrated in a small ~2 mm zone. This zone was collected and was dialyzed against sucrose buffer [10 mM Tris-HCL, 2 mM $MgCl_2$, 5% Sucrose, pH; 8] in a Slide-A-Lyzer® molecular weight cut-off (MWCO) 10000 (PIERCE; Rockfor, IL) dialysis cassette. The viral dilution was separated in 50 μl aliquots in 1.5 ml tubes and stored at -80^oC.

2.2.12. Plaque assay

911 cells were plated and grown to a monolayer, and subsequently were infected with serial dilutions of the virus. More specifically the viral particles were diluted $5x10^4$ to $5x10^7$ times in L-15 culture medium supplemented with 2 % HIHS and 1% P/S, and then were used to infect 911 cells that were seeded the previous day in 6-well plates at a concentration of $1.5x10^6$ cells per well. The cells after 20 minutes of incubation with the virus were fixed with culture medium [2x MEM, 4% HIHS, and 25 mM $MgCl_2$] diluted with agar [1.5% agar 40 mM Hepes, pH: 7.4]. The cells were incubated at 37^oC for 10 to 12 days. The plaques of lysis/infection of the cells were visual with naked eye and formed characteristic gray regions, in the case of the viruses we studied there was also expression of green fluorescence protein (GFP) and the plaques could be visualized under an optical microscope with the help of ultraviolet light. The plaques were counted for each dilution and the title of the virus was calculated.

2.2.13. Cell cultures

The cell lines used in these studies were HTB-13 (SW1783, human astrocytes), 911 (human embryonic retinoblasts), HEK-293 (human embryonic kidney), HEK293 EBNA-T and ldlA7 (Chinese hamster ovaries) expressing mouse SR-BI. The stocks of the cultures are kept at -80^{o}C. The cells are placed in 37^{o}C water bath to thaw and then transferred in flasks with culture medium which is replaced the next day. The cells were grown in 25 or 175 cm^{2} flasks or 6 or 24-well plates in a HeraCell, Heraeus incubator (ThermoFisher Scientific; Waltham, MA) in 5% CO_2 at 37^{o}C. The cells were grown in L15 medium for HTB-13 and HEK-293 cell lines, DMEM for 911 cell line or high glucose DMEM for the HEK293 EBNA-T cell line and HamsF12for the ldlA7 cells supplemented with 10% FBS and 1% P/S. The medium in the flasks is replaced every 72 hours. The cells are split when the monolayer is confluent, with the use of trypsin-EDTA, to the desired concentration with the addition of culture medium.

2.2.14. Analyses of expression and secretion of the wild type (WT) and the mutated forms of apoA-I

To estimate the expression and secretion of the various apoA-I forms that were generated (wt and mutant), HTB-13 cells were cultured in 80% confluence in 6-well plates using 2 ml of L-15 medium supplemented with 2% HIHS and 1% P/S. The cells were infected with adenoviruses that express WT apoA-I and its mutant forms with multiplicity of infection (moi) 10, 15, and 20. As moi we define the number of viral particles per cell. Twenty four hours post infection the cells were washed with 1x PBS and were incubated

for 2 hours in medium that did not have any serum. Then new serum-free medium was added. The cells were incubated for 24 hours at 37^{o}C and then the medium was collected. An aliquot of the medium (100 μl) was analyzed by SDS-PAGE (see below) to estimate the expression/secretion of the apoA-I protein. The amount of protein was estimated by analyzing on the same gel a known amount of BSA protein.

2.2.15. SDS-polyacrylamide gel electrophoresis (SDS-PAGE)

In every sample I added the appropriate amount of 4x SDS Loading Buffer [2.5 ml 1M Tris-HCl pH 8, 1.6 ml β-mercaptoethanol, 8 ml 20% SDS, 4 ml glycerol, 8 mg bromophenol blue]. In the experiments I used 14% polyacrylamide gels for the running gel [2.2 ml ddH_2O, 3.5 ml 30% bis-acrylamide, 1.8 ml running buffer (Tris-HCl 1.5 M, SDS 0.4%, pH 8.8), 37 μl 10% ammonium persulfate (APS), 5 μl TEMED] and 4% for the stacking gel [1.8 ml ddH_2O, 0.45 ml 30% bis-acrylamide, 0.75 ml stacking buffer (0.5M Tris-HCL, 0.4% SDS, pH 6.8, 30 μl 10% APS, 3 μl TEMED]. The electrophoreses were performed in 500 ml of 1x TGS dilution [1L 10x TGS : 30.2 g Tris-HCl, 144 g Glycine, 10 g SDS, pH 8.3], at 120 V with the use of Bio-Rad Protean electroblot.

The gels were stained and fixed with Coomasie Brilliant Blue [2.5 g Coomasie Brilliant Blue R, 50 % methanol and 10% acetic acid] for 30 minutes and then destained in destaining solution [50% methanol, 10% acetic acid] for 20 minutes or more in order to obtain a clear image of the protein bands. The gels were dried in a Bio-Rad gel dryer under vacuum at 80^{o}C for 1 hour.

2.2.16. Analysis by Western blotting

The proteins analyzed by SDS-PAGE are transferred to nylon PVDF membranes. Prior to transfer the membranes are incubated first in methanol for 15 s, then in water for 2 min, and finally in transfer buffer [700 ml H_2O, 100 ml 10x TGS and 200 ml methanol] to equilibrate for at least 5 min.

The transfer was performed using Bio-Rad Protean electroblot apparatus in 1L transfer buffer with electrophoresis at 35 V, at 4^oC for 16 hours. After the transfer, the membranes are washed with TBS-T [1x TBS, 0.05% Tween-20], (1L 10x TBS: 90 g NaCl, 0.5M Tris-HCl, pH 7.3) for 10 minutes at room temperature. Then the membranes are incubated with blocking buffer [1x TBS-T, 5% non-fat milk] for 1 hour at room temperature. Then the membranes are incubated for 1 hour at 37^oC with primary antibody specific for the protein we want to detect, that is diluted usually 1:1000 in blocking buffer. The membranes are washed three times for 10 minutes with TBS-T at room temperature. The secondary antibody is applied usually in 1:3000 dilution in blocking buffer. This secondary antibody recognizes the primary and it has also attached to it the enzyme horse radish peroxidase (HRP). The incubation again is for 1 hour at 37^oC. Then we wash 3 times for 10 minutes each time with TBS-T and wash for an additional 5 minutes with TBS at room temperature. The detection of the proteins is accomplished with the ECL system and by exposing the films for different time intervals (usually 30 sec to 2 min were enough).

2.2.17. ApoA-I production

WT and mutant apoA-I proteins were obtained from the culture media of HTB-13 cells grown in roller bottles following infection with adenoviruses expressing the corresponding proteins. For protein production the cells were grown in L-15 medium supplemented with 10% FBS and 1% P/S. The cells of one T175 flask were transferred after trypsinization to one roller bottle which has ~10 times (1700 cm^2) the surface of a T175. The cells were plated evenly and were placed to grow in an Roll In incubator at 37^oC. When cells reached confluency after about 1 week the cells from the initial roller bottle were split into 7 roller bottles and were again grown for about 1½ week. The six roller bottles were used for the production of a protein and the one left was used for making more cells. When cells reached 90% confluency the medium was switched to L-15 supplemented with 2% HIHS, 1% P/S and were infected with apoA-I-expressing adenoviruses at a moi of 20. The next day the medium was switched to serum free L-15 supplemented with P/S. The culture medium was collected for the next six days. At each harvest a 0.5 ml sample form each roller bottle was kept in an eppendorf tube and from this sample 20 μl were analyzed on SDS page to estimate the production of the protein. The collected medium was filtered and stored at -80^oC. For the purification the medium was frozen in Labconco® fast freeze flasks, placed on the lyophilizer and concentrated 5-fold. Then the concentrated media was placed in a 15000 MWCO dialysis tube and dialyzed against 25 mM ammonium bicarbonate at 4^oC. The dialysis media was changed three times and each time the protein was left to dialyze for at least 4 hours. After dialysis the protein was dried by lyophylization.

2.2.18. ApoA-I purification

The lyophilized apoA-I was combined with β-oleoyl-γ-palmitoyl-L-α-phosphatidylcholine (POPC), cholesterol and sodium cholate at a ratio of 1 mg/9.5 mg/0.47 mg/4.5 mg. Briefly POPC was combined with cholesterol and dissolved in chloroform:methanol 2:1. The non-polar solvent was dried under N_2 and the lipids were resuspended in 0.42 ml of salt buffer (150 mM NaCl, 10 mM Tris HCl, 0.01% EDTA). When they were completely dissolved, after approximately 1 h of incubation, sodium cholate was added and the mixture was incubated for an additional hour until the mixture was cleared. Finally, the apoA-I (resuspended in salt buffer at a 2 mg/ml concentration) was added and again the mixture was incubated for 1 h at 4ºC. The proteoliposomes were extensively dialyzed against salt buffer and then were fractionated by density gradient ultracentrifugation and the fractions that contained the pure apoA-I were collected. For the fractionation the proteoliposomes were adjusted with KBr at a density of d= 1.21 g/ml. 13.2 ml of proteoliposomes were overlayed by 6.6 ml of salt buffer with density adjusted at 1.063 g/ml by KBr. The other two layers were 6.6 ml of salt buffer at a density of 1.019 g/ml and 13.2 ml of salt buffer with no KBr added. The samples were centrifuged at 22.5K rpm overnight in a Beckman centrifuge and were separated into 2 ml fractions. The 2 ml fractions were dialyzed against water to remove the KBr and the protein content was assessed by SDS-PAGE analysis and visualization of the protein content by Coomassie staining. Usually the fractions 8-13 from the top of the tube contained the apoA-I protein.

2.2.19. Delipidation (Folch method)

The dialyzed fractions containing the pure protein were pooled and ammonium bicarbonate was added to final concentration 0.05 M. Subsequently, 10 ml were mixed with 38.4 ml of chloroform:methanol (2:1) in 50 ml corex tubes. The tubes were placed on ice for 2 hours and were vortexed several times. The two phases were separated by centrifugation at 3000 rpm for 20 minutes and the non-polar layer was removed carefully using a sterile glass pipette. The mixture was consequently placed under N_2 flow to remove the methanol from the polar phase. When methanol was removed the remaining lipids were extracted again in the same way. Usually after three delipidation cycles proteins were clean of lipids. A sample was obtained and phosphorus and protein content were measured (see below). Then the protein was aliquoted into 0.5 mg samples in sterile microcentrifuge tubes, lyophilized and stored at -80 ^{o}C.

2.2.20. Quantification of protein using DC protein assay

Protein was quantified with a microplate reader using the Bio-Rad DC Protein Assay (Bio-Rad; Hercules, CA), which is based on the procedure of Lowry. 20 μl of Reagent S were mixed with 1 ml of reagent A in a 1.5 ml microcentrifuge tube to make the working reagent A'. 25 μl of working reagent A' was pipetted into each well of a 96-well plate with 5 μl of samples or standard BSA amounts per well. 200 μl of reagent B was added to each well and the plate was mixed briefly. The plate was assayed at 750 nm wavelength. The standards used were dilutions of BSA at concentrations 1.5 mg/ml, 1 mg/ml, 0.6

mg/ml, 0.2 mg/ml and 0 mg/ml (PBS only). A regression of the standards was made and used to calculate concentration of unknown samples from absorbance at 750 nm.

2.2.21. Phosphorus quantification (Bartlett method)

Following at least three delipidation cycles a 30 and a 60 μl sample were used to estimate the lipid content of the pure protein. The estimation was performed by measuring the phosphorus content of the polar phase using the Bartlett method. Samples along with seven standard amounts of phosphorus (0-4 μg) were placed in glass tubes. Half ml of 10N sulfuric acid was added and each tube was covered with a marble. Then all the samples and standards were placed in oven at 150-160ºC overnight to digest the molecules. The next day after the samples were left to cool down, 0.5 ml of 30% H_2O_2 was added and the marbles were placed again over each tube and then returned to the oven for 3 more hours to complete combustion and to decompose the peroxide. After this step 4.6 ml of 0.22 % ammonium molybdate is added in each tube along with 0.2 ml of Fiske and SubbaRow reagent. The mixture is vortexed, the marbles are replaced on each test tube and the samples are heated in boiling water bath for seven minutes. Finally when the samples cool down absorbance at 830 nm is measured.

To estimate the purity of the proteins, the protein/phosphorus ratio was calculated and samples with protein/phosphorous (mg/mg) over 15 were used for the experiments requiring lipid free apoA-I.

2.2.22. LCAT production and purification

LCAT was purified from the culture medium of human HTB13 cells that were infected with an adenovirus expressing the human LCAT cDNA. The cells were grown in roller bottles as described for apoA-I in L-15 medium without phenol red. The production of LCAT was assessed in the medium by Western blotting with an antibody specific for human LCAT. The medium was collected for four days and the protein was purified by chromatography on Phenyl-Sepharose CL-4B column. Prior to loading, the column was equilibrated with 5 mM sodium phosphate, pH 7.4, 0.3M NaCl. The concentration of NaCl of the harvested medium was adjusted to 0.3 M and 450 ml were passed through a 50 ml Phenyl-Sepharose CL-4B column (see below) at a rate of 1.5 ml/min. Subsequently, the column was washed with the equilibration buffer until absorbance at 280 nm was below 0.01. The next step was to elute the LCAT with deionized H_2O at the rate of 1.5 ml/min. Twenty 10 ml fractions were collected and were analyzed by Western blot using an antibody specific for human LCAT. The collected fractions were adjusted to 5 mM sodium phosphate, pH 7.4, 5 mM EDTA and the ones that contained LCAT were concentrated using a Centriplus concentrator (Millipore; Billerica, MA) with a MWCO of 10,000. The concentrated enzyme (~100 μl) was adjusted to 10% glycerol and was divided into single use aliquots of 2 μl and stored at -80°C.

2.2.23. Column preparation for LCAT purification

A 1.6x20cm column was placed in a vertical position and the outlet was closed. The bottle containing Phenyl Sepharose CL-4B (GE Healthcare; Piscataway, NJ) was shaken

well and 70 ml of the suspension were placed in a beaker. After the slurry settled the supernatant was discarded. The slurry was washed 2 more times with 500 ml of water and the supernatant was again discarded. Finally the slurry was reconstituted in 20 ml of 5 mM sodium phosphate, pH 7.4, 0.3M NaCl and was poured into the column in one continued motion down a glass rod held against the wall of the column. When the slurry settled, the adaptor was inserted and adjusted on top of the column and the column was equilibrated with 5 column volumes of 5 mM sodium phosphate, pH7.4, 0.3M NaCl.

2.2.24. LCAT assay

For LCAT analysis, the rHDL particles used as substrate contained cholesterol + [^{3}C]cholesterol ([^{3}C]cholesterol; 0.04 mCi/ml, specific activity 45 mCi/mmol -Perkin Elmer Life Sciences, Inc.; Boston, MA), β-oleoyl-γ-palmitoyl-L-α-phosphatidylcholine (POPC) (Avanti; Alabaster, AL) and apoA-I and were prepared by the sodium cholate dialysis method as described for the apoA-I purification. The main difference was the amount of the reagents used. The molar ratio of POPC/Cholesterol and [^{3}H]Cholesterol/apoA-I/Na-Cholate was 100/10/1/100. The ratio of cholesterol to [^{3}H]cholesterol was around 5:2 and the goal was to obtain 5000-7000 counts per minute per 1 nmole of cholesterol. For the reactions a series of apoA-I amounts (ranging from 1.5 to 32 ng) were combined with 50 μl fatty acid free BSA at 40 mg/ml concentration, 20 μl β-mercapto-ethanol 100 mM, and salt buffer to a final volume of 450 μl. The reactions were placed at 37ºC and after 10 minutes 50 μl of LCAT was added. The LCAT used was a dilution of the concentrated purified enzyme. Usually a 1:10000 dilution was

used. This was calculated by adjusting the dilution so that at 30 minutes, 15 % of the cholesterol of rHDL containing 4 μg of WT apoA-I was converted to cholesterol esters. The reactions were carried on for 30 minutes and then they were terminated by adding 5 ml choloform:methanol 2:1 containing 0.2 mg cholesterol and 0.2 mg cholesteryl oleate. The reactions were let to settle down so that the two phases could separate. The upper, aqueous phase was carefully removed with a glass pipetteand discarded and the lower, non-polar phase that contained the cholesterol was dried under N_2. The dried lipids were solubilized in chloroform and were spotted on ITLC (Pall) paper. They were then developed for 1.5 min in a TLC tank that was presaturated with petroleum ether:ethyl ether:acetic acid at a volume ratio of 85:15:1. The cholesterol was visualized under iodine and the ITLC was cut. The upper band contained the cholesteryl esters that moved faster and the middle the free cholesterol. These two pieces were placed in two scintillation vials containing 10 ml scintillation cocktail ECONOMICAL biodegenerable counting cocktail (Econo-Safe™; Canton, MA) and their radioactivity was measured. The lower band was the oxidized cholesterol that moved even slower and its radioactivity was not assessed. The cholesterol esterification rate was expressed as nanomoles of cholesteryl ester formed per hour. To convert the counts per minute that were recorded by the Beckman LS6500 scintillator to nanomoles the following formula was used:

$$nmol\,CE/hour = CPM_{CE} \times \frac{nmol_{TC}}{CPM_{TC}} \times \frac{1}{0.5\ hours}$$

where $nmol_{TC}$ represents the nanomoles of proteoliposomes cholesterol in the 500 μl reaction, CPM_{CE} the counts per minute of cholesteryl esters and CPM_{TC} represents the combined counts per minute of cholesterol and cholesteryl esters. To calculate the

apparent $Vmax_{app}$ and Km_{app}, the rate of cholesteryl ester formation was plotted versus the concentration of apoA-I. The data were fitted to Michaelis-Menten kinetics, using the Prism software (GraphPad Software, Inc.).

2.2.25. ABCA1 transfection and cholesterol efflux assay

For the ABCA1-mediated cholesterol efflux assay, HEL293-EBNA-T cells were plated in a 24 well plate that was precoated with poly-D-lysine at a $2x10^5$ cells/well concentration. The cells were cultured in antibiotic free high glucose DMEM medium supplemented with 10% FBS. The next day the medium was removed and fresh medium was added (0.5 ml/well). The cells were then transfected with a pcDNA3.1 plasmid expressing ABCA1 or a Mock plasmid. Briefly for each well 1 μg of plasmid DNA was diluted in 50 μl of opti-MEM I (Invitrogen) and 2.5 μl of Lipofectamine 2000 (Invitrogen) was diluted in 50 μl of opti-MEM I. After a 5 min incubation the diluted DNA was combined with the Lipofectamin 2000. Following a 20 min incubation at RT the liposome complexes were added to the cells. The next day the medium was switched to high glucose DMEM/10% heat inactivated FBS supplement with 0.5 μCi [^{3}H]cholesterol/ml. The cells were allowed to load [^{3}H]cholesterol for 24 h. Then the cells were washed twice with warm PBS. Subsequently they were incubated in 0.5 ml of 2 mg/ml fatty-acid free BSA in high glucose DMEM for 1 h. The medium was removed and 0.5 ml of medium containing 2 mg/ml fatty-acid free BSA in high glucose DMEM supplemented with 1 μM apoA-I WT (28 μg/ml) or mutants was added.

Following incubation at 37°C for 4 h, the medium was collected in eppendorf tubes and was centrifuged at 8000prm for 5 min. The next step was to transfer 300 μl of the efflux medium into a scintillation vial containing 10 ml of scintillation fluid, mix and count the radioactivity. As for the calculation of the total cholesterol present in the cells 1 ml of 0.1 M NaOH was added in each well and after incubation for 1 h the lysate was transferred in 10 ml of scintillation fluid and radioactivity was measured. The percentage of efflux was calculated as the counts in the efflux medium divided by the combined counts of the lysate and the efflux medium. The ABCA1-mediated efflux was calculated after subtracting from the ABCA1 transfected cells the efflux of the Mock-transfected cells.

2.2.26. Cholesterol efflux from ldlA7 cells stably transfected with mSR-BI

For the SR-BI-mediated cholesterol efflux assay ldlA7 and ldlA7 cells expressing mSR-BI were plated in 6 well plates at a $2x10^5$ cells/well concentration. The cells were cultured in HamsF12 medium supplemented with 1% P/S and 10% FBS. The next day the medium was removed and fresh HamsF12 medium supplemented with 10% delipidated and heat inactivated fetal calf serum, 1% P/S and [^{3}H]-cholesterol at a concentration 1μCi/ml (2ml/well). On day 3 the cells were washed with HamsF12 medium and then equilibrated in HamsF12 medium supplemented with 1% fatty acid free BSA and 1% P/S. Four days after the cells were plated the cells were washed with HamsF12 medium and incubated in fresh HamsF12, 1% P/S medium for 45 minutes. Then the efflux medium was added. The efflux medium contained HamsF12 medium, 1%

P/S, 10mM Hepes, pH 7. Additionally the acceptor lipid particles were added at a protein concentration of 1 μM of protein.

Following incubation at 37°C for 4 h, the medium was collected in eppendorf tubes and was centrifuged at 8000prm for 5 min. The next step was to transfer 50 μl of the efflux medium in a scintillation vial containing 10 ml of scintillation fluid, mix and count the radioactivity. As for the calculation of the total cholesterol present in the cells 0.8 ml of 0.1% Triton were added in each well and after a 20 min incubation, 50 μl of the lysate were transferred in 10 ml of scintillation fluid and radioactivity was measured. The percentage of efflux was calculated as the counts in the efflux medium divided by the combined counts in the lysate and the efflux medium. The SR-BI mediated efflux was calculated after subtracting the efflux of the untransfected ldlA7 cells from the efflux of ldlA7-mSR-BI cells.

2.2.27. Animal studies

ApoA-I$^{-/-}$ (ApoA-I^{tm1Unc}) C57BL/6J mice (3) were purchased from Jackson Laboratories (Bar Harbor, ME). The mice were maintained on a 12 h light/dark cycle and standard rodent chow diet. All procedures performed on the mice were in accordance with National Institutes of Health and institutional guidelines. Four to six male apoA-I $^{-/-}$ mice 6-8 weeks old were injected via tail vein with 1-2.5 x 10^9 pfu of recombinant adenovirus per animal and the animals were sacrificed 4 days post-injection following a 4 h fast.

2.2.28. Plasma isolation from mice blood

For the collection of blood sample and the subsequent plasma isolation from the mouse vein we used the Microvette CB 300 K2E (STARSTEDT) tubes. For the collection of larger volume of blood before the sacrifice of the animals we used Microtube 1.3 ml KE microcentrifuge tubes. From each mouse around 750 μl of blood were collected. Then the samples were centrifuged at 3500 rpm for 10 min and the plasma was separated. The plasma was transferred in a new microcentrifuge tube and was stored at 4^{o}C until further analyses were performed.

2.2.29. Plasma lipid levels

The concentration of total cholesterol, free cholesterol, triglycerides, phospholipids and apoA-I of plasma drawn 4 days post-infection was determined using the cholesterol E, free cholesterol C, Phospholipids C reagents, apoA-I (Wako Chemicals USA, Inc.) and Infinity^{TM} Triglycerides (ThermoScientific; Middletown, VA) respectively, according to the manufacturer's instructions. The concentration of cholesteryl esters was determined by subtracting the concentration of free cholesterol from the concentration of total cholesterol.

2.2.30. Fast protein liquid chromatography (FPLC)

For the analysis of plasma with FPLC 17 μl of plasma were used. The plasma obtained from mice infected with adenovirus-expressing WT or mutant apoA-I forms was loaded onto a Sepharose 6 PC column in a SMART microFPLC system (Amersham

Biosciences) and eluted with PBS. A total of 25 fractions of 50 µl volume each were collected for further analysis using the following program.

```
0.00 FLOW                50.0
0.00 CON_B               100.0
0.00 LOOP                1
0.00 FILL                B, 2, 10, 15000
0.20 INJECT
0.90 NEEDLE_POSITION     DOWN
0.90 GOTO_TUBE           1
0.90 FRACTION_SIZE       50
2.15 FRAC_STOP
2.15 FLOW                75
3.15 LOAD
3.15 NEW_CHROMATOGRAM
3.15 END_LOOP
```

The concentration of lipids in the FPLC fractions was determined as described above.

2.2.31. Fractionation of plasma by density gradient ultracentrifugation

For this analysis, 300 µl of plasma obtained from adenovirus-infected mice was diluted with saline to a total volume of 0.5 ml. The mixture was adjusted to a density of 1.23 g/ml with KBr and overlaid with 1 ml of KBr solution of d = 1.21 g/ml, 2.5 ml of KBr solution of d = 1.063 g/ml, 0.5 ml of KBr solution of d = 1.019 g/ml, and 0.5 ml of normal saline. The mixture was centrifuged for 22 h in SW55 rotor at 30000 rpm. Following ultracentrifugation, 0.5 ml fractions were collected from the top for further analyses. The refractive index of the fractions was measured using a refractometer

(American Optical Corp.) and it was converted to density for each sample based on a standard curve derived from solutions of known densities. The fractions were dialyzed against ammonium acetate and carbonate buffer (126 mM ammonium acetate, 2.6 mM ammonium carbonate, 0.26 mM EDTA, pH 7.4). Aliquots of the fractions were subjected to SDS-PAGE, and the protein bands were visualized by staining with Coomassie Brilliant Blue.

2.2.32. Electron microscopy (EM) analysis of the apoA-I containing fractions

For EM analysis, fractions 6-8 that float in the HDL ($1.100\ g/ml \leq d \leq 1.152\ gr/ml$) region were dialyzed against ammonium acetate and carbonate buffer. The samples were applied on carbon-coated grids, were stained with sodium phosphotungstate, were visualized in the Philips CM-120 electron microscope (Philips Electron Optics, Eindhoven, Netherlands) and photographed; these procedures were performed by Dr. Donald Gantz at the Department of Biophysics of Boston University. The photographs have been magnified 225,000 times.

2.2.33. Non-denaturing two-dimensional (2D) gel electrophoresis

The distribution of HDL subfractions in plasma was analyzed by 2D electrophoresis as described by Fielding and Fielding 1996 with some modifications. In the first dimension, 0.5 to 1 μl of plasma sample was separated by electrophoresis at $4^{o}C$ in a 0.75% agarose gel using a 50 mM barbital buffer (pH 8.6, Sigma, St Louis, MO) until the bromophenol blue marker had migrated 5.5 cm. Agarose gel strips containing the separated lipoproteins

were then transferred to a 4-20% polyacrylamide gradient gel. Separation in the second dimension was performed at 90 V for 2-3 h at 4^{o}C using non-denaturing 1x TGS buffer [1l 10x TGS: 30.2g Tris-HCl, 144g Glycine]. The proteins were transferred to a nitrocellulose membrane and apoA-I was detected by using the goat polyclonal anti-human apoA-I antibody AB740 (Chemicon International) in a 1:1000 dilution.

2.2.34. RNA isolation

Total cellular RNA was isolated from the mouse liver using the Trizol® procedure (Invitrogen Corp.) as recommended by the manufacturer. More specifically approximately 5 mm^3 of hepatic tissue and 1 ml of Trizol® were used. The tissue was homogenized for 30s in Minibeadbeater homogenizer (Biospec Products). The sample was extracted with 100 μl of chloroform and the sample was homogenized for 10 sec. The RNA was isolated in the aqueous phase after centrifugation at 13000 rpm for 15 minutes. The aqueous phase was then transferred to a new microcentrifuge tube and was precipitated with equal volume of isopropanol and centrifugation at 13000 rpm for 20 min. Finally the RNA was reconstituted in DEPC (Diethylpyrocarbonate) treated water. Pellet dissolution was promoted by heating the tube at 65 ^{o}C for 7 minutes. After measuring its concentration, RNA was stored at -80 ^{o}C.

2.2.35. Quantification of RNA by UV spectrophotometry

The RNA concentration was measured using the Beckman DU530 UV/Vis Spectrophotometer. The program “single-stranded RNA” that measures optical density at

260 nm was selected and the dilution factor was set at 250. A quartz optical cuvette of 1 cm path length was used for all the measurements. The baseline was obtained by measuring only water and setting that measurement as "blank". RNA was diluted into water (4 µl RNA into 1 ml water), was placed in the cuvette and its absorption was measured. The RNA program then subtracts the base line value and returns the concentration value.

2.2.36. Synthesis of cDNA from RNA

RNA samples were adjusted to 0.1 µg/µl. One microgram of RNA was used to make complementary DNA (cDNA) using the high capacity cDNA Reverse transcription Kit (Applied Biosystems, Foster City, CA, USA), according to the manufacturer's instructions. Briefly 1 µl of 0.5 µM 18S-RNA-specific primer (5'-GAGCTGGAATTACCG CGGCT-3') and 1 µl of 50 µM oligo-$(dT)_{16}$ primer (Applied Biosystems, Foster City, CA, USA) were combined with 10 µl of RNA (1 µg), 2 µl of 10X reaction buffer, 0.8 µl of 25x dNTP mix (100mM), 1 µl of RNase inhibitor, 1 µl of MultiScribe™ Reverse Transcriptase (50 U/µl) and 3.2 µl of nuclease-free water (Integrated DNA technologies, Inc.) to a final reaction volume of 20 µl. The reactions were subjected to a four-step program according to the manufacturer's instructions. They were incubated at 25 ^{o}C for 10 min, then incubated at 37 ^{o}C for 120 min, then at 85 ^{o}C for 5 min and finally the samples were placed at 4^{o}C.

2.2.37. Quantitative Real Time PCR (qPCR) using TaqMan probe/primer sets

QPCR was carried out in a 96-well plate in 20 µl reaction volume containing 10 µl of TaqMan® Gene expression PCR Master Mix (Applied Biosystems, Foster City, CA, Cat# 4370048), 0.5 µl of apo A-I Applied Biosystems Gene Array TaqMan® primers (Applied Biosystems, Foster City, CA, Cat# Hs00985000_g1), 0.5 µl of 18s rRNA (Cat# 4319413E), 1 µl of 1:1000 diluted cDNA template and 8 µl nuclease-free water (Integrated DNA technologies, Inc.). All qPCR reactions were performed using the Applied Biosystems 7300 Real-Time PCR System (Applied Biosystems, Foster City, CA, USA). Triplicate reactions of each sample were incubated for 2 min at 50^{o}C, denaturated at 95 ^{o}C for 10 min and subjected to 40 cycles of denaturation at 95 ^{o}C for 15 s with annealing/extension at 60 ^{o}C for 1 min (standard two-step cycling program). After running the relative values were calculated using the ddCt method (SDS v2.3 Applied Biosystems, Foster City, CA, USA).

2.3. Biophysical studies

2.3.1. Preparation of apoA-I for physicochemical measurements

Several days prior to the physicochemical analyses, the lyophilized proteins were dissolved in 4M guanidine hydrochloride (GndHCl) and then refolded by subsequent dialysis against 2.5 M and 1.25 M GndHCl solutions in PBS, followed by extensive dialysis against the appropriate buffer (10 mM sodium phosphate, pH 7.4, for circular dichroism (CD) experiments or PBS for fluorescent and dimyristoyl-L-α-phosphatidylcholine (DMPC) clearance measurements).

2.3.2. Secondary structure and thermal unfolding of apoA-I forms

CD-measurements were performed on an AVIV 62DS or AVIV 215 spectropolarimeter (AVIV Associates, Inc.; Lakewood, NJ) equipped with a thermoelectric temperature control and calibrated with d-10-camphor sulfonic acid, in 2 or 5 mm path length quartz cuvettes. Far-UV CD spectra were recorded at protein concentration 20-55 μg/mL as described previously (*33;469*). Thermal unfolding of apoA-I in solution was monitored by changes in ellipticity at 222 nm. For each protein, spectra were recorded at several protein concentrations, then normalized to the protein concentration and expressed as mean residue ellipticity $[\Theta] = [\Theta_{222}] \times MRW/(10 \times l \times c)$ where $[\Theta_{222}]$ is the measured ellipticity, MRW is the mean residue weight (about 115), l is the cell path length (cm) and c is the protein concentration (g/ml). The α-helix content was estimated from the mean residue ellipticity at 222 nm, $[\Theta_{222}]$. The thermodynamic parameters of the transitions, melting temperature, T_m, and van't Hoff enthalpy, ΔH_v, were determined from the van't Hoff analysis of the melting curves as described previously (*33;469*).

2.3.3. 8-anilino-1-naphthalene-sulfonate (ANS) fluorescence measurements

Fluorescence emission spectra were collected on a FluoroMax-2 fluorescence spectrometer (Instruments S.A., Inc.; Edison, NJ) as previously described (*470*). Fluorescence of ANS was recorded in PBS buffer at ANS concentration of 125 μM in the presence or absence of 25 μg/mL WT apoA-I or the mutant apoA-I forms. For comparison, 25 μg/ml of carbonic anhydrase were used as a "reference" for a globular water-soluble protein. The wavelength of maximum fluorescence (WMF) and intensity of

fluorescence emission at WMF were determined from each spectra after subtraction of the buffer base line.

2.3.4. DMPC clearance studies

The solubilization of DMPC multilamellar vesicles by apoA-I was monitored by the decrease in absorbance at 325 nm following the administration of apoA-I to a suspension of DMPC in PBS as described previously (*471*). The experiment was performed four times with proteins from different preparations and was reproducible.

2.3.5. Binding of WT and mutant apoA-I to triglyceride-rich emulsion particles

Triglyceride-rich emulsions were prepared as described (*471;472*). The particles were analyzed for phospholipids and triglyceride content and by electron microscopy to determine their morphology and size and were used for apoA-I binding assays within 2 days. For these assays, 120 µg of WT and mutant apoA-I (freshly dialyzed) were incubated for 1h at 27°C using increasing amounts of emulsion in 1.8 ml of Tris buffer to give a phosphatidylcholine to protein molar ratio ranging from 180 to 710. The apoA-I bound to the emulsions was recovered by ultracentrifugation and quantitated as described (*471*). Experiments were performed 3 to 4 times using emulsions from three different preparations.

3. RESULTS

The results are divided in sections 3.1, 3.2, 3.3, 3.4 and 3.5. Section 3.1 deals with plasmid construction, generation and validation of recombinant adenoviruses, section 3.2 with functional in vitro studies and section 3.4 with physicochemical studies. These sections are common to project I and project II that are presented in the abstract and the discussion. Sections 3.3 deals with the in vivo functions of apoA-I[D89A/E91A/E92A] and apoA-I[K94A/K96A] mutants and 3.5 deals with the in vivo functions of apoA-I[L218A/L219A/V221A/L222A] and apoA-I[K223A/K226A] mutants designated as Project I and Project II in the abstract and the discussion.

3.1. Plasmid construction and generation of recombinant adenoviruses that express naturally occurring mutated forms of apoA-I

3.1.1. Plasmid construction and cloning of the WT and mutant apoA-I genes into the adenovirus shuttle vector

ApoA-I mutants were generated by site-directed mutagenesis using the primers described in Table III and the plasmid pCDNA3.1apoA-IWTΔBglII (Fig. 3.1) was used as a template employing the QuickChange® II XL mutagenesis kit. In the case of apoA-I [L218A/L219A/V221A/L222A/F225A/V227A/F229A/L230A] mutant the template was pCDNA3.1apoA-I[L218A/L219A/V221A/L222A]. The template plasmid DNA was incubated with the appropriate primers, PfuUltra® polymerase, and dNTPs. Following a 18-cycle PCR reaction the DNA product was digested with DpnI to eliminate the

template plasmid. Cells provided by Stratagene (XL10-Gold®) were then transformed with the PCR product and ten colonies resistant to ampicillin were selected for each mutation. DNA was extracted from these colonies and was sequenced at the Core Facility of Tufts University. DH5a bacterial cells were transformed with the positive clones and plasmid DNA was generated by large scale plasmid preparation. The DNA plasmids were digested with BglII and EcoRV and the digest was analysed on 1% agarose gel (Fig. 3.2 A).

A 2.2 kb band corresponding to the apoA-I gene, was extracted from the gel and then it was ligated to the shuttle vector pAdTrack-CMV that was previously linearized with the same restriction enzymes (Fig. 3.2A right lane). This ligation was designed to generate the pAdTrackCMVapoA-I vectors (Fig. 3.1) that were used to create by homologous recombination the recombinant apoA-I expressing adenoviruses that are described later. Successful cloning of the apoA-I gene into the pAdTrackCMV vector was confirmed by digestion with BglII and EcoRV that releases a 2.2 kb fragment that corresponds to apoA-I gene and a ~10 kb fragment that corresponds to the pAdTrackCMV vector (Fig. 3.2B).

Table III. Nucleotide sequence of primers used in PCR amplifications

Name	Sequence	Location of sequence
apoA-I [D89A/E91A/E92A]F	5´-G GAG ATG AGC AAG G**C**[a]T CTG G**C**G G**C**G GTG AAG GCC AAG G-3´	nt 359-396[b] (sense) (aminoacids +84 to +97)[c]
apoA-I [D89A/E91A/E92A]R	5´-C CTT GGC CTT CAC C**G**C C**G**C CAG A**G**C CTT GCT CAT CTC C-3´	nt 396-359 (antisense) (aminoacids +97 to +84)
apoA-I [K94A/K96A]F	5´-G GAT CTG GAG GAG GTG **GC**G GCC **GC**G GTG CAG CCC TAC CTG-3´	nt 371-410 (sense) (aminoacids +88 to +102)
apoA-I [K94A/K96A]R	5´-CAG GTA GGG CTG CAC C**GC** GGC C**GC** CAC CTC CTC CAG ATC C-3´	nt 410-371 (antisense) (aminoacids +102 to +88)
apoA-I [L218A/L219A/ V221A/L222A]F	5´- G GAC CTC CGC CAA GGC **GC**G **GC**G CCC G**C**G **GC**G GAG AGC TTC AAG GTC -3´	nt 743-788 (sense) (aminoacids +212 to +227)
apoA-I [L218A/L219A/ V221A/L222A]R	5´- GAC CTT GAA GCT CTC C**GC** C**G**C GGG C**GC** C**GC** GCC TTG GCG GAG GTC C -3´	nt 788-743 (antisense) (aminoacids +227 to +212)
apoA-I [F225A/V227A/ F229A/L230A]F	5´- G CCC GTG CTG GAG AGC **GC**C AAG G**C**C AGC **GC**C **GC**G AGC GCT CTC GAG GAG-3'	nt 764-812 (sense) (aminoacids +219 to +235)
apoA-I [F225A/V227A/ F229A/L230A]R	5´- CTC CTC GAG AGC GCT C**GC** G**GC** GCT G**G**C CTT G**GC** GCT CTC CAG CAC GGG C-3'	nt 812-764 (antisense) (aminoacids +235 to +219)
apoA-I [E223A/K226A]R	5´- CTG CCC GTG CTG G**C**G AGC TTC **GC**G GTC AGC TTC CTG-3'	nt 762-797 (sense) (aminoacids +219 to +230)
apoA-I [E223A/K226A]R	5´- CAG GAA GCT GAC C**GC** GAA GCT C**G**C CAG CAC GGG CAG-3'	nt 797-762 (antisense) (aminoacids +230 to +219)
apoA-I [F71A/W72A]F	5'- GGC CCT GTG ACC CAG GAG **GC**C GCG GAT AAC CTG GAA AAG GA-3'	nt 300-340 (sense) (aminoacids +65 to +78)
apoA-I [F71A/W72A]R	5'- TC CTT TTC CAG GTT ATC CGC G**GC** CTC CTG GGT CAC AGG GCC-3'	nt 340-300 (antisense) (aminoacids +78 to +65)
[d]apoA-I [L218A/L219A/ V221A/L222A/F225A/ V227A/F229A/L230A]F	5'- CCC GCG GCG GAG AGC **GC**C AAG G**C**C AGC **GC**C **GC**G AGC GCT CTC GAG GA -3'	nt 765-811 (sense) (aminoacids +220 to +235)
apoA-I [L218A/L219A/ V221A/L222A/F225A/ V227A/F229A/L230A]R	5'- TC CTC GAG AGC GCT C**GC** G**GC** GCT G**G**C CTT G**GC** GCT CTC CAG CAC GGG-3'	nt 811-765 (antisense) (aminoacids +235 to +220)

[a]Mutagenized residues are marked in boldface type and are underlined.
[b]Nucleotide number of the human apoA-I cDNA sequence, oligonucleotide position relative to the translation initiation ATG condon.
[c]Aminoacid position (+) refers to the mature plasma apoA-I sequence.
[d]For the generation of this mutant the template used was pCDNA3.1apoA-IWTΔBglII containing the L218A/L219A/V221A/L222A substitutions in the apoA-I gene.

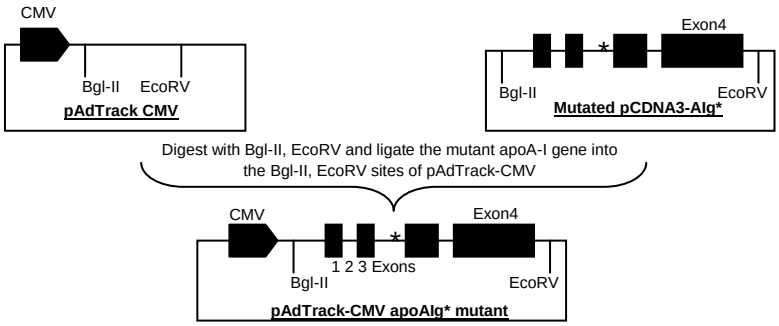

Figure 3.1: Schematic representation of the cloning strategies for the construction of the recombinant adenoviruses expressing WT and mutant apoA-I forms. * indicates elimination of the BglII site.

3.1.2. Generation, amplification, isolation and titration of the recombinant adenoviruses

For the generation of the recombinant adenoviruses that express the mutated forms of apoA-I the system pAdEasy® was used as described in materials and methods. The pAdTrackCMVapoA-I vector was linearized with PmeI and was used to transform by electroporation electro-competent cells containing the pAdEasy-1 plasmid. A number of colonies resistant to kanamycin were selected and DNA was extracted as described in materials and methods and digested with PacI to find positive clones that produce a 3 or 4.5 kb band (Fig. 3.2C). The DNA obtained from positive clones was then transformed to DH5a competent cells and large amount of plasmid DNA was isolated and purified (Fig. 3.3). The DNA was linearized with PacI and used to transfect by Lipofectamine™ 2000 911 cells in a T_{25} flask. Cells were lysed after 10 to 12 days and the lysate was used to infect HEK293 cells initially grown in T_{175} flasks and lysates obtained from theses flasks five to six days post-infection were used to infect HEK293 grown in ten triple T_{175} flasks. Cell extracts obtained from the triple flasks were then purified by two consecutive CsCl gradient ultracentrifugations. The titers of the viruses were estimated with plaque assay as described in materials and methods (Table IV).

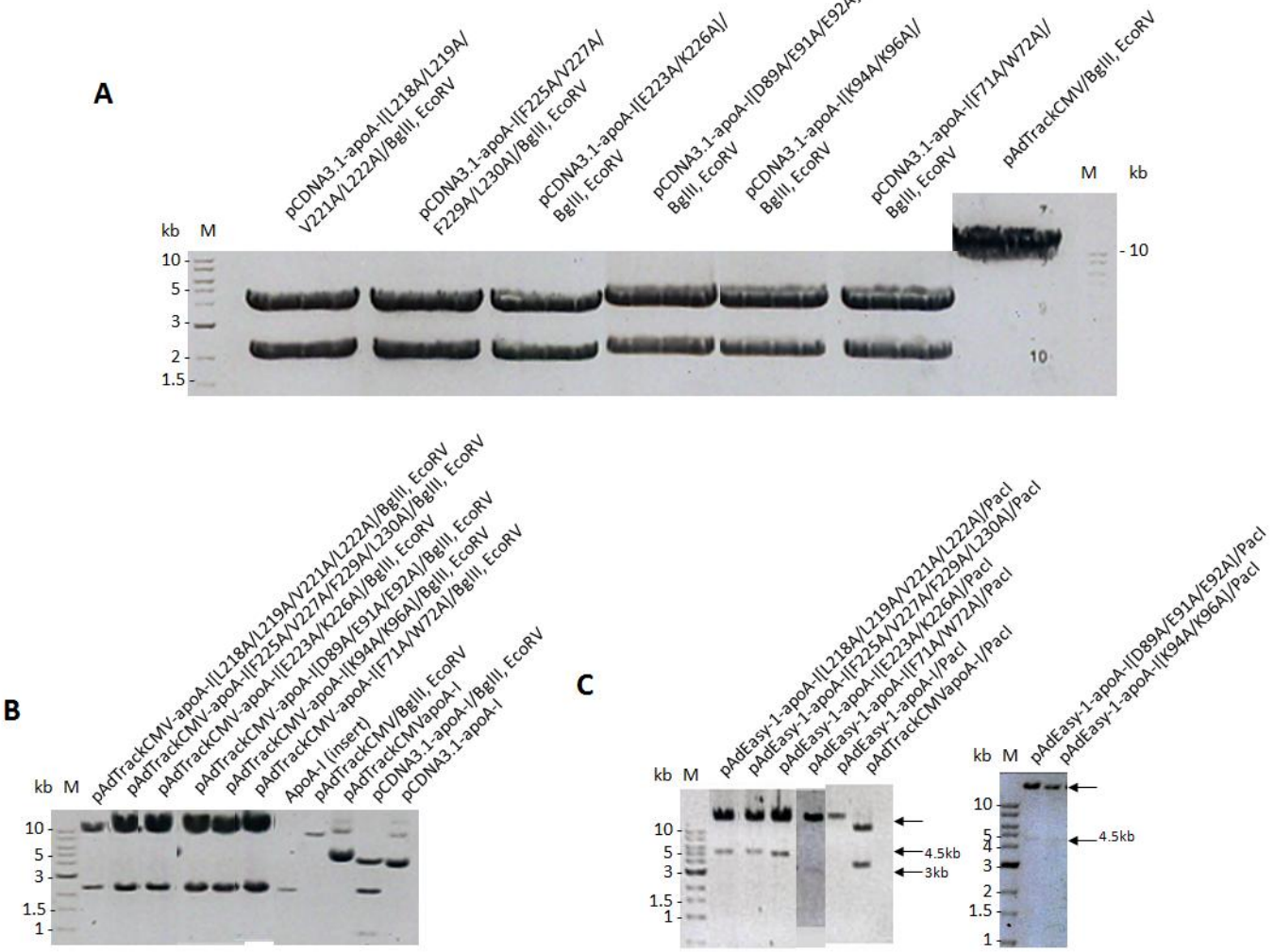

Figure 3.2 (A-C). Caption on next page.

Figure 3.2 (A-C): Restriction analysis of intermediate plasmids that lead to the formation of the recombinant adenoviruses expressing different apoA-I forms. (A) Digestion of pCDNA3.1apoA-IΔBglII with BglII and EcoRV, leading to the formation of two fragments, a 2.2 kb fragment encompassing the apoA-I gene and a ~4.5 kb fragment containing part of the pCDNA3.1 vector. (B) Digestion of pAdTrack-CMV-apoA-I with BglII and EcoRV, leading to the formation of two fragments, a 2.2 kb fragment encompassing the apoA-I gene and a 10 kB fragment containing the pAdTrack-CMV vector. (C) Digestion of pAdEasy-1-apoA-I with PacI, leading to the formation of two fragments, a 4.5 or 3 kB fragment containing the bacterial origin of replication and the ampicillin resistance gene and an approximately 30 kB fragment containing the remaining recombinant adenovirus containing apoA-I.

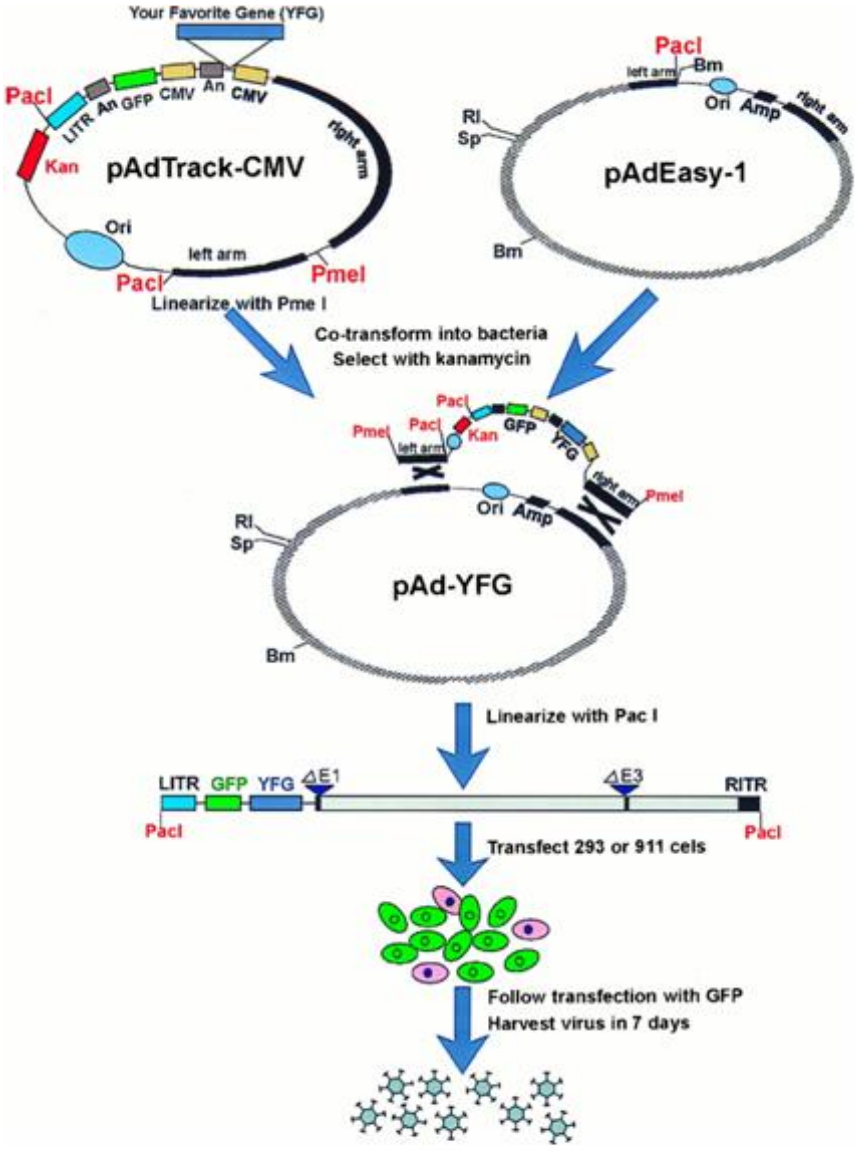

Figure 3.3. Schematic representation of the steps that lead to the generation of the recombinant adenoviruses expressing wild-type and mutant apoA-I forms. Obtained from (*473*).

Table IV. Adenoviruses produced

Name of the adenovirus	Titer (pfu/ml)	Rationale of the mutation
apoA-I [D89A/E91A/E92A]	6.53 x 10^{10}	Conserved amino acids in mammals D89 and E92 are involved in strong interhelix interactions Deletion of 89-99 region of apoA-I caused dyslipidemia
apoA-I [K94A/K96A]	4.5 x 10^{11}	Conserved amino acids in mammals K96 is involved in intra-helix interaction Deletion of 89-99 region of apoA-I caused dyslipidemia
apoA-I [L218A/L219A/ V221A/L222A]	8.1 x 10^{10}	Deletion of 220-231 region of apoA-I helix 6 inhibited apoA-I-ABCA1 interaction
apoA-I [F225A/V227A/ F229A/L230A]	1.1 x 10^{11}	
[a]apoA-I [L218A/L219A/ V221A/L222A/F225A/ V227A/F229A/L230A]	1.4 x 10^{11}	
apoA-I [E223A/K226A]	2.75 x 10^{10}	
apoA-I [F71A/W72A]	1.4 x 10^{11}	Deletion of the 62-80 region of apoA-I induced hypertriglyceridemia

[a]The mutagenic pCDNA3.1apoA-I[L218A/L219A/V221A/L222A/F225A/V227A/ F229A/L230A] construct was generated by Ioanna Tiniakou.

3.1.3. Expressing the WT apoA-I and the apoA-I mutants following infection of HTB-13 cells with the recombinant adenoviruses and purification of apoA-I

To evaluate the expression of apoA-I WT and the mutant apoA-I forms HTB-13 cells were infected with adenoviruses expressing apoA-I WT and apoA-I[D89A/E91A/E92A], apoA-I [K94A/K96A], apoA-I [L218A/L219A/V221A/ L222A], apoA-I [F225A/V227A/ F229A/L230A], apoA-I [L218A/L219A/V221A/ L222A/F225A/V227A/F229A/L230A], apoA-I [E223A/K226A] and apoA-I [F71A/W72A] mutants at various moi (10, 15, and 20 as indicated). Twenty four hours post-infection the cells were washed, new serum free medium was added and the medium was harvested 24 hours later. An aliquot of 100 μl was dissolved in SDS-sample buffer and analyzed by SDS-PAGE. The analysis showed that the infected cells secreted efficiently apoA-I into the culture medium. The molecular mass of WT and six of the apoA-I mutants was as expected, approximately 24 kDa. The protein secreted by apoA-I[F71A/W72A] had a slightly increased molecular mass of approximately 25 kDa (Fig. 3.4A-E).

Large quantities of apoA-I were also produced by adenovirus infection of large scale cultures of HTB13 cells grown in roller bottles as described in experimental procedures. Serum-free media were collected up to six days post infection and analyzed for secretion of apoA-I. Each harvest was 250 ml and the protein concentration was 0.5-1.5 mg/ml. These analyses indicated that the cultures produced approximately 20-50 mg apoA-I per litre (Fig. 3.5).

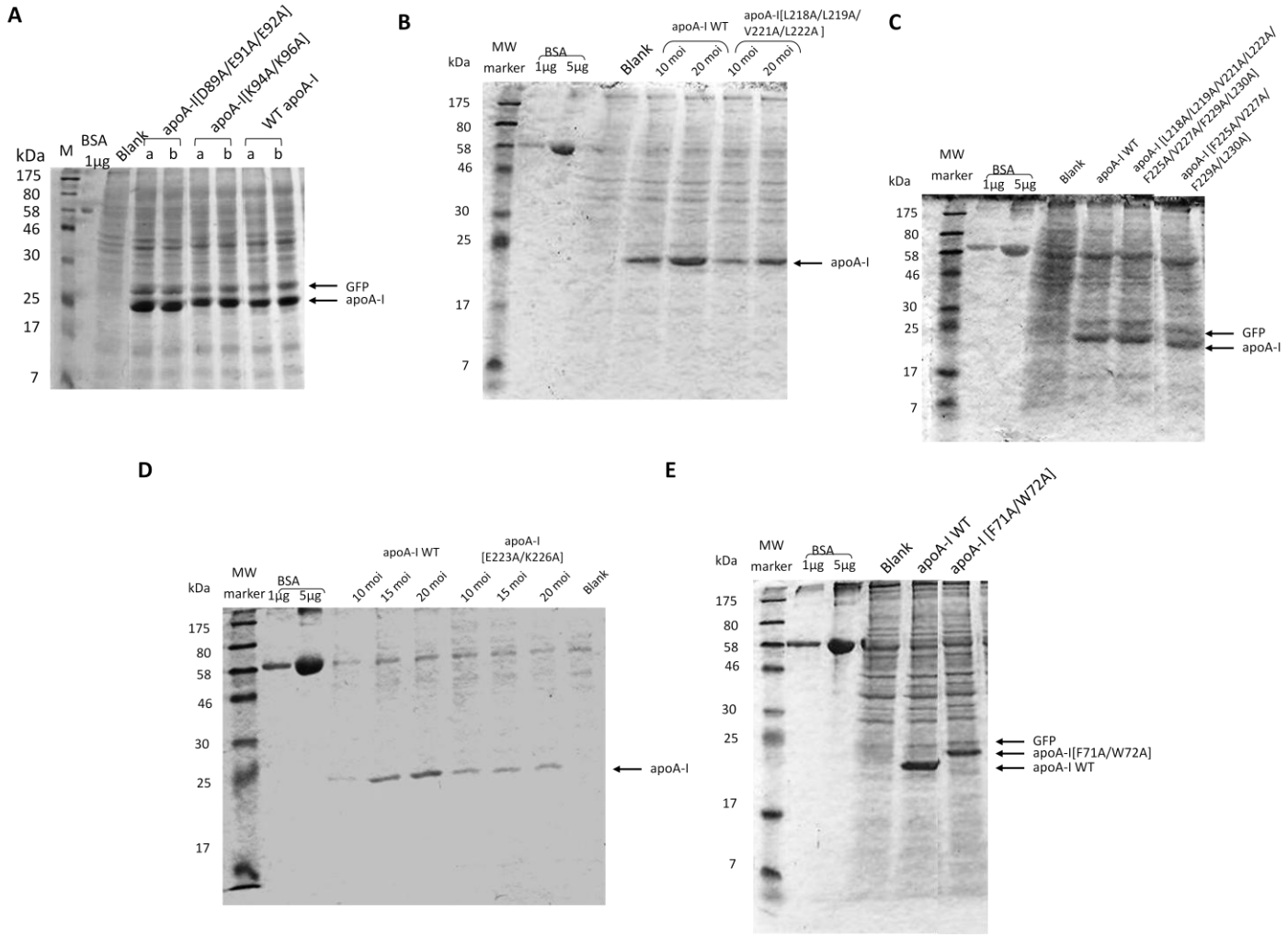

Figure 3.4 (A-E). Caption on next page.

Figure 3.4 (A-E): ApoA-I secretion following infection of HTB-13 cells with apoA-I expressing adenoviruses. SDS-PAGE analysis of 100 μL of culture medium of HTB-13 cells infected with adenoviruses expressing the WT and mutant apoA-I forms at a moi of 10-20 viruses per cell as described in experimental procedures.

For purification of apoA-I from the culture medium the apoA-I containing medium was dialyzed against 25 mM ammonium bicarbonate, lyophilized and used to produce POPC/apoA-I/cholesterol proteoliposomes by the sodium cholate method as described in the experimental procedures. The proteoliposomes were fractionated by density gradient ultracentrifugation and fractions containing apoA-I were collected and analysed by SDS-PAGE. Fractions containing pure apoA-I, usually 6-13, were collected. Using this analysis it was possible to isolate approximately 20 mg pure apoA-I for WT apoA-I and apoA-I[D89A/E91A/E92A], apoA-I [K94A/K96A], apoA-I [L218A/L219A/V221A/L222A] and apoA-I [E223A/K226A] that were used for physicochemical and cell culture studies (Fig. 3.6 A-E).

For experiments that required lipid free apoA-I proteoliposomes isolated by density gradient ultracentrifugation were extensively delipidated by three to five extractions with 2:1 chloroform:methanol till the phosphorus levels of the apoA-I were very low. Protein/phosphorous ratios over 15 mg/ml were considered lipid-free. Thorough delipidation is important in order to assess the physicochemical and cholesterol efflux properties of lipid-free apoA-I.

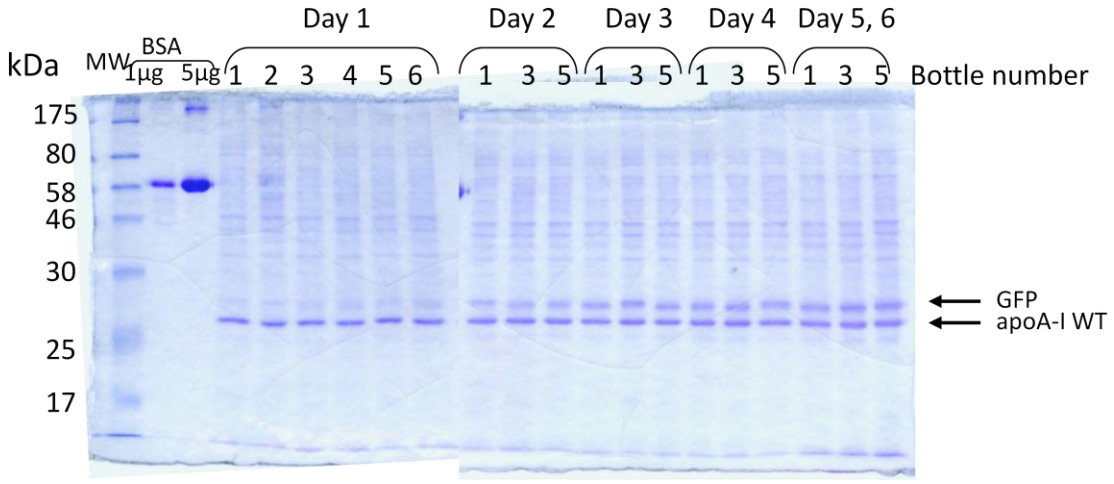

Figure 3.5: Analysis of production of apoA-I by SDS PAGE. SDS PAGE analysis of apoA-I secreted into the culture medium of HTB-13 cells infected with an adenovirus expressing apoA-I. The cells were grown in roller bottles as described in experimental procedures and serum free medium was collected on days 1-6 post infection. The position of the apoA-I and the molecular markers are indicated.

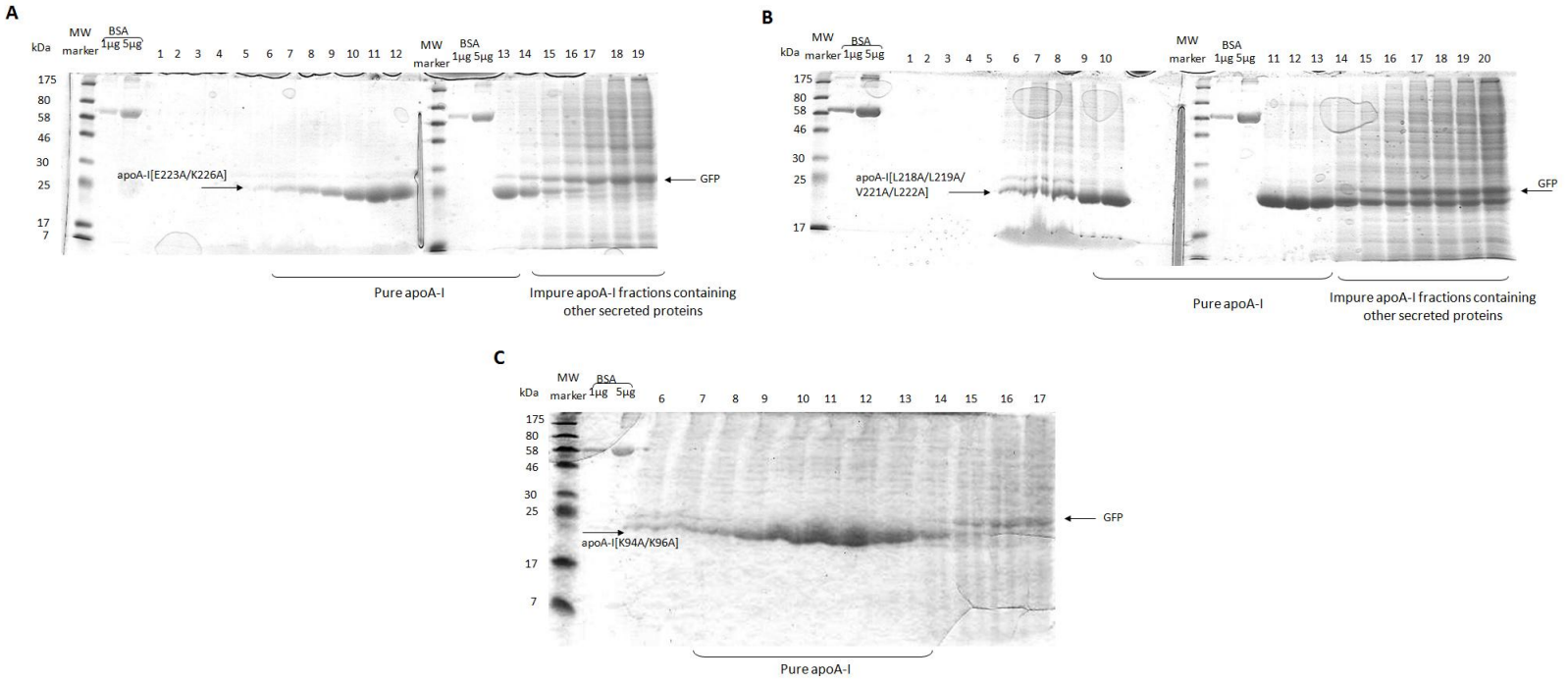

Figure 3.6 (A-C). Continued.

D

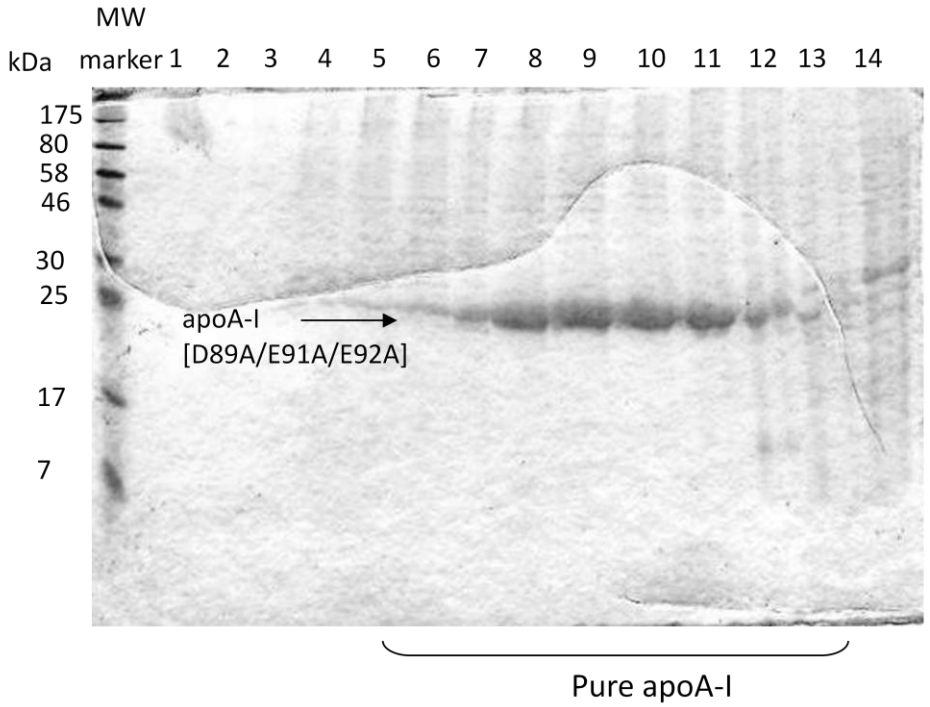

E

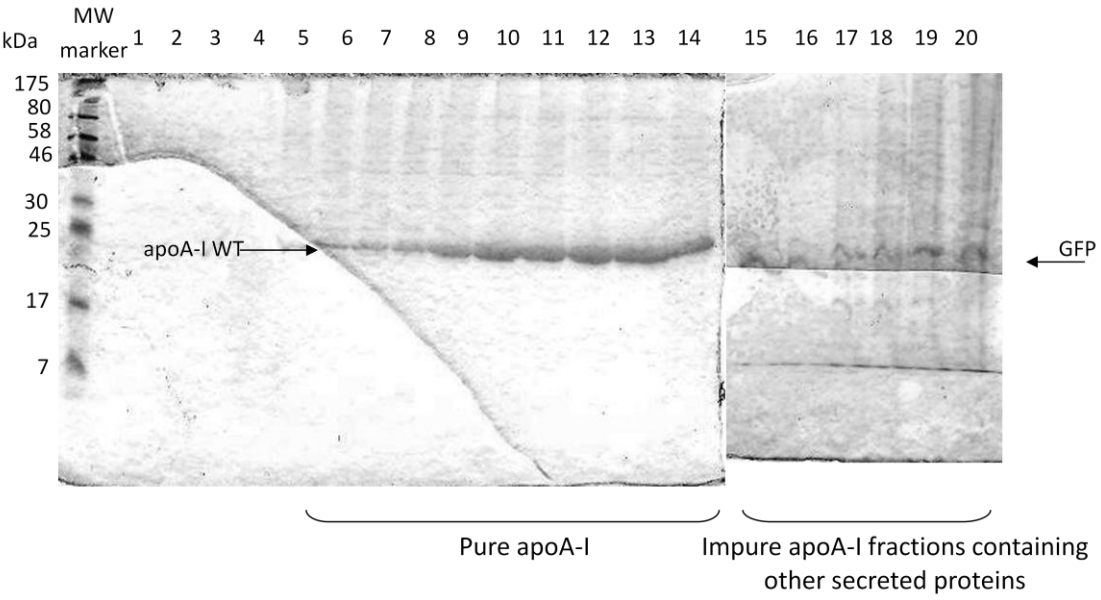

Figure 3.6 (D, E). Caption on next page.

Figure 3.6 (A-E): Analysis of purification of apoA-I by SDS PAGE. SDS PAGE analysis of apoA-I purified from the cultured medium following formation of POPC proteoliposomes and density gradient ultracentrifugation as described in the experimental procedures. The position of the apoA-I and the molecular markers are indicated.

3.2 Functional *in vitro* studies

3.2.1. Production of LCAT following infection of HTB-13 cells with LCAT-expressing recombinant adenovirus and purification of LCAT by Phenyl-Sepharose column

Large quantities of human LCAT was also produced by adenovirus infection of large scale cultures of HTB13 cells grown in roller bottles as described in experimental procedures. Serum-free media were collected up to six days post infection and analyzed for secretion of LCAT. These analyses showed efficient production of LCAT up to day five post infection. Secreted LCAT consisted of two protein bands of approximately 50 and 63 kDa molecular mass. The size heterogeneity indicates different degrees of post-translational modification of LCAT (Fig. 3.7 A). LCAT was purified by Phenyl-Sepharose affinity chromatography as described in the experimental procedures. Pure LCAT was eluted between fractions 8 and 14 (Fig. 3.7 B) and was used for LCAT assays.

3.2.2. Ability of WT and mutant apoA-I forms to activate LCAT

The LCAT activity was assayed as the rate of production of labeled cholesteryl esters from rHDL particles containing WT and apoA-I mutants. The apparent catalytic efficiency ($V\text{max}_{app}/K_{Mapp}$) of the enzyme with rHDL particles containing apoA-I[D89A/E91A/E92A], apoA-I[L144R], apoA-I[A164S] and apoA-I[L218A/L219A/V221A/L222A] mutant forms was reduced approximately to 67%, 35%,

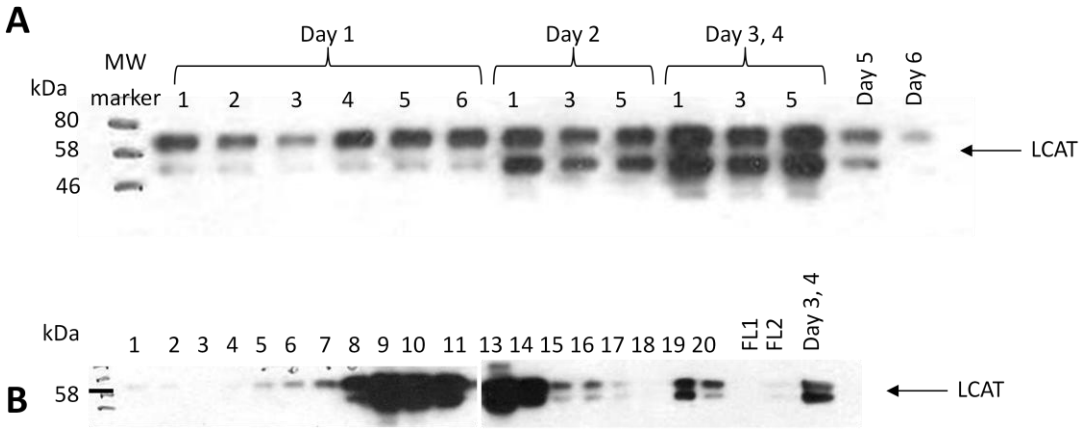

Figure 3.7 (A, B): Analysis of production and purification of LCAT by Western Blotting. (A) Western blot analysis of LCAT secreted into the culture medium of HTB-13 cells infected with an adenovirus expressing LCAT. The cells were grown in roller bottles as described in experimental procedures and serum free medium was collected on days 1-4 post infection. (B) Western blot analysis of cultured medium containing LCAT following fractionation on phenyl Sepharose column as described in experimental procedure. The position of the LCAT and the molecular markers are indicated.

90% and 82% respectively as compared to rHDL particles containing WT apoA-I (Fig. 3.8 A, B).

3.2.3. ABCA1-mediated cholesterol efflux by WT apoA-I apoE and apoAIV and the apoA-I variants [D89A/E91A/E92A], [L144R] and [A164S] mutants

To evaluate the capacity of apoA-I WT, apoA-I[D89A/E91A/E92A], apoA-I[L144R] and apoA-I[A164S] mutants as well as apoE and apoAIV to promote ABCA1-mediated cholesterol efflux, studies were performed in HEK293-EBNA cells transfected with empty vector or an ABCA1 expressing plasmid for 16h as described in experimental procedures. Following transfections the cells were labeled with [^{3}H] cholesterol for 24h and then incubated with or without 1 μM lipid-free WT apoA-I, mutant forms of apoA-I, apoE or apoAIV.

The net efflux values (difference of efflux of ABCA1-transfected cells minus the efflux of empty vector-transfected cells) obtained for apoA-I was set as 100 %. Compared with apoA-I WT, ABCA1-mediated efflux was 64% in the presence of apoA-I[D89A/E91A/E92A], 91 and 79% in the presence of apoA-I[L144R] and apoA-I[A164S] (Fig. 3.9 A-B). The capacity of lipid-free apoAIV to promote ABCA1-mediated efflux was also assayed and it was shown that its capacity at 1 μM concentration was 92% and at higher concentration (3 μM) it was 107% (Fig. 3.9 C).

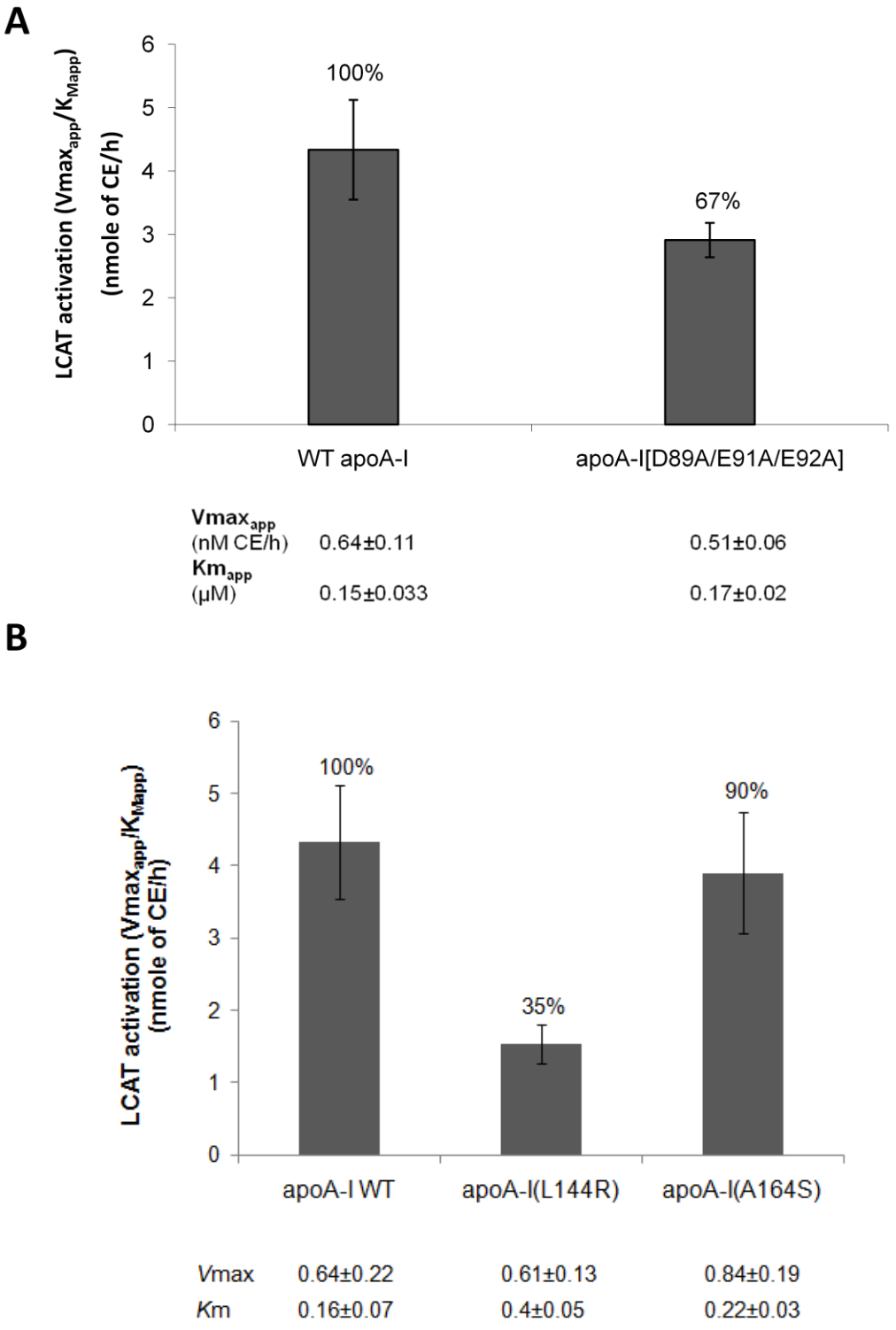

Figure 3.8 (A, B). Caption on next page

Figure 3.8 (A, B): Activation of LCAT by rHDL containing wild type apoA-I, apoA-I[D89A/E91A/E92A], apoA-I[L144R] and apoA-I[A164S] form. Diagram showing the $V\text{max}_{app}/K\text{m}_{app}$ values of wild-type, apoA-I[D89A/E91A/E92A] (A), apoA-I[L144R] (B) and apoA-I[A164S] (B) mutant forms. The kinetic parameters of wild-type, apoA-I[D89A/E91A/E92A], apoA-I[L144R] and apoA-I[A164S] are listed. Values are the mean ± SE from three independent experiments.

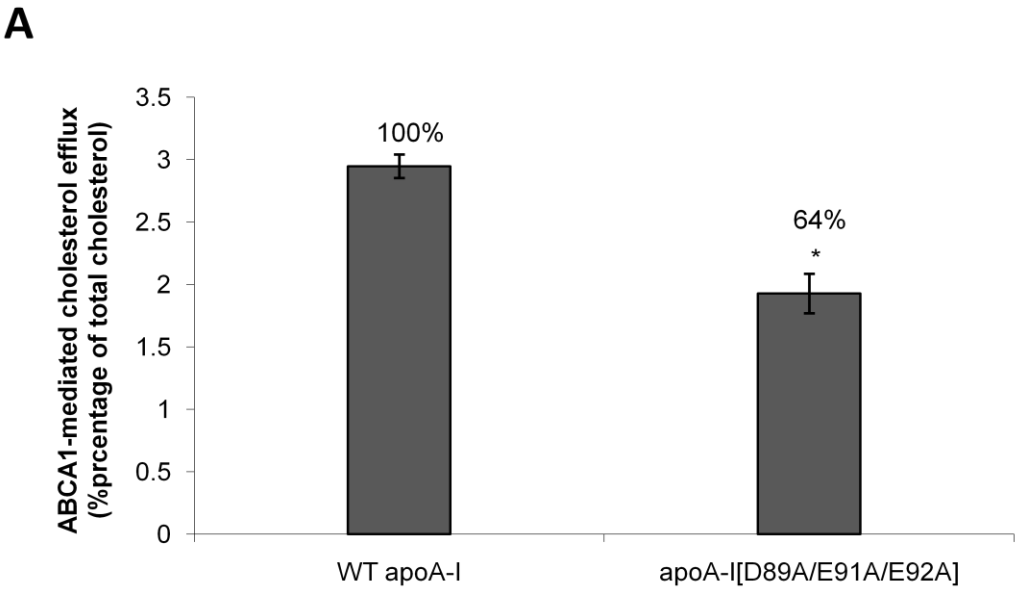

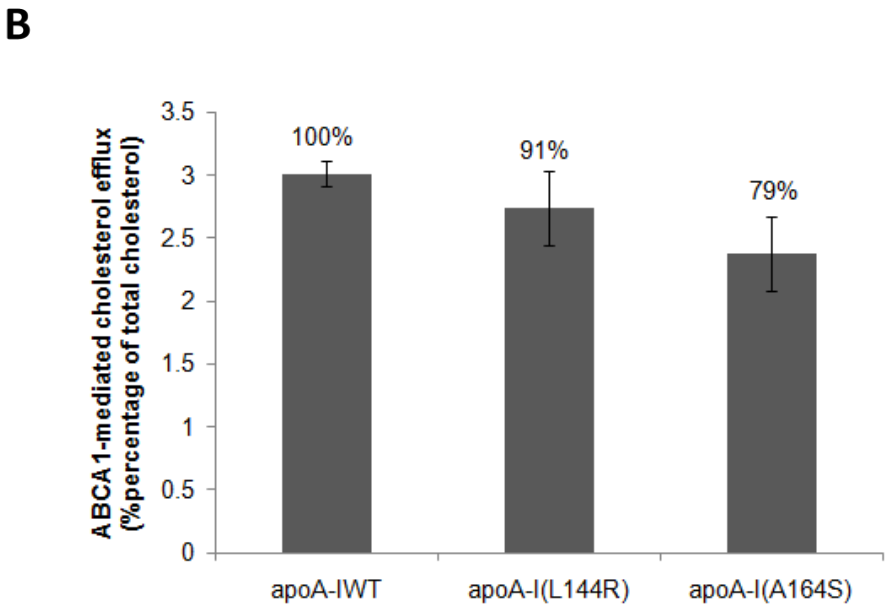

Figure 3.9 (A-B). Continued.

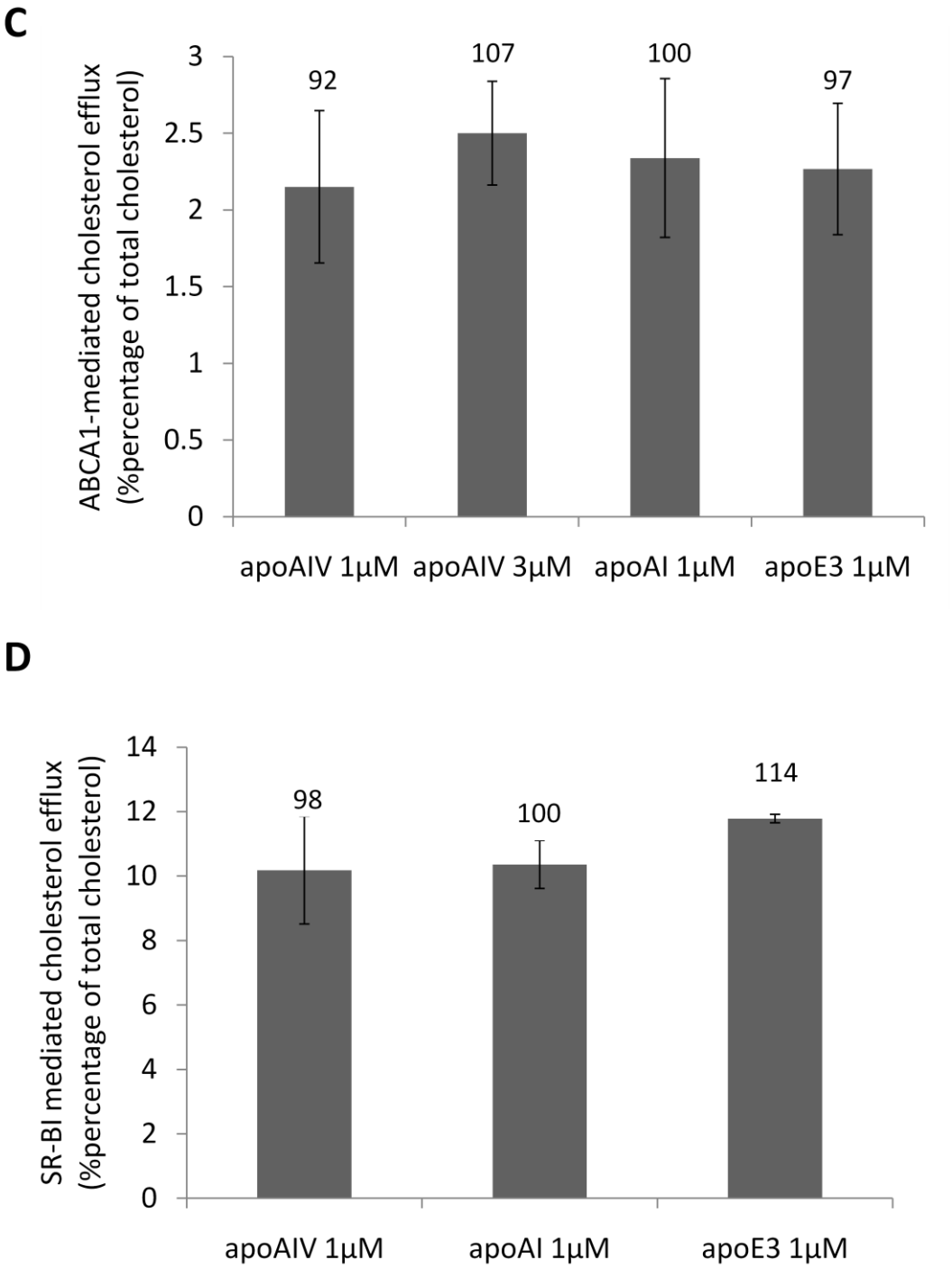

Figure 3.9 (C-D). Caption on next page.

Figure 3.9 (A-D): Cholesterol efflux by wild type apoA-I, apoA-I[D89A/E91A/E92A], apoA-I[L144R] and apoA-I[A164S] mutant forms as well as WT apoE and apoA-IV from HEK293 EBNA-T cells and cholesterol efflux by rHDL containing WT apoA-I, WT apoE3 and apoA-IV from CHO cells. ABCA1-mediated cholesterol efflux in the presence of WT apoA-I, apoA-I[D89A/E91A/E92A] (A), apoA-I[L144R] and apoA-I[A164S] mutant forms (B) as well as WT apoE and apoA-IV (C) was determined as described in Experimental Procedures. The concentration of the acceptor apoA-I in the medium was 1 μM. (D) SR-BI-mediated cholesterol efflux in the presence of rHDL containing WT apoA-I, WT apoE and apoA-IV was determined as described in Experimental Procedures. The concentration of the acceptor proteins in the medium was 1 μM. Values are the means ± SE from three experiments performed in duplicate.

3.2.4. SR-BI mediated cholesterol efflux by rHDL containing apoA-I, apoE3 and apoAIV

SR-BI mediated cholesterol efflux was measured using ldlA7 CHO cells expressing the mSR-BI as described in the experimental procedures using proteoliposomes containing apoA-I, apoE3 and apoAIV as acceptors. This analysis showed that the cholesterol efflux capacity of proteoliposomes containing these three proteins were similar (Fig. 3.9 D).

3.3. Functional *in vivo* studies

3.3.1. Alteration of negatively charged residues in the 89 to 99 domain of apoA-I affects lipid homeostasis and the maturation of HDL

The objective of these analyses was to investigate the role of positively and negatively charged amino acids within the 89-99 region of apolipoprotein A-I (apoA-I), that are highly conserved in mammals, on plasma lipid homeostasis and the biogenesis of HDL. We have shown previously that deletion of the 89-99 region of apoA-I increased plasma cholesterol and phospholipids but did not affect plasma triglycerides.

3.3.2. Secretion of the WT and the two apoA-I mutants

To assess the expression and secretion of the two mutant proteins relative to WT apoA-I, we infected HTB-13 cells with recombinant adenoviruses expressing the WT or the mutant apoA-I genes using a multiplicity of infection of 10. Analysis of the medium 24

hours post infection showed that the WT and the two mutant forms of apoA-I were secreted at comparable levels in the medium (Fig. 3.4A).

3.3.3. Expression of the apoA-I transgene following adenovirus infection

Total hepatic RNA was isolated from the mouse livers four days post infection with adenoviruses expressing the WT and the [D89A/E91A/E92A] and [K94A/K96A] mutant apoA-I forms. The relative expression of the WT and the mutant apoA-I transgenes was determined by qPCR as described in the experimental procedures. This analysis showed that the expression of WT and apoA-I[D89A/E91A/E92A] were comparable, whereas the expression of apoA-I[K94A/K96A] was 56% of the WT apoA-I (Fig. 3.10).

3.3.4. Plasma lipids and apoA-I measurements

Plasma lipids and apoA-I were determined four days post infection of apoA-$I^{-/-}$ mice with adenoviruses expressing the WT and the two apoA-I mutants. It was found that the apoA-I[D89A/E91A/E92A] mutant caused dyslipidemia characterized by severe hypertriglyceridemia, increased plasma cholesterol and phospholipids and decreased cholesteryl ester to total cholesterol (CE/TC) ratio. The lipid parameters in mice expressing the apoA-I[K94A/K96A] mutant were comparable to those of mice expressing WT apoA-I with the exception of TC/apoA-I ratio which was reduced for this mutant (Table V, Fig. 3.11 A-C).

Table V. Plasma lipids, apoA-I and hepatic mRNA levels of apoA-I$^{-/-}$ mice expressing WT and mutant forms of apoA-I obtained 4 days post infection[a]

Protein expressed	Total Cholesterol (TC) (mg/dL)	TC/ apoA-I	Free cholesterol (mg/dL)	CE/TC	Phospholipids (PL) (mg/dL)	Triglycerides (mg/dL)	Relative apoA-I mRNA (%)	Plasma apoA-I (mg/dL)
GFP	28±7	-	12±3	0.58±0.04	33±22	34±3	-	-
WT apoA-I	268±55	0.95±0.16	75±34	0.72±0.06	296±96	70±11	100±32	283±84
apoA-I [D89A/E91A/E92A]	497±139	2.52±0.84	347±147	0.36±0.31	603±406	2106±1629	101±24	235±106
apoA-I [K94A/K96A]	108±23	0.53±0.04	46±21	0.58±0.15	190±14	66±9	56±20	220±51
apoA-I [D89A/E91A/ E92A] + hLPL	122±56	1±0.2	56±20	0.44±0.14	255±128	49±16	41±6	99±18

[a] The values are means ± S.D. (n = 4-6)

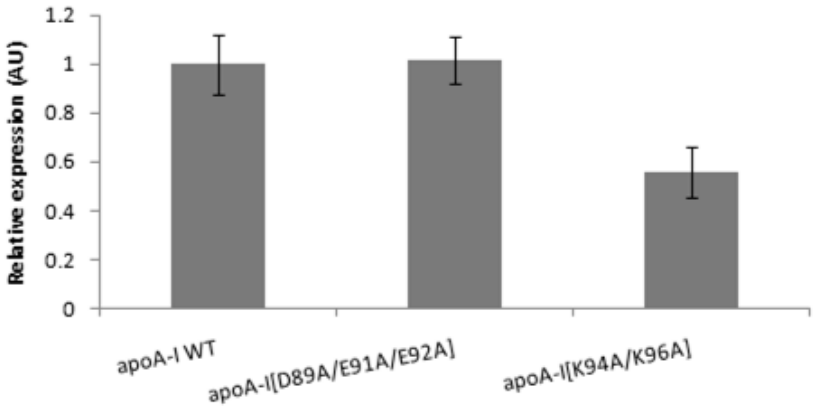

Figure 3.10: Hepatic apoA-I mRNA levels of mice infected with apoA-I expressing adenoviruses. Mice infected with $2x10^9$ adenoviruses expressing WT apoA-I, apoA-I[D89A/E91A/E92A] and apoA-I[K94A/K96A]. RNA was extracted from livers 4 days post infection and apoA-I mRNA was quantitated by real time qPCR as described in experimental procedures.

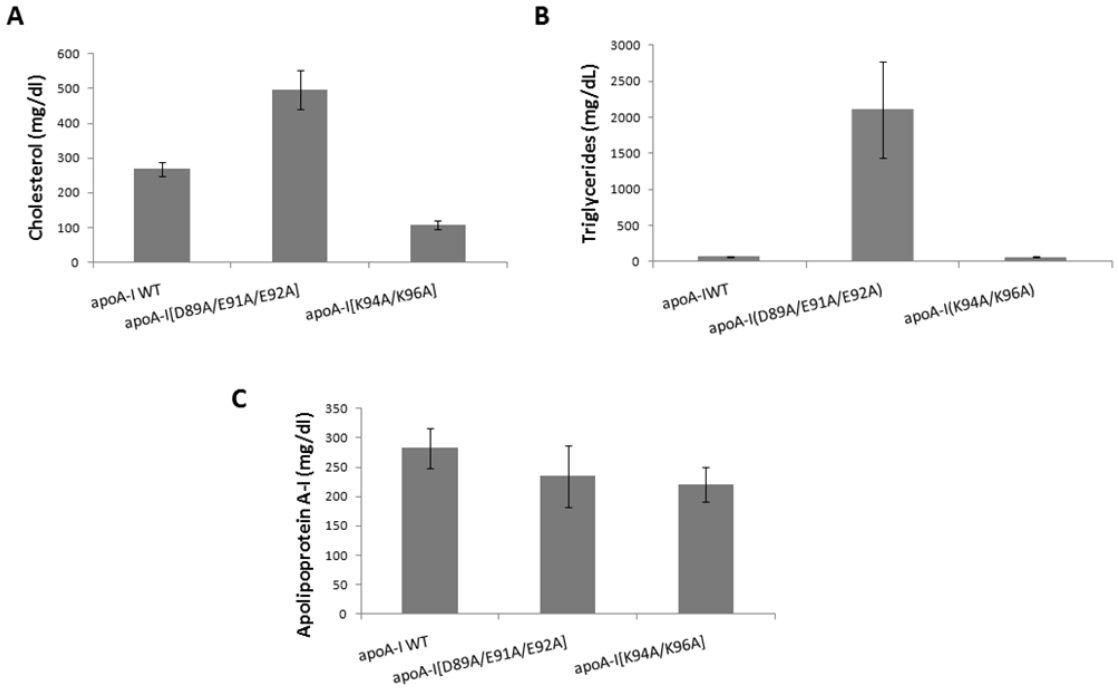

Figure 3.11: Plasma lipid and apoA-I levels four days post infection of mice infected with apoA-I expressing adenoviruses. (A)Plasma cholesterol, (B) plasma triglycerides and (C) plasma apoA-I levels obtained from mice infected with adenovirus expressing WT apoA-I, apoA-I[D89A/E91A/E92A] or apoA-I[K94A/K96A].

3.3.5. FPLC profiles of plasma isolated from apoA-I$^{-/-}$ mice infected with adenoviruses expressing the WT and the two apoA-I mutants

FPLC analysis of plasma from apoA-I$^{-/-}$ mice infected with the recombinant adenovirus expressing either WT apoA-I or the two apoA-I mutants showed that in mice expressing WT apoA-I cholesterol was distributed predominantly in the HDL2/HDL3 region. The distribution of cholesterol in the apoA-I[K94A/K96A] mutant was similar to that of WT apoA-I with an additional shoulder in the IDL and LDL regions. In contrast, in mice expressing the apoA-I[D89A/E91A/E92A] mutant cholesterol was distributed predominantly in the VLDL/IDL/LDL region (Fig. 3.12 A). All the triglycerides of the apoA-I[D89A/E91A/E92A] mutant were found in the VLDL region. The VLDL triglyceride peak of WT apoA-I and apoA-I[K94A/K96A] mutant were negligible (Fig. 3.12 B).

3.3.6. Fractionation of plasma of mice expressing the WT and the two apoA-I mutants by density gradient ultracentrifugation

Fractionation of plasma by density gradient ultracentrifugation and subsequent analysis of the resulting fractions by SDS-PAGE served two purposes. It gave important information on the distribution of apoA-I in different lipoprotein fractions and provided the HDL fractions that were used for EM analysis. It was found that the WT apoA-I and apoA-I[K94A/K96A] mutant are predominantly distributed in the HDL2 and HDL3 region (Fig. 3.13 A, C). In contrast, in the case of apoA-I[D89A/E91A/E92A] mutant

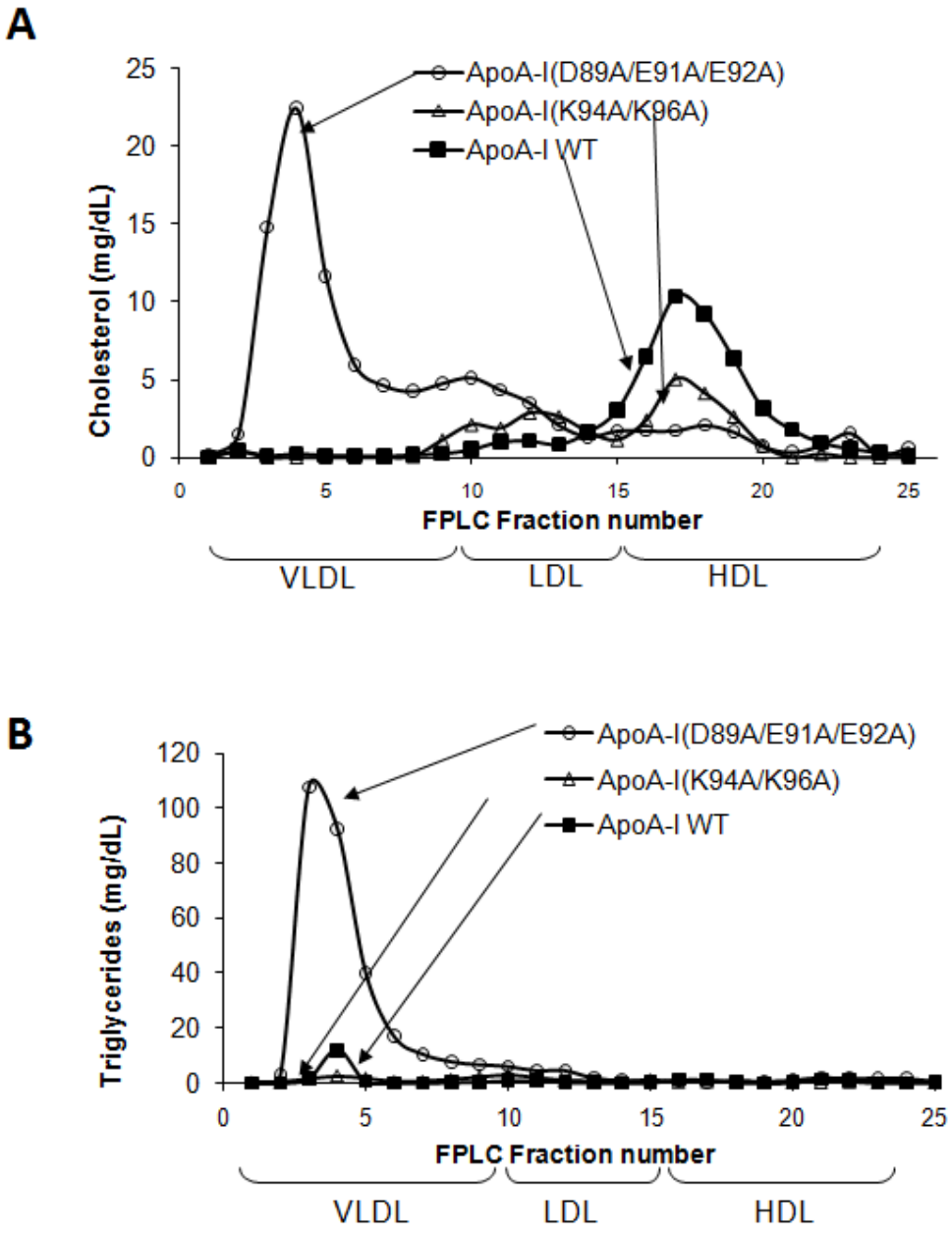

Figure 3.12 (A, B): FPLC profiles of total cholesterol (*A*) or triglycerides (*B*) of apoA-I$^{-/-}$ mice infected with adenoviruses expressing the WT apoA-I, apoA-I[D89A/E91A/E92A], or apoA-I[K94A/K96A] as indicated. Plasma samples were obtained 4 days post-infection.

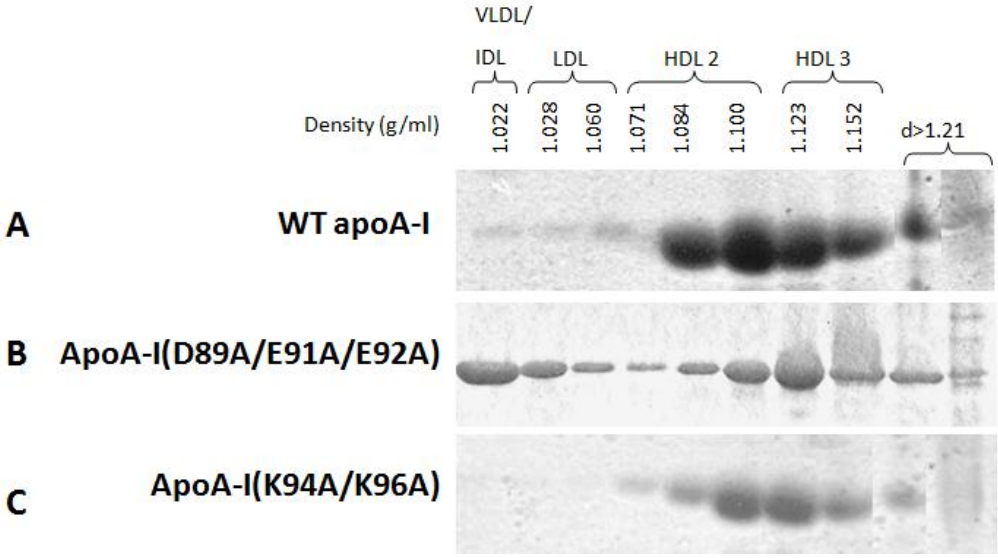

Figure 3.13 (A-C): Analysis of plasma of apoA-I$^{-/-}$ mice infected with adenoviruses expressing the WT apoA-I (*A)*, the apoA-I[D89A/E91A/E92A] (*B*), and the apoA-I[K94A/K96A] (*C*), by density gradient ultracentrifugation and SDS-PAGE.

approximately 40% of apoA-I was distributed in the VLDL/IDL/LDL region and the remaining in the HDL3 and to a lesser extent in the HDL2 region (Fig. 3.13 B).

3.3.7. EM analysis of the HDL fractions

Analysis of the HDL fractions 6 and 7 obtained following density gradient ultracentrifugation by EM showed that the WT apoA-I and the apoA-I[K94A/K96A] mutant generated spherical particles (Fig. 3.14 A and C) and the apoA-I[D89A/E91A/E92A] mutant generated mostly spherical and few discoidal particles (Fig. 3.14 B). Control experiments showed that HDL density fractions obtained from GFP expressing apoA-$I^{-/-}$ mice, which cannot form HDL, contained very few spherical particles (Fig. 3.14 D).

3.3.8. Two-dimensional gel electrophoresis of plasma of mice expressing the WT and the two apoA-I mutants

Two-dimensional gel electrophoresis of plasma showed that WT apoA-I and the apoA-I[K94A/K96A] mutant formed normal α subpopulations with small amount of preβ HDL particles (Fig. 3.15 A and C). In contrast the apoA-I[D89A/E91A/E92A] mutant formed predominantly preβ1 and α4 HDL particles at a ratio of approximately 2:1 (Fig. 3.15 B).

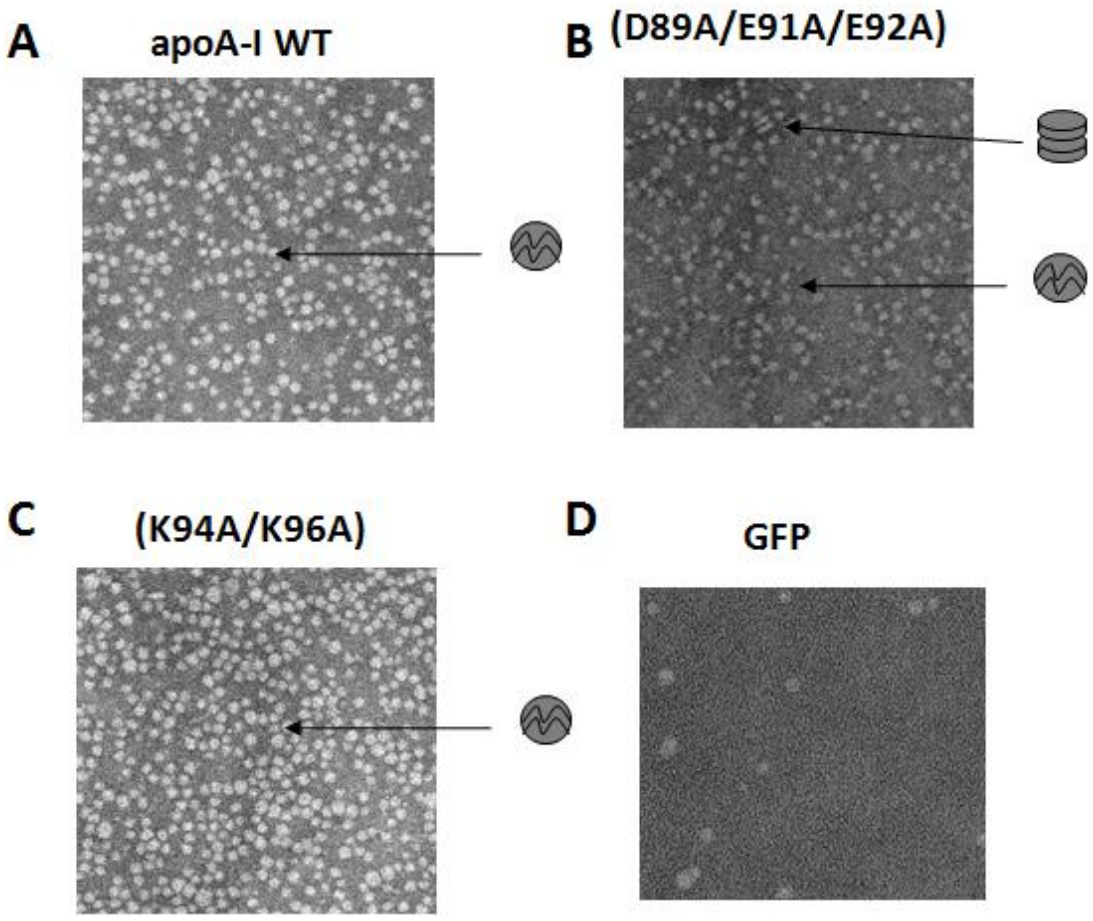

Figure 3.14 (A-D): EM analysis of HDL fractions 6-7 obtained from apoA-I$^{-/-}$ mice expressing the WT apoA-I (*A)*, the apoA-I[D89A/E91A/E92A] (*B*), and the apoA-I[K94A/K96A] (*C*), or GFP control virus (*D*) following density gradient ultracentrifugation of plasma as indicated. The electron micrographs were taken at 75,000× magnification and enlarged 3 times.

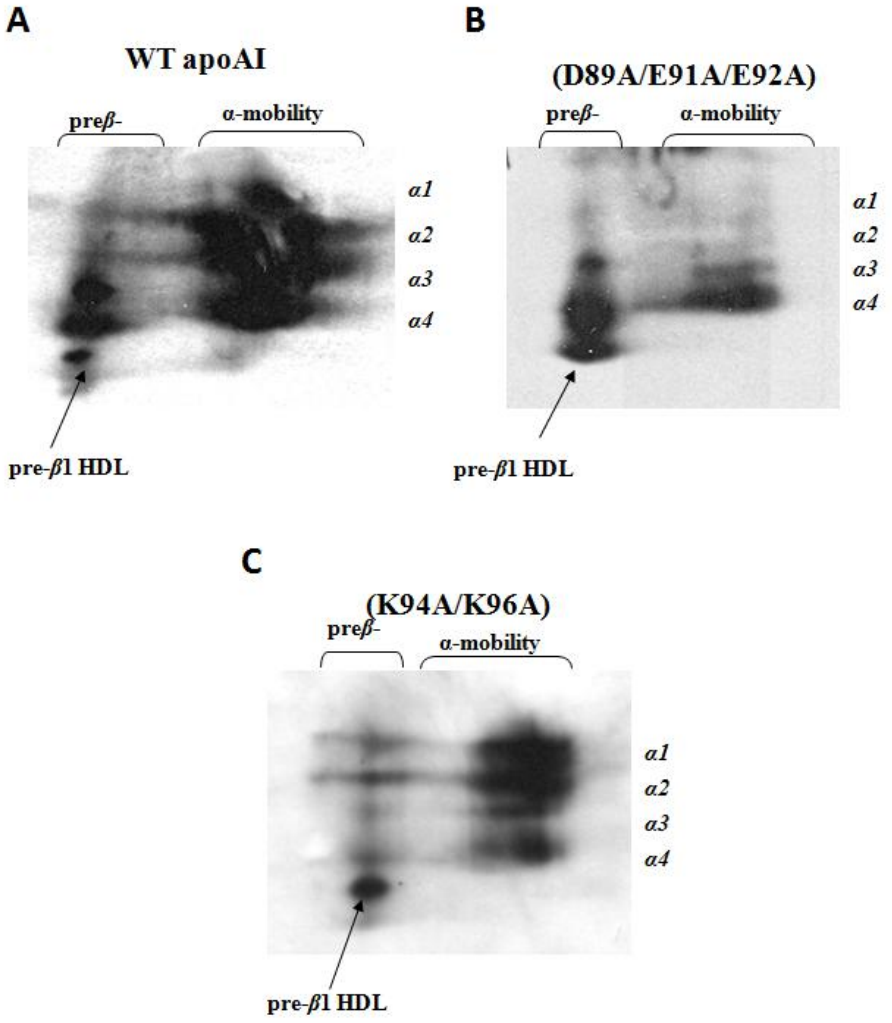

Figure 3.15 (A-C): Analysis of plasma obtained from mice expressing the WT apoA-I (*A)*, the apoA-I[D89A/E91A/E92A] (*B*), and the apoA-I[K94A/K96A] (*C*), following two-dimensional gel electrophoresis and Western blotting.

3.3.9. Ability of lipoprotein lipase to normalize the lipid and lipoprotein abnormalities induced by the apoA-I[D89A/E91A/E92A] mutation

ApoA-I$^{-/-}$ mice were co-infected with 2 x 10^9 pfu of an adenovirus expressing apoA-I[D89A/E91A/E92A] mutant and 5 x 10^8 pfu of an adenovirus expressing the hLPL and their lipid and lipoprotein profiles were compared to those of mice infected with 2 x 10^9 pfu of an adenovirus expressing WT apoA-I. This analysis showed that the lipoprotein lipase treatment abolished hypertriglyceridemia but did not correct the CE/TC ratio in mice that received the apoA-I[D89A/E91A/E92A] mutant and hLPL (Table V).

The plasma of the apoA-I$^{-/-}$ mice that were co-infected with the apoA-I[D89A/E91A/E92A] mutant and hLPL was fractionated by density gradient ultracentrifugation and SDS-PAGE and the HDL fraction was analyzed by electron microscopy. This analysis showed that in mice co-infected with the apoA-I[D89A/E91A/E92A] mutant and hLPL the HDL was distributed mostly into the HDL3 and to a lesser extent to HDL2. ApoA-I was not found in the VLDL/IDL fraction (Fig. 3.16 A). HDL fraction contained both discoidal and spherical HDL particles (Fig. 3.16 B). The observed decrease in plasma apoA-I levels can be explained by the decreased expression of the apoA-I transgene in the co-infection experiment and possibly by faster catabolism of the smaller size HDL particles.

Two-dimensional gel electrophoresis of plasma obtained from mice that were co-infected with the apoA-I[D89A/E91A/E92A] mutant and human lipoprotein lipase showed that the hLPL treatment restored in part the α1, 2, 3, 4 HDL subpopulations (Fig. 3.16C).

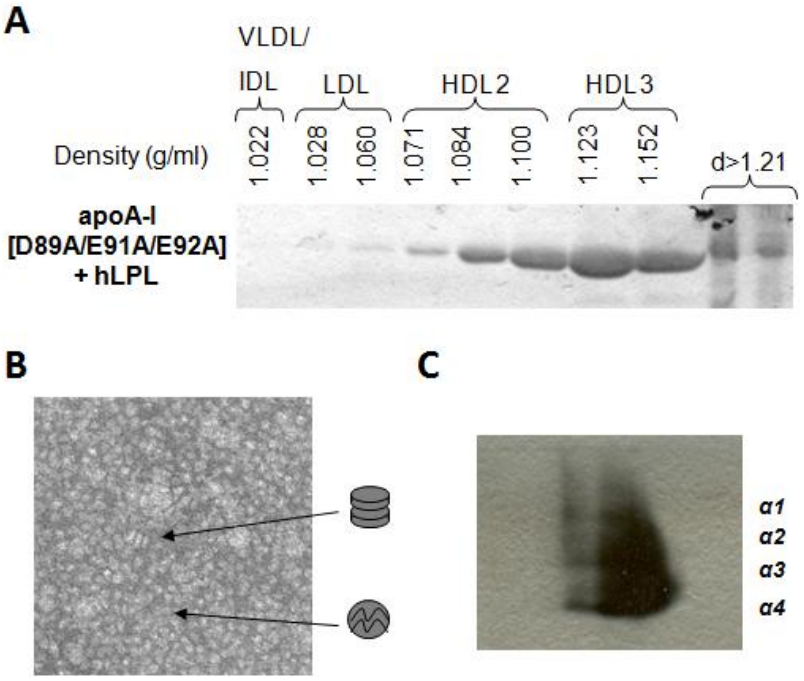

Figure 3.16 (A-C): Analyses of plasma of apoA-I$^{-/-}$ mice infected with adenoviruses expressing the apoA-I[D89A/E91D/E92A] and hLPL. (*A*) SDS-PAGE analysis of fractions obtained by density gradient ultracentrifugation of plasma of apoA-I$^{-/-}$ mice infected with 2×10^9 pfu of adenovirus expressing apoA-I[D89A/E91A/E92A] and 5×10^8 pfu of an adenovirus expressing the human lipoprotein lipase. (*B)* EM picture of HDL fractions 6-7 obtained from apoA-I$^{-/-}$ mice expressing the apoA-I[D89A/E91A/E92A] mutant and human lipoprotein lipase, following density gradient ultracentrifugation as indicated in (*A*). The sample was concentrated 2 times. The electron micrographs were taken at 75,000× magnification and enlarged 3 times. *(C)* Analysis of plasma obtained from mice expressing the apoA-I[D89A/E91A/E92A] mutant and human lipoprotein lipase following two-dimensional gel electrophoresis and Western blotting.

3.4. Physicochemical properties of the WT and the apoA-I[D89A/E91A/E92A] and apoA-I[K94A/K96A] mutant forms (Physicochemical experiments were performed in collaboration with Irina Gorshkova)

3.4.1. Thermal stability and conformation of apoA-I

Analysis of the normalized far-UV CD spectra of WT apoA-I and the apoA-I[D89A/E91A/E92A] and apoA-I[K94A/K96A] mutants showed that compared to WT apoA-I, the two mutant proteins had an ~9% reduction and ~6% increase respectively in their α-helical content. This corresponds to a loss of ~22 and gain of ~15 residues in the helical conformation of apoA-I respectively (Table VI).

The thermal unfolding of the WT apoA-I, apoA-I[D89A/E91A/E92A] and apoA-I[K94A/K96A] mutants was monitored by the ellipticity at 222 nm. The parameters of the thermal unfolding determined from the van't Hoff analysis are listed in Table VI. The apoA-I[D89A/E91A/E92A] mutation caused a small (~2°C) but statistically significant decrease in the melting temperature T_m indicating a destabilizing effect of the mutation. The T_m of apoA-I[K94A/K96A] did not differ from that of WT apoA-I. Large (approximately 13 kcal/mol) decrease in the effective enthalpy ΔH_v for the apoA-I[D89A/E91A/E92A] mutant as compared to WT apoA-I is consistent with the less cooperative (less sharp) thermally induced unfolding of this mutant and suggests a significantly lower cooperativity of the thermal transition of the apoA-I[D89A/E91A/E92A] mutant . The effective enthalpy ΔH_v for the apoA-I[K94A/K96A] mutant was lower than that for WT apoA-I by approximately 5 kcal/mol.

3.4.2. ANS-fluorescence and DMPC-clearance kinetics

To investigate if the apoA-I[D89A/E91A/E92A] and apoA-I[K94A/K96A] mutations affect the tertiary structure of apoA-I, the intrinsic fluorescence of the amphipathic fluorescent dye ANS was recorded in the presence of each of these proteins and in the presence of WT apoA-I. It was found that in the presence of the WT and the mutant apoA-I forms, ANS fluorescence was significantly enhanced and blue-shifted as compared to ANS fluorescence in buffer alone or in the presence of carbonic anhydrase, which represents a typical globular protein. This is consistent with the molten-globular-like conformation of apoA-I. However, in the presence of the apoA-I[D89A/E91A/E92A], the increase in the fluorescence intensity was 43% larger and the blue shift in WMF was ~3 nm greater than in the presence of WT apoA-I (Table VI). This suggests that compared to WT apoA-I, the [D89A/E91A/E92A] mutant has additional exposed hydrophobic surfaces. The fluorescence intensity and WMF of the apoA-I[K94A/K96A] were close to those of WT apoA-I (Table VI).

The kinetics of solubilization of multilamellar DMPC vesicles by WT and the apoA-I[D89A/E91A/E92A] mutant was monitored at 325 nM by the clearance of the turbidity of DMPC suspension following the addition of apoA-I. It was found that the apoA-I[D89A/E91A/E92A] mutant clears turbidity slightly faster than WT apoA-I and the apoA-I[K94/K96A] clears turbidity at a rate similar to that of WT apoA-I (Fig. 3.17).

3.4.3. Binding of apoA-I forms to triglyceride-rich emulsions

The weight ratio triolein:PC in the emulsions was 4.1±0.3 (mean ± SD of three isolated emulsions). The average size of particles in a typical isolated emulsion calculated from the electron microphotographs was 54±21 nm (mean± SD, n=201). The large standard deviations reflect a broad size distribution that resembles a size distribution of plasma VLDL. Data of the binding assays (Fig. 3.18 A) show that at each emulsion to protein ratio in the incubation mixtures, the portion of the bound protein is higher for the apoA-I[D89A/E91A/E92A] mutant than for WT apoA-I. Figure 3.18 B shows that for each emulsion to protein ratio in the incubation mixtures, the number of protein molecules bound to one particle are significantly higher for the apoA-I[D89A/E91A/E92A] mutant than for WT apoA-I.

Table VI. α-helical Content and Thermodynamic Parameters of Lipid-free WT apoA-I and the apoA-I mutant forms and parameters of ANS fluorescence in the presence of the proteins

Protein	α-helix[a] (%)	Number of residues in α-helix	T_m,[b] (°C)	ΔH_v,[b] (kcal/mol)	I[c] (relative units)	WMF[c] (nm)
WT apoA-I	~58	144	61±0.5	39±1	4.6	480
apoA-I [D89A/E91A/E92A]	~49	122	59±0.5[e]	26±2[f]	6.6	477
apoA-I [K94A/K96A]	~ 64	159	60±1.0	34±2[d]	4.8	479

[a] Estimated from the $[\Theta_{222}]$ at 25°C; Systematic and statistical errors are ±3%.

[b] The melting temperature T_m and the effective enthalpy ΔH_v were determined from van't Hoff analysis of the thermal unfolding curves monitored by CD at 222 nm.

[c] Parameters of ANS fluorescence determined in the presence of WT apoA-I, apoA-I [D89A/E91A/E92A] or apoA-I[K94A/K96A] (Fig. 5C). *I* is ANS fluorescence intensity in relative units compared to the fluorescence in buffer alone.

[d] Significance of differences from the value for WT: $p<0.05$.

[e] Significance of differences from the value for WT: $p<0.01$.

[f] Significance of differences from the value for WT: $p<0.005$.

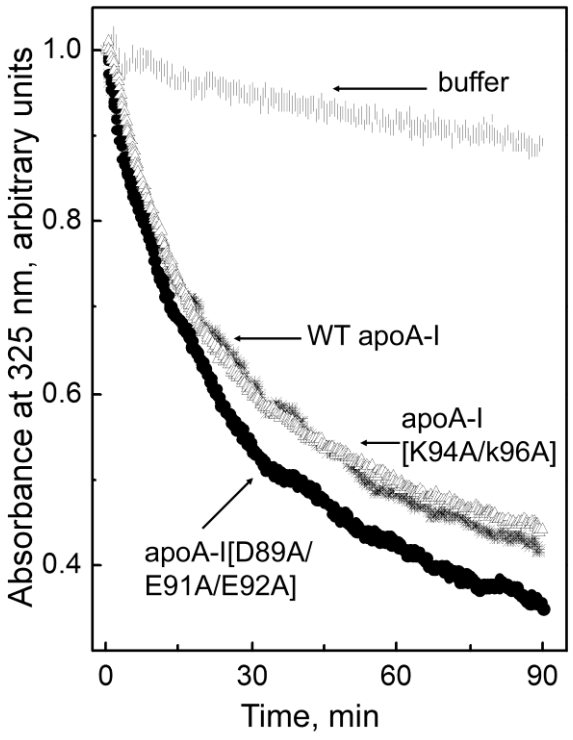

Figure 3.17: Physicochemical properties of the WT apoA-I, apoA-I[D89A/E91A/E92A] and apoA-I[K94A/K96A]. The time course of DMPC clearance by the apoA-I forms or in buffer alone. DMPC multilamellar vesicles (100 μg/mL lipids) were preincubated at 24°C and the clearance was triggered by addition of protein to reach final concentration in cuvette 40 μg/mL. The turbidity was monitored by absorbance at 325 nm at the controlled temperature 24°C. WT apoA-I (✳), apoA-I[D89A/E91A/E92A] (●), apoA-I[K94A/K96A] (△).

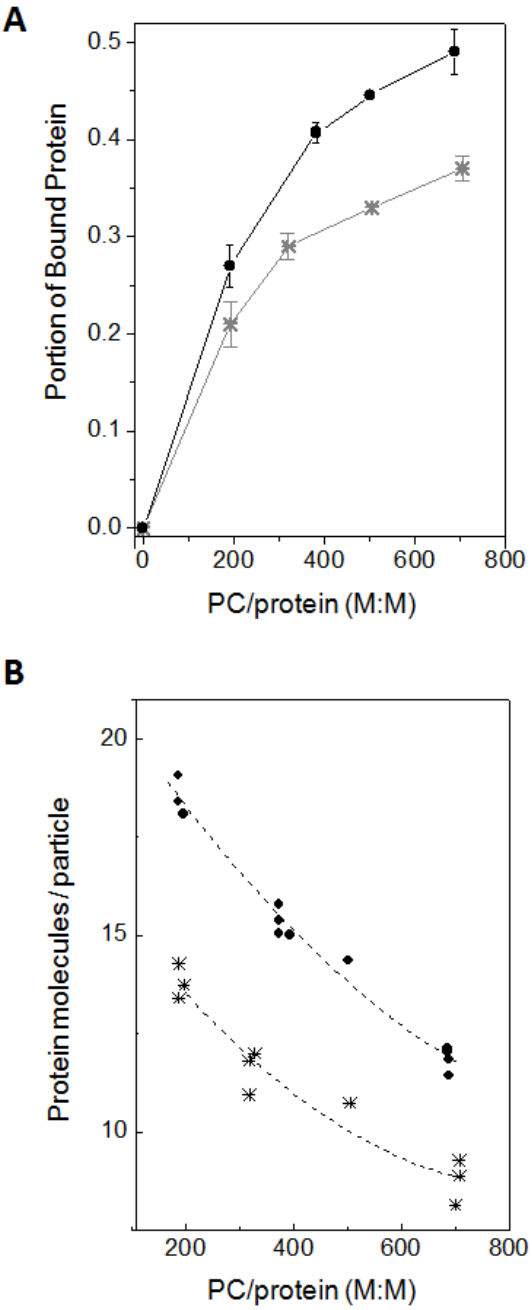

Figure 3.18 (A, B). Caption on next page.

Figure 3.18 (A, B): Binding of the WT apoA-I and the apoA-I[D89A/E91A/E92A] mutant to triglyceride-rich emulsion particles. (*A)* Portion of bound protein at different PC:protein ratios. (*B)* Bound WT apoA-I or apoA-I[D89A/E91A/E92A] per one emulsion particle. WT apoA-I (✳), apoA-I[D89A/E91A/E92A] (●).

3.5. Contribution of the residues 218 to 226 of apoA-I in the biogenesis of HDL

Previous studies showed that apoA-I deletion mutants that lack residues 220 to 231 have diminished capacity to promote cholesterol efflux and fail to synthesize HDL (*84;91*). The objective of the present study was to investigate the role of four hydrophobic residues (L218, L219, V221, L222) and two charged residues (E223, K226) on the biogenesis of HDL. These questions were addressed by the in vitro and in vivo studies described below.

3.5.1. Secretion of the WT and the two apoA-I mutants

The secretion in the culture medium of HTB-13 cells following transfection with recombinant adenoviruses expressing the WT or the mutant apoA-I proteins was assessed as described in the experimental procedures. This analysis showed that apoA-I[L218A/L219A/V221A/L222A] and apoA-I[E223A/K226A] were secreted at comparable levels in the culture medium (Fig. 3.4 B, D).

3.5.2. Expression of the apoA-I transgene following adenovirus infection

Total hepatic RNA was isolated from the mouse livers four days post infection with adenoviruses expressing the WT and the [L218A/L219A/V221A/L222A] and [E223A/K226A] mutant apoA-I forms. The relative expression of the WT and the mutant apoA-I transgenes was determined by qPCR as described in the experimental procedures. This analysis showed that the expression of WT and apoA-I[L218A/L219A/V221A/

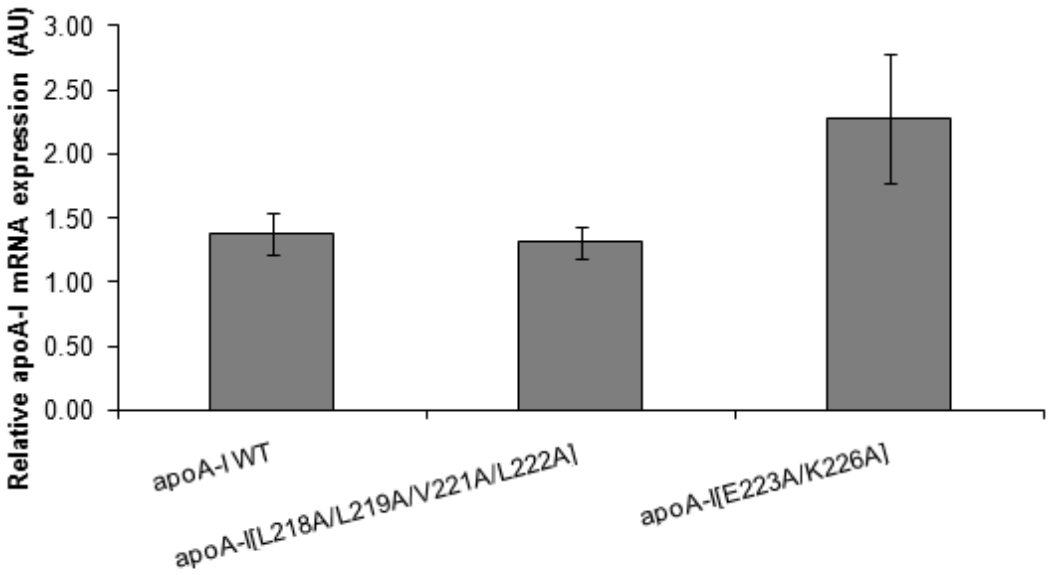

Figure 3.19: Hepatic apoA-I mRNA levels of mice infected with apoA-I expressing adenoviruses. Mice infected with $2x10^9$ adenoviruses expressing WT apoA-I, apoA-I[L218A/L219A/V221A/L222A] or apoA-I[E223A/K226A]. RNA was extracted from livers 4 days post-infection and apoA-I mRNA was quantitated by real time qPCR as described in experimental procedures.

L222A] were comparable, whereas the expression of apoA-I[E223A/K226A] was approximately 165% of that of WT apoA-I (Fig. 3.19).

3.5.3. Plasma lipid and apoA-I measurements

Plasma lipids and apoA-I were determined four days post infection of apoA-I$^{-/-}$mice with adenoviruses expressing the WT and the two apoA-I mutants. It was found that the [L218A/L219A/V221A/L222A] mutation decreased plasma cholesterol and apoA-I levels to approximately 10 % as compared to WT. The plasma cholesterol and apoA-I levels of [E223A/K226A] mutation were within the normal range (62% of total plasma cholesterol and 120% of plasma apoA-I as compared to WT apoA-I) (Fig. 3.20 A, B).

3.5.4. FPLC profiles of plasma isolated from apoA-I$^{-/-}$ mice infected with adenoviruses expressing the WT and the two apoA-I mutants

FPLC analysis of plasma from apoA-I$^{-/-}$ mice infected with the recombinant adenovirus expressing either WT apoA-I or the two apoA-I mutants showed that in all cases cholesterol was distributed in the HDL region and the HDL cholesterol peak of apoA-I[L218A/L219A/V221A/L222A] was greatly diminished (Fig. 3.21).

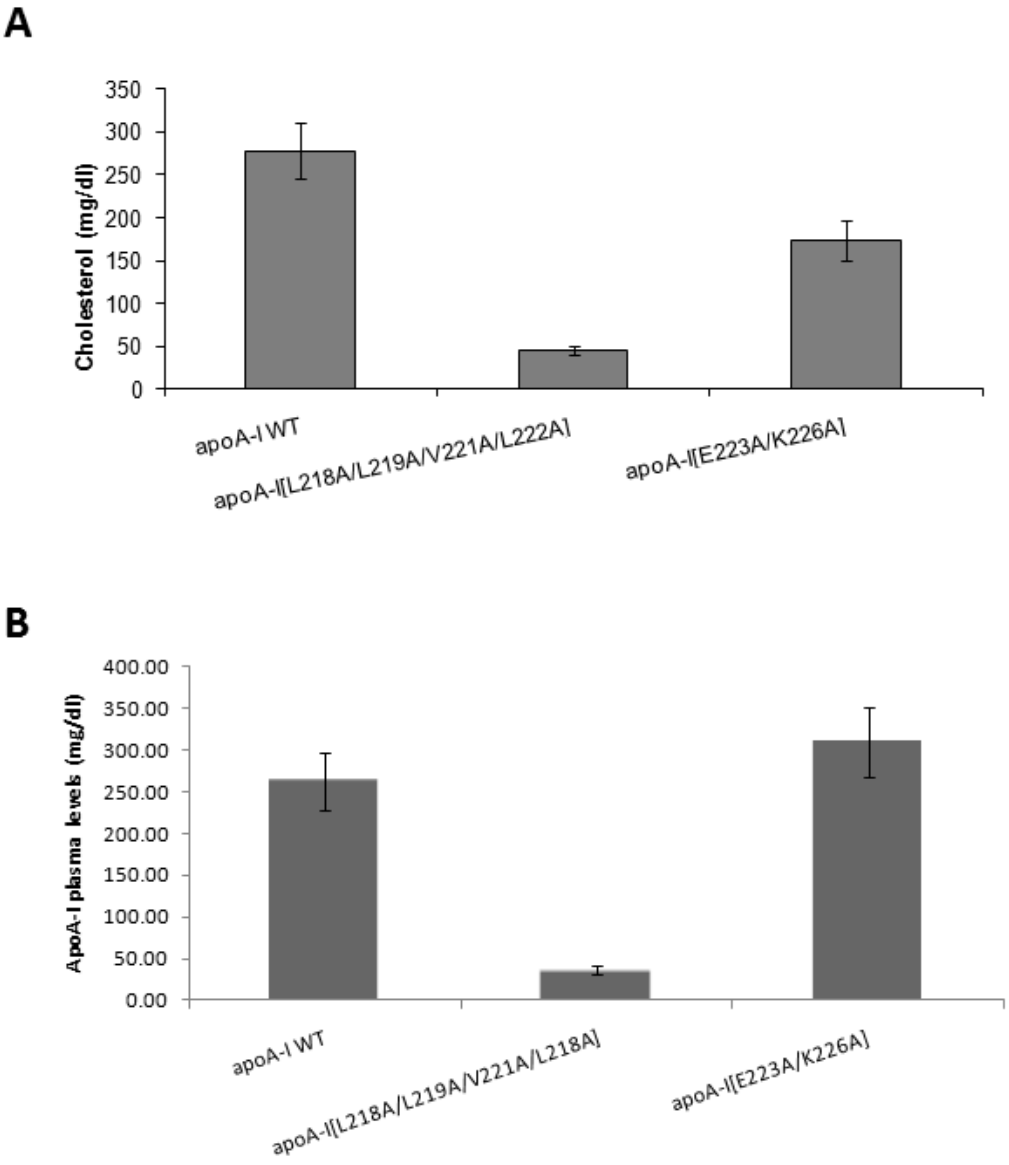

Figure 3.20 (A, B): Plasma lipid and apoA-I levels four days post infection of mice infected with apoA-I expressing adenoviruses. (*A*) Plasma cholesterol, (*B*) plasma apoA-I levels obtained from mice infected with adenovirus expressing WT apoA-I, apoA-I[L218A/L219A/V221A/L222A] or apoA-I[E223A/K226A].

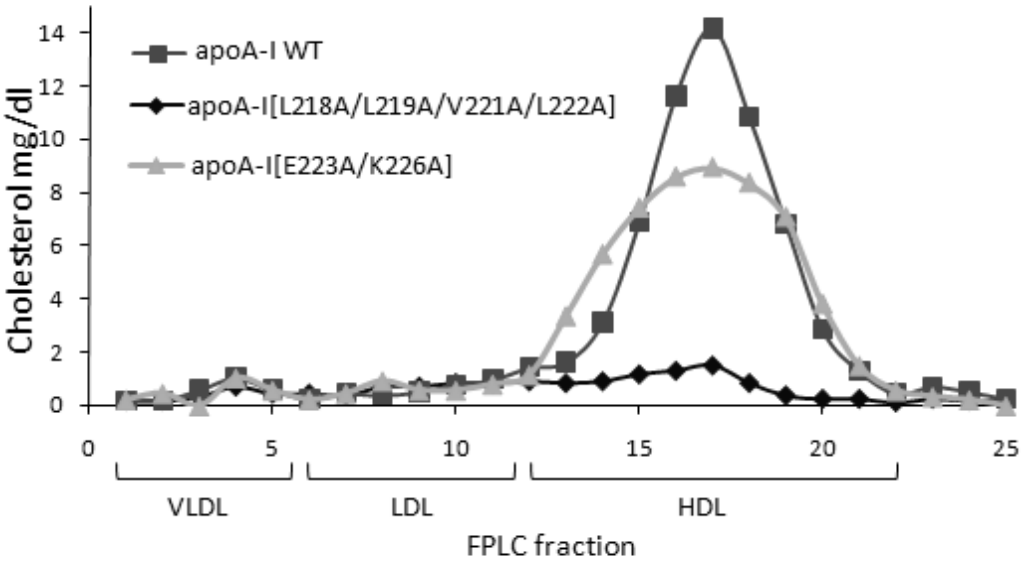

Figure 3.21: FPLC profile of total cholesterol of apoA-I$^{-/-}$ mice infected with adenoviruses expressing the WT apoA-I, apoA-I[L218A/L219A/V221A/L222A] or apoA-I[E223A/K226A] as indicated. Plasma samples were obtained 4 days post-infection.

3.5.5. Fractionation of plasma of mice expressing the WT and the two apoA-I mutants by density gradient ultracentrifugation

Fractionation of plasma by density gradient ultracentrifugation and subsequent analysis of the resulting fractions by SDS-PAGE showed that the WT apoA-I was equally distributed in the HDL_2 and HDL_3 region and the apoA-I[E223A/K226A] and apoA-I[L218A/L219A/V221A/L222A] were predominantly distributed in the HDL_3 and to a lesser extend the HDL2 region (Fig. 3.22 A-C). The apoA-I[L218A/L219A/V221A/L222A] mutant was characterized by low levels of apoA-I and increased levels of apoE that floated in the HDL2/3 but also in the VLDL/IDL/LDL region.

3.5.6. EM analysis of the HDL fraction

Analysis of the HDL fractions 6 and 7 obtained following density gradient ultracentrifugation by EM showed that the WT apoA-I as well as the two apoA-I mutants generated spherical particles (Fig. 3.22 D-F). The particles generated by the apoA-I[L218A/L219A/V221A/L222A] mutant appear smaller in size and may contain both apoA-I and apoE.

To ascertain the ability of the apoA-I[L218A/L219A/V221A/L222A] mutant to form HDL particles we used adenovirus mediated gene transfer in mice deficient in apoA-I and apoE. Separation of the plasma by density gradient ultracentrifugation showed that WT apoA-I was distributed in the HDL2 and HDL3 region and that in the case of apoA-I [L218A/L219A/V221A/L222A] very small amounts of apoA-I were

found in the HDL2/3 regions (Fig. 3.23 A, B). EM analysis of the fractions 6 and 7 obtained by density gradient ultracentrifugation of the plasma showed that WT apoA-I generated spherical particles whereas the apoA-I[L218A/L219A/V221A/L222A] failed to form HDL particles (Fig. 3.23 C, F).

3.5.7. Two-dimensional gel electrophoresis of plasma of mice expressing the WT and the two apoA-I mutants

Two-dimensional gel electrophoresis of plasma showed that WT apoA-I formed normal preβ and α HDL subpopulations, the apoA-I[E223A/K226A] contained predominantly α2, α3 and α4 and had increased preβ subpopulations whereas the apoA-I[L218A/L219A/V221A/L222A] had small amount of α4 and preβ subpopulations. The preβ subpopulations could be visualized by loading 2 μl of plasma as opposed to 0.5 μl used for WT apoA-I (Fig. 3.24 A-D).

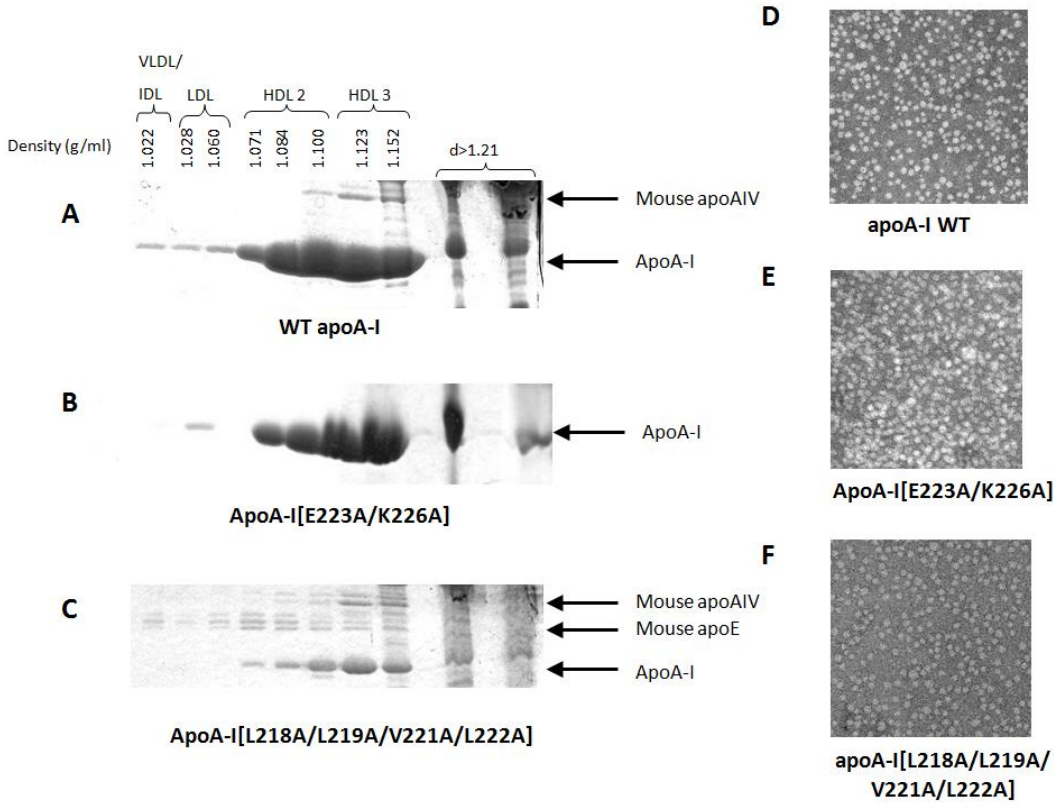

Figure 3.22 (A-F): Analysis of plasma of apoA-I$^{-/-}$ mice infected with adenoviruses expressing the WT apoA-I (*A*), apoA-I[L218A/L219A/V221A/ L222A] (*B*) or apoA-I[E223A/K226A] (*C*), by density gradient ultracentrifugation and SDS-PAGE. EM analysis of HDL fractions 6-7 obtained from apoA-I$^{-/-}$ mice expressing the WT apoA-I (*D)*, apoA-I[L218A/L219A/V221A/L222A] (*E*) or apoA-I[E223A/K226A] (*F*) following density gradient ultracentrifugation of plasma as indicated. The electron micrographs were taken at 75,000× magnification and enlarged 3 times.

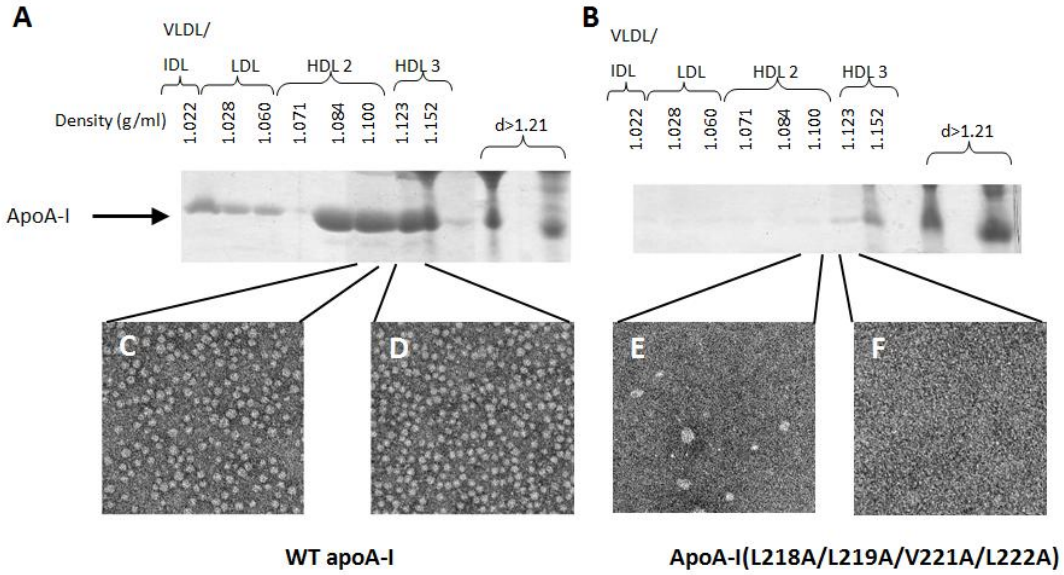

Figure 3.23 (A-F): Analysis of plasma of apoA-I$^{-/-}$ x apoE$^{-/-}$ mice infected with adenoviruses expressing the WT apoA-I (*A*) or apoA-I[L218A/L219A/ V221A/L222A] (*B*) by density gradient ultracentrifugation and SDS-PAGE. EM analysis of HDL fractions 6-7 obtained from apoA-I$^{-/-}$ x apoE$^{-/-}$ mice expressing the WT apoA-I (*C, D)* or apoA-I[L218A/L219A/V221A/L222A] (*E, F*) following density gradient ultracentrifugation of plasma as indicated. The electron micrographs were taken at 75,000× magnification and enlarged 3 times.

3.5.8. Physicochemical properties of the apoA-I[L218A/L219A/V221A/L222A] mutant

Preliminary physicochemical studies of the lipid-free apoA-I[L218A/L219A/ V221A/L222A] mutant were performed in collaboration with Dimitra Georgiadou at Dr. Stratikos lab at the National center for scientific research Demokritos, Greece. Two important finding of this analyses which are still under progress are:

1. There was a small but significant decrease in the α-helical content of the mutant protein as determined by CD.
2. There was a significant decrease of binding of ANS to the mutant protein as compared to WT apoA-I. This finding indicated a loss of hydrophobic exposed sites. This might occur if the mutated amino acids were part of an exposed hydrophobic surface or if the mutation caused structural changes that resulted in the burring of another normally exposed hydrophobic surface.

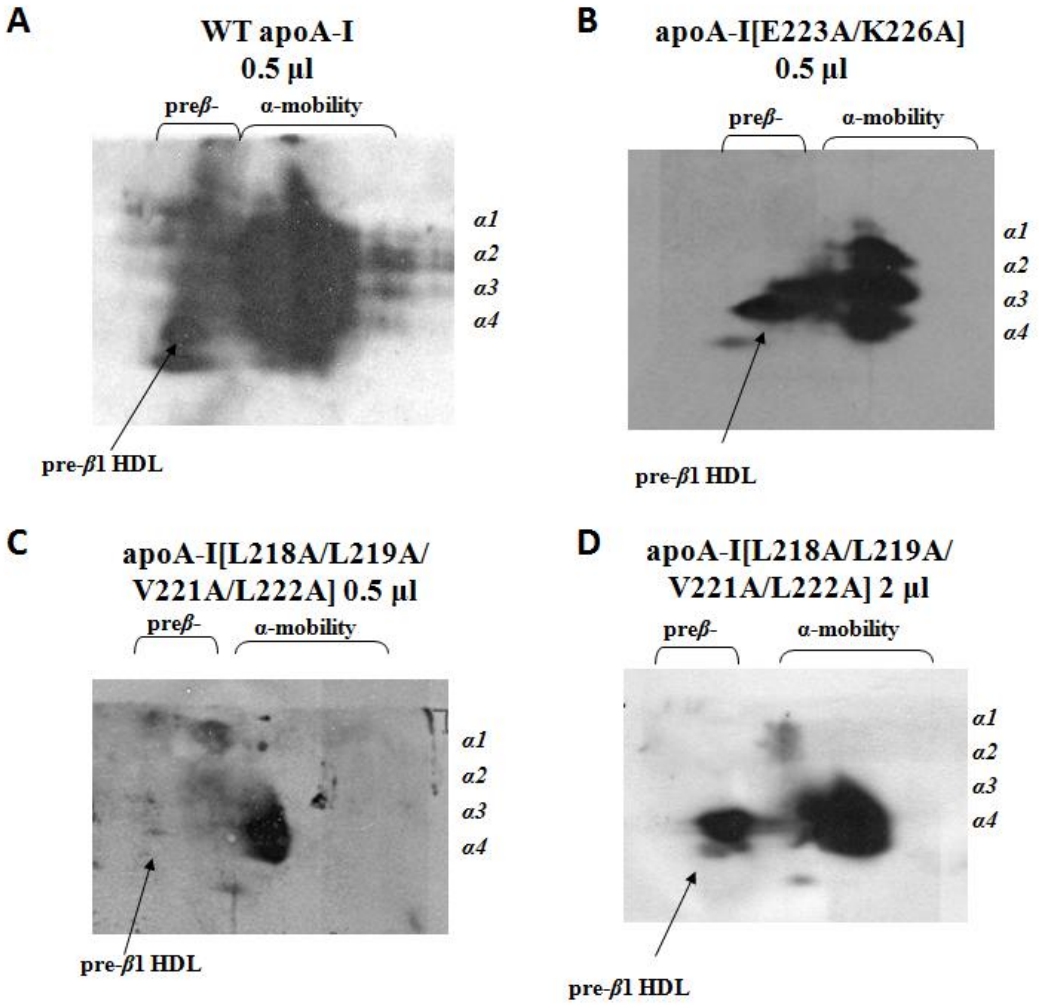

Figure 3.24 (A-D): Analysis of plasma obtained from mice expressing the WT apoA-I (*A*), apoA-I[E223A/K226A] (*B*) or apoA-I[L218A/L219A/V221A/L222A] (*C*, *D*), following two-dimensional gel electrophoresis and Western blotting.

4. DISCUSSION

The discussion encompasses Project I: section 4.1, Project II: section 4.2 and Collaborative projects: section 4.3. Section 4.1 deals with the consequences of the mutations in residues 89 to 99 of apoA-I on lipid homeostasis and the maturation of HDL. Section 4.2 deals with the consequences of the mutations in the region 218 to 226 on the biogenesis of HDL and section 4.3 summarizes collaborative studies on the effects of mutations in the region 218 to 222 and other regions of apoA-I on the bactericidal activity of apoA-I and its ability to promote retro-endocytosis in endothelial cells.

4.1. Project I: Alteration of negatively charged residues in the 89 to 99 domain of apoA-I affects lipid homeostasis and the maturation of HDL

4.1.1. Rationale for selection of the mutations

The 89-99 region of apoA-I contains several residues that are highly conserved in animal species and particularly in mammals (*474*). Thus amino acid position 89 is occupied in twenty nine species by D and has a conservative E substitution in two species. Positions 91 and 92 are occupied by negatively charged E and in few cases D residues in mammals and birds. Position 93 is occupied exclusively by hydrophobic residues in all species (predominantly V). The cluster of the positively charged K residues at positions 94 and 96 also shows remarkable sequence preservation in amphibian mammals and birds. Position 94 is occupied in twenty one species by K and in nine species by R whereas position 96 is occupied by K in all but one of the mammals and birds and diverges in fish (*474*). It is also interesting that non charged residues in the 89 to 99 region are

conserved. Positions 90, 93 and 97 are occupied mostly by V or other hydrophobic amino acids. Residues D89, E91 and E92 and residues K94 and K96 are located in the α11/3 helical wheel positions 2, 4, 5, 7 and 9 respectively. Residue D89 may form a strong solvent inaccessible salt bridge with residue R177 of the antiparallel helix and residues E92 and K96 may form weaker solvent inaccessible salt bridges with residues R173 and E169 respectively of the antiparallel helix. Residues E91 and K94 may interact with the aqueous phase.

Previous studies have shown that deletion of the 89-99 region of apoA-I caused dyslipidemia characterized by increased plasma cholesterol and phospholipids that were distributed in the VLDL/IDL region, decreased plasma PLTP activity and normal plasma triglycerides. The deletion caused a modest (20-30%) reduction in the capacity of the mutant protein to promote ABCA1 mediated cholesterol efflux and to activate LCAT *in vitro* (*252*). The drastic alteration of the structure of apoA-I caused by the 89-99 deletion may have caused realignment of the helices of apoA-I on the spherical HDL particles that may be responsible for the observed phenotype.

For these reasons we have chosen to probe further the importance of the 89-99 region of apoA-I by focusing on the impact of the conserved clusters of three negatively and two positively charged residues, on lipid homeostasis and the biogenesis of HDL in mouse models.

4.1.2. The apoA-I mutations D89A/E91A/E92A alter the functions of apoA-I, affect profoundly plasma triglyceride homeostasis and prevent the maturation of HDL

The present study showed that the expression of the apo-I[D89A/E91A/E92A] mutant in apoA-I$^{-/-}$ mice resulted in dyslipidemia characterized by severe hypertriglyceridemia, increased plasma cholesterol, decreased HDL cholesterol, reduced esterification of plasma cholesterol and the generation of few discoidal HDL particles and small size HDL particles that form preβ and α4-HDL subpopulations. The mutation caused only a minor 15% decrease in plasma PLTP activity (data not shown). On the other hand, the phenotype generated by adenovirus mediated gene transfer of apoA-I[K94A/K96A] in apoA-I$^{-/-}$ mice was normal. These findings suggested that the negatively charged D89, E91, and E92 residues of apoA-I are crucial for maintenance of plasma cholesterol and triglyceride homeostasis as well as the biogenesis and/or catabolism of HDL.

4.1.3. Changes in the structure and the lipid binding properties of the lipid-free apoA-I induced by the D89A/E91A/E92A and the K94A/K96A mutations

Estimation of the α-helical content and the thermodynamic stability by far-UV CD spectroscopy indicated that apoA-I[D89A/E91A/E92A] has 22 fewer residues in the α-helical conformation, slightly reduced thermal stability and greatly reduced cooperativity of thermal unfolding as compared to the WT apoA-I (Table VI). ANS fluorescence measurements indicated that the apoA-I [D89A/E91A/E92A] mutant has more

hydrophobic surfaces exposed to the solvent as compared to WT apoA-I, suggesting a looser tertiary folding of the mutant protein. Similar characteristics have been described for the apoA-I[E110A/E111A] and apoA-I[Δ(61-78)] mutants (*470*) that have been previously associated with dyslipidemia (*93;252*). The apoA-I[K94A/K96A] mutant had increased helical content and reduced cooperativity of thermal unfolding whereas the ANS characteristics and the DMPC clearance kinetics where similar to those of WT apoA-I.

4.1.4. Potential mechanism of dyslipidemia induced by the D89A/E91A/E92A mutations

The apoA-I[D89A/E91A/E92A] mutant has two similar characteristics with two other mutants in different regions of apoA-I, the apoA-I[Δ(61-78)] and the apoA-I [E110A/E111A] (*93;252*). The first characteristic is that all three mutants caused accumulation of apoA-I in the VLDL/IDL region and as shown previously this affects the *in vitro* lipolysis of the VLDL/IDL fraction by exogenous lipoprotein lipase (*93;252*). The second characteristic of the three apoA-I mutants is the negatively charged residues E78, D89 and E111 that occur in the WT sequence to have the ability to form solvent inaccessible salt bridges with positively charged residues present in the antiparallel apoA-I molecule of a discoidal HDL particle (*25*). The affinity of all three mutants for triglyceride rich lipoprotein particles is further supported by binding studies to triglyceride-rich emulsion particles (*475*).

Analysis of the 93 Å spherical HDL in solution by small angle neutron scattering (SANS) showed that apoA-I folds around a central lipid core that has 88.4 Å x 62.8 Å dimensions to form a spheroidal HDL (sHDL) particle. The following three possible arrangements of the apoA-I on the sHDL particle were considered. A model designated HdHp where two apoA-I molecules are arranged in anti-parallel planar orientation and a third molecule assumes a hairpin structure. A model designated 3Hp where three apoA-I molecules were folded as hairpins. A model designated integrated trimer (iT) where three apoA-I molecules interact with each other on the HDL surface (*34*). Similar but not identical arrangements were proposed in the "trefoil" model where the right hand half of two anti-parallel apoA-I molecules of the double belt model are displaced by 60° out of their planar position and are aligned in antiparallel orientation with a third molecule bent on a 60° angle (*39*). In these models the apoA-I monomers or dimers are juxtapositioned in the vicinity of helices 5 and 6 (*34;39*). In these arrangements of the apoA-I molecules on the sHDL particle residues E78 in helix 2, D89 in helix 3 and E111 in helix 4, can form solvent inaccessible salt bridges with residues R188 in helix 8, R177 in helix 7 and H155 in helix 6 respectively of the antiparallel strand. It is interesting that in the 11/3 α-helical wheel residues E78, D89 and E111 are all located in wheel position 2. With the exception of R188 all other five residues involved in salt bridges are conserved in mammals. Consistently with these observations temperature jump molecular dynamic simulation (*52;53*) indicated that the E89-R177 and E111-H155 are more stable than the E78-R188 salt bridge. Thus it is possible that elimination of the negatively charged residues D89 and E111 and to a lesser extend E78, may destabilize the inter-molecular

interactions of the apoA-I dimer or the hairpin bound to HDL and may predispose to dyslipidemia.

The interference of apoA-I[D89A/E91A/E92A] with lipolysis, was tested *in vivo* by co-infection of mice with adenoviruses expressing apoA-I[D89A/E91A/E92A] and the human lipoprotein lipase. This treatment abolished hypertriglyceridemia, restored in part the α1,2,3,4 HDL subpopulations, redistributed apoA-I in the HDL2 and HDL3 region, but did not alter the CE/TC ratio or the formation of discoidal HDL. The findings suggest that the increased abundance of apoA-I in the VLDL/IDL region may create lipoprotein lipase insufficiency that is responsible for the induction of hypertriglyceridemia.

The present study also indicates a direct effect of the [D89A/E91A/E92A] mutation in the activation of LCAT *in vivo*. This is documented by the persistence of the discoidal particles, the low CE/TC ratio and preponderance of the smaller α4 and α3 subpopulations following normalization of the plasma triglyceride levels by the lipoprotein lipase treatment. Previous studies showed that discoidal and small size HDL particles and LCAT associated with them may be catabolized fast by the kidney and thus lead to LCAT insufficiency and reduced plasma HDL levels (*78;134;141*). *In vitro* studies also indicated that increased catabolism by the kidney and the liver may also occur following triglyceride hydrolysis of the hypertriglyceridemic HDL by the hepatic lipase (*476*).

It is conceivable that loosening of the structure of apoA-I around the D89 or E92 area due to the substitution of the original residues by A, may provide new surfaces for interaction of HDL with other proteins or lipoprotein particles such as VLDL in ways that

inhibit triglyceride hydrolysis. Furthermore, the accumulation of discoidal HDL as well as the formation of preβ and small α4-HDL particles as shown by the *in vivo* experiments indicates that replacement of D89, E91 and E92 by A has a direct impact on the activation of LCAT. A schematic representation of this putative mechanism is shown in figure 4.1.

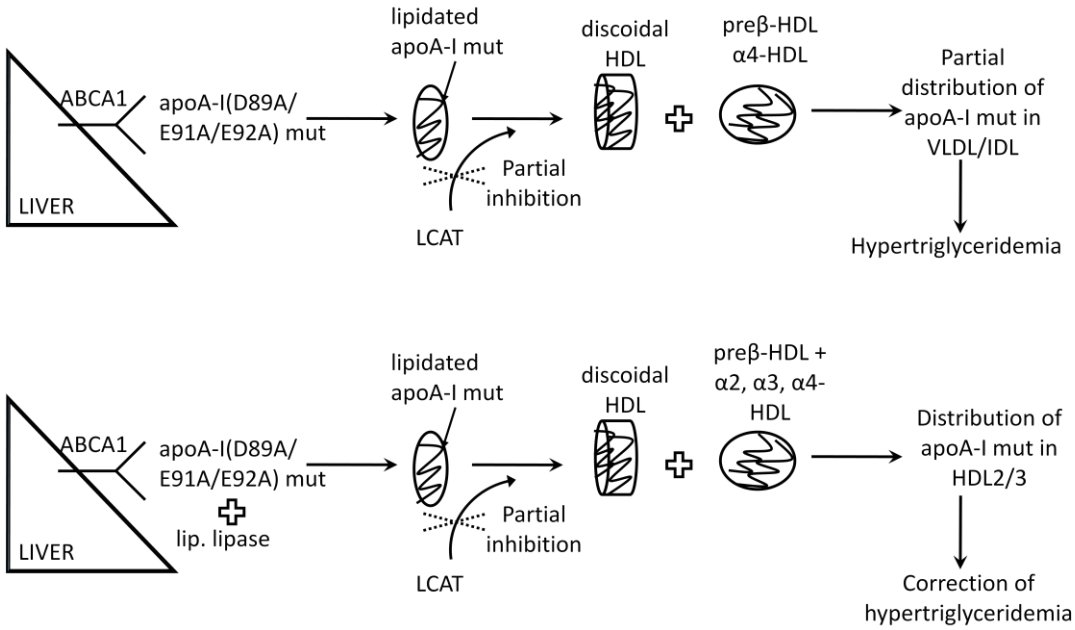

Figure 4.2. Schematic representation of the effect of apoA-I[D89A/E91A/E92A] on the induction of hypertriglyceridemia.

4.1.5. **Clinical implications**

Genome wide association studies provided statistical evidence that loci that affect HDL-C and triglyceride levels are associated with risk for coronary artery disease (*427*). The molecular etiology of most forms of hypertriglyceridemia in humans remains unclear. Early studies established that severe genetically transmitted hypertriglyceridemia occurs

as a result of mutations in lipoprotein lipase and apoCII (*477;478*). Subsequently, it has been shown that hypertriglyceridemia can be also induced by overexpression of apoCIII, apoCII, apoCI, apoA-II and apoE in transgenic mice, following adenovirus-mediated gene transfer (*479-484*) or by inactivation of the apoA-V gene in mice (*485*). In addition, in humans plasma apoE and apoCIII levels correlate with plasma triglyceride levels (*486;487*). Moderate hypertriglyceridemia has been observed in patients with Tangier disease, in carriers of apoA-I_{MILANO}, as well as in male carriers of apoA-IΔLys107 (*488-491*). These findings support the hypothesis that normal apoA-I structure and functions may be required for plasma triglyceride homeostasis.

The present and two previous studies (*93;252*) raise the possibility that subtle changes in the structure of apoA-I caused by mutations may induce hypertriglyceridemia. To the extent that similar mutations exist in humans, the genetic predisposition to hyprtriglyceridemia may be further aggravated by other genetic and environmental factors such as diabetes, thyroid status, etc. The potential contribution of apoA-I mutations to hypertriglyceridemia could be addressed in future studies in selected populations of patients with hypertriglyceridemia of unknown etiology.

4.2. Project II. Contribution of the residues 218 to 226 of apoA-I in the biogenesis of HDL

4.2.1. Rationale for selection of the mutations

Lipid-free or minimally lipidated apoA-I promote ABCA1-mediated cholesterol efflux and thus serve as acceptors of cellular phospholipid and cholesterol. The functional

interaction between apoA-I and ABCA1 are important for cholesterol efflux and also initiate the biogenesis of HDL (*68;69;91*).

The domains of apoA-I that are required for the functional interactions with ABCA1 were previously investigated by adenovirus mediated gene transfer in apoA-I-/- mice. This analysis showed that C-terminal deletion mutants that remove the 220-231 region of apoA-I prevent the biogenesis of normal α-HDL particles but allow the formation of preβ-HDL particles by processes which appear to be independent of apoA-I/ABCA1 interactions (*84;91*). To identify the specific residues of apoA-I that are required for interactions with ABCA1 that lead to the formation of HDL I generated a group of mutations that span the 218-230 region of apoA-I and include apoA-I[L218A/L219A/V221A/L222A], apoA-I[E223A/K226A], apoA-I[F225A/V227A/F229A/L230A] and apoA-I[L218A/L219A/V221A/L222A/F225A/V227A/F229A/L230A]. Detailed analyses were performed for the first two mutants.

4.2.2. Ability of apoA-I[L218A/L219A/V221A/L222A] mutant to promote biogenesis of HDL

Adenovirus mediated gene transfer of the WT apoA-I and apoA-I[L218A/L219A/V221A/L222A] in apoA-$I^{-/-}$ mice showed that at comparable levels of gene expression the plasma cholesterol and apoA-I levels of mice expressing apoA-I[L218A/L219A/V221A/L222A] were greatly reduced as compared to WT apoA-I. The reduction was due to the great decrease in the HDL cholesterol levels as determined by FPLC fractionation and density gradient ultracentrifugation of plasma. The ability of the mutant

apoA-I[L218A/L219A/V221A/L222A] to form HDL particles was assessed by EM analysis of HDL fractions obtained by fractionation of plasma of apoA-I deficient as well as both apoA-I x apoE double deficient mice following adenovirus mediated gene transfer. This analysis showed that compared to WT apoA-I the apoA-I[L218A/ L219A/V221A/L222A] mutant was mainly distributed in the HDL3 fraction and its quantity was greatly reduced. The HDL fraction contained also substantial amount of mouse apoE. The HDL fraction of the double deficient mice that were infected with apoA-I[L218A/L219A/V221A/L222A] mutant contained only small amounts of apoA-I in the HDL_3 and larger amounts in the lipoprotein-free (d>1.21 g/ml) fractions. The EM analysis showed absence of HDL particles in the plasma of double deficient mice but the presence of smaller size HDL particles in the plasma of apoA-I deficient mice that were infected with the apoA-I[L218A/L219A/V221A/L222A] mutant. Since the HDL fraction contained both apoA-I[L218A/L219A/V221A/L222A] mutant and mouse apoE it is possible that some of these particles may represent a mixture of apoA-I and apoE containing HDL. Two-dimensional gel electrophoresis of plasma showed that the apoA-I[L218A/L219A/V221A/L222A] generated preβ and α4 HDL particles in apoA-I deficient mice and did not show the presence of HDL particles in the double deficient mice. Taken together these data indicate that the apoA-I[L218A/L219A/V221A/L222A] mutation affected the biogenesis of HDL. It is possible that due to defective apoA-I/ABCA1 interactions the lipidation of HDL is defective and the particles formed are catabolized fast by the kidney (*78;140*). The defective interactions between ABCA1 and the mutant apoA-I give the opportunity to the mouse apoE to be lipidated and form apoE

containing HDL particles which float in the HDL2/HDL3 regions. The lipidated particles that contain the apoA-I[L218A/L219A/V221A/L222A] mutant accumulate in the plasma in the form of preβ and α4 HDL suggesting that the mutation also affected the conversion of the nascent to mature HDL particles that are enriched in the mature α3, α2 and α1 subpopulations that are generated in mice expressing the WT apoA-I. It has been previously shown that interactions of apoproteins with ABCA1 stabilize the transporter and protect it from degradation by thiol-proteases (*100;492*). Stabilization of ABCA1 by the mouse apoE may allow it to form HDL particles that contain both mouse apoE and the apoA-I[L218A/L219A/V221A/L222A] mutant that float in the HDL region.

The absence of both apoA-I and apoE in the double deficient mice destabilizes ABCA1 and this diminishes the lipidation of the apoA-I[L218A/L219A/V221A/ L222A] mutant and essentially prevents the biogenesis of HDL. This interpretation is supported by the density gradient ultracentrifugation analysis, EM and two-dimensional gel electrophoresis analyses of the plasma of the double deficient mice that were infected with the apoA-I[L218A/L219A/V221A/L222A] mutant that could not promote biogenesis of HDL particles. A schematic representation of this putative mechanism is shown in figure 4.2.

4.2.3. Ability of apoA-I[E223A/K226A] mutant to promote biogenesis of HDL

The studies with the apoA-I[E223A/K226A] mutant showed that at similar level of gene expression the plasma apoA-I levels and the EM profile were comparable, although the HDL was shifted towards the HDL3 region and total HDL cholesterol levels for the

mutant were 2/3 of that obtained from apoA-I$^{-/-}$ mice expressing WT apoA-I. Slight differences were also observed in the two-dimensional pattern of the mutant that contained increased ratio of preβ to α HDL particles and decreased α1HDL particles. Overall the data suggest that this mutation had only small but detectable effects on the biogenesis of HDL.

Complete interpretation of the data requires additional experiments of the apoA-I[L218A/L219A/V221A/L222A], apoA-I[F225A/V227A/F229A/L230A] and apoA-I[L218A/L219A/V221A/L222A/F225A/V227A/F229A/L230A] mutants.

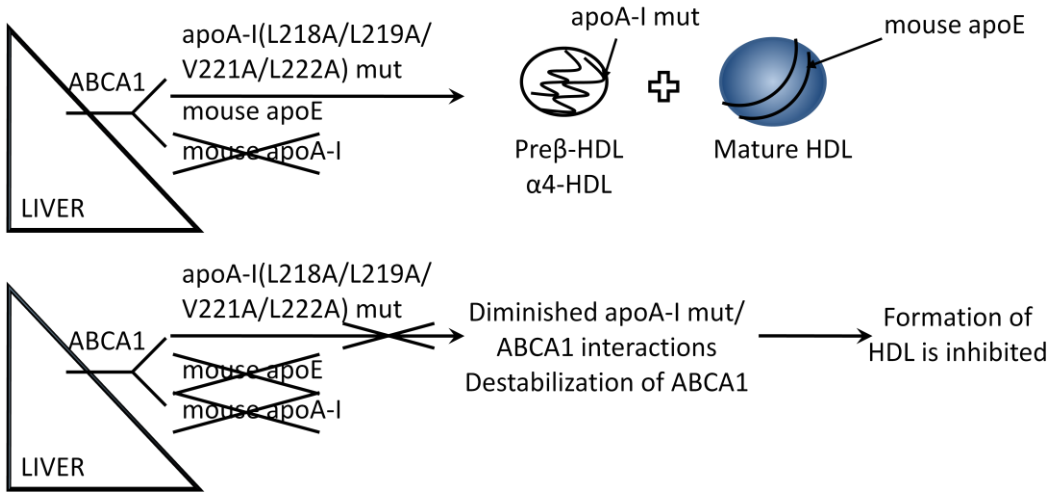

Figure 4.2. Schematic representation of the effect of apoA-I[L218A/L219A/V221A/L222A] on the biogenesis of HDL.

4.3. Collaborative projects

4.3.1. Carboxyl terminus of apolipoprotein A-I is necessary for the transport of lipid-free apoA-I but not prelipidated apoA-I particles through aortic endothelial cells

In collaboration with Dr. von Eckarstein's laboratory (Institute of Clinical Chemistry, University Hospital of Zurich) we have tested the ability of WT apoA-I and apoA-I[Δ(144-165)], apoA-I[Δ(185-243)], apoA-I[Δ(1-59)] and apoA-I[Δ(1-59/Δ185-243)] generated previously (*91*) and apoA-I[L218A/L219A/V221A/L222A] mutant generated in the context of this work to be transcytosed by endothelial cells. The most dramatic effect for binding and transcytosis was observed with the lipid-free apoA-I[Δ(185-243)] and apoA-I[L218A/L219A/V221A/L222A]) mutants. These mutants had had 80% decreased specific binding and 90% decreased specific transport by aortic endothelial cells. Following lipidation of these mutants the rHDL particles formed were transported through endothelial cells by ABCG1 and SR-BI dependent processes. Amino and combined amino and carboxy terminal apoA-I deletion mutants displayed increased non-specific binding but absence of specific binding or transport (*82*). My contribution was the purification of the WT and several of the mutant apoA-I forms that made the experiments described in figures 1, 2, 3, 5, 6 and 7 possible.

This work has been published in J Biol Chem. 2011 Mar 11;286(10):7744-54 and the complete article is attached.

4.3.2. Apolipoprotein A-I exerts bactericidal activity against *Yersinia enterocolitica* serotypre O:3

In a collaborative study with Dr. Jauhiainen's laboratory (Department of Chronic Disease Prevention, Public Health Genomics Research Unit, National Institute for Health and Welfare and FIMM, Institute for Molecular Medicine Finland, Helsinki) that is currently under review we tested the ability of WT apoA-I and various apoA-I mutants (apoA-I[Δ(220-243)], apoA-I[Δ(185-243)], apoA-I[Δ(1-59)/Δ(185-243)], apoA-I[Δ(61-78)], apoA-I[L218A/L219A/V221A/L222A] and apoA-I[E223A/K226A]) to affect the killing of *Yersinia enterocolitica* (Serotype O:3) by the complement pathway. It was shown that WT apoA-I kills 90-95% of the *Yersinia enterocolitica* (Serotype O:3) cultures whereas killing is inhibited by 80 to 90% by the C-terminal deletion mutants. A C-terminal apoA-I mutant [L218A/L219A/V221A/L222A] lost 80% of its bactericidal activity whereas apoA-I[E223A/K226A] and apoA-I[Δ(61-78)] mutants lost 45 and 20 % respectively of their bactericidal activity. These studies showed that lipid-free and HDL associated apoA-I had bactericidal activity. Furthermore apoA-I did not interact directly with the bacteria surface and the association of apoA-I with the bacteria required the exposure of the bacteria to the serum proteins.

My contribution has been the purification of the WT and several of the mutant apoA-I forms that made the experiments described in figure 4B possible. This manuscript is under review.

4.3.3. Mutation in apoA-I predicts increased risk of ishaemic heart disease and total mortality without low HDL cholesterol levels

This work has been performed in collaboration with Dr. Tybjaerg-Hansen and her colleagues at the Department of Clinical Biochemistry, Rigshospitalet, University of Copenhagen, Denmark and is currently in press in J Intern Med. 2011 Mar 28. doi: 10.1111 and is attached. Figure 2 and 3 of this manuscript describe the properties of apoA-I[L144R] and apoA-I[A164S] and were part of my Master's thesis. One of the major findings of the study was that heterozigosity for the apoA-I[A164S] substitution that has been identified by the Copenhagen City Heart Study and is present in one out of 500 of the general population, predicts risk for IHD and is associated with increased mortality (mean reduction of lifespan by 10 years). Interestingly heterozygote carriers for this mutant had normal plasma lipid and apoA-I levels a finding that was confirmed by adenovirus mediated gene transfer of the apoA-I[A164S] mutant in apoA-$I^{-/-}$ mice.

Additional work that contributed to this publication that was not in my Master's thesis was the determination of LpA-I levels and ratio of LpA-I over total plasma apoA-I in plasma of heterozygous carriers of apoA-I WT, apoA-I[A164S], apoA-I[L144R] and apoA-I[R160L] by two-dimensional gel electrophoresis (Figure 2C and D of the supplementary data). These analyses showed that the carriers of apoA-I[L144R] and apoA-I[R160L] mutations had decreased LpA-I to total apoA-I ratio as compared to non-carriers whereas the heterozygote carriers and non-carriers of apoA-I[A164S] mutation had similar LpA-I to total apoA-I ratio.

4.4. Future directions

The study of naturally occurring and bioengineered mutations contributes to the clarification of the molecular pathways that are involved in the several steps of biogenesis of HDL. It also helps develop new diagnostic methods and can also help in the prognosis and even the therapy of dyslipidemias.

The experimental approaches used in the present thesis will be used in future studies to investigate the functions of apoA-I mutants that affect the interactions of apoA-I with other important proteins of the HDL pathway such as LCAT, PLTP, and SR-BI.

Several viruses expressing mutant forms of apoA-I have been generated in this study. A next step is to complete the analysis of the two other C-terminal point mutants in the biogenesis of HDL and the mechanisms that lead to low HDL levels. In particular, I want to explore how the C-terminal mutations affect the stability of ABCA1.

Another study that could be a continuation of this work is to identify by Ala scanning mutagenesis of the apoA-I gene other residues of apoA-I that contribute to hypertriglyceridemia and also find the mechanism that accounts for the induction of hypertriglyceridemia (ie altered protein interactions). Furthermore I could analyse the role of the C-terminal mutations and the mutations that cause hypertriglyceridemia on the pathogenesis of atherosclerosis.

Based on the review of the literature it is clear that HDL and apoA-I have pleiotropic implications on pathways that do not exclusively involve lipid transport. It would be interesting to explore these functions and study the ability of HDL that contain specific apoA-I mutants to suppress induction of inflammatory cytokines from macrophages and

promote activation of eNOS in endothelial cells. These latter studies are crucial for the identification of important functions of HDL that contribute to atheroprotection and other human diseases.

5. REFERENCES

1. Brewer, H. B., Jr., Fairwell, T., LaRue, A., Ronan, R., Houser, A., and Bronzert, T. J. (1978) *Biochem. Biophys. Res. Commun. 80*, 623-630.

2. Zannis, V. I., Cole, F. S., Jackson, C. L., Kurnit, D. M., and Karathanasis, S. K. (1985) *Biochemistry 24*, 4450-4455.

3. Karathanasis, S. K., Zannis, V. I., and Breslow, J. L. (1983) *Proc. Natl. Acad. Sci. U. S. A 80*, 6147-6151.

4. Zannis, V. I., Chroni, A., and Krieger, M. (2006) *J. Mol. Med. 84*, 276-294.

5. Williamson, R., Lee, D., Hagaman, J., and Maeda, N. (1992) *Proc. Natl. Acad. Sci. U. S. A 89*, 7134-7138.

6. Rubin, E. M., Krauss, R. M., Spangler, E. A., Verstuyft, J. G., and Clift, S. M. (1991) *Nature 353*, 265-267.

7. Benoit, P., Emmanuel, F., Caillaud, J. M., Bassinet, L., Castro, G., Gallix, P., Fruchart, J. C., Branellec, D., Denefle, P., and Duverger, N. (1999) *Circulation 99*, 105-110.

8. Castelli, W. P., Doyle, J. T., Gordon, T., Hames, C. G., Hjortland, M. C., Hulley, S. B., Kagan, A., and Zukel, W. J. (1977) *Circulation 55*, 767-772.

9. Heiss, G. and Tyroler, H. Are apolipoproteins useful for evaluating ischemic heart disease? A brief overview of the literature. [83-1266], 7-24. 1982. Bethesda, MD, U.S. Department of Health and Human Services, National Institutes of Health. Proceedings of the Workshop on Apolipoprotein Quantification.

10. Glueck, C. J., Gartside, P., Fallat, R. W., Sielski, J., and Steiner, P. M. (1976) *J. Lab Clin. Med. 88*, 941-957.

11. Patsch, W., Kuisk, I., Glueck, C., and Schonfeld, G. (1981) *Arteriosclerosis 1*, 156-161.

12. Arinami, T., Hirano, T., Kobayashi, K., Yamanouchi, Y., and Hamaguchi, H. (1990) *Human Genetics 85*, 39-40.

13. Karathanasis, S. K., McPherson, J., Zannis, V. I., and Breslow, J. L. (1983) *Nature 304*, 371-373.

14. Sorci-Thomas, M. G. and Thomas, M. J. (2002) *Trends Cardiovasc. Med. 12*, 121-128.

15. Zannis, V. I., Kardassis, D., and Zanni, E. E. (1993) *Adv. Hum. Genet. 21*, 145-319.

16. Zannis, V. I., Kan, H. Y., Kritis, A., Zanni, E. E., and Kardassis, D. (2001) *Curr. Opin. Lipidol. 12*, 181-207.

17. Srivastava, R. and Srivastava, N. (2000) *Molecular and Cellular Biochemistry 209*, 131-144.

18. Malik, S. (2003) *Frontiers in Bioscience 8*, D360-D368.

19. Lewis, G. F. and Rader, D. J. (2005) *Circ. Res. 96*, 1221-1232.

20. Nolte, R. T. and Atkinson, D. (1992) *Biophys. J. 63*, 1221-1239.

21. Segrest, J. P., Jackson, R. L., Morrisett, J. D., and Gotto, A. M., Jr. (1974) *FEBS Lett. 38*, 247-258.

22. Rogers, D. P., Roberts, L. M., Lebowitz, J., Engler, J. A., and Brouillette, C. G. (1998) *Biochemistry 37*, 945-955.

23. Gursky, O. and Atkinson, D. (1996) *Proc. Natl. Acad. Sci. U. S. A 93*, 2991-2995.

24. Davidson, W. S., Arnvig-McGuire, K., Kennedy, A., Kosman, J., Hazlett, T. L., and Jonas, A. (1999) *Biochemistry 38*, 14387-14395.

25. Segrest, J. P., Jones, M. K., Klon, A. E., Sheldahl, C. J., Hellinger, M., De Loof, H., and Harvey, S. C. (1999) *J. Biol. Chem. 274*, 31755-31758.

26. Segrest, J. P. (1977) *Chem. Phys. Lipids 18*, 7-22.

27. Segrest, J. P., Li, L., Anantharamaiah, G. M., Harvey, S. C., Liadaki, K. N., and Zannis, V. (2000) *Curr. Opin. Lipidol. 11*, 105-115.

28. Panagotopulos, S. E., Horace, E. M., Maiorano, J. N., and Davidson, W. S. (2001) *J. Biol. Chem. 276*, 42965-42970.

29. Marcel, Y. L. and Kiss, R. S. (2003) *Curr. Opin. Lipidol. 14*, 151-157.

30. Martin, D. D., Budamagunta, M. S., Ryan, R. O., Voss, J. C., and Oda, M. N. (2006) *J. Biol. Chem.*

31. Borhani, D. W., Rogers, D. P., Engler, J. A., and Brouillette, C. G. (1997) *Proc. Natl. Acad. Sci. U. S. A 94*, 12291-12296.

32. Roosbeek, S., Vanloo, B., Duverger, N., Caster, H., Breyne, J., De, B., I, Patel, H., Vandekerckhove, J., Shoulders, C., Rosseneu, M., and Peelman, F. (2001) *J. Lipid Res. 42*, 31-40.

33. Gorshkova, I. N., Liu, T., Zannis, V. I., and Atkinson, D. (2002) *Biochemistry 41*, 10529-10539.

34. Wu, Z., Gogonea, V., Lee, X., May, R. P., Pipich, V., Wagner, M. A., Undurti, A., Tallant, T. C., Baleanu-Gogonea, C., Charlton, F., Ioffe, A., Didonato, J. A., Rye, K. A., and Hazen, S. L. (2011) *J. Biol. Chem.*

35. Zhang, L., Song, J., Cavigiolio, G., Ishida, B. Y., Zhang, S., Kane, J. P., Weisgraber, K. H., Oda, M. N., Rye, K. A., Pownall, H. J., and Ren, G. (2011) *J. Lipid Res. 52*, 175-184.

36. Thomas, M. J., Bhat, S., and Sorci-Thomas, M. G. (2008) *J. Lipid Res. 49*, 1875-1883.

37. Wu, Z., Wagner, M. A., Zheng, L., Parks, J. S., Shy, J. M., III, Smith, J. D., Gogonea, V., and Hazen, S. L. (2007) *Nat. Struct. Mol. Biol. 14*, 861-868.

38. Silva, R. A., Hilliard, G. M., Li, L., Segrest, J. P., and Davidson, W. S. (2005) *Biochemistry 44*, 8600-8607.

39. Silva, R. A., Huang, R., Morris, J., Fang, J., Gracheva, E. O., Ren, G., Kontush, A., Jerome, W. G., Rye, K. A., and Davidson, W. S. (2008) *Proc. Natl. Acad. Sci. U. S A 105*, 12176-12181.

40. Davidson, W. S. and Hilliard, G. M. (2003) *J. Biol. Chem. 278*, 27199-27207.

41. Breslow, J. L. (1991) *Annu. Rev. Med. 42*, 357-371.

42. Wang, J., Sykes, B. D., and Ryan, R. O. (2002) *Proc. Natl. Acad. Sci. U. S. A 99*, 1188-1193.

43. Oda, M. N., Forte, T. M., Ryan, R. O., and Voss, J. C. (2003) *Nat. Struct. Biol. 10*, 455-460.

44. Wang, L., Atkinson, D., and Small, D. M. (2005) *J. Biol. Chem. 280*, 4154-4165.

45. Lagerstedt, J. O., Cavigiolio, G., Budamagunta, M. S., Pagani, I., Voss, J. C., and Oda, M. N. (2011) *J. Biol. Chem. 286*, 2966-2975.

46. Bhat, S., Sorci-Thomas, M. G., Tuladhar, R., Samuel, M. P., and Thomas, M. J. (2007) *Biochemistry 46*, 7811-7821.

47. Bhat, S., Sorci-Thomas, M. G., Alexander, E. T., Samuel, M. P., and Thomas, M. J. (2005) *J. Biol. Chem. 280*, 33015-33025.

48. Tanaka, M., Koyama, M., Dhanasekaran, P., Nguyen, D., Nickel, M., Lund-Katz, S., Saito, H., and Phillips, M. C. (2008) *Biochemistry 47*, 2172-2180.

49. Catte, A., Patterson, J. C., Bashtovyy, D., Jones, M. K., Gu, F., Li, L., Rampioni, A., Sengupta, D., Vuorela, T., Niemela, P., Karttunen, M., Marrink, S. J., Vattulainen, I., and Segrest, J. P. (2008) *Biophys. J. 94*, 2306-2319.

50. Shih, A. Y., Sligar, S. G., and Schulten, K. (2008) *Biophys. J. 94*, L87-L89.

51. Vuorela, T., Catte, A., Niemela, P. S., Hall, A., Hyvonen, M. T., Marrink, S. J., Karttunen, M., and Vattulainen, I. (2010) *PLoS. Comput. Biol. 6*, e1000964.

52. Jones, M. K., Catte, A., Patterson, J. C., Gu, F. F., Chen, J. G., Li, L., and Segrest, J. P. (2009) *Biophysical Journal 96*, 354-371.

53. Gogonea, V., Wu, Z. P., Lee, X., Pipich, V., Li, X. M., Ioffe, A. I., Didonato, J. A., and Hazen, S. L. (2010) *Biochemistry 49*, 7323-7343.

54. Zannis, V. I., Chroni, A., Kypreos, K. E., Kan, H. Y., Cesar, T. B., Zanni, E. E., and Kardassis, D. (2004) *Curr Opin Lipidol. 15*, 151-166.

55. Barter, P. J., Brewer, H. B., Jr., Chapman, M. J., Hennekens, C. H., Rader, D. J., and Tall, A. R. (2003) *Arterioscler. Thromb. Vasc. Biol. 23*, 160-167.

56. Lusa, S., Jauhiainen, M., Metso, J., Somerharju, P., and Ehnholm, C. (1996) *Biochem. J. 313 (Pt 1)*, 275-282.

57. Krieger, M. (2001) *J. Clin. Invest 108*, 793-797.

58. Wang, N., Lan, D., Chen, W., Matsuura, F., and Tall, A. R. (2004) *Proc. Natl. Acad. Sci. U. S. A 101*, 9774-9779.

59. Ishida, T., Choi, S., Kundu, R. K., Hirata, K., Rubin, E. M., Cooper, A. D., and Quertermous, T. (2003) *J. Clin. Invest 111*, 347-355.

60. Krauss, R. M., Levy, R. I., and Fredrickson, D. S. (1974) *J. Clin. Invest 54*, 1107-1124.

61. Breckenridge, W. C., Little, J. A., Alaupovic, P., Wang, C. S., Kuksis, A., Kakis, G., Lindgren, F., and Gardiner, G. (1982) *Atherosclerosis 45*, 161-179.

62. Brunzell, J. D. and Deeb, S. S. (2001) in *The Metabolic & Molecular Bases of Inherited Disease* (Scriver, C. R., Beaudet, A. L., Valle, D., and Sly, W. S., Eds.) pp 2789-2816, McGraw-Hill, New York.

63. Zannis, V. I., Zanni, E. E., Papapanagiotou, A., Kardassis, D., and Chroni, A. (2006) in *High-Density Lipoproteins. From Basic Biology to Clinical Aspects* pp 237-265, Wiley-VCH, Weinheim.

64. Langmann, T., Klucken, J., Reil, M., Liebisch, G., Luciani, M. F., Chimini, G., Kaminski, W. E., and Schmitz, G. (1999) *Biochem. Biophys. Res. Commun. 257*, 29-33.

65. Kielar, D., Dietmaier, W., Langmann, T., Aslanidis, C., Probst, M., Naruszewicz, M., and Schmitz, G. (2001) *Clin. Chem. 47*, 2089-2097.

66. Neufeld, E. B., Demosky, S. J., Jr., Stonik, J. A., Combs, C., Remaley, A. T., Duverger, N., Santamarina-Fojo, S., and Brewer, H. B., Jr. (2002) *Biochem. Biophys. Res. Commun. 297*, 974-979.

67. Neufeld, E. B., Remaley, A. T., Demosky, S. J., Stonik, J. A., Cooney, A. M., Comly, M., Dwyer, N. K., Zhang, M., Blanchette-Mackie, J., Santamarina-Fojo, S., and Brewer, H. B., Jr. (2001) *J. Biol. Chem. 276*, 27584-27590.

68. Wang, N., Silver, D. L., Costet, P., and Tall, A. R. (2000) *J. Biol. Chem. 275*, 33053-33058.

69. Remaley, A. T., Stonik, J. A., Demosky, S. J., Neufeld, E. B., Bocharov, A. V., Vishnyakova, T. G., Eggerman, T. L., Patterson, A. P., Duverger, N. J., Santamarina-Fojo, S., and Brewer, H. B., Jr. (2001) *Biochem. Biophys. Res. Commun. 280*, 818-823.

70. Schmitz, G., Assmann, G., Robenek, H., and Brennhausen, B. (1985) *Proc. Natl. Acad. Sci. U. S. A 82*, 6305-6309.

71. Schmitz, G., Robenek, H., Lohmann, U., and Assmann, G. (1985) *EMBO J. 4*, 613-622.

72. Duong, P. T., Weibel, G. L., Lund-Katz, S., Rothblat, G. H., and Phillips, M. C. (2008) *J. Lipid Res. 49*, 1006-1014.

73. Brunham, L. R., Singaraja, R. R., and Hayden, M. R. (2006) *Annu. Rev. Nutr. 26*, 105-129.

74. Orso, E., Broccardo, C., Kaminski, W. E., Bottcher, A., Liebisch, G., Drobnik, W., Gotz, A., Chambenoit, O., Diederich, W., Langmann, T., Spruss, T., Luciani,

M. F., Rothe, G., Lackner, K. J., Chimini, G., and Schmitz, G. (2000) *Nat. Genet. 24*, 192-196.

75. Assmann, G., von Eckardstein, A., and Brewer, H. B. (2001) in *The Metabolic and Molecular Basis of Inherited Disease* (Scriver, C. R., Beaudet, A. L., Sly, W. S., and Valle, D., Eds.) pp 2937-2960, McGraw-Hill, New York.

76. McNeish, J., Aiello, R. J., Guyot, D., Turi, T., Gabel, C., Aldinger, C., Hoppe, K. L., Roach, M. L., Royer, L. J., de Wet, J., Broccardo, C., Chimini, G., and Francone, O. L. (2000) *Proc. Natl. Acad. Sci. U. S. A 97*, 4245-4250.

77. Christiansen-Weber, T. A., Voland, J. R., Wu, Y., Ngo, K., Roland, B. L., Nguyen, S., Peterson, P. A., and Fung-Leung, W. P. (2000) *Am. J. Pathol. 157*, 1017-1029.

78. Timmins, J. M., Lee, J. Y., Boudyguina, E., Kluckman, K. D., Brunham, L. R., Mulya, A., Gebre, A. K., Coutinho, J. M., Colvin, P. L., Smith, T. L., Hayden, M. R., Maeda, N., and Parks, J. S. (2005) *J. Clin. Invest 115*, 1333-1342.

79. Takahashi, Y. and Smith, J. D. (1999) *Proc. Natl. Acad. Sci. U. S. A 96*, 11358-11363.

80. Smith, J. D., Waelde, C., Horwitz, A., and Zheng, P. (2002) *J. Biol. Chem. 277*, 17797-17803.

81. Cavelier, C., Rohrer, L., and von Eckardstein, A. (2006) *Circulation Research 99*, 1060-1066.

82. Ohnsorg, P. M., Rohrer, L., Perisa, D., Kateifides, A., Chroni, A., Kardassis, D., Zannis, V. I., and von, E. A. (2011) *J. Biol. Chem. 286*, 7744-7754.

83. Iwamoto, N., Lu, R., Tanaka, N., Abe-Dohmae, S., and Yokoyama, S. (2010) *Arterioscler. Thromb. Vasc. Biol.*

84. Chroni, A., Koukos, G., Duka, A., and Zannis, V. I. (2007) *Biochemistry 46*, 5697-5708.

85. Marcil, M., Brooks-Wilson, A., Clee, S. M., Roomp, K., Zhang, L. H., Yu, L., Collins, J. A., van Dam, M., Molhuizen, H. O., Loubster, O., Ouellette, B. F., Sensen, C. W., Fichter, K., Mott, S., Denis, M., Boucher, B., Pimstone, S., Genest, J., Jr., Kastelein, J. J., and Hayden, M. R. (1999) *Lancet 354*, 1341-1346.

86. Francis, G. A., Knopp, R. H., and Oram, J. F. (1995) *J. Clin. Invest 96*, 78-87.

87. Bodzioch, M., Orso, E., Klucken, J., Langmann, T., Bottcher, A., Diederich, W., Drobnik, W., Barlage, S., Buchler, C., Porsch-Ozcurumez, M., Kaminski, W. E., Hahmann, H. W., Oette, K., Rothe, G., Aslanidis, C., Lackner, K. J., and Schmitz, G. (1999) *Nat. Genet. 22*, 347-351.

88. Rust, S., Rosier, M., Funke, H., Real, J., Amoura, Z., Piette, J. C., Deleuze, J. F., Brewer, H. B., Duverger, N., Denefle, P., and Assmann, G. (1999) *Nat. Genet. 22*, 352-355.

89. Brooks-Wilson, A., Marcil, M., Clee, S. M., Zhang, L. H., Roomp, K., van Dam, M., Yu, L., Brewer, C., Collins, J. A., Molhuizen, H. O., Loubser, O., Ouelette, B. F., Fichter, K., Ashbourne-Excoffon, K. J., Sensen, C. W., Scherer, S., Mott, S., Denis, M., Martindale, D., Frohlich, J., Morgan, K., Koop, B., Pimstone, S., Kastelein, J. J., and Hayden, M. R. (1999) *Nat. Genet. 22*, 336-345.

90. Lawn, R. M., Wade, D. P., Garvin, M. R., Wang, X., Schwartz, K., Porter, J. G., Seilhamer, J. J., Vaughan, A. M., and Oram, J. F. (1999) *J. Clin. Invest 104*, R25-R31.

91. Chroni, A., Liu, T., Gorshkova, I., Kan, H. Y., Uehara, Y., von Eckardstein, A., and Zannis, V. I. (2003) *J. Biol. Chem. 278*, 6719-6730.

92. Reardon, C. A., Kan, H. Y., Cabana, V., Blachowicz, L., Lukens, J. R., Wu, Q., Liadaki, K., Getz, G. S., and Zannis, V. I. (2001) *Biochemistry 40*, 13670-13680.

93. Chroni, A., Kan, H. Y., Kypreos, K. E., Gorshkova, I. N., Shkodrani, A., and Zannis, V. I. (2004) *Biochemistry 43*, 10442-10457.

94. Chroni, A., Liu, T., Fitzgerald, M. L., Freeman, M. W., and Zannis, V. I. (2004) *Biochemistry 43*, 2126-2139.

95. Remaley, A. T., Thomas, F., Stonik, J. A., Demosky, S. J., Bark, S. E., Neufeld, E. B., Bocharov, A. V., Vishnyakova, T. G., Patterson, A. P., Eggerman, T. L., Santamarina-Fojo, S., and Brewer, H. B. (2003) *J. Lipid Res. 44*, 828-836.

96. Fitzgerald, M. L., Morris, A. L., Chroni, A., Mendez, A. J., Zannis, V. I., and Freeman, M. W. (2004) *J. Lipid Res. 45*, 287-294.

97. Fitzgerald, M. L., Morris, A. L., Rhee, J. S., Andersson, L. P., Mendez, A. J., and Freeman, M. W. (2002) *J. Biol. Chem. 277*, 33178-33187.

98. Fitzgerald, M. L., Mendez, A. J., Moore, K. J., Andersson, L. P., Panjeton, H. A., and Freeman, M. W. (2001) *J. Biol. Chem. 276*, 15137-15145.

99. Vedhachalam, C., Ghering, A. B., Davidson, W. S., Lund-Katz, S., Rothblat, G. H., and Phillips, M. C. (2007) *Arterioscler. Thromb. Vasc. Biol.*

100. Hajj, H. H., Denis, M., Donna Lee, D. Y., Iatan, I., Nyholt, D., Ruel, I., Krimbou, L., and Genest, J. (2007) *J. Lipid Res.*

101. Yokoyama, S. (2006) *Arteriosclerosis Thrombosis and Vascular Biology 26*, 20-27.

102. Wang, N. and Tall, A. R. (2003) *Arteriosclerosis Thrombosis and Vascular Biology 23*, 1178-1184.

103. Oram, J. F. (2003) *Arterioscler. Thromb. Vasc. Biol. 23*, 720-727.

104. Denis, M., Haidar, B., Marcil, M., Bouvier, M., Krimbou, L., and Genest, J., Jr. (2004) *J. Biol. Chem. 279*, 7384-7394.

105. Brunham, L. R., Kruit, J. K., Iqbal, J., Fievet, C., Timmins, J. M., Pape, T. D., Coburn, B. A., Bissada, N., Staels, B., Groen, A. K., Hussain, M. M., Parks, J. S., Kuipers, F., and Hayden, M. R. (2006) *J. Clin. Invest 116*, 1052-1062.

106. Singaraja, R. R., Stahmer, B., Brundert, M., Merkel, M., Heeren, J., Bissada, N., Kang, M., Timmins, J. M., Ramakrishnan, R., Parks, J. S., Hayden, M. R., and Rinninger, F. (2006) *Arterioscler. Thromb. Vasc. Biol. 26*, 1821-1827.

107. Chambenoit, O., Hamon, Y., Marguet, D., Rigneault, H., Rosseneu, M., and Chimini, G. (2001) *J. Biol. Chem. 276*, 9955-9960.

108. Oram, J. F., Lawn, R. M., Garvin, M. R., and Wade, D. P. (2000) *J. Biol. Chem. 275*, 34508-34511.

109. Oram, J. F., Johnson, C. J., and Brown, T. A. (1987) *J. Biol. Chem. 262*, 2405-2410.

110. Lorenzi, I., von Eckardstein, A., Cavelier, C., Radosavljevic, S., and Rohrer, L. (2008) *Journal of Molecular Medicine-Jmm 86*, 171-183.

111. Singaraja, R. R., Brunham, L. R., Visscher, H., Kastelein, J. J., and Hayden, M. R. (2003) *Arterioscler. Thromb. Vasc. Biol. 23*, 1322-1332.

112. Joyce, C. W., Amar, M. J., Lambert, G., Vaisman, B. L., Paigen, B., Najib-Fruchart, J., Hoyt, R. F., Jr., Neufeld, E. D., Remaley, A. T., Fredrickson, D. S., Brewer, H. B., Jr., and Santamarina-Fojo, S. (2002) *Proc. Natl. Acad. Sci. U. S. A 99*, 407-412.

113. Aiello, R. J., Brees, D., Bourassa, P. A., Royer, L., Lindsey, S., Coskran, T., Haghpassand, M., and Francone, O. L. (2002) *Arterioscler. Thromb. Vasc. Biol. 22*, 630-637.

114. Haghpassand, M., Bourassa, P. A., Francone, O. L., and Aiello, R. J. (2001) *J. Clin. Invest 108*, 1315-1320.

115. Van Eck, M., Bos, I. S., Kaminski, W. E., Orso, E., Rothe, G., Twisk, J., Bottcher, A., Van Amersfoort, E. S., Christiansen-Weber, T. A., Fung-Leung, W. P., van Berkel, T. J., and Schmitz, G. (2002) *Proc. Natl. Acad. Sci. U. S. A 99*, 6298-6303.

116. Van Eck, M., Singaraja, R. R., Ye, D., Hildebrand, R. B., James, E. R., Hayden, M. R., and van Berkel, T. J. (2006) *Arterioscler. Thromb. Vasc. Biol. 26*, 929-934.

117. Vaisman, B. L., Lambert, G., Amar, M., Joyce, C., Ito, T., Shamburek, R. D., Cain, W. J., Fruchart-Najib, J., Neufeld, E. D., Remaley, A. T., Brewer, H. B., Jr., and Santamarina-Fojo, S. (2001) *J. Clin. Invest 108*, 303-309.

118. Groen, A. K., Bloks, V. W., Bandsma, R. H., Ottenhoff, R., Chimini, G., and Kuipers, F. (2001) *J. Clin. Invest 108*, 843-850.

119. Frikke-Schmidt, R., Nordestgaard, B. G., Stene, M. C., Sethi, A. A., Remaley, A. T., Schnohr, P., Grande, P., and Tybjaerg-Hansen, A. (2008) *JAMA 299*, 2524-2532.

120. Frikke-Schmidt, R., Nordestgaard, B. G., Jensen, G. B., Steffensen, R., and Tybjaerg-Hansen, A. (2008) *Arterioscler. Thromb. Vasc. Biol. 28*, 180-186.

121. Acuna-Alonzo, V., Flores-Dorantes, T., Kruit, J. K., Villarreal-Molina, T., Arellano-Campos, O., Hunemeier, T., Moreno-Estrada, A., Ortiz-Lopez, M. G., Villamil-Ramirez, H., Leon-Mimila, P., Villalobos-Comparan, M., Jacobo-Albavera, L., Ramirez-Jimenez, S., Sikora, M., Zhang, L. H., Pape, T. D., Granados-Silvestre, M. D., Montufar-Robles, I., Tito-Alvarez, A. M., Zurita-Salinas, C., Bustos-Arriaga, J., Cedillo-Barron, L., Gomez-Trejo, C., Barquera-Lozano, R., Vieira-Filho, J. P., Granados, J., Romero-Hidalgo, S., Huertas-Vazquez, A., Gonzalez-Martin, A., Gorostiza, A., Bonatto, S. L., Rodriguez-Cruz, M., Wang, L., Tusie-Luna, T., Aguilar-Salinas, C. A., Lisker, R., Moises, R. S., Menjivar, M., Salzano, F. M., Knowler, W. C., Bortolini, M. C., Hayden, M. R., Baier, L. J., and Canizales-Quinteros, S. (2010) *Hum. Mol. Genet.*

122. Zannis, V. I., Chroni, A., Liu, T., Liadaki, K. N., and Laccotripe, M. (2004) (Simionescu, M., Ed.) pp 33-72.

123. Jonas, A. (2000) *Biochim. Biophys. Acta 1529*, 245-256.

124. Chroni, A., Duka, A., Kan, H. Y., Liu, T., and Zannis, V. I. (2005) *Biochemistry 44*, 14353-14366.

125. Santamarina-Fojo, S., Hoeg, J. M., Assmann, G., and Brewer, H. B., Jr. (2001) in *The Metabolic & Molecular Bases of Inherited Disease* (Scriver, C. R., Beaudet, A. L., Sly, W. S., and Valle, D., Eds.) pp 2817-2834, McGraw-Hill, New York.

126. Shao, B., Cavigiolio, G., Brot, N., Oda, M. N., and Heinecke, J. W. (2008) *Proc. Natl. Acad. Sci. U. S A 105*, 12224-12229.

127. Calabresi, L., Baldassarre, D., Castelnuovo, S., Conca, P., Bocchi, L., Candini, C., Frigerio, B., Amato, M., Sirtori, C. R., Alessandrini, P., Arca, M., Boscutti, G., Cattin, L., Gesualdo, L., Sampietro, T., Vaudo, G., Veglia, F., Calandra, S., and Franceschini, G. (2009) *Circulation 120*, 628-635.

128. Calabresi, L., Favari, E., Moleri, E., Adorni, M. P., Pedrelli, M., Costa, S., Jessup, W., Gelissen, I. C., Kovanen, P. T., Bernini, F., and Franceschini, G. (2009) *Atherosclerosis 204*, 141-146.

129. Jones, M. K., Catte, A., Li, L., and Segrest, J. P. (2009) *Biochemistry 48*, 11196-11210.

130. Kuivenhoven, J. A., Pritchard, H., Hill, J., Frohlich, J., Assmann, G., and Kastelein, J. (1997) *J. Lipid Res. 38*, 191-205.

131. Miccoli, R., Bertolotto, A., Navalesi, R., Odoguardi, L., Boni, A., Wessling, J., Funke, H., Wiebusch, H., Eckardstein, A., and Assmann, G. (1996) *Circulation 94*, 1622-1628.

132. Pisciotta, L., Miccoli, R., Cantafora, A., Calabresi, L., Tarugi, P., Alessandrini, P., Bittolo, B. G., Franceschini, G., Cortese, C., Calandra, S., and Bertolini, S. (2003) *Atherosclerosis 167*, 335-345.

133. Navalesi, R., Miccoli, R., Odoguardi, L., Funke, H., von Eckardstein, A., Wiebusch, H., and Assmann, G. (1995) *Lancet 346*, 708-709.

134. Miettinen, H. E., Gylling, H., Miettinen, T. A., Viikari, J., Paulin, L., and Kontula, K. (1997) *Arterioscler. Thromb. Vasc. Biol. 17*, 83-90.

135. Miettinen, H. E., Jauhiainen, M., Gylling, H., Ehnholm, S., Palomaki, A., Miettinen, T. A., and Kontula, K. (1997) *Arterioscler. Thromb. Vasc. Biol. 17*, 3021-3032.

136. Daum, U., Langer, C., Duverger, N., Emmanuel, F., Benoit, P., Denefle, P., Chirazi, A., Cullen, P., Pritchard, P. H., Bruckert, E., Assmann, G., and von Eckardstein, A. (1999) *J. Mol. Med. 77*, 614-622.

137. Bruckert, E., von Eckardstein, A., Funke, H., Beucler, I., Wiebusch, H., Turpin, G., and Assmann, G. (1997) *Atherosclerosis 128*, 121-128.

138. Leren, T. P., Bakken, K. S., Daum, U., Ose, L., Berg, K., Assmann, G., and von Eckardstein, A. (1997) *J. Lipid Res. 38*, 121-131.

139. Haase, C. L., Frikke-Schmidt, R., Nordestgaard, B. G., Kateifides, A. K., Kardassis, D., Nielsen, L. B., Andersen, C. B., Kober, L., Johnsen, A. H., Grande, P., Zannis, V. I., and Tybjaerg-Hansen, A. (2011) *J. Intern. Med.*

140. Koukos, G., Chroni, A., Duka, A., Kardassis, D., and Zannis, V. I. (2007) *Biochem. J. 406*, 167-174.

141. Koukos, G., Chroni, A., Duka, A., Kardassis, D., and Zannis, V. I. (2007) *Biochemistry 46*, 10713-10721.

142. Amar, M. J., Shamburek, R. D., Vaisman, B., Knapper, C. L., Foger, B., Hoyt, R. F., Jr., Santamarina-Fojo, S., Brewer, H. B., Jr., and Remaley, A. T. (2009) *Metabolism 58*, 568-575.

143. Krieger, M. (1999) *Annu. Rev. Biochem. 68*, 523-558.

144. Acton, S., Rigotti, A., Landschulz, K. T., Xu, S., Hobbs, H. H., and Krieger, M. (1996) *Science 271*, 518-520.

145. Murao, K., Terpstra, V., Green, S. R., Kondratenko, N., Steinberg, D., and Quehenberger, O. (1997) *J. Biol. Chem. 272*, 17551-17557.

146. Acton, S. L., Scherer, P. E., Lodish, H. F., and Krieger, M. (1994) *J. Biol. Chem. 269*, 21003-21009.

147. Wang, N., Arai, T., Ji, Y., Rinninger, F., and Tall, A. R. (1998) *J. Biol. Chem. 273*, 32920-32926.

148. Ueda, Y., Royer, L., Gong, E., Zhang, J., Cooper, P. N., Francone, O., and Rubin, E. M. (1999) *J. Biol. Chem. 274*, 7165-7171.

149. Rigotti, A., Trigatti, B. L., Penman, M., Rayburn, H., Herz, J., and Krieger, M. (1997) *Proc. Natl. Acad. Sci. U. S. A 94*, 12610-12615.

150. Webb, N. R., de Beer, M. C., Yu, J., Kindy, M. S., Daugherty, A., van der Westhuyzen, D. R., and de Beer, F. C. (2002) *J. Lipid Res. 43*, 1421-1428.

151. Chroni, A., Nieland, T. J., Kypreos, K. E., Krieger, M., and Zannis, V. I. (2005) *Biochemistry 44*, 13132-13143.

152. Liadaki, K. N., Liu, T., Xu, S., Ishida, B. Y., Duchateaux, P. N., Krieger, J. P., Kane, J., Krieger, M., and Zannis, V. I. (2000) *J. Biol. Chem. 275*, 21262-21271.

153. Xu, S., Laccotripe, M., Huang, X., Rigotti, A., Zannis, V. I., and Krieger, M. (1997) *J. Lipid Res. 38*, 1289-1298.

154. Urban, S., Zieseniss, S., Werder, M., Hauser, H., Budzinski, R., and Engelmann, B. (2000) *J. Biol. Chem. 275*, 33409-33415.

155. Greene, D. J., Skeggs, J. W., and Morton, R. E. (2001) *J. Biol. Chem. 276*, 4804-4811.

156. Thuahnai, S. T., Lund-Katz, S., Williams, D. L., and Phillips, M. C. (2001) *J. Biol. Chem. 276*, 43801-43808.

157. Stangl, H., Hyatt, M., and Hobbs, H. H. (1999) *J. Biol. Chem. 274*, 32692-32698.

158. Gu, X., Lawrence, R., and Krieger, M. (2000) *J. Biol. Chem. 275*, 9120-9130.

159. Gu, X., Trigatti, B., Xu, S., Acton, S., Babitt, J., and Krieger, M. (1998) *J. Biol. Chem. 273*, 26338-26348.

160. Ji, Y., Jian, B., Wang, N., Sun, Y., Moya, M. L., Phillips, M. C., Rothblat, G. H., Swaney, J. B., and Tall, A. R. (1997) *J. Biol. Chem. 272*, 20982-20985.

161. Gu, X., Kozarsky, K., and Krieger, M. (2000) *J. Biol. Chem. 275*, 29993-30001.

162. Cuchel, M., Lund-Katz, S., Llera-Moya, M., Millar, J. S., Chang, D., Fuki, I., Rothblat, G. H., Phillips, M. C., and Rader, D. J. (2010) *Arterioscler. Thromb. Vasc. Biol. 30*, 526-532.

163. Parathath, S., Sahoo, D., Darlington, Y. F., Peng, Y., Collins, H. L., Rothblat, G. H., Williams, D. L., and Connelly, M. A. (2004) *J. Biol. Chem. 279*, 24976-24985.

164. Liu, T., Krieger, M., Kan, H. Y., and Zannis, V. I. (2002) *J. Biol. Chem. 277*, 21576-21584.

165. Vergeer, M., Korporaal, S. J. A., Franssen, R., Meurs, I., Out, R., Hovingh, G. K., Hoekstra, M., Sierts, J. A., Dallinga-Thie, G. M., Motazacker, M. M., Holleboom, A. G., Van Berkel, T. J. C., Kastelein, J. J. P., Van Eck, M., and Kuivenhoven, J. A. (2011) *New England Journal of Medicine 364*, 136-145.

166. Yates, M., Kolmakova, A., Zhao, Y., and Rodriguez, A. (2011) *Hum. Reprod.*

167. Out, R., Hoekstra, M., Spijkers, J. A., Kruijt, J. K., Van Eck, M., Bos, I. S., Twisk, J., and van Berkel, T. J. (2004) *J. Lipid Res. 45*, 2088-2095.

168. Out, R., Kruijt, J. K., Rensen, P. C., Hildebrand, R. B., De Vos, P., Van Eck, M., and van Berkel, T. J. (2004) *J. Biol. Chem. 279*, 18401-18406.

169. Out, R., Hoekstra, M., de Jager, S. C., Vos, P. D., van der Westhuyzen, D. R., Webb, N. R., Van Eck, M., Biessen, E. A., and van Berkel, T. J. (2005) *J. Lipid Res. 46*, 1172-1181.

170. Mardones, P., Quinones, V., Amigo, L., Moreno, M., Miquel, J. F., Schwarz, M., Miettinen, H. E., Trigatti, B., Krieger, M., VanPatten, S., Cohen, D. E., and Rigotti, A. (2001) *J. Lipid Res. 42*, 170-180.

171. Ji, Y., Wang, N., Ramakrishnan, R., Sehayek, E., Huszar, D., Breslow, J. L., and Tall, A. R. (1999) *J. Biol. Chem. 274*, 33398-33402.

172. Trigatti, B., Rayburn, H., Vinals, M., Braun, A., Miettinen, H., Penman, M., Hertz, M., Schrenzel, M., Amigo, L., Rigotti, A., and Krieger, M. (1999) *Proc. Natl. Acad. Sci. U. S. A 96*, 9322-9327.

173. Holm, T. M., Braun, A., Trigatti, B. L., Brugnara, C., Sakamoto, M., Krieger, M., and Andrews, N. C. (2002) *Blood 99*, 1817-1824.

174. Yesilaltay, A., Morales, M. G., Amigo, L., Zanlungo, S., Rigotti, A., Karackattu, S. L., Donahee, M. H., Kozarsky, K. F., and Krieger, M. (2006) *Endocrinology 147*, 1577-1588.

175. Yesilaltay, A., Morales, M. G., Amigo, L., Zanlungo, S., Rigotti, A., Karackattu, S. L., Donahee, M. H., Kozarsky, K. F., and Krieger, M. (2006) *Endocrinology 147*, 1577-1588.

176. Browne, R. W., Bloom, M. S., Shelly, W. B., Ocque, A. J., Huddleston, H. G., and Fujimoto, V. Y. (2009) *J. Assist. Reprod. Genet. 26*, 557-560.

177. Mineo, C., Yuhanna, I. S., Quon, M. J., and Shaul, P. W. (2003) *J. Biol. Chem. 278*, 9142-9149.

178. Shaul, P. W. (2003) *J. Physiol 547*, 21-33.

179. Yuhanna, I. S., Zhu, Y., Cox, B. E., Hahner, L. D., Osborne-Lawrence, S., Lu, P., Marcel, Y. L., Anderson, R. G., Mendelsohn, M. E., Hobbs, H. H., and Shaul, P. W. (2001) *Nat. Med. 7*, 853-857.

180. Li, X. A., Titlow, W. B., Jackson, B. A., Giltiay, N., Nikolova-Karakashian, M., Uittenbogaard, A., and Smart, E. J. (2002) *J. Biol. Chem. 277*, 11058-11063.

181. Gong, M., Wilson, M., Kelly, T., Su, W., Dressman, J., Kincer, J., Matveev, S. V., Guo, L., Guerin, T., Li, X. A., Zhu, W., Uittenbogaard, A., and Smart, E. J. (2003) *J. Clin. Invest 111*, 1579-1587.

182. Li, X. A., Guo, L., Dressman, J. L., Asmis, R., and Smart, E. J. (2005) *J. Biol. Chem. 280*, 19087-19096.

183. Arai, T., Wang, N., Bezouevski, M., Welch, C., and Tall, A. R. (1999) *J. Biol. Chem. 274*, 2366-2371.

184. Ueda, Y., Gong, E., Royer, L., Cooper, P. N., Francone, O. L., and Rubin, E. M. (2000) *J. Biol. Chem. 275*, 20368-20373.

185. Kozarsky, K. F., Donahee, M. H., Glick, J. M., Krieger, M., and Rader, D. J. (2000) *Arterioscler. Thromb. Vasc. Biol. 20*, 721-727.

186. Huszar, D., Varban, M. L., Rinninger, F., Feeley, R., Arai, T., Fairchild-Huntress, V., Donovan, M. J., and Tall, A. R. (2000) *Arterioscler. Thromb. Vasc. Biol. 20*, 1068-1073.

187. Braun, A., Trigatti, B. L., Post, M. J., Sato, K., Simons, M., Edelberg, J. M., Rosenberg, R. D., Schrenzel, M., and Krieger, M. (2002) *Circ. Res. 90*, 270-276.

188. Braun, A., Zhang, S., Miettinen, H. E., Ebrahim, S., Holm, T. M., Vasile, E., Post, M. J., Yoerger, D. M., Picard, M. H., Krieger, J. L., Andrews, N. C., Simons, M., and Krieger, M. (2003) *Proc. Natl. Acad. Sci. U. S. A 100*, 7283-7288.

189. Karackattu, S. L., Picard, M. H., and Krieger, M. (2005) *Arterioscler. Thromb. Vasc. Biol. 25*, 803-808.

190. Karackattu, S. L., Trigatti, B., and Krieger, M. (2006) *Arterioscler. Thromb. Vasc. Biol. 26*, 548-554.

191. Hildebrand, R. B., Lammers, B., Meurs, I., Korporaal, S. J., De Haan, W., Zhao, Y., Kruijt, J. K., Pratico, D., Schimmel, A. W., Holleboom, A. G., Hoekstra, M.,

Kuivenhoven, J. A., van Berkel, T. J., Rensen, P. C., and Van Eck, M. (2010) *Arterioscler. Thromb. Vasc. Biol.*

192. Zhang, S., Picard, M. H., Vasile, E., Zhu, Y., Raffai, R. L., Weisgraber, K. H., and Krieger, M. (2005) *Circulation 111*, 3457-3464.

193. Savary, S., Denizot, F., Luciani, M., Mattei, M., and Chimini, G. (1996) *Mamm. Genome 7*, 673-676.

194. Croop, J. M., Tiller, G. E., Fletcher, J. A., Lux, M. L., Raab, E., Goldenson, D., Son, D., Arciniegas, S., and Wu, R. L. (1997) *Gene 185*, 77-85.

195. Nakamura, K., Kennedy, M. A., Baldan, A., Bojanic, D. D., Lyons, K., and Edwards, P. A. (2004) *J. Biol. Chem. 279*, 45980-45989.

196. Klucken, J., Buchler, C., Orso, E., Kaminski, W. E., Porsch-Ozcurumez, M., Liebisch, G., Kapinsky, M., Diederich, W., Drobnik, W., Dean, M., Allikmets, R., and Schmitz, G. (2000) *Proc. Natl. Acad. Sci. U. S. A 97*, 817-822.

197. Venkateswaran, A., Repa, J. J., Lobaccaro, J. M., Bronson, A., Mangelsdorf, D. J., and Edwards, P. A. (2000) *J. Biol. Chem. 275*, 14700-14707.

198. Wang, N., Ranalletta, M., Matsuura, F., Peng, F., and Tall, A. R. (2006) *Arterioscler. Thromb. Vasc. Biol. 26*, 1310-1316.

199. Vaughan, A. M. and Oram, J. F. (2005) *J. Biol. Chem. 280*, 30150-30157.

200. Wang, X., Collins, H. L., Ranalletta, M., Fuki, I. V., Billheimer, J. T., Rothblat, G. H., Tall, A. R., and Rader, D. J. (2007) *J. Clin. Invest 117*, 2216-2224.

201. Kennedy, M. A., Barrera, G. C., Nakamura, K., Baldan, A., Tarr, P., Fishbein, M. C., Frank, J., Francone, O. L., and Edwards, P. A. (2005) *Cell Metab 1*, 121-131.

202. Yvan-Charvet, L., Ranalletta, M., Wang, N., Han, S., Terasaka, N., Li, R., Welch, C., and Tall, A. R. (2007) *J. Clin. Invest 117*, 3900-3908.

203. Out, R., Jessup, W., Le Goff, W., Hoekstra, M., Gelissen, I. C., Zhao, Y., Kritharides, L., Chimini, G., Kuiper, J., Chapman, M. J., Huby, T., van Berkel, T. J., and Van Eck, M. (2008) *Circ. Res. 102*, 113-120.

204. Stefulj, J., Panzenboeck, U., Becker, T., Hirschmugl, B., Schweinzer, C., Lang, I., Marsche, G., Sadjak, A., Lang, U., Desoye, G., and Wadsack, C. (2009) *Circulation Research 104*, 600-U79.

205. Zhang, Y., McGillicuddy, F. C., Hinkle, C. C., O'Neill, S., Glick, J. M., Rothblat, G. H., and Reilly, M. P. (2010) *Circulation 121*, 1347-1355.

206. Favari, E., Calabresi, L., Adorni, M. P., Jessup, W., Simonelli, S., Franceschini, G., and Bernini, F. (2009) *Biochemistry 48*, 11067-11074.

207. Rohrer, L., Cavelier, C., Fuchs, S., Schluter, M. A., Volker, W., and von Eckardstein, A. (2006) *Biochim. Biophys. Acta 1761*, 186-194.

208. Rohrer, L., Ohnsorg, P. M., Lehner, M., Landolt, F., Rinninger, F., and von Eckardstein, A. (2009) *Circ. Res. 104*, 1142-1150.

209. Martinez, L. O., Jacquet, S., Esteve, J. P., Rolland, C., Cabezon, E., Champagne, E., Pineau, T., Georgeaud, V., Walker, J. E., Terce, F., Collet, X., Perret, B., and Barbaras, R. (2003) *Nature 421*, 75-79.

210. Moser, T. L., Stack, M. S., Asplin, I., Enghild, J. J., Hojrup, P., Everitt, L., Hubchak, S., Schnaper, H. W., and Pizzo, S. V. (1999) *Proceedings of the National Academy of Sciences of the United States of America 96*, 2811-2816.

211. Radojkovic, C., Genoux, A., Pons, V., Combes, G., de Jonge, H., Champagne, E., Rolland, C., Perret, B., Collet, X., Terce, F., and Martinez, L. O. (2009) *Arteriosclerosis Thrombosis and Vascular Biology 29*, 1125-U214.

212. Fabre, A. C., Vantourout, P., Champagne, E., Terce, F., Rolland, C., Perret, B., Collet, X., Barbaras, R., and Martinez, L. O. (2006) *Cell Mol. Life Sci. 63*, 2829-2837.

213. Chung, B. H., Segrest, J. P., Ray, M. J., Brunzell, J. D., Hokanson, J. E., Krauss, R. M., Beaudrie, K., and Cone, J. T. (1986) *Methods Enzymol. 128*, 181-209.

214. Nichols, A. V., Krauss, R. M., and Musliner, T. A. (1986) *Methods Enzymol. 128*, 417-431.

215. Davidson, W. S., Sparks, D. L., Lund-Katz, S., and Phillips, M. C. (1994) *J. Biol. Chem. 269*, 8959-8965.

216. Asztalos, B. F., Brousseau, M. E., McNamara, J. R., Horvath, K. V., Roheim, P. S., and Schaefer, E. J. (2001) *Atherosclerosis 156*, 217-225.

217. Fielding, C. J. and Fielding, P. E. (1996) *Methods Enzymol. 263*, 251-259.

218. Asztalos, B. F., Sloop, C. H., Wong, L., and Roheim, P. S. (1993) *Biochim. Biophys. Acta 1169*, 291-300.

219. Fielding, C. J. and Fielding, P. E. (1995) *J. Lipid Res. 36*, 211-228.

220. Nanjee, M. N., Cooke, C. J., Olszewski, W. L., and Miller, N. E. (2000) *Arterioscler. Thromb. Vasc. Biol. 20*, 2148-2155.

221. Reichl, D., Hathaway, C. B., Sterchi, J. M., and Miller, N. E. (1991) *Eur. J. Clin. Invest 21*, 638-643.

222. Asztalos, B. F., Sloop, C. H., Wong, L., and Roheim, P. S. (1993) *Biochim. Biophys. Acta 1169*, 301-304.

223. Heideman, C. L. and Hoff, H. F. (1982) *Biochim. Biophys. Acta 711*, 431-444.

224. Smith, E. B., C.Ashall, and J.E.Walker. High density lipoprotein (HDL) subfractions in interstitial fluid from human aortic intima and atherosclerostic lesions. Biochem.Soc.Trans. 12, 843-844. 1984.
Ref Type: Generic

225. Nakamura, Y., Kotite, L., Gan, Y., Spencer, T. A., Fielding, C. J., and Fielding, P. E. (2004) *Biochemistry 43*, 14811-14820.

226. Castro, G. R. and Fielding, C. J. (1988) *Biochemistry 27*, 25-29.

227. Forte, T. M., Goth-Goldstein, R., Nordhausen, R. W., and McCall, M. R. (1993) *J. Lipid Res. 34*, 317-324.

228. Forte, T. M., Bielicki, J. K., Goth-Goldstein, R., Selmek, J., and McCall, M. R. (1995) *J. Lipid Res. 36*, 148-157.

229. Clay, M. A., Newnham, H. H., and Barter, P. J. (1991) *Arterioscler. Thromb. 11*, 415-422.

230. Hennessy, L. K., Kunitake, S. T., and Kane, J. P. (1993) *Biochemistry 32*, 5759-5765.

231. Settasatian, N., Duong, M., Curtiss, L. K., Ehnholm, C., Jauhiainen, M., Huuskonen, J., and Rye, K. A. (2001) *J. Biol. Chem. 276*, 26898-26905.

232. Weisgraber, K. H., Bersot, T. P., Mahley, R. W., Franceschini, G., and Sirtori, C. R. (1980) *J. Clin. Invest 66*, 901-907.

233. Franceschini, G., Sirtori, C. R., Capurso, A., Weisgraber, K. H., and Mahley, R. W. (1980) *J. Clin. Invest 66*, 892-900.

234. Weisgraber, K. H., Rall, S. C., Jr., Bersot, T. P., Mahley, R. W., Franceschini, G., and Sirtori, C. R. (1983) *J. Biol. Chem. 258*, 2508-2513.

235. Franceschini, G., Baio, M., Calabresi, L., Sirtori, C. R., and Cheung, M. C. (1990) *Biochim. Biophys. Acta 1043*, 1-6.

236. Utermann, G., Haas, J., Steinmetz, A., Paetzold, R., Rall, S. C., Jr., Weisgraber, K. H., and Mahley, R. W. (1984) *Eur. J. Biochem. 144*, 325-331.

237. Utermann, G., Feussner, G., Franceschini, G., Haas, J., and Steinmetz, A. (1982) *J. Biol. Chem. 257*, 501-507.

238. Rall, S. C., Jr., Weisgraber, K. H., Mahley, R. W., Ogawa, Y., Fielding, C. J., Utermann, G., Haas, J., Steinmetz, A., Menzel, H. J., and Assmann, G. (1984) *J. Biol. Chem. 259*, 10063-10070.

239. Funke, H., von Eckardstein, A., Pritchard, P. H., Karas, M., Albers, J. J., and Assmann, G. (1991) *J. Clin. Invest 87*, 371-376.

240. Nichols, W. C., Dwulet, F. E., Liepnieks, J., and Benson, M. D. (1988) *Biochem. Biophys. Res. Commun. 156*, 762-768.

241. Nichols, W. C., Gregg, R. E., Brewer, H. B., Jr., and Benson, M. D. (1990) *Genomics 8*, 318-323.

242. Schaefer, E. J., Ordovas, J. M., Law, S. W., Ghiselli, G., Kashyap, M. L., Srivastava, L. S., Heaton, W. H., Albers, J. J., Connor, W. E., Lindgren, F. T., and . (1985) *J. Lipid Res. 26*, 1089-1101.

243. Matsunaga, T., Hiasa, Y., Yanagi, H., Maeda, T., Hattori, N., Yamakawa, K., Yamanouchi, Y., Tanaka, I., Obara, T., and Hamaguchi, H. (1991) *Proc. Natl. Acad. Sci. U. S. A 88*, 2793-2797.

244. Recalde, D., Velez-Carrasco, W., Civeira, F., Cenarro, A., Gomez-Coronado, D., Ordovas, J. M., and Pocovi, M. (2001) *Atherosclerosis 154*, 613-623.

245. Gylling, H., Relas, H., Miettinen, H. E., Radhakrishnan, R., and Miettinen, T. A. (1996) *Atherosclerosis 127*, 239-243.

246. Wada, M., Iso, T., Asztalos, B. F., Takama, N., Nakajima, T., Seta, Y., Kaneko, K., Taniguchi, Y., Kobayashi, H., Nakajima, K., Schaefer, E. J., and Kurabayashi, M. (2009) *Atherosclerosis 207*, 157-161.

247. Pisciotta, L., Fasano, T., Calabresi, L., Bellocchio, A., Fresa, R., Borrini, C., Calandra, S., and Bertolini, S. (2008) *Atherosclerosis 198*, 145-151.

248. Dastani, Z., Dangoisse, C., Boucher, B., Desbiens, K., Krimbou, L., Dufour, R., Hegele, R. A., Pajukanta, P., Engert, J. C., Genest, J., and Marcil, M. (2006) *Atherosclerosis 185*, 127-136.

249. Favari, E., Gomaraschi, M., Zanotti, I., Bernini, F., Lee-Rueckert, M., Kovanen, P. T., Sirtori, C. R., Franceschini, G., and Calabresi, L. (2007) *J. Biol. Chem. 282*, 5125-5132.

250. Franceschini, G., Calabresi, L., Chiesa, G., Parolini, C., Sirtori, C. R., Canavesi, M., and Bernini, F. (1999) *Arterioscler. Thromb. Vasc. Biol. 19*, 1257-1262.

251. Weibel, G. L., Alexander, E. T., Joshi, M. R., Rader, D. J., Lund-Katz, S., Phillips, M. C., and Rothblat, G. H. (2007) *Arterioscler. Thromb. Vasc. Biol. 27*, 2022-2029.

252. Chroni, A., Kan, H. Y., Shkodrani, A., Liu, T., and Zannis, V. I. (2005) *Biochemistry 44*, 4108-4117.

253. Pussinen, P. J., Jauhiainen, M., Metso, J., Pyle, L. E., Marcel, Y. L., Fidge, N. H., and Ehnholm, C. (1998) *J. Lipid Res. 39*, 152-161.

254. Huuskonen, J., Olkkonen, V. M., Jauhiainen, M., and Ehnholm, C. (2001) *Atherosclerosis 155*, 269-281.

255. Jauhiainen, M., Metso, J., Pahlman, R., Blomqvist, S., van Tol, A., and Ehnholm, C. (1993) *J. Biol. Chem. 268*, 4032-4036.

256. Tu, A. Y., Nishida, H. I., and Nishida, T. (1993) *J. Biol. Chem. 268*, 23098-23105.

257. von Eckardstein, A., Jauhiainen, M., Huang, Y., Metso, J., Langer, C., Pussinen, P., Wu, S., Ehnholm, C., and Assmann, G. (1996) *Biochim. Biophys. Acta 1301*, 255-262.

258. Jiang, X. C., Bruce, C., Mar, J., Lin, M., Ji, Y., Francone, O. L., and Tall, A. R. (1999) *J. Clin. Invest 103*, 907-914.

259. Zeiher, A. M., Schachlinger, V., Hohnloser, S. H., Saurbier, B., and Just, H. (1994) *Circulation 89*, 2525-2532.

260. Li, X. P., Zhao, S. P., Zhang, X. Y., Liu, L., Gao, M., and Zhou, Q. C. (2000) *Int. J. Cardiol. 73*, 231-236.

261. Kuvin, J. T., Patel, A. R., Sidhu, M., Rand, W. M., Sliney, K. A., Pandian, N. G., and Karas, R. H. (2003) *Am. J. Cardiol. 92*, 275-279.

262. Kuvin, J. T., Ramet, M. E., Patel, A. R., Pandian, N. G., Mendelsohn, M. E., and Karas, R. H. (2002) *Am. Heart J. 144*, 165-172.

263. Ramet, M. E., Ramet, M., Lu, Q., Nickerson, M., Savolainen, M. J., Malzone, A., and Karas, R. H. (2003) *Journal of the American College of Cardiology 41*, 2288-2297.

264. Assanasen, C., Mineo, C., Seetharam, D., Yuhanna, I. S., Marcel, Y. L., Connelly, M. A., Williams, D. L., Llera-Moya, M., Shaul, P. W., and Silver, D. L. (2005) *J. Clin. Invest 115*, 969-977.

265. Kocher, O., Birrane, G., Tsukamoto, K., Fenske, S., Yesilaltay, A., Pal, R., Daniels, K., Ladias, J. A. A., and Krieger, M. (2010) *Journal of Biological Chemistry 285*, 34999-35010.

266. Kocher, O., Yesilaltay, A., Cirovic, C., Pal, R., Rigotti, A., and Krieger, M. (2003) *J. Biol. Chem. 278*, 52820-52825.

267. Nofer, J. R., van der, G. M., Tolle, M., Wolinska, I., von Wnuck, L. K., Baba, H. A., Tietge, U. J., Godecke, A., Ishii, I., Kleuser, B., Schafers, M., Fobker, M., Zidek, W., Assmann, G., Chun, J., and Levkau, B. (2004) *J. Clin. Invest 113*, 569-581.

268. Shaul, P. W. and Mineo, C. (2004) *J. Clin. Invest 113*, 509-513.

269. Drew, B. G., Fidge, N. H., Gallon-Beaumier, G., Kemp, B. E., and Kingwell, B. A. (2004) *Proc. Natl. Acad. Sci. U. S. A 101*, 6999-7004.

270. Silver, D. L., Wang, N., Xiao, X., and Tall, A. R. (2001) *J. Biol. Chem. 276*, 25287-25293.

271. Yao, Y., Shao, E. S., Jumabay, M., Shahbazian, A., Ji, S., and Bostrom, K. I. (2008) *Arterioscler. Thromb. Vasc. Biol. 28*, 2266-2274.

272. Nofer, J. R., Remaley, A. T., Feuerborn, R., Wolinska, I., Engel, T., von Eckardstein, A., and Assmann, G. (2006) *Journal of Lipid Research 47*, 794-803.

273. Tsukamoto, K., Hirano, K., Tsujii, K., Ikegami, C., Zhongyan, Z., Nishida, Y., Ohama, T., Matsuura, F., Yamashita, S., and Matsuzawa, Y. (2001) *Biochemical and Biophysical Research Communications 287*, 757-765.

274. Zannis, V. I., Kypreos, K. E., Chroni, A., Kardassis, D., and Zanni, E. E. (2004) in *Molecular Mechanisms of Atherosclerosis* (Loscalzo, J., Ed.) pp 111-174, Taylor & Francis, New York, NY.

275. Cybulsky, M. I. and Gimbrone, M. A., Jr. (1991) *Science 251*, 788-791.

276. Peters, W. and Charo, I. F. (2001) *Curr Opin Lipidol. 12*, 175-180.

277. Navab, M., Hama, S. Y., Anantharamaiah, G. M., Hassan, K., Hough, G. P., Watson, A. D., Reddy, S. T., Sevanian, A., Fonarow, G. C., and Fogelman, A. M. (2000) *J. Lipid Res. 41*, 1495-1508.

278. Navab, M., Hama, S. Y., Cooke, C. J., Anantharamaiah, G. M., Chaddha, M., Jin, L., Subbanagounder, G., Faull, K. F., Reddy, S. T., Miller, N. E., and Fogelman, A. M. (2000) *J. Lipid Res. 41*, 1481-1494.

279. Cockerill, G. W., Rye, K. A., Gamble, J. R., Vadas, M. A., and Barter, P. J. (1995) *Arterioscler. Thromb. Vasc. Biol. 15*, 1987-1994.

280. Bursill, C. A., Castro, M. L., Beattie, D. T., Nakhla, S., van, d., V, Heather, A. K., Barter, P. J., and Rye, K. A. (2010) *Arterioscler. Thromb. Vasc. Biol. 30*, 1773-1778.

281. Nobecourt, E., Tabet, F., Lambert, G., Puranik, R., Bao, S., Yan, L., Davies, M. J., Brown, B. E., Jenkins, A. J., Dusting, G. J., Bonnet, D. J., Curtiss, L. K., Barter, P. J., and Rye, K. A. (2010) *Arterioscler. Thromb. Vasc. Biol. 30*, 766-772.

282. Okura, H., Yamashita, S., Ohama, T., Saga, A., Yamamoto-Kakuta, A., Hamada, Y., Sougawa, N., Ohyama, R., Sawa, Y., and Matsuyama, A. (2010) *Journal of Atherosclerosis and Thrombosis 17*, 568-577.

283. Norata, G. D., Callegari, E., Marchesi, M., Chiesa, G., Eriksson, P., and Catapano, A. L. (2005) *Circulation 111*, 2805-2811.

284. Nicholls, S. J., Dusting, G. J., Cutri, B., Bao, S., Drummond, G. R., Rye, K. A., and Barter, P. J. (2005) *Circulation 111*, 1543-1550.

285. Tabet, F., Remaley, A. T., Segaliny, A. I., Millet, J., Yan, L., Nakhla, S., Barter, P. J., Rye, K. A., and Lambert, G. (2010) *Arterioscler. Thromb. Vasc. Biol. 30*, 246-252.

286. Gomaraschi, M., Calabresi, L., Rossoni, G., Iametti, S., Franceschini, G., Stonik, J. A., and Remaley, A. T. (2008) *J. Pharmacol. Exp. Ther. 324*, 776-783.

287. Tolle, M., Pawlak, A., Schuchardt, M., Kawamura, A., Tietge, U. J., Lorkowski, S., Keul, P., Assmann, G., Chun, J., Levkau, B., van der Giet, M., and Nofer, J. R. (2008) *Arteriosclerosis Thrombosis and Vascular Biology 28*, 1542-1548.

288. Murphy, A. J., Woollard, K. J., Hoang, A., Mukhamedova, N., Stirzaker, R. A., McCormick, S. P., Remaley, A. T., Sviridov, D., and Chin-Dusting, J. (2008) *Arterioscler. Thromb. Vasc. Biol. 28*, 2071-2077.

289. Patel, S., Drew, B. G., Nakhla, S., Duffy, S. J., Murphy, A. J., Barter, P. J., Rye, K. A., Chin-Dusting, J., Hoang, A., Sviridov, D., Celermajer, D. S., and Kingwell, B. A. (2009) *J. Am. Coll. Cardiol. 53*, 962-971.

290. Mythreye, K., Satterwhite, L. L., Davidson, W. S., and Goldschmidt-Clermont, P. J. (2008) *Biochim. Biophys. Acta 1781*, 703-709.

291. Tang, C., Vaughan, A. M., and Oram, J. F. (2004) *J. Biol. Chem. 279*, 7622-7628.

292. Tang, C. R., Liu, Y. H., Kessler, P. S., Vaughan, A. M., and Oram, J. F. (2009) *Journal of Biological Chemistry 284*, 32336-32343.

293. Dimmeler, S., Haendeler, J., and Zeiher, A. M. (2002) *Curr. Opin. Lipidol. 13*, 531-536.

294. Li, D., Yang, B., and Mehta, J. L. (1998) *Am. J. Physiol 275*, H568-H576.

295. Choy, J. C., Granville, D. J., Hunt, D. W., and McManus, B. M. (2001) *J. Mol. Cell Cardiol. 33*, 1673-1690.

296. Dimmeler, S., Breitschopf, K., Haendeler, J., and Zeiher, A. M. (1999) *J. Exp. Med. 189*, 1815-1822.

297. Welch, G. N. and Loscalzo, J. (1998) *N. Engl. J. Med. 338*, 1042-1050.

298. Strawn, W. B. and Ferrario, C. M. (2002) *Curr. Opin. Lipidol. 13*, 505-512.

299. Sugano, M., Tsuchida, K., and Makino, N. (2000) *Biochem. Biophys. Res. Commun. 272*, 872-876.

300. Nofer, J. R., Levkau, B., Wolinska, I., Junker, R., Fobker, M., von Eckardstein, A., Seedorf, U., and Assmann, G. (2001) *J. Biol. Chem. 276*, 34480-34485.

301. Suc, I., Escargueil-Blanc, I., Troly, M., Salvayre, R., and Negre-Salvayre, A. (1997) *Arterioscler. Thromb. Vasc. Biol. 17*, 2158-2166.

302. Vantourout, P., Radojkovic, C., Lichtenstein, L., Pons, V., Champagne, E., and Martinez, L. O. (2010) *World J. Gastroenterol. 16*, 5925-5935.

303. Kimura, T., Sato, K., Malchinkhuu, E., Tomura, H., Tamama, K., Kuwabara, A., Murakami, M., and Okajima, F. (2003) *Arterioscler. Thromb. Vasc. Biol. 23*, 1283-1288.

304. Okajima, F., Sato, K., and Kimura, T. (2009) *Endocr. J. 56*, 317-334.

305. de Souza, J. A., Vindis, C., Negre-Salvayre, A., Rye, K. A., Couturier, M., Therond, P., Chantepie, S., Salvayre, R., Chapman, M. J., and Kontush, A. (2010) *J. Cell Mol. Med. 14*, 608-620.

306. Kontush, A. and Chapman, M. J. (2010) *Current Opinion in Lipidology 21*, 312-318.

307. de Souza, J. A., Vindis, C., Hansel, B., Negre-Salvayre, A., Therond, P., Serrano, C. V., Chantepie, S., Salvayre, R., Bruckert, E., Chapman, M. J., and Kontush, A. (2008) *Atherosclerosis 197*, 84-94.

308. Brodeur, M. R., Brissette, L., Falstrault, L., and Moreau, R. (2008) *J. Cell Biochem. 105*, 1374-1385.

309. Noor, R., Shuaib, U., Wang, C. X., Todd, K., Ghani, U., Schwindt, B., and Shuaib, A. (2007) *Atherosclerosis 192*, 92-99.

310. Mineo, C., Deguchi, H., Griffin, J. H., and Shaul, P. W. (2006) *Circ. Res. 98*, 1352-1364.

311. Uittenbogaard, A., Shaul, P. W., Yuhanna, I. S., Blair, A., and Smart, E. J. (2000) *Journal of Biological Chemistry 275*, 11278-11283.

312. Blair, A., Shaul, P. W., Yuhanna, I. S., Conrad, P. A., and Smart, E. J. (1999) *J. Biol. Chem. 274*, 32512-32519.

313. Terasaka, N., Westerterp, M., Koetsveld, J., Fernandez-Hernando, C., Yvan-Charvet, L., Wang, N., Sessa, W. C., and Tall, A. R. (2010) *Arterioscler. Thromb. Vasc. Biol. 30*, 2219-2225.

314. Yeh, M., Cole, A. L., Choi, J., Liu, Y., Tulchinsky, D., Qiao, J. H., Fishbein, M. C., Dooley, A. N., Hovnanian, T., Mouilleseaux, K., Vora, D. K., Yang, W. P., Gargalovic, P., Kirchgessner, T., Shyy, J. Y., and Berliner, J. A. (2004) *Circ. Res. 95*, 780-788.

315. Gharavi, N. M., Baker, N. A., Mouillesseaux, K. P., Yeung, W., Honda, H. M., Hsieh, X., Yeh, M., Smart, E. J., and Berliner, J. A. (2006) *Circ. Res. 98*, 768-776.

316. Ou, J., Ou, Z., Jones, D. W., Holzhauer, S., Hatoum, O. A., Ackerman, A. W., Weihrauch, D. W., Gutterman, D. D., Guice, K., Oldham, K. T., Hillery, C. A., and Pritchard, K. A., Jr. (2003) *Circulation 107*, 2337-2341.

317. Ou, J., Wang, J., Xu, H., Ou, Z., Sorci-Thomas, M. G., Jones, D. W., Signorino, P., Densmore, J. C., Kaul, S., Oldham, K. T., and Pritchard, K. A., Jr. (2005) *Circ. Res. 97*, 1190-1197.

318. Ou, Z., Ou, J., Ackerman, A. W., Oldham, K. T., and Pritchard, K. A., Jr. (2003) *Circulation 107*, 1520-1524.

319. Gotlieb, A. I. and Silver, M. D. (2001) in *Cardiovascular Pathology* (Gotlieb, A. I., Schoen, F. J., and Silver, M. D., Eds.) Churchill Livingstone, New York.

320. Ross, R. (1993) *Nature 362*, 801-809.

321. Werner, N., Junk, S., Laufs, U., Link, A., Walenta, K., Bohm, M., and Nickenig, G. (2003) *Circ. Res. 93*, e17-e24.

322. Tamagaki, T., Sawada, S., Imamura, H., Tada, Y., Yamasaki, S., Toratani, A., Sato, T., Komatsu, S., Akamatsu, N., Yamagami, M., Kobayashi, K., Kato, K., Yamamoto, K., Shirai, K., Yamada, K., Higaki, T., Nakagawa, K., Tsuji, H., and Nakagawa, M. (1996) *Atherosclerosis 123*, 73-82.

323. Murugesan, G., Sa, G., and Fox, P. L. (1994) *Circ. Res. 74*, 1149-1156.

324. Miura, S., Fujino, M., Matsuo, Y., Kawamura, A., Tanigawa, H., Nishikawa, H., and Saku, K. (2003) *Arterioscler. Thromb. Vasc. Biol. 23*, 802-808.

325. Seetharam, D., Mineo, C., Gormley, A. K., Gibson, L. L., Vongpatanasin, W., Chambliss, K. L., Hahner, L. D., Cummings, M. L., Kitchens, R. L., Marcel, Y. L., Rader, D. J., and Shaul, P. W. (2006) *Circulation Research 98*, 63-72.

326. Doggen, C. J. M., Smith, N. L., Lemaitre, R. N., Heckbert, S. R., Rosendaal, F. R., and Psaty, B. M. (2004) *Arteriosclerosis Thrombosis and Vascular Biology 24*, 1970-1975.

327. Gonzalez-Ordonez, A. J., Fernandez-Carreira, J. M., Fernandez-Alvarez, C. R., Obaya, R. V., Macias-Robles, M. D., Gonzalez-Franco, A., and Garcia, M. A. A. (2003) *Haematologica 88*, 1035-1043.

328. Deguchi, H., Pecheniuk, N. M., Elias, D. J., Averell, P. M., and Griffin, J. H. (2005) *Circulation 112*, 893-899.

329. Mineo, C., Deguchi, H., Griffin, J. H., and Shaul, P. W. (2006) *Circ. Res. 98*, 1352-1364.

330. Bombeli, T., Schwartz, B. R., and Harlan, J. M. (1999) *Blood 93*, 3831-3838.

331. Bombeli, T., Karsan, A., Tait, J. F., and Harlan, J. M. (1997) *Blood 89*, 2429-2442.

332. Durand, E., Scoazec, A., Lafont, A., Boddaert, J., Al Hajzen, A., Addad, F., Mirshahi, M., Desnos, M., Tedgui, A., and Mallat, Z. (2004) *Circulation 109*, 2503-2506.

333. Mallat, Z., Benamer, H., Hugel, B., Benessiano, J., Steg, P. G., Freyssinet, J. M., and Tedgui, A. (2000) *Circulation 101*, 841-843.

334. Martinez, M. C., Tesse, A., Zobairi, F., and Andriantsitohaina, R. (2005) *Am. J. Physiol Heart Circ. Physiol 288*, H1004-H1009.

335. Pajkrt, D., Lerch, P. G., vanderPoll, T., Levi, M., Illi, M., Doran, J. E., Arnet, B., vandenEnde, A., tenCate, J. W., and vanDeventer, S. J. H. (1997) *Thrombosis and Haemostasis 77*, 303-307.

336. Li, D. Y., Weng, S., Yang, B. C., Zander, D. S., Saldeen, T., Nichols, W. W., Khan, S., and Mehta, J. L. (1999) *Arteriosclerosis Thrombosis and Vascular Biology 19*, 378-383.

337. Fleisher, L. N., Tall, A. R., Witte, L. D., and Cannon, P. J. (1983) *Advances in Prostaglandin Thromboxane and Leukotriene Research 11*, 475-480.

338. Vane, J. R. and Botting, R. M. (1995) *American Journal of Cardiology 75*, A3-A10.

339. Vinals, M., Martinez-Gonzalez, J., Badimon, J. J., and Badimon, L. (1997) *Arteriosclerosis Thrombosis and Vascular Biology 17*, 3481-3488.

340. Escudero, I., Martinez-Gonzalez, J., Alonso, R., Mata, P., and Badimon, L. (2003) *European Journal of Clinical Investigation 33*, 779-786.

341. Martinez-Gonzalez, J., Escudero, I., and Badimon, L. (2004) *Atherosclerosis 174*, 305-313.

342. Wadham, C., Albanese, N., Roberts, J., Wang, L. J., Bagley, C. J., Gamble, J. R., Rye, K. A., Barter, P. J., Vadas, M. A., and Xia, P. (2004) *Circulation 109*, 2116-2122.

343. Griffin, J. H., Kojima, K., Banka, C. L., Curtiss, L. K., and Fernandez, J. A. (1999) *Journal of Clinical Investigation 103*, 219-227.

344. MacCallum, P. K., Cooper, J. A., Martin, J., Howarth, D. J., Meade, T. W., and Miller, G. J. (2000) *Thrombosis and Haemostasis 83*, 421-426.

345. Balicki, D. and Beutler, E. (2002) *Medicine (Baltimore) 81*, 69-86.

346. Nicholls, S. J., Cutri, B., Worthley, S. G., Kee, P., Rye, K. A., Bao, S., and Barter, P. J. (2005) *Arteriosclerosis Thrombosis and Vascular Biology 25*, 2416-2421.

347. Boffa, M. C. and Karmochkine, M. (1998) *Lupus 7*, S120-S125.

348. Deguchi, H., Fernandez, J. A., Pabinger, I., Heit, J. A., and Griffin, J. H. (2001) *Blood 97*, 1907-1914.

349. Deguchi, H., Fernandez, J. A., and Griffin, J. H. (2002) *Journal of Biological Chemistry 277*, 8861-8865.

350. Deguchi, H., Yegneswaran, S., and Griffin, J. H. (2004) *Journal of Biological Chemistry 279*, 12036-12042.

351. Grewal, T., de, D., I, Kirchhoff, M. F., Tebar, F., Heeren, J., Rinninger, F., and Enrich, C. (2003) *J. Biol. Chem. 278*, 16478-16481.

352. O'Connell, B. J. and Genest, J. (2001) *Circulation 104*, 1978-1983.

353. Eren, M., Painter, C. A., Atkinson, J. B., Declerck, P. J., and Vaughan, D. E. (2002) *Circulation 106*, 491-496.

354. Norata, G. D., Banfi, C., Pirillo, A., Tremoli, E., Hamsten, A., Catapano, A. L., and Eriksson, P. (2004) *British Journal of Haematology 127*, 97-104.

355. Naqvi, T. Z., Shah, P. K., Ivey, P. A., Molloy, M. D., Thomas, A. M., Panicker, S., Ahmed, A., Cercek, B., and Kaul, S. (1999) *American Journal of Cardiology 84*, 1011-1017.

356. Lerch, P. G., Spycher, M. O., and Doran, J. E. (1998) *Thrombosis and Haemostasis 80*, 316-320.

357. Oravec, S., Demuth, K., Myara, I., and Hornych, A. (1998) *Thrombosis Research 92*, 65-71.

358. Dole, V. S., Matuskova, J., Vasile, E., Yesilaltay, A., Bergmeier, W., Bernimoulin, M., Wagner, D. D., and Krieger, M. (2008) *Arterioscler. Thromb. Vasc. Biol. 28*, 1111-1116.

359. Brodde, M. F., Korporaal, S. J., Herminghaus, G., Fobker, M., van Berkel, T. J., Tietge, U. J., Robenek, H., Van, E. M., Kehrel, B. E., and Nofer, J. R. (2011) *Atherosclerosis*.

360. Tschoepe, D., Roesen, P., Kaufmann, L., Schauseil, S., Kehrel, B., Ostermann, H., and Gries, F. A. (1990) *European Journal of Clinical Investigation 20*, 166-170.

361. Eibl, N., Krugluger, W., Streit, G., Schrattbauer, K., Hopmeier, P., and Schernthaner, G. (2004) *European Journal of Clinical Investigation 34*, 205-209.

362. Davi, G., Catalano, I., Averna, M., Notarbartolo, A., Strano, A., Ciabattoni, G., and Patrono, C. (1990) *New England Journal of Medicine 322*, 1769-1774.

363. Li, Y., Woo, V., and Bose, R. (2001) *American Journal of Physiology-Heart and Circulatory Physiology 280*, H1480-H1489.

364. Calkin, A. C., Drew, B. G., Ono, A., Duffy, S. J., Gordon, M. V., Schoenwaelder, S. M., Sviridov, D., Cooper, M. E., Kingwell, B. A., and Jackson, S. P. (2009) *Circulation 120*, 2095-2104.

365. Rutti, S., Ehses, J. A., Sibler, R. A., Prazak, R., Rohrer, L., Georgopoulos, S., Meier, D. T., Niclauss, N., Berney, T., Donath, M. Y., and von Eckardstein, A. (2009) *Endocrinology 150*, 4521-4530.

366. Koseki, M., Matsuyama, A., Nakatani, K., Inagaki, M., Nakaoka, H., Kawase, R., Yuasa-Kawase, M., Tsubakio-Yamamoto, K., Masuda, D., Sandoval, J. C., Ohama, T., Nakagawa-Toyama, Y., Matsuura, F., Nishida, M., Ishigami, M., Hirano, K., Sakane, N., Kumon, Y., Suehiro, T., Nakamura, T., Shimomura, I., and Yamashita, S. (2009) *Journal of Atherosclerosis and Thrombosis 16*, 292-296.

367. Fryirs, M. A., Barter, P. J., Appavoo, M., Tuch, B. E., Tabet, F., Heather, A. K., and Rye, K. A. (2010) *Arteriosclerosis Thrombosis and Vascular Biology 30*, 1642-U296.

368. Drew, B. G., Duffy, S. J., Formosa, M. F., Natoli, A. K., Henstridge, D. C., Penfold, S. A., Thomas, W. G., Mukhamedova, N., de Court, Forbes, J. M., Yap, F. Y., Kaye, D. M., van Hall, G., Febbraio, M. A., Kemp, B. E., Sviridov, D., Steinberg, G. R., and Kingwell, B. A. (2009) *Circulation 119*, 2103-U134.

369. Brunham, L. R., Kruit, J. K., Pape, T. D., Timmins, J. M., Reuwer, A. Q., Vasanji, Z., Marsh, B. J., Rodrigues, B., Johnson, J. D., Parks, J. S., Verchere, C. B., and Hayden, M. R. (2007) *Nat. Med. 13*, 340-347.

370. Hao, M., Head, W. S., Gunawardana, S. C., Hasty, A. H., and Piston, D. W. (2007) *Diabetes 56*, 2328-2338.

371. Rizzo, M. A. and Piston, D. W. (2003) *Journal of Cell Biology 161*, 243-248.

372. Ishikawa, M., Iwasaki, Y., Yatoh, S., Kato, T., Kumadaki, S., Inoue, N., Yamamoto, T., Matsuzaka, T., Nakagawa, Y., Yahagi, N., Kobayashi, K., Takahashi, A., Yamada, N., and Shimano, H. (2008) *Journal of Lipid Research 49*, 2524-2534.

373. Sorrentino, S. A., Besler, C., Rohrer, L., Meyer, M., Heinrich, K., Bahlmann, F. H., Mueller, M., Horvath, T., Doerries, C., Heinemann, M., Flemmer, S., Markowski, A., Manes, C., Bahr, M. J., Haller, H., von Eckardstein, A., Drexler, H., and Landmesser, U. (2010) *Circulation 121*, 110-122.

374. Drew, B. G., Carey, A. L., Natoli, A. K., Formosa, M. F., Vizi, D., Reddy-Luthmoodoo, M., Weir, J. M., Barlow, C. K., van Hall, G., Meikle, P. J., Duffy, S. J., and Kingwell, B. A. (2011) *Journal of Lipid Research 52*, 572-581.

375. Han, R., Lai, R., Ding, Q., Wang, Z., Luo, X., Zhang, Y., Cui, G., He, J., Liu, W., and Chen, Y. (2007) *Diabetologia 50*, 1960-1968.

376. Abderrahmani, A., Niederhauser, G., Favre, D., Abdelli, S., Ferdaoussi, M., Yang, J. Y., Regazzi, R., Widmann, C., and Waeber, G. (2007) *Diabetologia 50*, 1304-1314.

377. Ruan, X., Li, Z., Zhang, Y., Yang, L., Pan, Y., Wang, Z., Feng, G. S., and Chen, Y. (2010) *J. Cell Mol. Med.*

378. Timmermans, F., Plum, J., Yoder, M. C., Ingram, D. A., Vandekerckhove, B., and Case, J. (2009) *J. Cell Mol. Med. 13*, 87-102.

379. Noor, R., Shuaib, U., Wang, C. X., Todd, K., Ghani, U., Schwindt, B., and Shuaib, A. (2007) *Atherosclerosis 192*, 92-99.

380. Petoumenos, V., Nickenig, G., and Werner, N. (2009) *J. Cell Mol. Med. 13*, 4623-4635.

381. Tso, C., Martinic, G., Fan, W. H., Rogers, C., Rye, K. A., and Barter, P. J. (2006) *Arteriosclerosis Thrombosis and Vascular Biology 26*, 1144-1149.

382. Knetsch, M. L. W., Aldenhoff, Y. B. J., and Koole, L. H. (2006) *Biomaterials 27*, 2813-2819.

383. Werner, N., Kosiol, S., Schiegl, T., Ahlers, P., Walenta, K., Link, A., Bohm, M., and Nickenig, G. (2005) *N. Engl. J. Med. 353*, 999-1007.

384. Tepper, O. M., Galiano, R. D., Capla, J. M., Kalka, C., Gagne, P. J., Jacobowitz, G. R., Levine, J. P., and Gurtner, G. C. (2002) *Circulation 106*, 2781-2786.

385. van Oostrom, O., Nieuwdorp, M., Westerweel, P. E., Hoefer, I. E., Basser, R., Stroes, E. S., and Verhaar, M. C. (2007) *Arterioscler. Thromb. Vasc. Biol. 27*, 1864-1865.

386. Sumi, M., Sata, M., Miura, S. I., Rye, K. A., Toya, N., Kanaoka, Y., Yanaga, K., Ohki, T., Saku, K., and Nagai, R. (2007) *Arteriosclerosis Thrombosis and Vascular Biology 27*, 813-818.

387. Feng, Y. M., Van Eck, M., Van Craeyveld, E., Jacobs, F., Carlier, V., Van Linthout, S., Erdel, M., Tjwa, M., and De Geest, B. (2009) *Blood 113*, 755-764.

388. Yvan-Charvet, L., Pagler, T., Gautier, E. L., Avagyan, S., Siry, R. L., Han, S., Welch, C. L., Wang, N., Randolph, G. J., Snoeck, H. W., and Tall, A. R. (2010) *Science 328*, 1689-1693.

389. Villarroel, F., Bastias, A., Casado, A., Amthauer, R., and Concha, M. I. (2007) *Fish & Shellfish Immunology 23*, 197-209.

390. Johnston, L. D., Brown, G., Gauthier, D., Reece, K., Kator, H., and Van Veld, P. (2008) *Comparative Biochemistry and Physiology B-Biochemistry & Molecular Biology 151*, 167-175.

391. Figueiredo, P. M. S., Catani, C. F., and Yano, T. (2003) *Fems Immunology and Medical Microbiology 38*, 53-57.

392. Grunfeld, C., Marshall, M., Shigenaga, J. K., Moser, A. H., Tobias, P., and Feingold, K. R. (1999) *Journal of Lipid Research 40*, 245-252.

393. Ma, J., Liao, X. L., Lou, B., and Wu, M. P. (2004) *Acta Biochimica et Biophysica Sinica 36*, 419-424.

394. Parker, T. S., Levine, D. M., Chang, J. C. C., Laxer, J., Coffin, C. C., and Rubin, A. L. (1995) *Infection and Immunity 63*, 253-258.

395. Jiao, Y. L. and Wu, M. P. (2008) *Cytokine 43*, 83-87.

396. Li, Y., Dong, J. B., and Wu, M. P. (2008) *European Journal of Pharmacology 590*, 417-422.

397. Sorensen, O., Bratt, T., Johnsen, A. H., Madsen, M. T., and Borregaard, N. (1999) *Journal of Biological Chemistry 274*, 22445-22451.

398. Suzuki, M., Pritchard, D. K., Becker, L., Hoofnagle, A. N., Tanimura, N., Bammler, T. K., Beyer, R. P., Bumgarner, R., Vaisar, T., de Beer, M. C., de Beer, F. C., Miyake, K., Oram, J. F., and Heinecke, J. W. (2010) *Circulation 122*, 1919-1U77.

399. Courtney, H. S., Zhang, Y. M., Frank, M. W., and Rock, C. O. (2006) *Journal of Biological Chemistry 281*, 5515-5521.

400. Wheeler, R. J. (2010) *Trends in Parasitology 26*, 457-464.

401. Vanhollebeke, B. and Pays, E. (2010) *Molecular Microbiology 76*, 806-814.

402. Samanovic, M., Molina-Portela, M. P., Chessler, A. D. C., Burleigh, B. A., and Raper, J. (2009) *Plos Pathogens 5*.

403. Singh, I. P., Chopra, A. K., Coppenhaver, D. H., Ananatharamaiah, G. M., and Baron, S. (1999) *Antiviral Research 42*, 211-218.

404. Srinivas, R. V., Venkatachalapathi, Y. V., Rui, Z., Owens, R. J., Gupta, K. B., Srinivas, S. K., Anantharamaiah, G. M., Segrest, J. P., and Compans, R. W. (1991) *Journal of Cellular Biochemistry 45*, 224-237.

405. Gaidukov, L. and Tawfik, D. S. (2005) *Biochemistry 44*, 11843-11854.

406. Harel, M., Aharoni, A., Gaidukov, L., Brumshtein, B., Khersonsky, O., Meged, R., Dvir, H., Ravelli, R. B. G., McCarthy, A., Toker, L., Silman, I., Sussman, J. L., and Tawfik, D. S. (2004) *Nature Structural & Molecular Biology 11*, 412-419.

407. Gaidukov, L., Viji, R. I., Yacobson, S., Rosenblat, M., Aviram, M., and Tawfik, D. S. (2010) *Biochemistry 49*, 532-538.

408. Fuhrman, B., Gantman, A., and Aviram, M. (2010) *Atherosclerosis 211*, 61-68.

409. Gamliel-Lazarovich, A., Gantman, A., Shiner, M., Coleman, R., Aviram, M., and Keidar, S. (2010) *Atherosclerosis 211*, 130-135.

410. James, R. W., Brulhart-Meynet, M. C., Singh, A. K., Riederer, B., Seidler, U., Out, R., Van Berkel, T. J. C., and Deakin, S. (2010) *Arteriosclerosis Thrombosis and Vascular Biology 30*, 2121-U247.

411. Evangelou, A. M. (1994) *Prostaglandins Leukotrienes and Essential Fatty Acids 50*, 1-28.

412. Imaizumi, T. A., Stafforini, D. M., Yamada, Y., McIntyre, T. M., Prescott, S. M., and Zimmerman, G. A. (1995) *Journal of Internal Medicine 238*, 5-20.

413. Stafforini, D. M., Prescott, S. M., and McIntyre, T. M. (1991) *Methods in Enzymology 197*, 411-425.

414. Tjoelker, L. W., Wilder, C., Eberhardt, C., Stafforini, D. M., Dietsch, G., Schimpf, B., Hooper, S., Letrong, H., Cousens, L. S., Zimmerman, G. A., Yamada, Y., McIntyre, T. M., Prescott, S. M., and Gray, P. W. (1995) *Nature 374*, 549-553.

415. Tselepis, A. D., Dentan, C., Karabina, S. A. P., Chapman, M. J., and Ninio, E. (1995) *Arteriosclerosis Thrombosis and Vascular Biology 15*, 1764-1773.

416. Tsaoussis, V. and Vakirtzilemonias, C. (1994) *Journal of Lipid Mediators and Cell Signalling 9*, 317-331.

417. Quarck, R., De Geest, B., Stengel, D., Mertens, A., Lox, M., Theilmeier, G., Michiels, C., Raes, M., Bult, H., Collen, D., Van Veldhoven, P., Ninio, E., and Holvoet, P. (2001) *Circulation 103*, 2495-2500.

418. Daugherty, A., Rateri, D. L., Dunn, J. L., and Heinecke, J. W. (1993) *Circulation 88*, 32.

419. Hurst, J. K. and Barrette, W. C. (1989) *Critical Reviews in Biochemistry and Molecular Biology 24*, 271-328.

420. Eiserich, J. P., Cross, C. E., Jones, A. D., Halliwell, B., and vanderVliet, A. (1996) *Journal of Biological Chemistry 271*, 19199-19208.

421. Gaut, J. P., Byun, J., Tran, H. D., Lauber, W. M., Carroll, J. A., Hotchkiss, R. S., Belaaouaj, A., and Heinecke, J. W. (2002) *Journal of Clinical Investigation 109*, 1311-1319.

422. Shao, B., Tang, C., Heinecke, J. W., and Oram, J. F. (2010) *J. Lipid Res.*

423. Zheng, L. M., Nukuna, B., Brennan, M. L., Sun, M. J., Goormastic, M., Settle, M., Schmitt, D., Fu, X. M., Thomson, L., Fox, P. L., Ischiropoulos, H., Smith, J. D., Kinter, M., and Hazen, S. L. (2004) *Journal of Clinical Investigation 114*, 529-541.

424. Zheng, L., Settle, M., Brubaker, G., Schmitt, D., Hazen, S. L., Smith, J. D., and Kinter, M. (2005) *Journal of Biological Chemistry 280*, 38-47.

425. Undurti, A., Huang, Y., Lupica, J. A., Smith, J. D., Didonato, J. A., and Hazen, S. L. (2009) *J. Biol. Chem. 284*, 30825-30835.

426. Peng, D. Q., Brubaker, G., Wu, Z., Zheng, L., Willard, B., Kinter, M., Hazen, S. L., and Smith, J. D. (2008) *Arterioscler. Thromb. Vasc. Biol. 28*, 2063-2070.

427. Teslovich, T. M., Musunuru, K., Smith, A. V., Edmondson, A. C., Stylianou, I. M., Koseki, M., Pirruccello, J. P., Ripatti, S., Chasman, D. I., Willer, C. J., Johansen, C. T., Fouchier, S. W., Isaacs, A., Peloso, G. M., Barbalic, M., Ricketts, S. L., Bis, J. C., Aulchenko, Y. S., Thorleifsson, G., Feitosa, M. F., Chambers, J., Orho-Melander, M., Melander, O., Johnson, T., Li, X., Guo, X., Li, M., Shin, C. Y., Jin, G. M., Jin, K. Y., Lee, J. Y., Park, T., Kim, K., Sim, X., Twee-Hee, O. R., Croteau-Chonka, D. C., Lange, L. A., Smith, J. D., Song, K., Hua, Z. J., Yuan, X., Luan, J., Lamina, C., Ziegler, A., Zhang, W., Zee, R. Y., Wright, A. F., Witteman, J. C., Wilson, J. F., Willemsen, G., Wichmann, H. E., Whitfield, J. B., Waterworth, D. M., Wareham, N. J., Waeber, G., Vollenweider, P., Voight, B. F., Vitart, V., Uitterlinden, A. G., Uda, M., Tuomilehto, J., Thompson, J. R., Tanaka, T., Surakka, I., Stringham, H. M., Spector, T. D., Soranzo, N., Smit, J. H., Sinisalo, J., Silander, K., Sijbrands, E. J., Scuteri, A., Scott, J., Schlessinger, D., Sanna, S., Salomaa, V., Saharinen, J., Sabatti, C., Ruokonen, A., Rudan, I., Rose, L. M., Roberts, R., Rieder, M., Psaty, B. M., Pramstaller, P. P., Pichler, I., Perola, M., Penninx, B. W., Pedersen, N. L., Pattaro, C., Parker, A. N., Pare, G., Oostra, B. A., O'Donnell, C. J., Nieminen, M. S., Nickerson, D. A., Montgomery, G. W., Meitinger, T., McPherson, R., McCarthy, M. I., McArdle, W., Masson, D., Martin, N. G., Marroni, F., Mangino, M., Magnusson, P. K., Lucas, G., Luben, R., Loos, R. J., Lokki, M. L., Lettre, G., Langenberg, C., Launer, L. J., Lakatta, E. G., Laaksonen, R., Kyvik, K. O., Kronenberg, F., Konig, I. R., Khaw, K. T., Kaprio, J., Kaplan, L. M., Johansson, A., Jarvelin, M. R., Cecile, J. W. J., Ingelsson, E., Igl, W., Kees, H. G., Hottenga, J. J., Hofman, A., Hicks, A. A., Hengstenberg, C., Heid, I. M., Hayward, C., Havulinna, A. S., Hastie, N. D., Harris, T. B., Haritunians, T., Hall, A. S., Gyllensten, U., Guiducci, C., Groop, L. C., Gonzalez, E., Gieger, C., Freimer, N. B., Ferrucci, L., Erdmann, J., Elliott, P., Ejebe, K. G., Doring, A., Dominiczak, A. F., Demissie, S., Deloukas, P., de Geus, E. J., de Faire, U., Crawford, G., Collins, F. S., Chen, Y. D., Caulfield, M. J., Campbell, H., Burtt, N. P., Bonnycastle, L. L., Boomsma, D. I., Boekholdt, S. M., Bergman, R. N., Barroso, I., Bandinelli, S., Ballantyne, C. M., Assimes, T. L., Quertermous, T., Altshuler, D., Seielstad, M., Wong, T. Y., Tai, E. S., Feranil, A. B., Kuzawa, C. W., Adair, L. S., Taylor, H. A., Jr., Borecki, I. B., Gabriel, S. B., Wilson, J. G., Holm, H., Thorsteinsdottir, U., Gudnason, V., Krauss, R. M., Mohlke, K. L., Ordovas, J. M., Munroe, P. B., Kooner, J. S., Tall, A. R., Hegele, R. A., Kastelein, J. J., Schadt, E. E., Rotter, J. I., Boerwinkle, E., Strachan, D. P., Mooser, V.,

Stefansson, K., Reilly, M. P., Samani, N. J., Schunkert, H., Cupples, L. A., Sandhu, M. S., Ridker, P. M., Rader, D. J., van Duijn, C. M., Peltonen, L., Abecasis, G. R., Boehnke, M., and Kathiresan, S. (2010) *Nature 466*, 707-713.

428. Richards, J. B., Waterworth, D., O'Rahilly, S., Hivert, M. F., Loos, R. J., Perry, J. R., Tanaka, T., Timpson, N. J., Semple, R. K., Soranzo, N., Song, K., Rocha, N., Grundberg, E., Dupuis, J., Florez, J. C., Langenberg, C., Prokopenko, I., Saxena, R., Sladek, R., Aulchenko, Y., Evans, D., Waeber, G., Erdmann, J., Burnett, M. S., Sattar, N., Devaney, J., Willenborg, C., Hingorani, A., Witteman, J. C., Vollenweider, P., Glaser, B., Hengstenberg, C., Ferrucci, L., Melzer, D., Stark, K., Deanfield, J., Winogradow, J., Grassl, M., Hall, A. S., Egan, J. M., Thompson, J. R., Ricketts, S. L., Konig, I. R., Reinhard, W., Grundy, S., Wichmann, H. E., Barter, P., Mahley, R., Kesaniemi, Y. A., Rader, D. J., Reilly, M. P., Epstein, S. E., Stewart, A. F., van Duijn, C. M., Schunkert, H., Burling, K., Deloukas, P., Pastinen, T., Samani, N. J., McPherson, R., Davey, S. G., Frayling, T. M., Wareham, N. J., Meigs, J. B., Mooser, V., and Spector, T. D. (2009) *PLoS Genet. 5*, e1000768.

429. Willer, C. J., Sanna, S., Jackson, A. U., Scuteri, A., Bonnycastle, L. L., Clarke, R., Heath, S. C., Timpson, N. J., Najjar, S. S., Stringham, H. M., Strait, J., Duren, W. L., Maschio, A., Busonero, F., Mulas, A., Albai, G., Swift, A. J., Morken, M. A., Narisu, N., Bennett, D., Parish, S., Shen, H., Galan, P., Meneton, P., Hercberg, S., Zelenika, D., Chen, W. M., Li, Y., Scott, L. J., Scheet, P. A., Sundvall, J., Watanabe, R. M., Nagaraja, R., Ebrahim, S., Lawlor, D. A., Ben Shlomo, Y., Davey-Smith, G., Shuldiner, A. R., Collins, R., Bergman, R. N., Uda, M., Tuomilehto, J., Cao, A., Collins, F. S., Lakatta, E., Lathrop, G. M., Boehnke, M., Schlessinger, D., Mohlke, K. L., and Abecasis, G. R. (2008) *Nat. Genet. 40*, 161-169.

430. Kathiresan, S., Willer, C. J., Peloso, G. M., Demissie, S., Musunuru, K., Schadt, E. E., Kaplan, L., Bennett, D., Li, Y., Tanaka, T., Voight, B. F., Bonnycastle, L. L., Jackson, A. U., Crawford, G., Surti, A., Guiducci, C., Burtt, N. P., Parish, S., Clarke, R., Zelenika, D., Kubalanza, K. A., Morken, M. A., Scott, L. J., Stringham, H. M., Galan, P., Swift, A. J., Kuusisto, J., Bergman, R. N., Sundvall, J., Laakso, M., Ferrucci, L., Scheet, P., Sanna, S., Uda, M., Yang, Q., Lunetta, K. L., Dupuis, J., de Bakker, P. I., O'Donnell, C. J., Chambers, J. C., Kooner, J. S., Hercberg, S., Meneton, P., Lakatta, E. G., Scuteri, A., Schlessinger, D., Tuomilehto, J., Collins, F. S., Groop, L., Altshuler, D., Collins, R., Lathrop, G. M., Melander, O., Salomaa, V., Peltonen, L., Orho-Melander, M., Ordovas, J. M., Boehnke, M., Abecasis, G. R., Mohlke, K. L., and Cupples, L. A. (2009) *Nat. Genet. 41*, 56-65.

431. Chasman, D. I., Pare, G., Mora, S., Hopewell, J. C., Peloso, G., Clarke, R., Cupples, L. A., Hamsten, A., Kathiresan, S., Malarstig, A., Ordovas, J. M.,

Ripatti, S., Parker, A. N., Miletich, J. P., and Ridker, P. M. (2009) *Plos Genetics 5*.

432. Sabatti, C., Service, S. K., Hartikainen, A. L., Pouta, A., Ripatti, S., Brodsky, J., Jones, C. G., Zaitlen, N. A., Varilo, T., Kaakinen, M., Sovio, U., Ruokonen, A., Laitinen, J., Jakkula, E., Coin, L., Hoggart, C., Collins, A., Turunen, H., Gabriel, S., Elliot, P., McCarthy, M. I., Daly, M. J., Jarvelin, M. R., Freimer, N. B., and Peltonen, L. (2009) *Nat. Genet. 41*, 35-46.

433. Waterworth, D. M., Ricketts, S. L., Song, K., Chen, L., Zhao, J. H., Ripatti, S., Aulchenko, Y. S., Zhang, W., Yuan, X., Lim, N., Luan, J., Ashford, S., Wheeler, E., Young, E. H., Hadley, D., Thompson, J. R., Braund, P. S., Johnson, T., Struchalin, M., Surakka, I., Luben, R., Khaw, K. T., Rodwell, S. A., Loos, R. J., Boekholdt, S. M., Inouye, M., Deloukas, P., Elliott, P., Schlessinger, D., Sanna, S., Scuteri, A., Jackson, A., Mohlke, K. L., Tuomilehto, J., Roberts, R., Stewart, A., Kesaniemi, Y. A., Mahley, R. W., Grundy, S. M., McArdle, W., Cardon, L., Waeber, G., Vollenweider, P., Chambers, J. C., Boehnke, M., Abecasis, G. R., Salomaa, V., Jarvelin, M. R., Ruokonen, A., Barroso, I., Epstein, S. E., Hakonarson, H. H., Rader, D. J., Reilly, M. P., Witteman, J. C., Hall, A. S., Samani, N. J., Strachan, D. P., Barter, P., van Duijn, C. M., Kooner, J. S., Peltonen, L., Wareham, N. J., McPherson, R., Mooser, V., and Sandhu, M. S. (2010) *Arterioscler. Thromb. Vasc. Biol. 30*, 2264-2276.

434. Kathiresan, S., Musunuru, K., and Orho-Melander, M. (2008) *Curr. Opin. Lipidol. 19*, 122-127.

435. Aulchenko, Y. S., Ripatti, S., Lindqvist, I., Boomsma, D., Heid, I. M., Pramstaller, P. P., Penninx, B. W., Janssens, A. C., Wilson, J. F., Spector, T., Martin, N. G., Pedersen, N. L., Kyvik, K. O., Kaprio, J., Hofman, A., Freimer, N. B., Jarvelin, M. R., Gyllensten, U., Campbell, H., Rudan, I., Johansson, A., Marroni, F., Hayward, C., Vitart, V., Jonasson, I., Pattaro, C., Wright, A., Hastie, N., Pichler, I., Hicks, A. A., Falchi, M., Willemsen, G., Hottenga, J. J., de Geus, E. J., Montgomery, G. W., Whitfield, J., Magnusson, P., Saharinen, J., Perola, M., Silander, K., Isaacs, A., Sijbrands, E. J., Uitterlinden, A. G., Witteman, J. C., Oostra, B. A., Elliott, P., Ruokonen, A., Sabatti, C., Gieger, C., Meitinger, T., Kronenberg, F., Doring, A., Wichmann, H. E., Smit, J. H., McCarthy, M. I., van Duijn, C. M., and Peltonen, L. (2009) *Nat. Genet. 41*, 47-55.

436. Vaisar, T., Pennathur, S., Green, P. S., Gharib, S. A., Hoofnagle, A. N., Cheung, M. C., Byun, J., Vuletic, S., Kassim, S., Singh, P., Chea, H., Knopp, R. H., Brunzell, J., Geary, R., Chait, A., Zhao, X. Q., Elkon, K., Marcovina, S., Ridker, P., Oram, J. F., and Heinecke, J. W. (2007) *J. Clin. Invest 117*, 746-756.

437. Davidson, W. S., Silva, R. A. G. D., Chantepie, S., Lagor, W. R., Chapman, M. J., and Kontush, A. (2009) *Arteriosclerosis Thrombosis and Vascular Biology 29*, 870-U234.

438. Gordon, S. M., Deng, J. Y., Lu, L. J., and Davidson, W. S. (2010) *Journal of Proteome Research 9*, 5239-5249.

439. Davidson, W. S., Silva, R. A., Chantepie, S., Lagor, W. R., Chapman, M. J., and Kontush, A. (2009) *Arterioscler. Thromb. Vasc. Biol. 29*, 870-876.

440. Green, P. S., Vaisar, T., Pennathur, S., Kulstad, J. J., Moore, A. B., Marcovina, S., Brunzell, J., Knopp, R. H., Zhao, X. Q., and Heinecke, J. W. (2008) *Circulation 118*, 1259-1267.

441. Durrington, P. (2003) *Lancet 362*, 717-731.

442. Freedman, D. S., Otvos, J. D., Jeyarajah, E. J., Barboriak, J. J., Anderson, A. J., and Walker, J. A. (1998) *Arteriosclerosis Thrombosis and Vascular Biology 18*, 1046-1053.

443. Asztalos, B. F., Cupples, L. A., Demissie, S., Horvath, K. V., Cox, C. E., Batista, M. C., and Schaefer, E. J. (2004) *Arterioscler. Thromb. Vasc. Biol. 24*, 2181-2187.

444. Asztalos, B. F., Collins, D., Cupples, L. A., Demissie, S., Horvath, K. V., Bloomfield, H. E., Robins, S. J., and Schaefer, E. J. (2005) *Arterioscler. Thromb. Vasc. Biol. 25*, 2185-2191.

445. Tall, A. R., Yvan-Charvet, L., Terasaka, N., Pagler, T., and Wang, N. (2008) *Cell Metab 7*, 365-375.

446. Paszty, C., Maeda, N., Verstuyft, J., and Rubin, E. M. (1994) *J. Clin. Invest 94*, 899-903.

447. Tangirala, R. K., Tsukamoto, K., Chun, S. H., Usher, D., Pure, E., and Rader, D. J. (1999) *Circulation 100*, 1816-1822.

448. Wilhelm, A. J., Zabalawi, M., Owen, J. S., Shah, D., Grayson, J. M., Major, A. S., Bhat, S., Gibbs, D. P., Jr., Thomas, M. J., and Sorci-Thomas, M. G. (2010) *J. Biol. Chem. 285*, 36158-36169.

449. Duverger, N., Kruth, H., Emmanuel, F., Caillaud, J. M., Viglietta, C., Castro, G., Tailleux, A., Fievet, C., Fruchart, J. C., Houdebine, L. M., and Denefle, P. (1996) *Circulation 94*, 713-717.

450. Nissen, S. E., Tsunoda, T., Tuzcu, E. M., Schoenhagen, P., Cooper, C. J., Yasin, M., Eaton, G. M., Lauer, M. A., Sheldon, W. S., Grines, C. L., Halpern, S., Crowe, T., Blankenship, J. C., and Kerensky, R. (2003) *JAMA 290*, 2292-2300.

451. Nicholls, S. J., Tuzcu, E. M., Sipahi, I., Schoenhagen, P., Crowe, T., Kapadia, S., and Nissen, S. E. (2006) *J. Am. Coll. Cardiol. 47*, 992-997.

452. Barter, P. J. and Rye, K. A. (2006) *J. Intern. Med. 259*, 447-454.

453. Ansell, B. J., Navab, M., Hama, S., Kamranpour, N., Fonarow, G., Hough, G., Rahmani, S., Mottahedeh, R., Dave, R., Reddy, S. T., and Fogelman, A. M. (2003) *Circulation 108*, 2751-2756.

454. Kim, T. H., Lee, Y. H., Kim, K. H., Lee, S. H., Cha, J. Y., Shin, E. K., Jung, S., Jang, A. S., Park, S. W., Uh, S. T., Kim, Y. H., Park, J. S., Sin, H. G., Youm, W., Koh, E. S., Cho, S. Y., Paik, Y. K., Rhim, T. Y., and Park, C. S. (2010) *American Journal of Respiratory and Critical Care Medicine 182*, 633-642.

455. Lapergue, B., Moreno, J. A., Dang, B. Q., Coutard, M., Delbosc, S., Raphaeli, G., Auge, N., Klein, I., Mazighi, M., Michel, J. B., Amarenco, P., and Meilhac, O. (2010) *Stroke 41*, 1536-1542.

456. Moradi, H., Pahl, M. V., Elahimehr, R., and Vaziri, N. D. (2009) *Translational Research 153*, 77-85.

457. Kalantar-Zadeh, K., Kopple, J. D., Kamranpour, N., Fogelman, A. M., and Navab, M. (2007) *Kidney International 72*, 1149-1156.

458. Yu, R., Yekta, B., Vakili, L., Gharavi, N., Navab, M., Marelli, D., and Ardehali, A. (2008) *Current Atherosclerosis Reports 10*, 171-176.

459. Haque, S., Mirjafari, H., and Bruce, I. N. (2008) *Current Opinion in Lipidology 19*, 338-343.

460. Ansell, B. J., Fonarow, G. C., and Fogelman, A. M. (2007) *Current Opinion in Lipidology 18*, 427-434.

461. Vaziri, N. D., Moradi, H., Pahl, M. V., Fogelman, A. M., and Navab, M. (2009) *Kidney International 76*, 437-444.

462. Theilmeier, G., Schmidt, C., Herrmann, J., Keul, P., Schafers, M., Herrgott, I., Mersmann, J., Larmann, J., Hermann, S., Stypmann, J., Schober, O., Hildebrand, R., Schulz, R., Heusch, G., Haude, M., Lipinski, K. V., Herzog, C., Schmitz, M., Erbel, R., Chun, J., and Levkau, B. (2006) *Circulation 114*, 1403-1409.

463. Matsuo, Y., Miura, S. I., Kawamura, A., Uehara, Y., Rye, K. A., and Saku, K. (2007) *Atherosclerosis 194*, 159-168.

464. Levkau, B., Hermann, S., Theilmeier, G., van der, G. M., Chun, J., Schober, O., and Schafers, M. (2004) *Circulation 110*, 3355-3359.

465. Bisoendial, R. J., Hovingh, G. K., Levels, J. H., Lerch, P. G., Andresen, I., Hayden, M. R., Kastelein, J. J., and Stroes, E. S. (2003) *Circulation 107*, 2944-2948.

466. Spieker, L. E., Sudano, I., Hurlimann, D., Lerch, P. G., Lang, M. G., Binggeli, C., Corti, R., Ruschitzka, F., Luscher, T. F., and Noll, G. (2002) *Circulation 105*, 1399-1402.

467. Van Linthout, S., Spillmann, F., Riad, A., Trimpert, C., Lievens, J., Meloni, M., Escher, F., Filenberg, E., Demir, O., Li, J., Shakibaei, M., Schimke, I., Staudt, A., Felix, S. B., Schultheiss, H. P., De Geest, B., and Tschope, C. (2008) *Circulation 117*, 1563-1573.

468. Roghani, A. and Zannis, V. I. (1988) *Biochemistry 27*, 7428-7435.

469. Gorshkova, I. N., Liadaki, K., Gursky, O., Atkinson, D., and Zannis, V. I. (2000) *Biochemistry 39*, 15910-15919.

470. Gorshkova, I. N., Liu, T., Kan, H. Y., Chroni, A., Zannis, V. I., and Atkinson, D. (2006) *Biochemistry 45*, 1242-1254.

471. Gorshkova, I. N., Kypreos, K. E., Gantz, D. L., Zannis, V. I., and Atkinson, D. (2008) *Biochemistry 47*, 12644-12654.

472. Derksen, A. and Small, D. M. (1989) *Biochemistry 28*, 900-906.

473. He, T. C., Zhou, S., da Costa, L. T., Yu, J., Kinzler, K. W., and Vogelstein, B. (1998) *Proc. Natl. Acad. Sci. U. S. A 95*, 2509-2514.

474. Bashtovyy, D., Jones, M. K., Anantharamaiah, G. M., and Segrest, J. P. (2011) *J. Lipid Res. 52*, 435-450.

475. Gorshkova, I. N. and Atkinson, D. (2011) *Biochemistry In press*.

476. Xiao, C., Watanabe, T., Zhang, Y., Trigatti, B., Szeto, L., Connelly, P. W., Marcovina, S., Vaisar, T., Heinecke, J. W., and Lewis, G. F. (2008) *Circ. Res. 103*, 159-166.

477. Brunzell, J. D. (1989) in *The Metabolic Basis of Inherited Disease* (Scriver, C. R., Beaudet, A. L., Sly, W. S., and Valle, D., Eds.) pp 1165-1180, McGraw-Hill, New York.

478. Baggio, G., Manzato, E., Gabelli, C., Fellin, R., Martini, S., Enzi, G. B., Verlato, F., Baiocchi, M. R., Sprecher, D. L., Kashyap, M. L., and . (1986) *J. Clin. Invest 77*, 520-527.

479. Ito, Y., Azrolan, N., O'Connell, A., Walsh, A., and Breslow, J. L. (1990) *Science 249*, 790-793.

480. de Silva, H. V., Lauer, S. J., Wang, J., Simonet, W. S., Weisgraber, K. H., Mahley, R. W., and Taylor, J. M. (1994) *J. Biol. Chem. 269*, 2324-2335.

481. Shachter, N. S., Hayek, T., Leff, T., Smith, J. D., Rosenberg, D. W., Walsh, A., Ramakrishnan, R., Goldberg, I. J., Ginsberg, H. N., and Breslow, J. L. (1994) *J. Clin. Invest 93*, 1683-1690.

482. Boisfer, E., Lambert, G., Atger, V., Tran, N. Q., Pastier, D., Benetollo, C., Trottier, J. F., Beaucamps, I., Antonucci, M., Laplaud, M., Griglio, S., Chambaz, J., and Kalopissis, A. D. (1999) *J. Biol. Chem. 274*, 11564-11572.

483. Kypreos, K. E., Van Dijk, K. W., van Der, Z. A., Havekes, L. M., and Zannis, V. I. (2001) *J. Biol. Chem. 276*, 19778-19786.

484. Kypreos, K. E., Li, X., Van Dijk, K. W., Havekes, L. M., and Zannis, V. I. (2003) *Biochemistry 42*, 9841-9853.

485. Pennacchio, L. A., Olivier, M., Hubacek, J. A., Cohen, J. C., Cox, D. R., Fruchart, J. C., Krauss, R. M., and Rubin, E. M. (2001) *Science 294*, 169-173.

486. Chait, A., Hazzard, W. R., Albers, J. J., Kushwaha, R. P., and Brunzell, J. D. (1978) *Metabolism 27*, 1055-1066.

487. Fredenrich, A. (1998) *Diabetes Metab 24*, 490-495.

488. Fredrickson, D. S., Altrocchi, P. H., Avioli, L. V., Goodman, D. S., and Goodman, H. C. (1961) *Ann. Intern. Med. 55*, 1016-1031.

489. Heinen, R. J., Herbert, P. N., and Fredrickson, D. S. (1978) *J. Clin. Invest 61*, 120-132.

490. Chiesa, G., Stoltzfus, L. J., Michelagnoli, S., Bielicki, J. K., Santi, M., Forte, T. M., Sirtori, C. R., Franceschini, G., and Rubin, E. M. (1998) *Atherosclerosis 136*, 139-146.

491. Nofer, J. R., von Eckardstein, A., Wiebusch, H., Weng, W., Funke, H., Schulte, H., Kohler, E., and Assmann, G. (1995) *Hum. Genet. 96*, 177-182.

492. Arakawa, R. and Yokoyama, S. (2002) *J. Biol. Chem. 277*, 22426-22429.

6. PUBLICATIONS

Alteration of negatively charged residues in the 89 to 99 domain of apoA-I affects lipid homeostasis and maturation of HDL[S]

Andreas K. Kateifides,*[,§] Irina N. Gorshkova,*[,†] Adelina Duka,* Angeliki Chroni, Dimitris Kardassis,[§] and Vassilis I. Zannis[1,*]**

Molecular Genetics,* Whitaker Cardiovascular Institute, Department of Physiology and Biophysics,[†] Boston University School of Medicine, Boston, MA; Department of Biochemistry,[§] University of Crete Medical School, Heraklion, Crete, Greece; and Institute of Biology,** National Center for Scientific Research "Demokritos", Athens, Greece

Abstract In this study, we investigated the role of positively and negatively charged amino acids within the 89-99 region of apolipoprotein A-I (apoA-I), which are highly conserved in mammals, on plasma lipid homeostasis and the biogenesis of HDL. We previously showed that deletion of the 89-99 region of apoA-I increased plasma cholesterol and phospholipids, but it did not affect plasma triglycerides. Functional studies using adenovirus-mediated gene transfer of two apoA-I mutants in apoA-I-deficient mice showed that apoA-I[D89A/E91A/E92A] increased plasma cholesterol and caused severe hypertriglyceridemia. HDL levels were reduced, and approximately 40% of the apoA-I was distributed in VLDL/IDL. The HDL consisted of mostly spherical and a few discoidal particles and contained preβ1 and α4-HDL subpopulations. The lipid, lipoprotein, and HDL profiles generated by the apoA-I[K94A/K96A] mutant were similar to those of wild-type (WT) apoA-I. Coexpression of apoA-I[D89A/E91A/E92A] and human lipoprotein lipase abolished hypertriglyceridemia, restored in part the α1,2,3,4 HDL subpopulations, and redistributed apoA-I in the HDL2/HDL3 regions, but it did not prevent the formation of discoidal HDL particles. Physicochemical studies showed that the apoA-I[D89A/E91A/E92A] mutant had reduced α-helical content and effective enthalpy of thermal denaturation, increased exposure of hydrophobic surfaces, and increased affinity for triglyceride-rich emulsions. We conclude that residues D89, E91, and E92 of apoA-I are important for plasma cholesterol and triglyceride homeostasis as well as for the maturation of HDL.—Kateifides, A. K., I. N. Gorshkova, A. Duka, A. Chroni, D. Kardassis, and V. I. Zannis. **Alteration of negatively charged residues in the 89 to 99 domain of apoA-I affects lipid homeostasis and the maturation of HDL. *J. Lipid Res.* 2011. 52: 1363–1372.**

Supplementary key words apolipoprotein A-I mutations • HDL biogenesis • preβ and α-HDL particles • dyslipidemia • hypertriglyceridemia • LCAT • lipoprotein lipase

Apolipoprotein A-I (apoA-I) is the major protein component of HDL, and it plays an essential role in the biogenesis, maturation, and the functions of HDL (1–4). It is generally believed that the biogenesis of HDL occurs through a complex pathway that requires apoA-I, ATP-binding cassette transporter A1 (ABCA1), LCAT, and several other proteins (4). Population studies have shown that genetic mutations in apoA-I, ABCA1, and LCAT occur with high frequency in subjects with low HDL levels (5–7).

In previous studies, systematic mutagenesis and gene transfer of human apoA-I mutants in apoA-I deficient (apoA-I$^{-/-}$) mice disrupted specific steps along the pathway of biogenesis of HDL or induced other lipid and lipoprotein abnormalities (8). The phenotypes generated by apoA-I gene transfer in mice were discrete and included inhibition of the biogenesis of HDL (1); generation of un-

Abbreviations: ANS, 8-anilino-1-naphthalene-sulfonate; apoA-I, apolipoprotein A-I; apoA-I$^{-/-}$, apoA-I-deficient; CD, circular dichroism; CE, cholesteryl ester; DMPC, dimyristoyl-L-α-phosphatidylcholine; EM, electron microscopy; FPLC, fast-protein liquid chromatography; GdnHCl, guanidine hydrochloride; GFP, green fluorescent protein; sHDL, spheroidal HDL; HEK293, human embryonic kidney 293; hLPL, human lipoprotein lipase; HTB-13, SW 1783 human astrocytoma; MRW, mean residue weight; pfu, plaque forming units; PL, phospholipid; PLTP, phospholipid transfer protein; POPC, β-oleoyl-γ-palmitoyl-L-α-phosphatidylcholine; SANS, small-angle neutron scattering; TC, total cholesterol; WMF, wavelength of maximum fluorescence; WT, wild-type.

[1] To whom correspondence should be addressed.
e-mail: vzannis@bu.edu

[S] The online version of this article (available at http://www.jlr.org) contains supplementary data in the form of two figures and two tables.

This work was supported by the National Institutes of Health Grants HL-48739 and PO HL-26335. Its contents are solely the responsibility of the authors and do not necessarily represent the official views of the National Institutes of Health. A.K.K. is a student of the graduate program "The Molecular Basis of Human Disease" of the University of Crete Medical School and was supported by the Greek Ministry of Development, General Secretariat for Research and Technology Grant PENED 03-780.

Manuscript received 19 November 2010 and in revised form 19 April 2011.

Published, JLR Papers in Press, April 19, 2011
DOI 10.1194/jlr.M012989

stable intermediates (9, 10); inhibition of the activation of LCAT (9–11); and increase in plasma cholesterol or increase in both plasma cholesterol and triglycerides (12, 13). These studies also showed that deletion of the 89-99 region increased the levels and density distribution of plasma cholesterol and phospholipids and generated discoidal HDL particles but did not affect plasma triglyceride levels (12).

In the present study, we investigated the importance of the conserved positively and negatively charged residues present in the 89-99 domain of apoA-I for cholesterol and triglyceride homeostasis and the biogenesis of HDL. In the lipid-bound form, charged residues within the 89-99 region are juxtaposed with the complementary amino acid of apoA-I dimer or hairpin-shaped monomer (14, 15) and can form solvent-inaccessible salt bridges (16). We have found that changes in the positively charged residues K94 and K96 caused structural changes but did not affect the lipid and lipoprotein levels and the biogenesis of HDL. In contrast, substitutions of the negatively charged residues D89, E91, and E92 by alanines altered the conformation of apoA-I, increased its affinity for VLDL/IDL, as well as for triglyceride-rich emulsions, affected the maturation of HDL, and caused severe hypertriglyceridemia. These findings combined with previous studies suggest that subtle changes in critical amino acids located in different domains of apoA-I may have severe effects not only on the biogenesis of HDL but also on plasma cholesterol and triglyceride homeostasis.

EXPERIMENTAL PROCEDURES

Materials

Materials not mentioned in the experimental procedures have been obtained from sources described previously (3, 13).

Methods

Generation of adenoviruses expressing the wild-type (WT) and the mutant apoA-I forms and human lipoprotein lipase. The apoA-I gene lacking the BglII restriction site, which is present at nucleotide position 181 of the genomic sequence relative to the ATG codon of the gene, was cloned into the pCDNA3.1 vector to generate the pCDNA3.1-apoA-I(ΔBglII) plasmid as described (10). This plasmid was used as a template to introduce the apoA-I mutations apoA-I[D89A/E91A/E92A] and apoA-I[K94A/K96A] using the QuickChange® XL mutagenesis kit (Stratagene, Santa Clara, CA) and the mutagenic primers shown in supplementary Table I. The recombinant adenoviruses were packaged in 911 cells, amplified in human embryonic kidney 293 (HEK 293) cells, purified, and titrated as described (10). The adenovirus expressing human lipoprotein lipase (hLPL) was a gift of Dr. Alex Vezeridis (17).

Secretion of WT and mutant apoA-I forms. To assess the secretion of WT and mutant apoA-I forms, SW1783 human astrocytoma (HTB-13) cells grown to 80% confluence in Leibovitz's L-15 medium containing 2% heat-inactivated horse serum in 6-well plates were infected with adenoviruses expressing WT and mutant apoA-I forms at a multiplicity of infection of 10. At 24 h postinfection, the cells were washed twice with PBS and incubated in serum-free medium for 2 h. Following an additional wash with PBS, fresh serum-free medium was added, and 24 h later, it was collected and analyzed by SDS-PAGE for apoA-I expression.

ApoA-I production, purification, and functional cholesterol efflux and LCAT assays. WT and the mutant apoA-I[D89A/E91A/E92A] were obtained from the culture media of HTB-13 cells grown in roller bottles following infection with adenoviruses expressing the corresponding proteins. For protein production, the culture medium was collected, concentrated 5-fold, dialyzed against 25 mM ammonium bicarbonate, and lyophilized. The lyophilized apoA-I was combined with β-oleoyl-γ-palmitoyl-L-α-phosphatidylcholine (POPC), cholesterol, and sodium cholate at the ratio 1 mg/9.5 mg/0.47 mg/4.5 mg. The proteoliposomes formed were fractionated by density gradient ultracentrifugation, and the fractions that contained pure apoA-I were collected and delipidated three times using 2:1 v/v chloroform:methanol (18).

ABCA1-mediated cholesterol efflux measurements using HEK293-EBNA cells and LCAT activation assays were performed as described (13, 19).

Animal studies, plasma lipids and apoA-I levels, FPLC fractionation, and two-dimensional gel electrophoresis. Male apoA-I$^{-/-}$ (ApoA1^{tm1Unc}) C57BL/6J mice (20) were purchased from Jackson Laboratories (Bar Harbor, ME). The mice were maintained on a 12-h light/dark cycle and standard rodent chow. All procedures performed on the mice were in accordance with National Institutes of Health and institutional guidelines. ApoA-I$^{-/-}$ mice, 6–8 weeks of age, were injected via the tail vein with 2×10^9 plaque forming units (pfu) of recombinant adenovirus per animal. The animals were euthanized four days postinjection following a 4 h fast.

The concentration of total cholesterol, free cholesterol, phospholipids, and triglycerides of plasma drawn four days postinfection was determined using the Total Cholesterol E, Free Cholesterol C, and Phospholipids C reagents (Wako Chemicals USA, Inc., Richmond, VA) and INFINITY triglycerides reagent (ThermoScientific, Waltham, MA), respectively, according to the manufacturer's instructions. The concentration of cholesteryl esters was determined by subtracting the concentration of free cholesterol from the concentration of total cholesterol. Plasma apoA-I levels were determined by a turbidometric assay using AutoKit A-I (Wako Chemicals). For fast-protein liquid chromatography (FPLC) analysis of plasma, 17 μl plasma obtained from mice infected with adenovirus-expressing WT or mutant apoA-I forms were loaded onto a Sepharose 6 PC column (Amersham Biosciences, Piscataway, NJ) in a SMART micro FPLC system (Amersham Biosciences) and eluted with PBS. A total of 25 fractions of 50 μl volume each were collected for further analysis. The concentration of lipids in the FPLC fractions was determined as described above. The plasma HDL subpopulations were separated by two-dimensional electrophoresis. The proteins were then transferred to a nitrocellulose membrane and apoA-I was detected by immunoblotting, using the goat polyclonal anti-human apoA-I antibody AB740 (Chemicon International, Billerica, MA) (12).

Fractionation of plasma by density gradient ultracentrifugation and EM analysis of the apoA-I-containing fractions. An aliquot of 300 μl of plasma obtained from adenovirus-infected mice was diluted with saline to a total volume of 0.5 ml and fractionated by density gradient ultracentrifugation. Following ultracentrifugation, 0.5 ml fractions were collected and analyzed by SDS-PAGE as previously described (12). Fractions 6-7 obtained by the density ultracentrifugation, which float in the HDL region, were analyzed by electron microscopy (EM) using a Philips CM-120 electron microscope.

ApoA-I mRNA quantification. Total hepatic RNA was isolated by the Trizol® method (Invitrogen, Carlsbad, CA) according to

the manufacturer's instructions. RNA samples were adjusted to 0.1 μg/μl, and cDNA was produced using the high-capacity reverse transcriptase cDNA kit (Applied Biosystems, Foster City, CA). Apo A-I mRNA was quantified using Applied Biosystems Gene Array TaqMan® primers for apoA-I cDNA (Cat# Hs00985000_g1) and 18s rRNA (Cat# 4319413E) with the TaqMan® Gene expression PCR Master Mix (Cat# 4370048), using the Applied Biosystems 7300 Real-Time PCR System (21).

Preparation of apoA-I for physicochemical measurements. Several days prior to the physicochemical analyses, the lyophilized proteins were dissolved in 4 M guanidine hydrochloride (GndHCl) and then refolded by subsequent dialysis against 2.5 M and 1.25 M GndHCl solutions in PBS, followed by extensive dialysis against the appropriate buffer [10 mM sodium phosphate and 0.02% NaN3 (pH 7.4) for circular dichroism (CD) experiments, PBS for fluorescence and dimyristoyl-L-α-phosphatidylcholine (DMPC) clearance measurements, or Tris for emulsion-binding experiments].

Secondary structure and thermal unfolding of apoA-I forms. Far-UV CD spectra were recorded at 25°C on an AVIV 62DS or AVIV 215 spectropolarimeter (AVIV Associates, Inc., Lakewood, NJ) equipped with a thermoelectric temperature control at protein concentrations 20-55 μg/ml as described previously (22, 23). For each protein, spectra were recorded at several protein concentrations, then normalized to the protein concentration and expressed as mean residue ellipticity [Θ], which was calculated by the equation: $[\Theta] = \Theta \times MRW / (10 \times l \times c)$, where Θ is the measured ellipticity, MRW is the mean residue weight (about 115), l is the cell path length (cm), and c is the protein concentration (g/ml). The α-helix content was estimated from the mean residue ellipticity at 222 nm, [Θ_{222}] (24). Thermal unfolding of apoA-I in solution was monitored by changes in ellipticity at 222 nm. The thermodynamic parameters of the transitions, melting temperature (T_m) and van't Hoff enthalpy (ΔH_v), were determined from the van't Hoff analysis of the melting curves as described previously (22, 23).

ANS fluorescence measurements and DMPC clearance studies. Fluorescence emission spectra of 8-anilino-1-naphthalene-sulfonate (ANS) were recorded in PBS buffer at ANS concentration of 125 μM in the presence of 25 μg/ml WT apoA-I, mutant apoA-I forms, or carbonic anhydrase, or in the absence of any protein using a FluoroMax-2 fluorescence spectrometer (25). The wavelength of maximum fluorescence (WMF) and the intensity of fluorescence emission at WMF were determined from each spectra after subtraction of the buffer baseline as described (25). The solubilization of DMPC multilamellar vesicles by apoA-I was monitored by the decrease in absorbance at 325 nm following the administration of apoA-I to a suspension of DMPC in PBS as described previously (25).

Binding of WT and mutant apoA-I to triglyceride-rich emulsion particles. Triglyceride-rich emulsions were prepared as described (26, 27). The particles, which were analyzed for phospholipid and triglyceride content as well as by EM to determine their morphology and size, were used for apoA-I binding assays within two days. For these assays, 120 μg of WT or mutant apoA-I (freshly dialyzed) were incubated for 1 h at 27°C with increasing amounts of emulsion in 1.8 ml of Tris buffer to give a phosphatidylcholine to protein molar ratio ranging from 180 to 710. The apoA-I bound to the emulsions was recovered by ultracentrifugation and quantitated as described (27). Experiments were performed three or four times using emulsions from three different preparations.

RESULTS

Expression and secretion of the WT apoA-I and the two apoA-I mutants

To assess the expression and secretion of the two mutant proteins relative to WT apoA-I, we infected HTB-13 cells with recombinant adenoviruses expressing the WT or the mutant apoA-I genes using a multiplicity of infection of 10. Analysis of the medium 24 h postinfection showed that the WT and the two mutant forms of apoA-I were secreted at comparable levels in the medium (supplementary Fig. IA).

Plasma lipid measurements

Plasma lipids, apoA-I, and hepatic apoA-I mRNA levels were determined four days postinfection of apoA-$I^{-/-}$ mice with adenoviruses expressing the WT apoA-I and the two apoA-I mutants. It was found that at comparable levels of mRNA expression the apoA-I[D89A/E91A/E92A] mutant caused dyslipidemia characterized by severe hypertriglyceridemia, increased plasma cholesterol and phospholipids, and decreased cholesteryl ester (CE) to total cholesterol (TC) ratio. The lipid parameters in mice expressing the apoA-I[K94A/K96A] mutant were comparable to those of mice expressing WT apoA-I with the exception of TC/apoA-I ratio, which was reduced for this mutant (**Table 1**).

FPLC profiles of plasma isolated from apoA-$I^{-/-}$ mice infected with adenoviruses expressing the WT apoA-I and the two apoA-I mutants

FPLC analysis of plasma from apoA-$I^{-/-}$ mice infected with the recombinant adenovirus expressing either WT apoA-I or the two apoA-I mutants showed that, in mice expressing WT apoA-I, cholesterol was distributed predominantly in the HDL2/HDL3 region. The distribution of cholesterol in the apoA-I[K94A/K96A] mutant was similar to that of WT apoA-I with an additional shoulder in the IDL and LDL regions. In contrast, in mice expressing the apoA-I[D89A/E91A/E92A] mutant, cholesterol was distributed predominantly in the VLDL/IDL/LDL region (**Fig. 1A**). All the triglycerides of the apoA-I[D89A/E91A/E92A] mutant were found in the VLDL region. The VLDL triglyceride peak of the WT apoA-I and apoA-I[K94A/K96A] mutant were negligible (Fig. 1B).

Fractionation of plasma of mice expressing the WT apoA-I and the two apoA-I mutants by density gradient ultracentrifugation and EM analysis of the HDL fraction

Fractionation of plasma by density gradient ultracentrifugation and subsequent analysis of the resulting fractions by SDS-PAGE served two purposes: it gave important information of the distribution of apoA-I in different lipoprotein fractions, and it provided the HDL fractions that were used for EM analysis. It was found that the WT apoA-I and apoA-I[K94A/K96A] mutant are predominantly distributed in the HDL2 and HDL3 regions (**Fig. 2A**, B). In contrast, in the case of the apoA-I[D89A/E91A/E92A] mutant, approximately 40% of apoA-I was distributed in the VLDL/IDL/LDL fractions and the remaining in the HDL3 and, to a lesser extent, the HDL2 fractions (Fig. 2C).

TABLE 1. Plasma Lipids, ApoA-I, and Hepatic mRNA Levels of ApoA-I$^{-/-}$ Mice Expressing WT and Mutant Forms of ApoA-I Obtained Four Days Postinfection

Protein Expressed	TC	TC/apoA-I	Free Cholesterol	CE/TC	PL	Triglyceride	Relative apoA-I mRNA	Plasma apoA-I
	mg/dl		*mg/dl*		*mg/dl*	*mg/dl*	*%*	*mg/dl*
GFP	28 ± 7	—	12 ± 3	0.58 ± 0.04	33 ± 22	34 ± 3	—	—
WT apoA-I	268 ± 55	0.95 ± 0.16	75 ± 34	0.72 ± 0.06	296 ± 96	70 ± 11	100 ± 32	283 ± 84
apoA-I [D89A/E91A/E92A]	497 ± 139	2.52 ± 0.84	347 ± 147	0.36 ± 0.31	603 ± 406	2106 ± 1629	101 ± 24	235 ± 106
apoA-I [K94A/K96A]	108 ± 23	0.53 ± 0.04	46 ± 21	0.58 ± 0.15	190 ± 14	66 ± 9	56 ± 20	220 ± 51
apoA-I [D89A/E91A/E92A] + hLPL	122 ± 56	1 ± 0.2	56 ± 20	0.44 ± 0.14	255 ± 128	49 ± 16	41 ± 6	99 ± 18

Values are means ± SD (n = 4-6).

Analysis of the HDL fractions 6 and 7 obtained following density gradient ultracentrifugation by EM showed that the WT apoA-I and the apoA-I[K94A/K96A] mutant generated spherical particles (Fig. 2D, E) and the apoA-I[D89A/E91A/E92A] mutant generated mostly spherical and a few discoidal particles (Fig. 2F). Control experiments showed that HDL density fractions obtained from green fluorescent protein (GFP)-expressing apoA-I$^{-/-}$ mice, which cannot form HDL, contained very few spherical particles (supplementary Fig. II).

Two-dimensional gel electrophoresis of plasma of mice expressing the WT apoA-I and the two apoA-I mutants

Two-dimensional gel electrophoresis of plasma showed that WT apoA-I and the apoA-I[K94A/K96A] mutant formed normal α subpopulations with a small amount of preβ HDL particles (Fig. 2G, H). In contrast, the apoA-I[D89A/E91A/E92A] mutant formed predominantly preβ1 and α4 HDL particles at a ratio of approximately 2:1 (Fig. 2I). Lipoprotein lipase normalizes the lipid and lipoprotein abnormalities induced by the apoA-I[D89A/E91A/E92A] mutation.

ApoA-I$^{-/-}$ mice were coinfected with 2×10^9 pfu of adenovirus expressing apoA-I[D89A/E91A/E92A] mutant and 5×10^8 pfu of adenovirus expressing the hLPL, and their lipid and lipoprotein profiles were compared with those mice infected with 2×10^9 pfu of adenovirus expressing WT apoA-I. This analysis showed that the lipoprotein lipase treatment abolished hypertriglyceridemia but did not correct the CE/TC ratio in mice that received the apoA-I[D89A/E91A/E92A] mutant and hLPL (Table 1).

The plasma of apoA-I$^{-/-}$ mice coinfected with the apoA-I[D89A/E91A/E92A] mutant and hLPL was fractionated by density gradient ultracentrifugation and SDS-PAGE, and then the HDL fraction was analyzed by EM. In mice coinfected with the apoA-I[D89A/E91A/E92A] mutant and hLPL, the HDL was distributed mostly into the HDL3 and, to a lesser extent, to HDL2. ApoA-I was not found in the VLDL/IDL fraction (**Fig. 3A**). The HDL fraction contained both discoidal and spherical HDL particles (Fig. 3B). The observed decrease in plasma apoA-I levels can be explained by the decreased expression of the apoA-I transgene in the coinfection experiment and possibly by faster catabolism of the smaller size HDL particles.

Two-dimensional gel electrophoresis of plasma obtained from mice coinfected with the apoA-I[D89A/E91A/E92A] mutant and hLPL showed that the hLPL treatment restored in part the α1, 2, 3, and 4 HDL subpopulations (Fig. 3C).

In vitro properties of apoA-I[D89A/E91A/E92A] mutant

To interpret the abnormalities in lipid and lipoprotein profiles of apoA-I$^{-/-}$ mice expressing the apoA-I[D89A/E91A/E92A] mutant, we investigated the ability of the lipid-free mutant protein to promote cholesterol efflux in HEK293 EBNA cells transfected with an ABCA1-expressing plasmid, as well as the ability of proteoliposomes containing this mutant to activate LCAT in vitro. The rHDL containing the apoA-I[D89A/E91A/E92A] mutant consisted predominantly of two populations of particles of 80 and 110 nm, whereas the rHDL containing WT apoA-I consisted predominantly of one subpopulation of particles of 96 nm (supplementary Fig. IB) The cholesterol

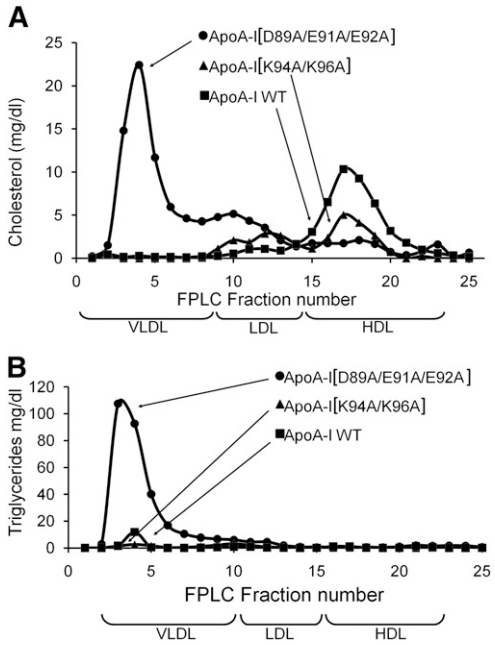

Fig. 1. FPLC profiles of total cholesterol (A) or triglycerides (B) of apoA-I$^{-/-}$ mice infected with adenoviruses expressing the WT apoA-I, apoA-I[D89A/E91A/E92A], and apoA-I[K94A/K96A] as indicated. Plasma samples were obtained four days postinfection.

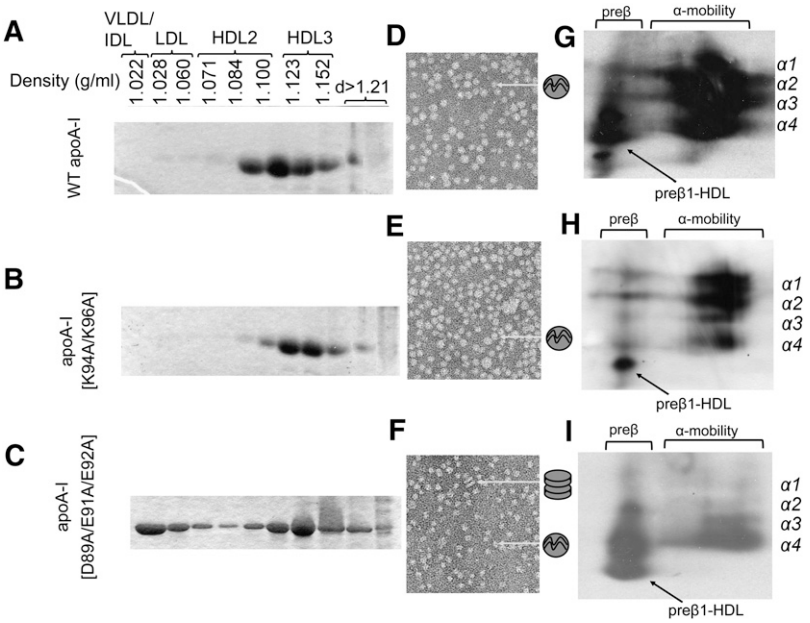

Fig. 2. Analyses of plasma of apoA-I$^{-/-}$ mice infected with adenoviruses expressing the WT apoA-I (A, D, G), the apoA-I[K94A/K96A] (B, E, H), and the apoA-I[D89A/E91A/E92A] (C, F, I) by density gradient ultracentrifugation, SDS-PAGE, two-dimensional gel electrophoresis, and EM. A–C: SDS-PAGE analysis of density gradient ultracentrifugation fractions. D–F: EM pictures of HDL fractions 6-7 obtained from apoA-I$^{-/-}$ mice expressing the WT and mutant forms of apoA-I following density gradient ultracentrifugation of plasma as indicated. The photomicrographs were taken at 75,000× magnification and enlarged three times. G–I: Analysis of plasma obtained from mice expressing the WT apoA-I or the mutant forms as indicated following two-dimensional gel electrophoresis and Western blotting.

efflux and LCAT assays showed that the capacity of the lipid-free apoA-I[D89A/E91A/E92A] mutant to promote ABCA1-mediated cholesterol efflux and the capacity of the rHDL containing this mutant to activate LCAT was approximately two-thirds of that of WT apoA-I (supplementary Fig. IC and D, respectively).

Effect of mutations on the α-helical content, thermal stability, and conformation of apoA-I

Analysis of the normalized far-UV CD spectra of WT apoA-I and the apoA-I[D89A/E91A/E92A] and apoA-I[K94A/K96A] mutants(**Fig. 4A**) showed that, compared with WT apoA-I, the two mutant proteins had an ∼9% reduction and ∼6% increase, respectively, in their α-helical content. This finding corresponds to a loss of ∼22 and gain of ∼15 residues, respectively, in the helical conformation of apoA-I (**Table 2**).

The thermal unfolding of the WT apoA-I, apoA-I[D89A/E91A/E92A], and apoA-I[K94A/K96A] mutants was monitored by the ellipticity at 222 nm (Fig. 4B). The parameters of thermal unfolding determined from the van't Hoff analysis are listed in Table 2. The apoA-I[D89A/E91A/E92A] mutation caused a small (∼2°C) but statistically significant decrease in the melting temperature T_m, indicating a destabilizing effect of the mutation. The T_m of apoA-I[K94A/K96A] did not differ from that of WT apoA-I. Large (∼13 kcal/mol) decrease in the effective enthalpy ΔH_v for the apoA-I[D89A/E91A/E92A] mutant compared with WT apoA-I was consistent with the less cooperative (less sharp) thermally induced unfolding of this mutant (Fig. 4B) and suggests a significantly lower cooperativity of the thermal transition of the apoA-I[D89A/E91A/E92A] mutant. The effective enthalpy ΔH_v

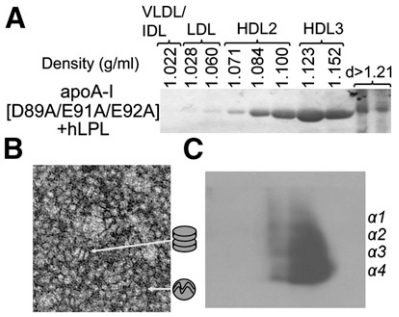

Fig. 3. Analyses of plasma of apoA-I$^{-/-}$ mice infected with adenoviruses expressing the apoA-I[D89A/E91D/E92A] and hLPL. A: SDS-PAGE analysis of fractions obtained by density gradient ultracentrifugation of plasma of apoA-I$^{-/-}$ mice infected with 2×10^9 pfu of adenovirus expressing apoA-I[D89A/E91A/E92A] and 5×10^8 pfu of an adenovirus expressing the hLPL. B: EM picture of HDL fractions 6-7 obtained from apoA-I$^{-/-}$ mice expressing the apoA-I[D89A/E91A/E92A] mutant and human lipoprotein lipase, following density gradient ultracentrifugation as indicated in panel A. The sample was concentrated two times. The photomicrographs were taken at 75,000× magnification and enlarged three times. C: Analysis of plasma obtained from mice expressing the apoA-I[D89A/E91A/E92A] mutant and hLPL following two-dimensional gel electrophoresis and Western blotting.

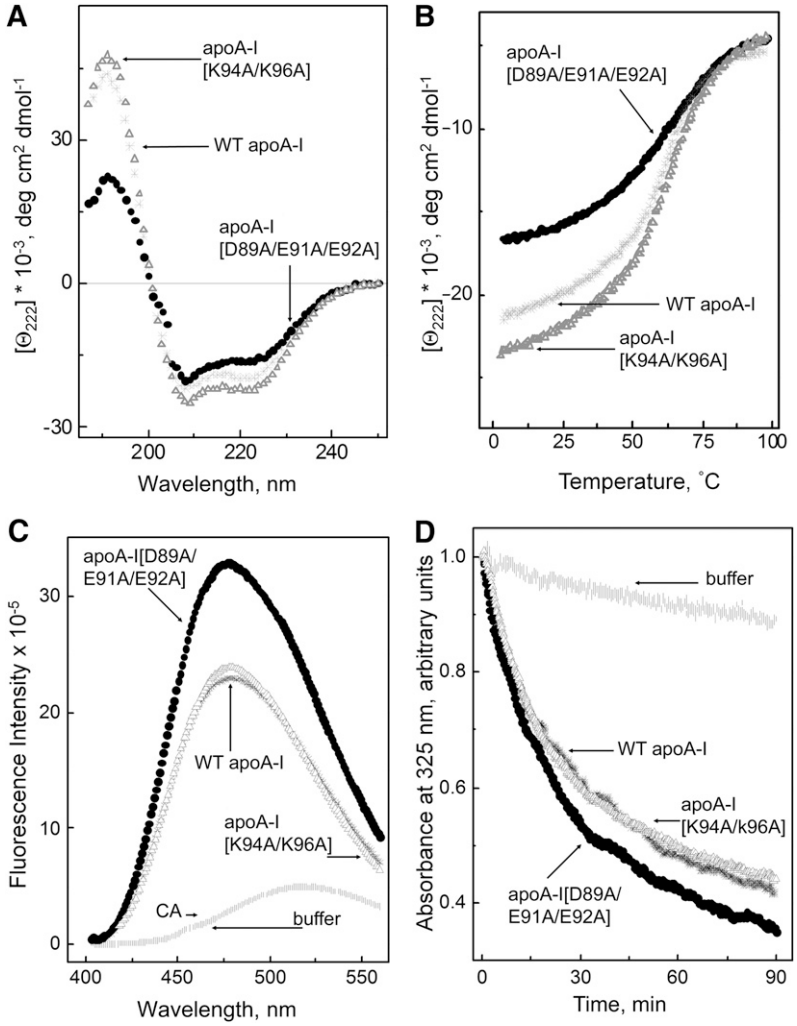

Fig. 4. Physicochemical properties of the WT apoA-I, apoA-I[D89A/E91A/E92A], and apoA-I[K94A/K96A]. A: Far-UV CD spectra of the apoA-I forms recorded at 25°C. Each sample contained 25 μg/ml protein in 10 mM PBS. Each spectrum is the average of four scans. B: Thermal unfolding of the apoA-I forms monitored by the ellipticity at 222 nm. Protein concentration in each sample was 40 μg/ml in 10 mM PBS. C: ANS fluorescence spectra obtained in the presence of the WT apoA-I, apoA-I[D89A/E91A/E92A], apoA-I[K94A/K96A] mutant, carbonic anhydrase, or in buffer alone, as indicated. The two latter spectra are superimposed. Final sample concentrations are 125 μM ANS and 25 μg/ml protein in 10 mM PBS. D: The time course of DMPC clearance by the apoA-I forms or in buffer alone. DMPC multilamellar vesicles (100 μg/ml lipids) were pre-incubated at 24°C, and the clearance was triggered by addition of protein to reach final concentration in cuvette 40 μg/ml. The turbidity was monitored by absorbance at 325 nm at the controlled temperature 24°C. ∗, WT apoA-I; ●, apoA-I[D89A/E91A/E92A]; △, apoA-I[K94A/K96A], indicated by arrows.

for the apoA-I[K94A/K96A] mutant was lower than that for WT apoA-I by ~5 kcal/mol.

Effect of the apoA-I mutations on ANS-fluorescence and DMPC-clearance kinetics

To investigate whether the apoA-I[D89A/E91A/E92A] and apoA-I[K94A/K96A] mutations affected the tertiary structure of apoA-I, the intrinsic fluorescence of the amphipathic fluorescent dye ANS was recorded in the presence of each of these proteins or in the presence of WT apoA-I. In the presence of the WT and mutant apoA-I forms, ANS fluorescence was significantly enhanced and blue-shifted compared with ANS fluorescence in buffer alone or in the presence of carbonic anhydrase, which represents a typical globular protein. This observation is consistent with the molten-globular-like conformation of apoA-I. However, in the presence of the apoA-I[D89A/E91A/E92A], the increase in the fluorescence intensity

TABLE 2. The α-Helical Content and Thermodynamic Parameters of Lipid-Free WT ApoA-I and the ApoA-I Mutant Forms and Parameters of ANS Fluorescence in the Presence of the Proteins

Protein	α-Helix[a]	Residues in α-Helix	T_m[b]	ΔH_v[b]	I[c]	WMF[c]
	%		°C	*kcal/mol*	*relative units*	*nm*
WT apoA-I	~58	144	61 ± 0.5	39 ± 1	4.6	480
apoA-I [D89A/E91A/E92A]	~49	122	59 ± 0.5[e]	26 ± 2[f]	6.6	477
apoA-I [K94A/K96A]	~64	159	60 ± 1.0	34 ± 2[d]	4.8	479

[a]Estimated from the $[\Theta_{222}]$ at 25°C. Systematic and statistical errors are ± 3%.
[b]The melting temperature T_m and the effective enthalpy ΔH_v were determined from van't Hoff analysis of the thermal unfolding curves monitored by CD at 222 nm.
[c]Parameters of ANS fluorescence determined in the presence of WT apoA-I, apoA-I [D89A/E91A/E92A], or apoA-I[K94A/K96A] (Fig. 4C). "I" is ANS fluorescence intensity in relative units compared with the fluorescence in buffer alone.
[d]Significance of differences from the value for WT: $P < 0.05$.
[e]Significance of differences from the value for WT: $P < 0.01$.
[f]Significance of differences from the value for WT: $P < 0.005$.

was 43% larger and the blue shift in WMF was ~3 nm greater than in the presence of WT apoA-I (Fig. 4C and Table 2). This finding suggests that, compared with WT apoA-I, the [D89A/E91A/E92A] mutant has additional exposed hydrophobic surfaces. The fluorescence intensity and WMF of the apoA-I[K94A/K96A] were close to those of WT apoA-I (Fig. 4C and Table 2).

The kinetics of solubilization of multilamellar DMPC vesicles by WT and the apoA-I[D89A/E91A/E92A] mutant was monitored at 325 nm by the clearance of the turbidity of DMPC suspension following the addition of apoA-I. It was found that the apoA-I[D89A/E91A/E92A] mutant clears turbidity slightly faster than WT apoA-I and the apoA-I[K94/K96A] clears turbidity at a rate similar to that of WT apoA-I (Fig. 4D).

Binding of apoA-I forms to triglyceride-rich emulsions

The weight ratio triolein:PC in the emulsions was 4.1 ± 0.3 (mean ± SD of three isolated emulsions). The average size of particles in a typical isolated emulsion calculated from the electron microphotographs was 54 ± 21 nm (mean± SD; n = 201). The large standard deviations reflect a broad size distribution that resembles a size distribution of plasma VLDL. Data of the binding assays (**Fig. 5A**) show that at each emulsion:protein ratio in the incubation mixtures, the portion of the bound protein is higher for the apoA-I[D89A/E91A/E92A] mutant than for WT apoA-I.

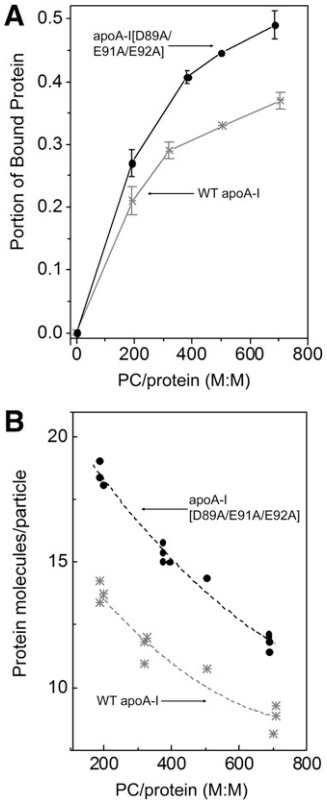

Fig. 5. Binding of the WT apoA-I and the apoA-I[D89A/E91A/E92A] mutant to triglyceride-rich emulsion particles. A: Portion of bound protein at different PC:protein ratios. B: Bound WT apoA-I or apoA-I[D89A/E91A/E92A] per one emulsion particle. *, WT apoA-I; ●, apoA-I[D89A/E91A/E92A].

Fig. 5B shows that for each emulsion:protein ratio in the incubation mixtures, the number of protein molecules bound to one particle is significantly higher for the apoA-I[D89A/E91A/E92A] mutant than for WT apoA-I.

DISCUSSION

Rationale for selection of the mutations

The 89-99 region of apoA-I contains several residues that are highly conserved in animal species, particularly mammals (16). Amino acid position 89 is occupied in 29 species by D and has a conservative E substitution in 2 species. Positions 91 and 92 are occupied by negatively charged E and, in a few cases, D residues in mammals and birds. The cluster of the positively charged K residues at positions 94 and 96 also shows remarkable sequence preservation in amphibian mammals and birds. Position 94 is occupied in 21 species by K and 9 by R, whereas position 96 is occupied by K in all but 1 of the mammals and birds and diverges in fish (16). It is also interesting that noncharged residues in the 89 to 99 region are conserved. Positions 90, 93, and 97 are occupied mostly by V or other hydrophobic amino acids (supplementary Table II). Residues D89, E91, E92, K94, and K96 are located in the α11/3 helical wheel positions 2, 4, 5, 7, and 9, respectively. Residue D89 may form a strong solvent-inaccessible salt bridge with residue R177 of the antiparallel helix, and residues E92 and K96 may form weaker solvent-inaccessible salt bridges with residues R173 and E169, respectively, of the antiparallel helix. Residues E91 and K94 may interact with the aqueous phase.

Previous studies have shown that deletion of the 89-99 region of apoA-I caused dyslipidemia characterized by increased plasma cholesterol and phospholipids that were distributed in the VLDL/IDL region, decreased plasma PLTP activity, normal plasma triglycerides, and formation of discoidal HDL particles. The deletion caused a modest (20–30%) reduction in the capacity of the mutant protein to promote ABCA1-mediated cholesterol efflux and to activate LCAT in vitro (12). The drastic alteration of the structure of apoA-I due to the 89-99 deletion may have caused realignment of the helices of apoA-I on the spherical HDL particles that may be responsible for the observed phenotype.

For these reasons, we chose to further probe the importance of the 89-99 region of apoA-I by focusing on the impact of the conserved clusters of three negatively charged and two positively charged residues on lipid homeostasis and the biogenesis of HDL in mouse models.

The apoA-I mutations D89A/E91A/E92A alter the functions of apoA-I, profoundly affect plasma triglyceride homeostasis, and prevent maturation of HDL

The present study showed that the expression of the apoA-I[D89A/E91A/E92A] mutant in apoA-I$^{-/-}$ mice resulted in dyslipidemia characterized by severe hypertriglyceridemia, increased plasma cholesterol, decreased HDL cholesterol, reduced esterification of plasma cholesterol, and the generation of a few discoidal HDL particles and small-

size HDL particles that form preβ and α4-HDL subpopulations. The mutation caused only a small 15% decrease in plasma PLTP activity (data not shown). On the other hand, the phenotype generated by adenovirus-mediated gene transfer of apoA-I[K94A/K96A] in apoA-I$^{-/-}$ mice was normal. These findings suggested that the negatively charged D89, E91, and E92 residues of apoA-I are crucial for maintenance of plasma cholesterol and triglyceride homeostasis as well as the biogenesis and/or catabolism of HDL.

Changes in the structure and the lipid binding properties of the lipid-free apoA-I induced by the D89A/E91A/E92A and the K94A/K96A mutations

Estimation of the α-helical content and the thermodynamic stability by far-UV CD spectroscopy indicated that apoA-I[D89A/E91A/E92A] has 22 fewer residues in the α-helical conformation, slightly reduced thermal stability, and greatly reduced cooperativity of thermal unfolding compared with the WT apoA-I (Table 2). ANS fluorescence measurements indicated that the apoA-I [D89A/E91A/E92A] mutant has more hydrophobic surfaces exposed to the solvent compared with WT apoA-I, suggesting a looser tertiary folding of the mutant protein. Similar characteristics have been described for the apoA-I[E110A/E111A] and apoA-I[Δ(61-78)] mutants (28) that have been previously associated with dyslipidemia (12, 13). The apoA-I[K94A/K96A] mutant had increased helical content and reduced cooperativity of thermal unfolding, whereas the ANS characteristics and the DMPC clearance kinetics were similar to those of WT apoA-I.

Potential mechanism of dyslipidemia induced by the D89A/E91A/E92A mutations

The apoA-I[D89A/E91A/E92A] mutant shares two characteristics with the apoA-I[Δ(61-78)] and apoA-I [E110A/E111A] mutants that were shown previously to cause hypertriglyceridemia (12, 13). The first characteristic is that all three mutants caused accumulation of apoA-I in the VLDL/IDL region, and as shown previously, this affected the in vitro lipolysis of the VLDL/IDL fraction by exogenous lipoprotein lipase (12, 13). The second characteristic of the three apoA-I mutants is that the negatively charged residues E78, D89, and E111 that occur in the WT sequence have the ability to form solvent-inaccessible salt bridges with positively charged residues present in the antiparallel apoA-I molecule of a discoidal HDL particle (29). The affinity of all three mutants for triglyceride-rich lipoproteins is further supported by binding of these mutants to triglyceride-rich emulsion particles (Ref. 27 and Fig. 5).

Analysis of the 93 Å spherical HDL in solution by small-angle neutron scattering (SANS) showed that apoA-I folds around a central lipid core that has 88.4 Å × 62.8 Å dimensions to form a spheroidal HDL (sHDL) particle. Three possible arrangements of the apoA-I on the sHDL particle were considered: *1*) An "HdHp" model where two apoA-I molecules are arranged in antiparallel planar orientation and a third molecule assumes a hairpin structure; *2*) a "3Hp" model where three apoA-I molecules are folded as hairpins; and *3*) an "integrated trimer (iT)" model where three apoA-I molecules interact with each other on the HDL surface (14). Similar but not identical arrangements were proposed in the "trefoil" model where the right-hand half of two antiparallel apoA-I molecules of the double belt model are displaced 60° out of their planar position and are aligned in antiparallel orientation with a third molecule bent on a 60° angle (15). In these models the apoA-I monomers or dimers are juxtaposed in the vicinity of helices 5 and 6 (14, 15). In these arrangements of apoA-I molecules on sHDL, particle residues E78 in helix 2, D89 in helix 3, and E111 in helix 4 can form solvent-inaccessible salt bridges with residues R188 in helix 8, R177 in helix 7, and H155 in helix 6, respectively, of the antiparallel strand. It is interesting that in the 11/3 α-helical wheel residues, E78, D89, and E111 are all located in wheel position 2. With the exception of R188, all other five residues involved in salt bridges are conserved in mammals. Consistently with these observations, temperature jump molecular dynamic simulation (30, 31) indicated that the E89-R177 and E111-H155 are more stable than the E78-R188 salt bridge. Thus it is possible that elimination of the negatively charged residues D89 and E111 and, to a lesser extent, E78, may destabilize the intermolecular interactions of the apoA-I dimer or the hairpin bound to HDL and may predispose to dyslipidemia.

The interference of apoA-I[D89A/E91A/E92A] with lipolysis was tested in vivo by coinfection of mice with adenoviruses expressing apoA-I[D89A/E91A/E92A] and human lipoprotein lipase. This treatment abolished hypertriglyceridemia, restored in part the α1,2,3,4 HDL subpopulations, and redistributed apoA-I in the HDL2 and HDL3 region; however, it did not alter the CE/TC ratio or the formation of discoidal HDL. The findings suggest that the increased abundance of apoA-I in the VLDL/IDL region may create lipoprotein lipase insufficiency that induces hypertriglyceridemia.

The present study also indicated a direct effect of the [D89A/E91A/E92A] mutation in the activation of LCAT in vivo. This is documented by the persistence of the discoidal particles, the low CE/TC ratio, and preponderance of the smaller α4 and α3 subpopulations following normalization of the plasma triglyceride levels by the lipoprotein lipase treatment. Previous studies have shown that discoidal and small-size HDL particles and the LCAT associated with them may be catabolized quickly by the kidney and thus lead to LCAT insufficiency and reduced plasma HDL levels (10, 32, 33). In vitro studies have also indicated that increased catabolism by the kidney and liver may occur following triglyceride hydrolysis of hypertriglyceridemic HDL by hepatic lipase (34).

It is conceivable that loosening of the structure of apoA-I around the D89 or E92 area due to the substitution of the original residues by A may provide new surfaces for interaction of HDL with other proteins or lipoprotein particles, such as VLDL, in ways that inhibit triglyceride hydrolysis. Furthermore, the accumulation of discoidal HDL and the formation of preβ and small α4-HDL particles shown by the in vivo experiments indicates that replacement of D89, E91, and E92 by A has a direct impact on the activation of LCAT.

Clinical implications

Genome-wide associated studies provided statistical evidence that loci that affect HDL-C and triglyceride levels are associated with risk for coronary artery disease (35). The molecular etiology of most forms of hypertriglyceridemia in humans remains unclear. Early studies established that severe genetically transmitted hypertriglyceridemia occurs as a result of mutations in lipoprotein lipase and apoCII (36, 37). Subsequently, it has been shown that hypertriglyceridemia can be induced by overexpression of apoCIII, apoCII, apoCI, apoA-II, and apoE in transgenic mice following adenovirus-mediated gene transfer (38–43) or by inactivation of the apoA-V gene in mice (44). In humans, plasma apoE and apoCIII levels correlate with plasma triglyceride levels (45, 46). Moderate hypertriglyceridemia has been observed in patients with Tangier disease, in carriers of apoA-I Milano, and in male carriers of apoA-IΔLys107 (47–50). These findings support the hypothesis that normal apoA-I structure and functions may be required for plasma triglyceride homeostasis.

The present and two previous studies (12, 13) raise the possibility that subtle changes in the structure of apoA-I caused by mutations may induce hypertriglyceridemia. To the extent that similar mutations exist in humans, the genetic predisposition to hypertriglyceridemia may be further aggravated by other genetic and environmental factors, such as diabetes and thyroid status. The potential contribution of apoA-I mutations to hypertriglyceridemia could be addressed in future studies in selected populations of patients with hypertriglyceridemia of unknown etiology.

The authors thank Dr. Mason Freeman for providing the ABCA1 expression plasmid; Dr. Silvia Santamarina-Fojo for providing the LPL and LCAT adenoviruses; Don Gantz for electron microscopy analysis; Gayle Forbes, Cheryl England, Michael Gigliotti, and Dimitra Georgiadou for technical assistance; and Dr. David Atkinson and Dr. Efstratios Stratikos for advice on the physicochemical studies.

REFERENCES

1. Chroni, A., T. Liu, I. Gorshkova, H. Y. Kan, Y. Uehara, A. von Eckardstein, and V. I. Zannis. 2003. The central helices of apoA-I can promote ATP-binding cassette transporter A1 (ABCA1)-mediated lipid efflux. Amino acid residues 220-231 of the wild-type apoA-I are required for lipid efflux in vitro and high density lipoprotein formation in vivo. *J. Biol. Chem.* **278:** 6719–6730.
2. Laccotripe, M., S. C. Makrides, A. Jonas, and V. I. Zannis. 1997. The carboxyl-terminal hydrophobic residues of apolipoprotein A-I affect its rate of phospholipid binding and its association with high density lipoprotein. *J. Biol. Chem.* **272:** 17511–17522.
3. Liu, T., M. Krieger, H. Y. Kan, and V. I. Zannis. 2002. The effects of mutations in helices 4 and 6 of apoA-I on scavenger receptor class B type I (SR-BI)-mediated cholesterol efflux suggest that formation of a productive complex between reconstituted high density lipoprotein and SR-BI is required for efficient lipid transport. *J. Biol. Chem.* **277:** 21576–21584.
4. Zannis, V. I., A. Chroni, K. E. Kypreos, H. Y. Kan, T. B. Cesar, E. E. Zanni, and D. Kardassis. 2004. Probing the pathways of chylomicron and HDL metabolism using adenovirus-mediated gene transfer. *Curr. Opin. Lipidol.* **15:** 151–166.
5. Kiss, R. S., N. Kavaslar, K. Okuhira, M. W. Freeman, S. Walter, R. W. Milne, R. McPherson, and Y. L. Marcel. 2007. Genetic etiology of isolated low HDL syndrome: incidence and heterogeneity of efflux defects. *Arterioscler. Thromb. Vasc. Biol.* **27:** 1139–1145.
6. Cohen, J. C., R. S. Kiss, A. Pertsemlidis, Y. L. Marcel, R. McPherson, and H. H. Hobbs. 2004. Multiple rare alleles contribute to low plasma levels of HDL cholesterol. *Science.* **305:** 869–872.
7. Frikke-Schmidt, R., B. G. Nordestgaard, G. B. Jensen, and A. Tybjaerg-Hansen. 2004. Genetic variation in ABC transporter A1 contributes to HDL cholesterol in the general population. *J. Clin. Invest.* **114:** 1343–1353.
8. Zannis, V. I., E. E. Zanni, A. Papapanagiotou, D. Kardassis, and A. Chroni. 2006. ApoA-I functions and synthesis of HDL: insights from mouse models of human HDL metabolism. *In* High-Density Lipoproteins. From Basic Biology to Clinical Aspects. Wiley-VCH, Weinheim. 237–265.
9. Koukos, G., A. Chroni, A. Duka, D. Kardassis, and V. I. Zannis. 2007. Naturally occurring and bioengineered apoA-I mutations that inhibit the conversion of discoidal to spherical HDL: the abnormal HDL phenotypes can be corrected by treatment with LCAT. *Biochem. J.* **406:** 167–174.
10. Koukos, G., A. Chroni, A. Duka, D. Kardassis, and V. I. Zannis. 2007. LCAT can rescue the abnormal phenotype produced by the natural ApoA-I mutations (Leu141Arg)Pisa and (Leu159Arg)FIN. *Biochemistry.* **46:** 10713–10721.
11. Chroni, A., A. Duka, H. Y. Kan, T. Liu, and V. I. Zannis. 2005. Point mutations in apolipoprotein a-I mimic the phenotype observed in patients with classical lecithin:cholesterol acyltransferase deficiency. *Biochemistry.* **44:** 14353–14366.
12. Chroni, A., H. Y. Kan, A. Shkodrani, T. Liu, and V. I. Zannis. 2005. Deletions of helices 2 and 3 of human apoA-I are associated with severe dyslipidemia following adenovirus-mediated gene transfer in apoA-I-deficient mice. *Biochemistry.* **44:** 4108–4117.
13. Chroni, A., H. Y. Kan, K. E. Kypreos, I. N. Gorshkova, A. Shkodrani, and V. I. Zannis. 2004. Substitutions of glutamate 110 and 111 in the middle helix 4 of human apolipoprotein A-I (apoA-I) by alanine affect the structure and in vitro functions of apoA-I and induce severe hypertriglyceridemia in apoA-I-deficient mice. *Biochemistry.* **43:** 10442–10457.
14. Wu, Z., V. Gogonea, X. Lee, R. P. May, V. Pipich, M. A. Wagner, A. Undurti, T. C. Tallant, C. Baleanu-Gogonea, F. Charlton, et al. 2011. The low resolution structure of ApoA1 in spherical high density lipoprotein revealed by small angle neutron scattering. *J. Biol. Chem.* **286:** 12495–12508.
15. Silva, R. A., R. Huang, J. Morris, J. Fang, E. O. Gracheva, G. Ren, A. Kontush, W. G. Jerome, K. A. Rye, and W. S. Davidson. 2008. Structure of apolipoprotein A-I in spherical high density lipoproteins of different sizes. *Proc. Natl. Acad. Sci. USA.* **105:** 12176–12181.
16. Bashtovyy, D., M. K. Jones, G. M. Anantharamaiah, and J. P. Segrest. 2011. Sequence conservation of apolipoprotein A-I affords novel insights into HDL structure-function. *J. Lipid Res.* **52:** 435–450.
17. Vezeridis, A. M., K. Drosatos, and V. I. Zannis. 2011. Molecular etiology of a dominant form of type III hyperlipoproteinemia caused by R142C substitution in apoE4. *J. Lipid Res.* **52:** 45–56.
18. Folch, J., M. Lees, and G. H. Sloane Stanley. 1957. A simple method for the isolation and purification of total lipides from animal tissues. *J. Biol. Chem.* **226:** 497–509.
19. Fitzgerald, M. L., A. J. Mendez, K. J. Moore, L. P. Andersson, H. A. Panjeton, and M. W. Freeman. 2001. ATP-binding cassette transporter A1 contains an NH2-terminal signal anchor sequence that translocates the protein's first hydrophilic domain to the exoplasmic space. *J. Biol. Chem.* **276:** 15137–15145.
20. Williamson, R., D. Lee, J. Hagaman, and N. Maeda. 1992. Marked reduction of high density lipoprotein cholesterol in mice genetically modified to lack apolipoprotein A-I. *Proc. Natl. Acad. Sci. USA.* **89:** 7134–7138.
21. Zhu, L. J., and S. W. Altmann. 2005. mRNA and 18S-RNA coapplication-reverse transcription for quantitative gene expression analysis. *Anal. Biochem.* **345:** 102–109.
22. Gorshkova, I. N., K. Liadaki, O. Gursky, D. Atkinson, and V. I. Zannis. 2000. Probing the lipid-free structure and stability of apolipoprotein A-I by mutation. *Biochemistry.* **39:** 15910–15919.
23. Gorshkova, I. N., T. Liu, V. I. Zannis, and D. Atkinson. 2002. Lipid-free structure and stability of apolipoprotein A-I: probing the central region by mutation. *Biochemistry.* **41:** 10529–10539.
24. Chen, Y. H., J. T. Yang, and H. M. Martinez. 1972. Determination of the secondary structures of proteins by circular dichroism and optical rotatory dispersion. *Biochemistry.* **11:** 4120–4131.

25. Gorshkova, I. N., K. E. Kypreos, D. L. Gantz, V. I. Zannis, and D. Atkinson. 2008. Biophysical properties of apolipoprotein E4 variants: implications in molecular mechanisms of correction of hypertriglyceridemia. *Biochemistry.* **47:** 12644–12654.
26. Derksen, A., and D. M. Small. 1989. Interaction of ApoA-1 and ApoE-3 with triglyceride-phospholipid emulsions containing increasing cholesterol concentrations. Model of triglyceride-rich nascent and remnant lipoproteins. *Biochemistry.* **28:** 900–906.
27. Gorshkova, I. N., and D. Atkinson. 2011. Enhanced binding of apolipoprotein A-I variants associated with hypertriglyceridemia to triglyceride-rich particles. *Biochemistry.* **50:** 2040–2047.
28. Gorshkova, I. N., T. Liu, H. Y. Kan, A. Chroni, V. I. Zannis, and D. Atkinson. 2006. Structure and stability of apolipoprotein A-I in solution and in discoidal high-density lipoprotein probed by double charge ablation and deletion mutation. *Biochemistry.* **45:** 1242–1254.
29. Segrest, J. P., M. K. Jones, A. E. Klon, C. J. Sheldahl, M. Hellinger, H. De Loof, and S. C. Harvey. 1999. A detailed molecular belt model for apolipoprotein A-I in discoidal high density lipoprotein. *J. Biol. Chem.* **274:** 31755–31758.
30. Jones, M. K., A. Catte, J. C. Patterson, F. F. Gu, J. G. Chen, L. Li, and J. P. Segrest. 2009. Thermal stability of apolipoprotein A-I in high-density lipoproteins by molecular dynamics. *Biophys. J.* **96:** 354–371.
31. Gogonea, V., Z. P. Wu, X. Lee, V. Pipich, X. M. Li, A. I. Ioffe, J. A. Didonato, and S. L. Hazen. 2010. Congruency between Biophysical Data from Multiple Platforms and Molecular Dynamics Simulation of the Double-Super Helix Model of Nascent High-Density Lipoprotein. *Biochemistry.* **49:** 7323–7343.
32. Timmins, J. M., J. Y. Lee, E. Boudyguina, K. D. Kluckman, L. R. Brunham, A. Mulya, A. K. Gebre, J. M. Coutinho, P. L. Colvin, T. L. Smith, et al. 2005. Targeted inactivation of hepatic Abca1 causes profound hypoalphalipoproteinemia and kidney hypercatabolism of apoA-I. *J. Clin. Invest.* **115:** 1333–1342.
33. Miettinen, H. E., H. Gylling, T. A. Miettinen, J. Viikari, L. Paulin, and K. Kontula. 1997. Apolipoprotein A-IFin. Dominantly inherited hypoalphalipoproteinemia due to a single base substitution in the apolipoprotein A-I gene. *Arterioscler. Thromb. Vasc. Biol.* **17:** 83–90.
34. Xiao, C., T. Watanabe, Y. Zhang, B. Trigatti, L. Szeto, P. W. Connelly, S. Marcovina, T. Vaisar, J. W. Heinecke, and G. F. Lewis. 2008. Enhanced cellular uptake of remnant high-density lipoprotein particles: a mechanism for high-density lipoprotein lowering in insulin resistance and hypertriglyceridemia. *Circ. Res.* **103:** 159–166.
35. Teslovich, T. M., K. Musunuru, A. V. Smith, A. C. Edmondson, I. M. Stylianou, M. Koseki, J. P. Pirruccello, S. Ripatti, D. I. Chasman, C. J. Willer, et al. 2010. Biological, clinical and population relevance of 95 loci for blood lipids. *Nature.* **466:** 707–713.
36. Brunzell, J. D. (1989) Familial lipoprotein lipase deficiency and other causes of the chylomicronemia syndrome. *In* The Metabolic Basis of Inherited Disease. C. R. Scriver, A. L. Beaudet, W. S. Sly, and D. Valle, editors. McGraw-Hill, New York. 1165–1180.
37. Baggio, G., E. Manzato, C. Gabelli, R. Fellin, S. Martini, G. B. Enzi, F. Verlato, M. R. Baiocchi, D. L. Sprecher, and M. L. Kashyap. 1986. Apolipoprotein C–II deficiency syndrome. Clinical features, lipoprotein characterization, lipase activity, and correction of hypertriglyceridemia after apolipoprotein C–II administration in two affected patients. *J. Clin. Invest.* **77:** 520–527.
38. Ito, Y., N. Azrolan, A. O'Connell, A. Walsh, and J. L. Breslow. 1990. Hypertriglyceridemia as a result of human apo CIII gene expression in transgenic mice. *Science.* **249:** 790–793.
39. de Silva, H. V., S. J. Lauer, J. Wang, W. S. Simonet, K. H. Weisgraber, R. W. Mahley, and J. M. Taylor. 1994. Overexpression of human apolipoprotein C–III in transgenic mice results in an accumulation of apolipoprotein B48 remnants that is corrected by excess apolipoprotein E. *J. Biol. Chem.* **269:** 2324–2335.
40. Shachter, N. S., T. Hayek, T. Leff, J. D. Smith, D. W. Rosenberg, A. Walsh, R. Ramakrishnan, I. J. Goldberg, H. N. Ginsberg, and J. L. Breslow. 1994. Overexpression of apolipoprotein CII causes hypertriglyceridemia in transgenic mice. *J. Clin. Invest.* **93:** 1683–1690.
41. Boisfer, E., G. Lambert, V. Atger, N. Q. Tran, D. Pastier, C. Benetollo, J. F. Trottier, I. Beaucamps, M. Antonucci, M. Laplaud, et al. 1999. Overexpression of human apolipoprotein A-II in mice induces hypertriglyceridemia due to defective very low density lipoprotein hydrolysis. *J. Biol. Chem.* **274:** 11564–11572.
42. Kypreos, K. E., K. W. Van Dijk, A. van Der Zee, L. M. Havekes, and V. I. Zannis. 2001. Domains of apolipoprotein E contributing to triglyceride and cholesterol homeostasis in vivo. Carboxyl-terminal region 203-299 promotes hepatic very low density lipoprotein-triglyceride secretion. *J. Biol. Chem.* **276:** 19778–19786.
43. Kypreos, K. E., X. Li, K. W. Van Dijk, L. M. Havekes, and V. I. Zannis. 2003. Molecular mechanisms of type III hyperlipoproteinemia: the contribution of the carboxy-terminal domain of ApoE can account for the dyslipidemia that is associated with the E2/E2 phenotype. *Biochemistry.* **42:** 9841–9853.
44. Pennacchio, L. A., M. Olivier, J. A. Hubacek, J. C. Cohen, D. R. Cox, J. C. Fruchart, R. M. Krauss, and E. M. Rubin. 2001. An apolipoprotein influencing triglycerides in humans and mice revealed by comparative sequencing. *Science.* **294:** 169–173.
45. Chait, A., W. R. Hazzard, J. J. Albers, R. P. Kushwaha, and J. D. Brunzell. 1978. Impaired very low density lipoprotein and triglyceride removal in broad beta disease: comparison with endogenous hypertriglyceridemia. *Metabolism.* **27:** 1055–1066.
46. Fredenrich, A. 1998. Role of apolipoprotein CIII in triglyceride-rich lipoprotein metabolism. *Diabetes Metab.* **24:** 490–495.
47. Fredrickson, D. S., P. H. Altrocchi, L. V. Avioli, D. S. Goodman, and H. C. Goodman. 1961. Tangier disease. Combined clinical staff conference at the National Institutes of Health. *Ann. Intern. Med.* **55:** 1016–1031.
48. Heinen, R. J., P. N. Herbert, and D. S. Fredrickson. 1978. Properties of the plasma very low and low density lipoproteins in Tangier disease. *J. Clin. Invest.* **61:** 120–132.
49. Chiesa, G., L. J. Stoltzfus, S. Michelagnoli, J. K. Bielicki, M. Santi, T. M. Forte, C. R. Sirtori, G. Franceschini, and E. M. Rubin. 1998. Elevated triglycerides and low HDL cholesterol in transgenic mice expressing human apolipoprotein A-I(Milano). *Atherosclerosis.* **136:** 139–146.
50. Nofer, J. R., A. von Eckardstein, H. Wiebusch, W. Weng, H. Funke, H. Schulte, E. Kohler, and G. Assmann. 1995. Screening for naturally occurring apolipoprotein A-I variants: apo A-I(delta K107) is associated with low HDL-cholesterol levels in men but not in women. *Hum. Genet.* **96:** 177–182.

THE JOURNAL OF BIOLOGICAL CHEMISTRY VOL. 286, NO. 10, pp. 7744–7754, March 11, 2011

Carboxyl Terminus of Apolipoprotein A-I (ApoA-I) Is Necessary for the Transport of Lipid-free ApoA-I but Not Prelipidated ApoA-I Particles through Aortic Endothelial Cells*

Received for publication, October 12, 2010, and in revised form, December 6, 2010 Published, JBC Papers in Press, January 5, 2011, DOI 10.1074/jbc.M110.193524

Pascale M. Ohnsorg[‡§], Lucia Rohrer[‡¶], Damir Perisa[‡¶], Andreas Kateifides[‖], Angeliki Chroni[‡‡], Dimitris Kardassis[**], Vassilis I. Zannis[‖**], and Arnold von Eckardstein[‡§¶1]**

*From the [‡]Institute of Clinical Chemistry, University Hospital of Zurich, 8091 Zurich, Switzerland, the [§]Competence Center for Systems Physiology and Metabolic Diseases, ETH and University of Zurich, 8091 Zurich, Switzerland, the [¶]Center for Integrative Human Physiology, University of Zurich, 8091 Zurich, Switzerland, [‖]Molecular Genetics, Whitaker Cardiovascular Institute, Boston University School of Medicine, Boston, Massachusetts 02118, the [‡‡]National Centre of Scientific Research "Demokritos," Institute of Biology, 15310 Athens, Greece, and the **Department of Biochemistry, Division of Basic Sciences, Institute of Molecular Biology and Biotechnology, University of Crete Medical School, 71201 Crete, Greece*

High density lipoproteins (HDL) and apolipoprotein A-I (apoA-I) must leave the circulation and pass the endothelium to exert their atheroprotective actions in the arterial wall. We previously demonstrated that the transendothelial transport of apoA-I involves ATP-binding cassette transporter (ABC) A1 and re-secretion of lipidated particles. Transendothelial transport of HDL is modulated by ABCG1 and the scavenger receptor BI (SR-BI). We hypothesize that apoA-I transport is started by the ABCA1-mediated generation of a lipidated particle which is then transported by ABCA1-independent pathways. To test this hypothesis we analyzed the endothelial binding and transport properties of initially lipid-free as well as prelipidated apoA-I mutants. Lipid-free apoA-I mutants with a defective carboxyl-terminal domain showed an 80% decreased specific binding and 90% decreased specific transport by aortic endothelial cells. After prior cell-free lipidation of the mutants, the resulting HDL-like particles were transported through endothelial cells by an ABCG1- and SR-BI-dependent process. ApoA-I mutants with deletions of either the amino terminus or both the amino and carboxyl termini showed dramatic increases in nonspecific binding but no specific binding or transport. Prior cell-free lipidation did not rescue these anomalies. Our findings of stringent structure-function relationships underline the specificity of transendothelial apoA-I transport and suggest that lipidation of initially lipid-free apoA-I is necessary but not sufficient for specific transendothelial transport. Our data also support the model of a two-step process for the transendothelial transport of apoA-I in which apoA-I is initially lipidated by ABCA1 and then further processed by ABCA1-independent mechanisms.

Atherosclerosis is a progressive disease that is characterized by lipid accumulation in macrophages in the arterial wall and leads to complications like heart attacks and strokes (1). Low plasma levels of high density lipoprotein (HDL) cholesterol as well as apolipoprotein A-I (apoA-I)[2] are associated with increased risk of coronary heart disease (2).

Mature HDL particles are synthesized mainly in the liver and intestine by a multistep process that is initiated by the binding of cellular phospholipids and cholesterol to initially lipid-free apoA-I. This step requires the presence of the ATP-binding cassette transporter (ABC) A1 (3). Based on x-ray crystallography and computer modeling, most of the 243 amino acid residues of apoA-I are grouped in amphipathic α-helices, 11 or 2 × 11 amino acids in length (4–10), that embrace the carbon chains of several phospholipid molecules like a belt.

Both HDL and apoA-I were found to exert multiple antiatherogenic properties, for example on the function and viability of the endothelium, the cholesterol homoeostasis and inflammatory state of macrophages, lipoprotein oxidation, coagulation, and thrombosis (2, 11). One major antiatherogenic effect is the removal of excess cholesterol from macrophage foam cells of atherosclerotic lesions and its delivery to the liver for biliary excretion (12).

To fulfill their atheroprotective actions in the subendothelial space of arteries, HDL or its precursor, lipid-poor apoA-I, have to leave the circulation and pass the endothelium. This cellular monolayer of the interior surface of blood vessels forms a semipermeable barrier and regulates liquid and solute transport between intra- and extravascular compartments (13). Little is known on how plasma proteins including HDL and apoA-I cross this endothelial barrier and enter the vascular wall (14). Morphological, biochemical, and physiological studies have suggested both paracellular and transcellular transport of proteins through the intact endothelium. We previously demon-

* This work was supported, in whole or in part, by National Institutes of Health Grant HL48739. This work was also supported by Swiss National Research Foundation Grants 3100AO-116404/1, 31003A_130836/1 and European Grant LSHM-CT-2006-0376331.

[1] To whom correspondence should be addressed: Institute of Clinical Chemistry, University Hospital of Zurich, Raemistrasse 100, 8091 Zurich, Switzerland. Tel.: 41-44-255-22-60; Fax: 41-44-255-45-90; E-mail: arnold.voneckardstein@usz.ch.

[2] The abbreviations used are: apoA-I, apolipoprotein A-I; ABC, ATP-binding cassette transporter; EC, aortic endothelial cell; POPC, 2-oleoyl-1-palmitoyl-*sn*-glycero-3 phosphocholine; rHDL, reconstituted HDL; SR-BI, scavenger receptor BI.

strated that the transendothelial transport of both HDL and apoA-I involves saturable and specific processes. Transport of HDL is modulated by ABCG1 and the scavenger receptor BI (SR-BI) (15) whereas the transendothelial transport of lipid-free apoA-I is modulated by ABCA1.

After apical-to-basolateral transport though aortic endothelial cells (ECs) the initially lipid-free apoA-I was recovered as a lipidated particle (16, 17). From this observation and in analogy to similar observations on apoA-I- and ABCA1-mediated lipid efflux from macrophages (18–20), we hypothesize that the transendothelial transport of apoA-I is a two-step process. First, a functional interaction between apoA-I and ABCA1 is required to generate a lipidated particle that is subsequently transported by ABCA1-independent processes. To test this hypothesis, we investigated the endothelial binding and transport properties of initially lipid-free as well as prelipidated apoA-I mutants that have been previously well characterized for their capacity to induce ABCA1-dependent phospholipid and cholesterol efflux from macrophage cell lines and to form HDL both *in vitro* and *in vivo* (21). Specifically, we compared recombinant wild-type (WT) apoA-I, two mutants with either a deletion (apoA-I(Δ185–243)) or multiple amino acid substitutions in the carboxyl-terminal domain, which are both defective in eliciting ABCA1-mediated lipid efflux from macrophages as well as three apoA-I mutants with deletions of either the amino terminus (apoA-I(Δ1–59)) or midregional domains (apoA-I(Δ144–165)) or both the amino- and carboxyl-terminal domains (apoA-I(Δ1–59/Δ185–243)), which have no or only slightly impaired lipid efflux capacity (22). Our data show that the carboxyl-terminal ABCA1 interaction domain of apoA-I is mandatory for the transendothelial transport of lipid-free apoA-I but not of prelipidated apoA-I particles and thus support the model of a two-step process for transendothelial apoA-I transport.

EXPERIMENTAL PROCEDURES

Cell Culture—ECs were isolated from bovine aortas as described previously (23) and cultured in Dulbecco's modified Eagle's medium (DMEM) (Sigma) supplemented with 5% fetal calf serum (FCS) at 37 °C in a humidified 5% CO_2, 95% air incubator.

Small Interfering (si)RNA Transfection—ECs were transfected with 100 nM Stealth siRNA against ABCA1, ABCG1, ABCA1/ABCG1, or SR-BI and 34 nM BLOCK-iT fluorescent oligonucleotide (Invitrogen) as described previously (15). Binding and transport assays were conducted between 65 and 72 h after transfection. The efficiency of the silencing was evaluated by quantitative RT-PCR and Western blotting, as shown previously (15, 17).

Isolation of HDL and ApoA-I from Plasma—Human HDL ($1.063<d<1.21$ kg/liter) was isolated from fresh normolipidemic plasmas of blood donors by sequential ultracentrifugation (24). The purity of the lipoprotein preparation was verified by SDS-PAGE to ensure no contamination with LDL or albumin. Lipid-free human plasma WT apoA-I was further purified from delipidated HDL as described previously (25).

Production and Isolation of Recombinant ApoA-I—Production of the recombinant WT apoA-I and of the apoA-I mutants Δ(185–243), Δ(144–165), Δ(1–59), and Δ(1–59)/Δ(185–243) was described previously (22, 26–29).

Generation of Adenoviruses Expressing ApoA-I(L218A/L219A/V221A/L222A)—The apoA-I gene lacking the BglII restriction site (that is present at nucleotide positions 181 of the genomic sequence relative to the ATG codon of the gene) was cloned into the pcDNA3.1 vector to generate the pcDNA3.1-apoA-I(ΔBglII) plasmid as described (30). This plasmid was used as a template to introduce the apoA-I(L218A/L219A/V221A/L222A) mutations in apoA-I using the mutagenesis kit QuikChange® XL (Stratagene) and the mutagenic primers. The forward and reverse primers used are: forward, 5′-GGACCTC-CGCCAAGGCGCGGCGCCCGCGGCGGAGAGCTTCAA-GGTC-3′ and reverse, 5′-GACCTTGAAGCTCTCCGCCGC-GGGCGCCGCGCCTTGGCGGAGGTCC-3′ (sites of the mutagenesis are underlined). Following 18 cycles of PCR amplification of the template DNA, the PCR product was treated with DpnI to digest plasmids containing methylated DNA in one or both of their strands. The reaction product consisting of plasmids containing newly synthesized DNA carrying the mutations of interest were used to transform competent XL-10 blue bacteria cells (Stratagene). Ampicillin-resistant clones were selected, and plasmid DNA was isolated from these clones and subjected to sequencing to confirm the presence of the point mutations. The 2.2-kb apoA-I inserts containing the apoA-I mutant were cloned into the pAdTrack CMV vector that was used to generate the adenoviral constructs by recombination with the Ad-Easy-1 helper virus in the bacteria cells BJ-5183-pAD1(Stratagene), which contain the Ad-Easy-1 helper virus. Correct clones were propagated in DH5a bacteria cells. The recombinant adenoviral constructs were linearized after incubation with PacI and used to transfect 911 cells. Following large scale infection of human embryonic kidney 293 cell cultures, the recombinant adenoviruses were purified by two consecutive CsCl ultracentrifugation steps, dialyzed, and titrated. The mutant protein was isolate from the culture medium of HTB-13 cells infected with the apoA-I(L218A/L219A/V221A/L222A)-expressing adenovirus as described (22, 26).

Lyophilized apoA-I mutants were dissolved in 5 M guanidinium hydrochloride and dialyzed against 0.01 M Tris-HCl, pH 8, 0.15 M NaCl. The iodination was carried out by the same procedure as described before for WT apoA-I adjusted to pH 8, and the extensive dialysis was against 0.01 M Tris-HCl, pH 8, 0.15 M NaCl.

Radiolabeling of ApoA-I—ApoA-I was labeled with ^{125}I using Iodination Beads (Pierce) and $Na^{125}I$ (Hartmann Analytic) according to the manufacturers' instructions. In a typical reaction, we used 0.5 mCi of $Na^{125}I$, 0.7 mg of apoA-I, and two beads. Protein was separated from unincorporated ^{125}I with a Sephadex G-25 column (Amersham Biosciences) followed by extensive dialysis (against 0.15 M NaCl, 0.3 mM EDTA, pH 7.4) to remove residual free iodine. The specific activity expressed as cpm/ng protein was calculated based on the protein concentration measured by the DC protein assay (Bio-Rad) and the activity measured using a γ-counter (PerkinElmer Life Sciences). Specific activities of 600–1200 cpm/ng protein were obtained.

Preparation of Reconstituted HDL (rHDL)—Discoidal rHDL particles were produced by the cholate dialysis method (18) and contained WT or mutant apoA-I, POPC (Sigma), and sodium cholate (Sigma) in a molar ratio of 1:40:100 ((mutant) ApoA-I 1:40). Reconstituted HDL was iodinated as described above for apoA-I. Electron microscopy analysis of the particles was performed as described (22).

Binding and Cell Association Assays—Binding and cell association assays with ^{125}I-apoA-I or ^{125}I-rHDL were performed as described previously (16). ECs were incubated with the indicated concentrations of ^{125}I-apoA-I or ^{125}I-rHDL without (total) or with (nonspecific) a 40-fold excess of the indicated competitor for 2 h at 4 °C (binding) or 1 h at 37 °C (cell association). Specific binding/cell association was calculated by subtracting the values of nonspecific binding/cell association from those of total binding/cell association. All experiments were performed at least in triplicate.

Transport Assays—Transport assays were performed as previously described (16). In brief, ECs were seeded 2 days in advance on inserts (0.4 μm; BD Biosciences) precoated with collagen type I (BD Biosciences). Medium containing either ^{125}I-apoA-I or ^{125}I-rHDL at the indicated concentrations was added to the apical compartment together with (nonspecific transport) or in the absence (total transport) of a 40-fold excess of unlabeled apoA-I and rHDL, respectively. After incubation for 60 min at 37 °C the media of the basolateral compartment were collected to measure radioactivity. Specific transport was calculated by subtracting the values of nonspecific transport from those of total transport.

Gel Filtration Chromatography—The size of apoA-I and mutant apoA-I before and after transendothelial transport was analyzed by gel filtration chromatography as described (31). In brief, transport assays were performed in four transwell cell culture wells as described above. The media (2 ml) were isolated from the basolateral compartments, combined, and concentrated to 50 μl by centrifugal concentrators (Vivaspin 500; Sartorius Stedim Biotech). The concentrate was loaded onto a Superdex^{TM} 200 preparation grade HiLoad^{TM} 16/60 column (GE Healthcare) of an Akta fast protein liquid chromatography (FPLC) system and eluted with Tris saline (0.01 M Tris, 0.15 M NaCl, 0.1 mM EDTA, pH 7.5) at a flow rate of 1.5 ml/min. Fractions (0.5 ml) were collected, and the amounts of transported radioactivity were determined using a PerkinElmer Life Sciences γ-counter.

Native Agarose Gel Electrophoresis—Equal amounts of proteins were used for mobility analysis and were loaded on a 1% native agarose gel (0.05 M barbital buffer, pH 8.6). Electrophoresis was performed at 4 °C. After that, the gel was stained with Coomassie Blue (protein staining) and Sudan Black (lipid staining) using standard protocols.

Statistical Analyses—The data for all experiments were analyzed using the GraphPad Prism 5 software program. Comparisons between groups were performed using *t* test methods. Experiments were routinely performed in triplicate or quadruplicate. Each experiment shown is a representative of at least three similar experiments. If not indicated otherwise, the data are graphically represented as means ± S.D.

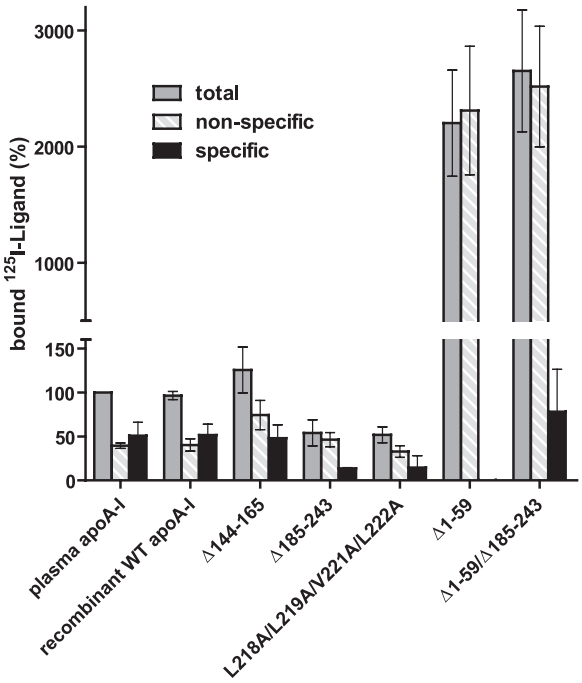

FIGURE 1. **Binding of WT and mutant apoA-I to ECs.** Cells were cultured in 12-well dishes for 48 h. Then, after prechilling on ice, the cells were incubated with 5 μg/ml of the indicated WT or mutant ^{125}I-apoA-I isoform in the absence (*total*) or presence (*nonspecific*) of a 40-fold excess of unlabeled WT apoA-I. After 2 h of incubation at 4 °C, the specific binding was determined by subtracting the values of nonspecific binding from those of total binding. The results are represented as means ± S.D. (*error bars*) of at least three individual experiments.

RESULTS

Binding and Association of Lipid-free ApoA-I Mutants to ECs—Initially we compared the endothelial binding properties of WT apoA-I either isolated from plasma or produced as a recombinant protein. ECs were incubated with radiolabeled lipid-free WT apoA-I at 4 °C in the absence (total) or presence of a 40-fold excess of unlabeled plasma WT apoA-I (nonspecific). The difference between the total and the nonspecific binding corresponds to the specific binding. The recombinant and plasma-derived WT isoproteins of apoA-I showed the same total and specific binding to ECs. Therefore, in further experiments, plasma WT apoA-I was used as a control to compare the behavior of the different apoA-I mutants.

The apoA-I(Δ144–165) mutant showed total and specific binding to ECs similar to those of WT apoA-I. The two mutants with a defective carboxyl-terminal sequence, apoA-I(Δ185–243) and apoA-I(L218A/L219A/V221A/L222A), showed 50 and 80% decreases in total and specific endothelial binding, respectively (Fig. 1). In contrast, apoA-I(Δ1–59) and apoA-I(Δ1–59/Δ185–243) showed a dramatic 25-fold increase in total binding. The binding of apoA-I(Δ1–59) could not be competed by unlabeled WT apoA-I so that no specific binding could be recorded (Fig. 1). The calculated specific binding of apoA-I(Δ1–59/Δ185–243) did not differ from that of WT apoA-I.

We repeated these experiments at 37 °C where ligands are not only bound but also internalized by ECs (16, 32), and therefore the absolute amount of cell-associated radioactivity is higher. In principle, we made the same observations as described for binding at 4 °C: WT apoA-I from plasma, recom-

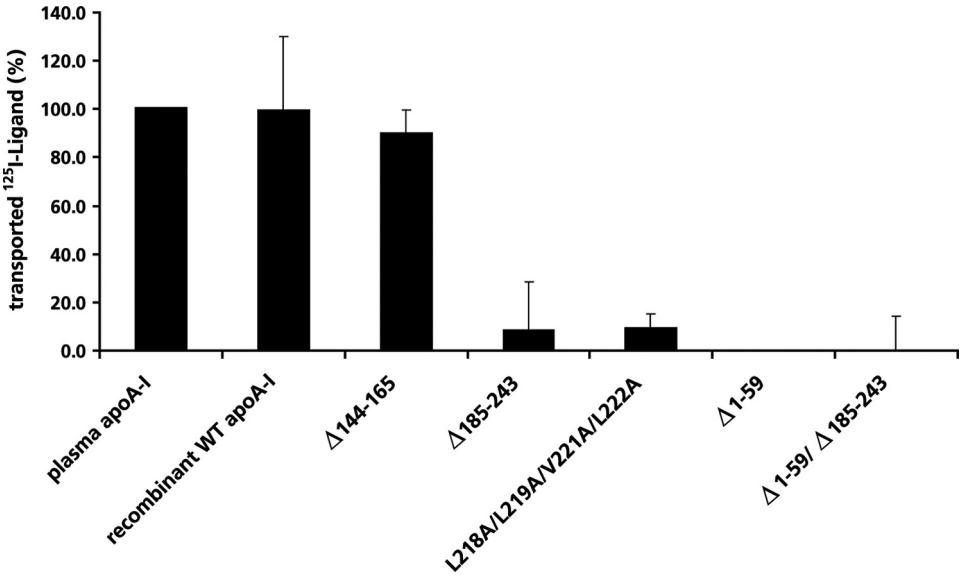

FIGURE 2. **Transport of WT and mutant apoA-I through ECs.** Cells were cultured on membrane inserts 48 h before the assay. 5 μg/ml of the indicated WT or mutant ^{125}I-apoA-I isoform as well as no or a 40-fold excess of unlabeled WT apoA-I were added to the apical compartment. The media of the basolateral compartments of the transwell chambers were collected after incubation for 1 h at 37 °C to measure the radioactivity. Specific transport from the apical to the basolateral compartment was calculated as the difference in radioactivity between the samples with (nonspecific transport) and without (total transport) excess of WT apoA-I. The results are represented as means ± S.D. (*error bars*) of at least three individual experiments.

binant WT apoA-I, and apoA-I(Δ144–165) did not differ from each other whereas the apoA-I(Δ185–243) and apoA-I(L218A/L219A/V221A/L222A) mutants showed strongly reduced total and specific cell association, and the apoA-I(Δ1–59) and apoA-I(Δ1–59/Δ185–243) mutants showed massively increased total cell association which could not be competed by WT apoA-I (data not shown).

Transport of Lipid-free ApoA-I Mutants through ECs—Next, we analyzed the transport of the different apoA-I mutants though ECs cultivated in a transwell system. Radiolabeled lipid-free WT or mutant apoA-I was added to the apical side with or without 40-fold excess of unlabeled competitor (WT apoA-I). After a 1-h incubation at 37 °C, the medium of the basolateral compartment was collected to measure radioactivity. The specific transport was calculated as the difference between total transport (radioactivity after incubation without competitor) and nonspecific transport (radioactivity after incubation with competitor). As shown in Fig. 2, specific transports of plasma WT apoA-I, recombinant WT apoA-I, and apoA-I(Δ144–165) were similar. In contrast, the specific transports of apoA-I(Δ185–243) and apoA-I(L218A/L219A/V221A/L222A) were decreased by 90%. No specific transports could be calculated for apoA-I(Δ1–59) and apoA-I(Δ1–59/Δ185–243) mutants because both in the presence or absence of the competitor the same amounts of radioactivity were recovered in the basolateral compartment of the transwell cell culture dish.

ApoA-I with Mutations in the Carboxyl Terminus Is Not Lipidated after Transendothelial Transport—In previous studies we observed a change in particle size and electrophoretic mobility of lipid-free WT apoA-I after the transport through ECs which we interpreted as a result of lipidation (16, 17). Therefore, we compared the particle sizes of WT apoA-I and the dysfunctional apoA-I(L218A/L219A/V221A/L222A) mutant before and after transport through ECs (Fig. 3). After transport and recovery from the basolateral compartment, WT apoA-I was fractionated by gel filtration into two peaks, one peak with identical elution volume (87.6 ml ± 0.5 ml) and hence size of the starting material and one new peak with lower elution volume (72.6 ml ± 0.5 ml) and hence larger particle size (Fig. 3*A*). By contrast, the comparison of the gel filtration profiles of the binding- and transport-defective apoA-I(L218A/L219A/V221A/L222A) mutant before and after incubation with ECs did not reveal the occurrence of any new peak (Fig. 3*B*). Already before incubation with cells and hence in the lipid-free state, this mutant was eluted in two peaks, one with the size of WT apoA-I (87.6 ml ± 0.5 ml) and one corresponding to larger particle size (77.1 ml ± 0.5 ml). The larger sized fraction of apoA-I(L218A/L219A/V221A/L222A) has a higher elution volume than the fraction formed after transport of WT apoA-I and did not change after transport. We therefore assume that this fraction represents lipid-free aggregates of apoA-I(L218A/L219A/V221A/L222A).

Role of ABCA1, ABCG1, and SR-BI for Binding, Cell Association, and Transport of Lipid-free WT ApoA-I—Using specific siRNAs (15), we investigated the effects of ABCA1, ABCG1, and SR-BI knockdown alone and the silencing of both ABCA1 and ABCG1 together on endothelial binding, cell association, and transport of lipid-free WT apoA-I (Fig. 4). ABCA1, ABCG1, and SR-BI transcription were reduced by approximately 80–90% in cells transfected with specific siRNA. The remaining protein expression of ABCA1, ABCG1, and SR-BI after silencing was ~50% as assessed by Western blotting and already shown previously (15, 17). Also as reported previously, knockdown of ABCA1, but not ABCG1 or SR-BI, reduced the binding of lipid-free WT apoA-I at 4 °C (Fig. 4*A*). The knockdown of ABCA1 and ABCG1 together revealed the same reduction of apoA-I binding as the single knock-down of ABCA1 by approximately 60%. At 37 °C, suppression of ABCA1 and ABCG1 either individually or both together but not the knockdown of SR-BI diminished the cell association (Fig. 4*B*) and

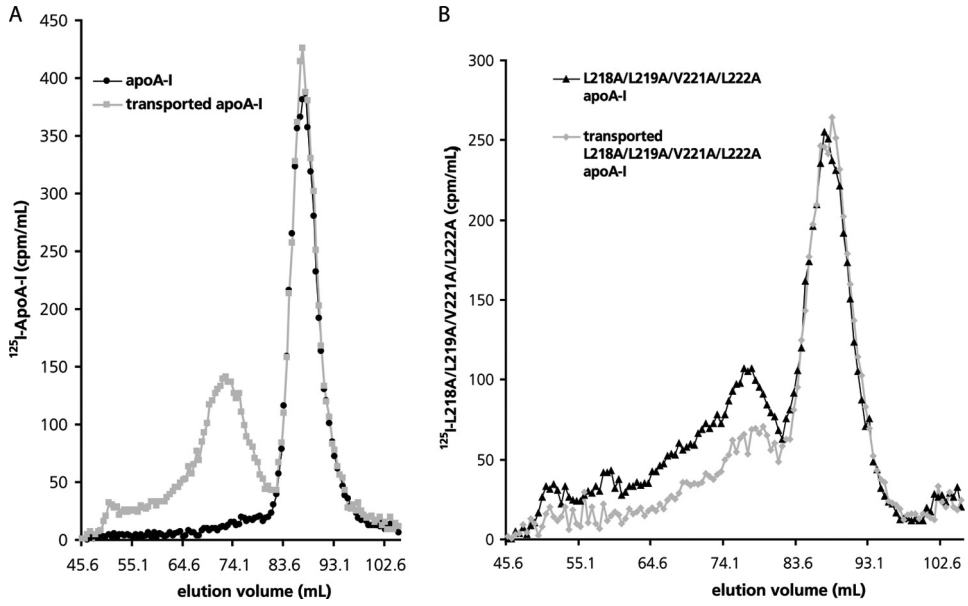

FIGURE 3. **Particle size of WT apoA-I and apoA-I(L218A/L219A/V221A/L222A) before and after transport through ECs.** The transport experiment was performed as described in Fig. 2, however only in the absence of excess unlabeled apoA-I. Both lipid-free apoA-I not incubated with cells and the material in the basolateral compartment were fractionated by gel filtration. *A*, WT ^{125}I-apoA-I. *B*, ^{125}I-apoA-I(L218A/L219A/V221A/L222A).

transendothelial transport of initially lipid-free apoA-I (Fig. 4*C*) by approximately 40%.

These at first sight discrepant observations at 4 °C and 37 °C could be explained by a previously proposed two-step model in which ABCA1-mediated lipid efflux generates a lipidated particle that secondarily interacts with ABCG1 (18–20). To test this hypothesis we analyzed the binding, association, and transport of HDL reconstituted artificially with WT or mutant apoA-I.

Interactions of rHDL with ECs—We first compared the binding (at 4 °C) and association properties (at 37 °C) of WT apoA-I in either the lipid-free or prelipidiated forms. The binding of lipid-free apoA-I was competed by rHDL to a similar degree as by lipid-free apoA-I itself or native HDL (Fig. 5*A*). The binding of rHDL was not competed by lipid-free apoA-I but by both reconstituted and native HDL (Fig. 5*A*). Cell association experiments yielded similar findings. EC association of lipid-free apoA-I was competed with 40-fold excesses of unlabeled apoA-I, lipidated apoA-I, or HDL to a similar degree (Fig. 5*B*). Cell association of rHDL was competed with an excess of either rHDL or native HDL (Fig. 5*B*). By contrast with the binding experiment, we however observed that also lipid-free apoA-I competed the cell association of rHDL, although to less extent (approximately 35%) than rHDL or native HDL (approximately 60%). These observations provide further evidence that at 37 °C the lipidation of apoA-I by ABCA1 generates a lipidated particle that can then compete with the cellular interaction of prelipidated apoA-I.

Binding and Transport of Reconstituted HDL Containing WT ApoA-I or ApoA-I(L218A/L219A/V221A/L222A)—Next, we exploited the apoA-I(L218A/L219A/V221A/L222A) mutant with defects in ABCA1-mediated lipid efflux as well as specific endothelial binding and transport to test the hypothesis that transendothelial transport of lipid-free apoA-I occurs by a two-step mechanism in which apoA-I is first lipidated by ABCA1-dependent lipid efflux to then undergo ABCA1-independent transport through ECs. We first lipidated WT apoA-I or apoA-I(L218A/L219A/V221A/L222A). The lipidation and resulting particle formation were verified by native agarose gel electrophoresis and electron microscopy. Both WT apoA-I and apoA-I(L218A/L219A/V221A/L222A) formed particles that had a higher electrophoretic mobility than the respective lipid-free apolipoproteins. rHDL containing apoA-I(L218A/L219A/V221A/L222A) were slightly less negatively charged than rHDL containing WT apoA-I (Fig. 6*A*). In addition, the Sudan Black staining of the agarose gel clearly reveals the lipidation of both WT apoA-I and apoA-I(L218A/L219A/V221A/L222A). After lipid staining, the bands containing rHDL with WT or mutant apoA-I were similarly intense (Fig. 6*B*). Electron microscopy revealed that both WT apoA-I and apoA-I(L218A/L219A/V221A/L222A) formed discoidal particles (Fig. 6*C*).

We then used the prelipidated particles to perform binding and transport studies. Neither the specific binding (Fig. 6*D*) nor the specific transport (Fig. 6*E*) differed between particles containing either WT apoA-I or the mutant apoA-I(L218A/L219A/V221A/L222A). Thus prelipidation can overcome the binding and transport defects of the dysfunctional apoA-I(L218A/L219A/V221A/L222A) mutant. These findings corroborate the hypothesis that lipidation of apoA-I is necessary for specific transcytosis.

Binding and Transport of rHDL Containing ApoA-I(Δ1–59) and ApoA-I(Δ1–59/Δ185–243)—We then investigated the effects of prior cell-free lipidation on binding and transport of the two apoA-I mutants which in the lipid-free form showed excessive nonspecific endothelial binding and transport, namely apoA-I(Δ1–59) and apoA-I(Δ1–59/Δ185–243). After cholate dialysis with POPC in a molar ratio of 1:40, both mutant rHDL particles showed higher electrophoretic mobility than the respective lipid-free apolipoproteins (Fig. 7*A*). The efficacy of lipidation was further confirmed by lipid staining of the agarose gel (Fig. 7*B*). The two mutant rHDL particles, however,

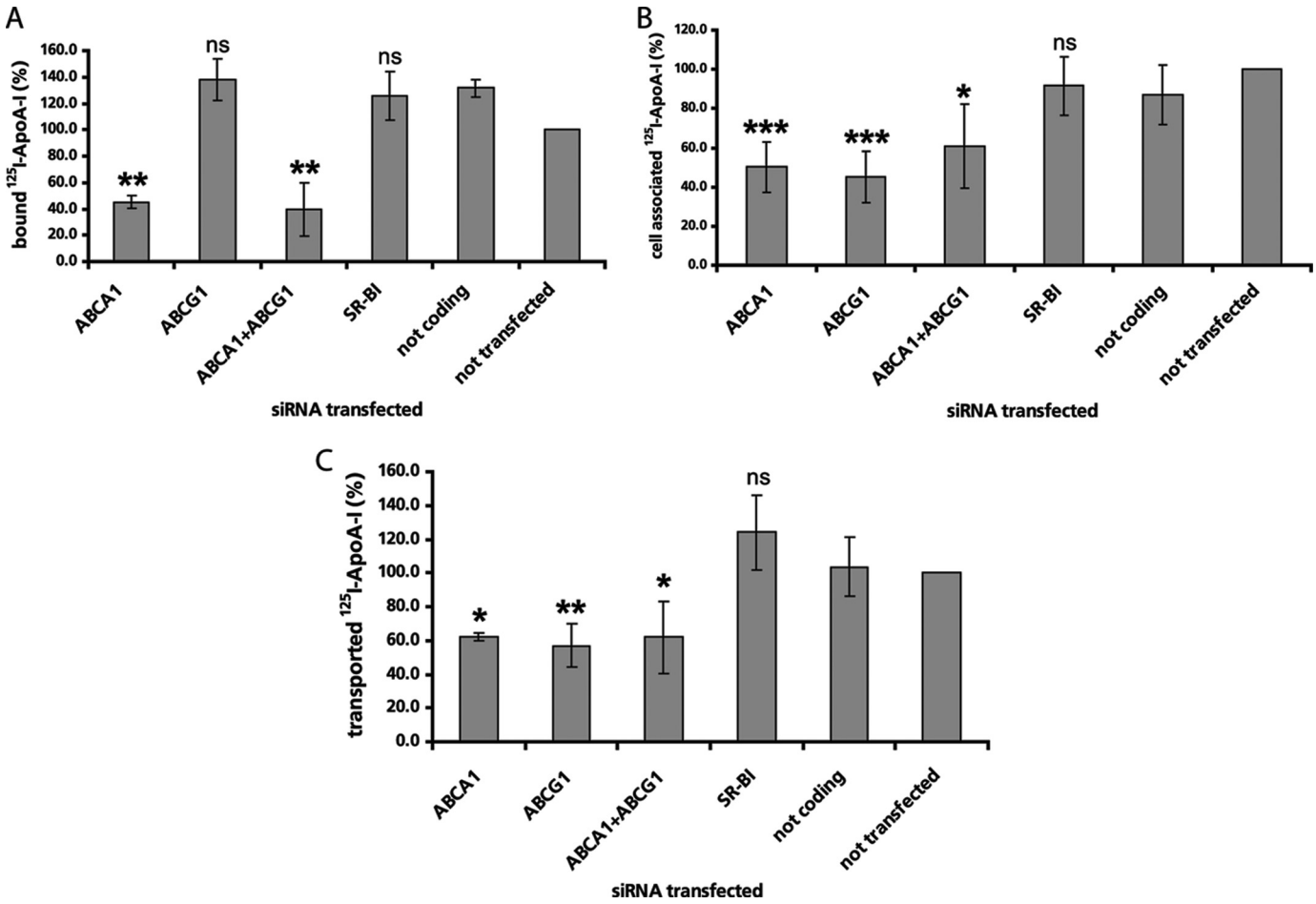

FIGURE 4. **Role of ABCA1, ABCG1, and SR-BI for binding, cell association, and transport of WT apoA-I.** ECs were transfected with specific siRNA against ABCA1, ABCG1, SR-BI, not coding siRNA, and mock (not transfected cells). 65–72 hours after transfection, ECs were incubated with 5 μg/ml of ^{125}I-apoA-I for 2 hours at 4 °C (*A*, binding) or for 1 hour at 37 °C (*B*, cell association). *C*, transport assays were performed as described in Fig. 2. *, $p < 0.05$; **, $p < 0.01$; ***, $p < 0.001$; *ns*, not significantly different compared with not transfected cells.

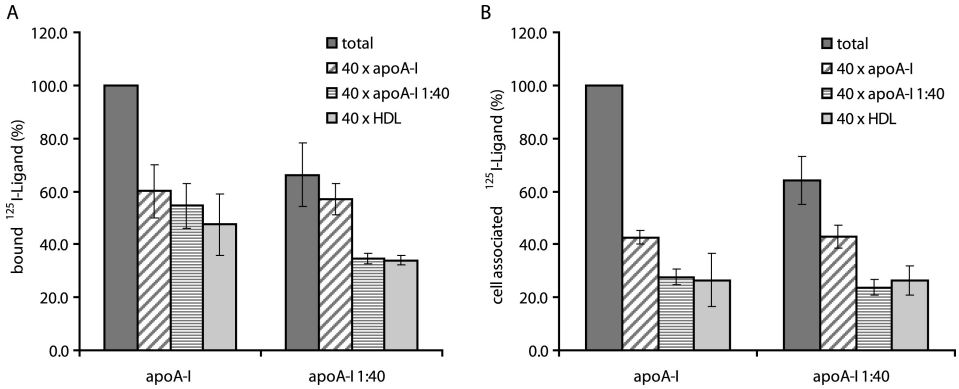

FIGURE 5. **Cross-competition of lipid-free and lipidated apoA-I.** Binding (*A*) and cell association (*B*) assays were performed. ECs were incubated with 5 μg/ml ^{125}I-apoA-I or ^{125}I-rHDL containing WT apoA-I for 2 h at 4 °C (binding) or for 1 h at 37 °C (cell association) in the absence (*total*) or presence of a 40-fold excess of the indicated competitor.

differed from each other and from normal rHDL by electrophoretic mobility (Fig. 7, *A* and *B*). Both mutants formed discoidal particles (Fig. 7*C*). With these lipidated mutants we performed binding and transport studies. We used native HDL as the competitor because reconstituted and native HDL competed equivalently (see Fig. 5). As shown in Fig. 7*D*, specific binding of the lipidated WT apoA-I was approximately 60% of the specific binding of lipid-free WT apoA-I. However, prelipidated apoA-I(Δ1–59) and prelipidated apoA-I(Δ1–59/Δ185–243) showed 4-fold and 8-fold higher total binding than prelipidated WT apoA-I. In contrast to lipidated WT apoA-I, it was not possible to compete this binding with excess HDL, indicating that these mutants keep their very high nonspecific endothelial binding properties also after prelipidation. In contrast to apoA-I(L218A/L219A/V221A/L222A), prelipidation of either apoA-I(Δ1–59) or apoA-I(Δ1–59/Δ185–243) did not rescue their

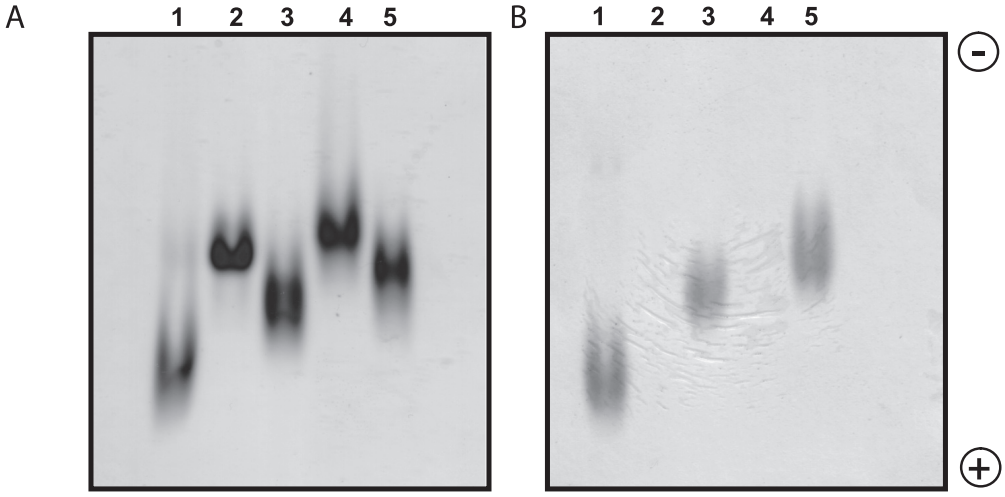

1 – HDL
2 – lipid-free apoA-I
3 – apoA-I/POPC 1:40
4 – lipid-free L218A/L219A/V221A/L222A
5 – L218A/L219A/V221A/L222A/POPC 1:40

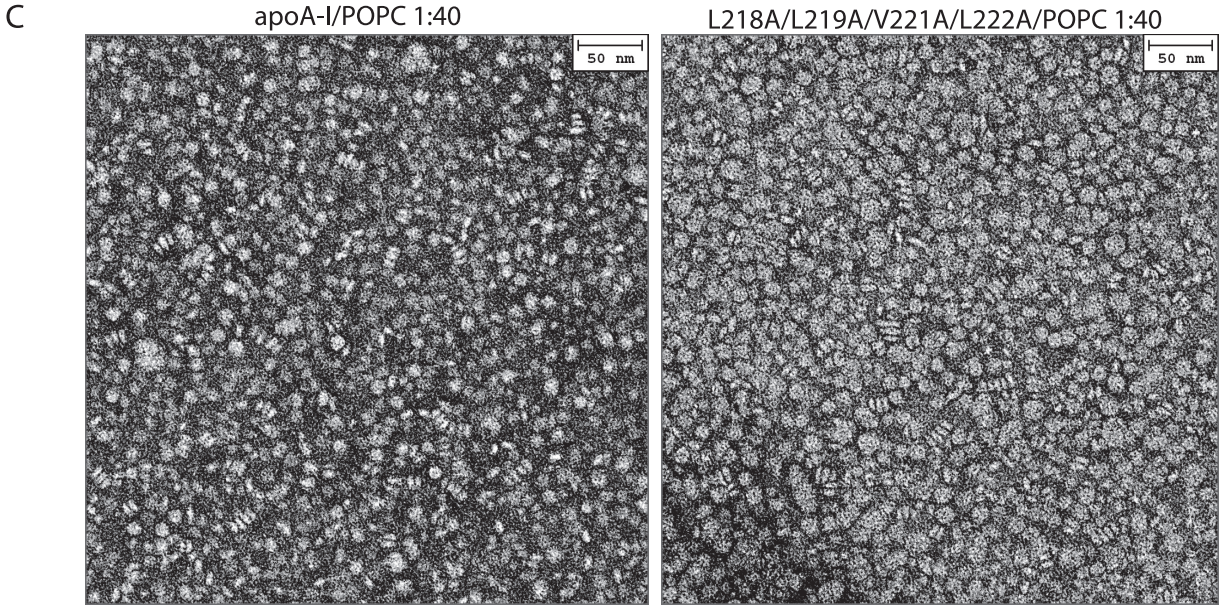

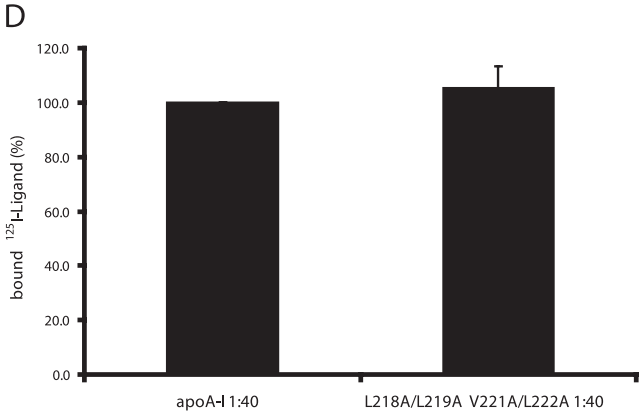

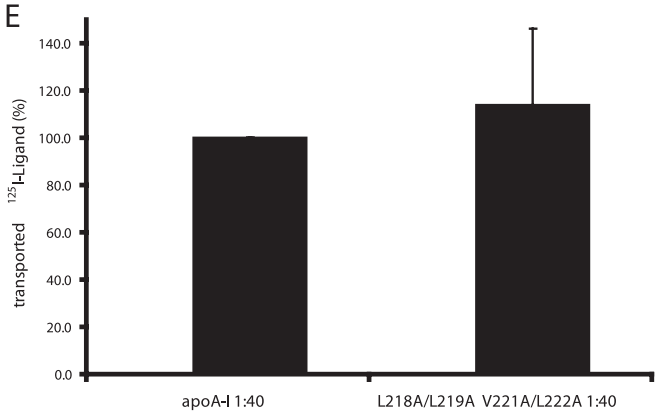

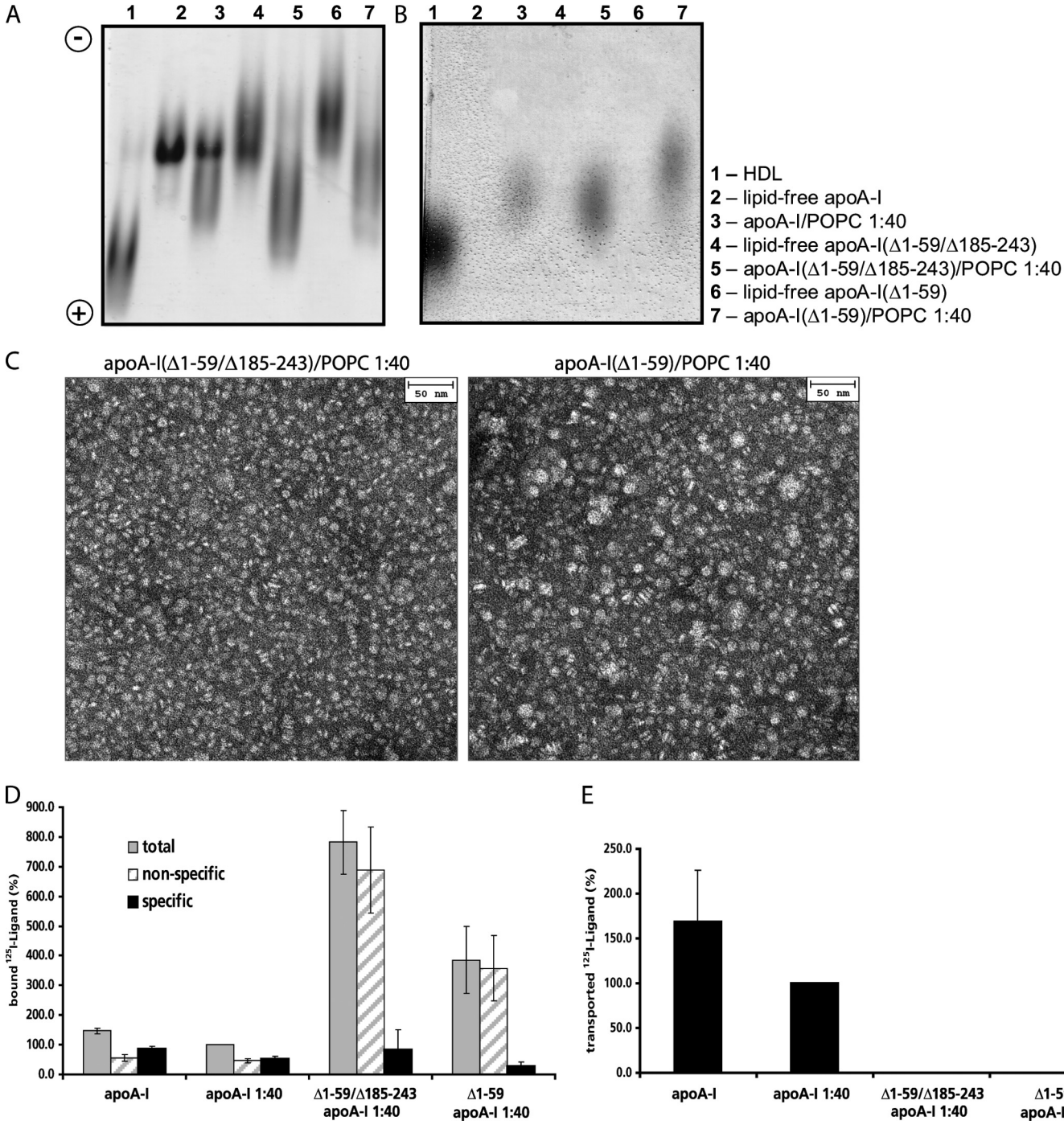

FIGURE 7. **Binding and transport of rHDL containing WT apoA-I, apoA-I(Δ1–59), or apoA-I(Δ1–59/Δ185–243).** *A*–*C*, Lipidation was verified by native agarose gel electrophoresis stained with Coomassie Blue for proteins (*A*) and with Sudan Black for lipids (*B*) and by electron microscopy (*C*). *D*, binding at 4 °C of 10 μg/ml ^{125}I-rHDL containing WT apoA-I, apoA-I(Δ1–59), or apoA-I(Δ1–59/Δ185–243) is shown. *E*, specific transport through a monolayer of ECs of 10 μg/ml ^{125}I-rHDL containing WT apoA-I, apoA-I(Δ1–59), or apoA-I(Δ1–59/Δ185–243) was determined.

defective specific transendothelial transport (Fig. 7*E*). These findings suggest that lipidation of initially lipid-free apoA-I is not sufficient for the specific transport through ECs of the apoA-I(Δ1–59) or apoA-I(Δ1–59/Δ185–243) mutants.

Role of ABCA1, ABCG1, and SR-BI for Transport of rHDL—To analyze which of the known apoA-I/HDL-binding proteins are participating in the transport of prelipidated apoA-I we used siRNAs to suppress ABCA1, ABCG1 or SR-BI. Knock-

FIGURE 6. **Binding and transport of rHDL containing WT apoA-I or apoA-I(L218A/L219A/V221A/L222A).** *A* and *B*, lipidation of the rHDL particles was performed by the cholate dialysis method, and the particle formation was analyzed by native agarose gel electrophoresis stained with Coomassie Blue for proteins (*A*) and with Sudan Black for lipids (*B*). *C*, electron microscopy of the formed particles was performed. *D*, specific binding at 4 °C of 10 μg/ml ^{125}I-rHDL particles containing either WT apoA-I or apoA-I(L218A/L219A/V221A/L222A) was determined. *E*, specific transport of 10 μg/ml ^{125}I-rHDL particles containing either WT apoA-I or apoA-I(L218A/L219A/V221A/L222A) through a monolayer of ECs was determined.

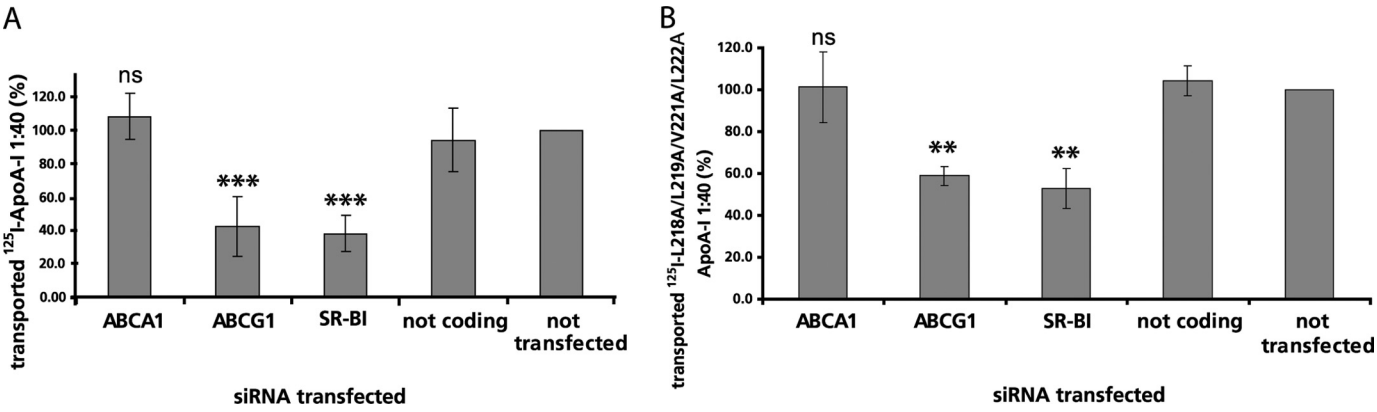

FIGURE 8. **Role of ABCA1, ABCG1, and SR-BI in the transport of rHDL containing WT apoA-I or apoA-I(L218A/L219A/V221A/L222A).** ECs were transfected with siRNA coding for ABCA1, ABCG1, SR-BI and not coding siRNA. 65–72 h after transfection transport assays were performed. ECs were incubated with 10 μg/ml ^{125}I-rHDL for 1 h in the absence or presence of a 40-fold excess of unlabeled rHDL. Specific transport was calculated by subtracting the values of nonspecific transport from those of total transport. *A*, specific transport of rHDL containing WT apoA-I. *B*, specific transport of rHDL containing apoA-I(L218A/L219A/V221A/L222A). **, $p < 0.01$; ***, $p < 0.001$; *ns*, not significantly different compared with nontransfected cells. *Error bars*, S.D.

down of ABCG1 and SR-BI but not of ABCA1 decreased the specific transendothelial transport of prelipidated WT apoA-I (Fig. 8*A*) and prelipidated apoA-I(L218A/L219A/V221A/L222A) (Fig. 8*B*). The reduction of the transport capacity of lipidated apoA-I(L218A/L219A/V221A/L222A) by knockdown of ABCG1 or SR-BI was smaller (−44% ±7%) compared with lipidated WT apoA-I (−60% ± 15%).

DISCUSSION

We recently provided several arguments that the transendothelial transport of apoA-I and HDL occurs by specific transport rather than unspecific filtration: (i) a considerable proportion of apoA-I and HDL transport is temperature-sensitive and can be competed by an excess of apoA-I and HDL, respectively, but not with albumin or LDL (15, 16). (ii) The specific fraction of transendothelial apoA-I transport can be inhibited by knockdown of ABCA1 and leads to the secretion of lipidated particles (17). (iii) The specific fraction of transendothelial HDL transport can be reduced by knockdown of ABCG1 or SR-BI and leads to the secretion of an HDL particle of reduced size (15). The findings of this study further support the specificity of transendothelial apoA-I and HDL transport by stringent structure-function relationships for apoA-I that reveals the importance of the carboxyl-terminal apoA-I domain for this process.

First, both the deletion of the carboxyl terminus of apoA-I as well as amino acid substitutions within the carboxyl terminus of apoA-I nearly abolished the specific endothelial binding and transendothelial transport of apoA-I (Figs. 1 and 2). The deletion of the carboxyl terminus was previously shown to be defective in inducing ABCA1-mediated phospholipid and cholesterol efflux from macrophages and to form nascent and mature HDL particles *in vivo* (22, 26, 33). Also, in our endothelial transwell cell culture model, both apoA-I(Δ185–243) and apoA-I(L218A/L219A/V221A/L222A) failed to form HDL-like particles although only the specific but not the nonspecific fraction of transendothelial transport was abolished.

Second, the deletion of the amino terminus of apoA-I, alone or together with the carboxyl terminus, tremendously increased the nonspecific binding of apoA-I(Δ1–59) and apoA-I(Δ1–59/Δ185–243), respectively, and interfered with the specific transport of these mutants both in the lipid-free and lipidated forms (Figs. 1, 2, and 7). Interestingly, these mutants were previously found to elicit normal or only moderately decreased ABCA1-dependent lipid efflux from macrophages, and similar mutations (apoA-I(Δ1–41) and apoA-I(Δ1–41/Δ185–243)) promoted biogenesis of HDL particles *in vivo* (22). However, in the large background of excessive cellular nonspecific binding to cells, we may have overlooked specific components of transendothelial transport. In fact, the double deletion mutant (apoA-I(Δ1–59/Δ185–243) but not the amino-terminal deletion apoA-I(Δ1–59) mutant showed more than normal specific binding to ECs (Fig. 1). Alternatively, the deletion of the amino terminus and especially both the amino terminus and carboxyl terminus may expose a midregional domain of prototypic antiparallel amphipathic α-helices which has a very high affinity to lipids (34). According to a model proposed by Phillips and co-workers, this central domain of apoA-I may bind very efficiently and solubilize lipids of plasma membranes which are generated by ABCA1 (35). In fact, pretreatment of ECs with cyclosporine A, which was shown by us and others to trap dysfunctional ABCA1 on the cells surface (17, 36), reduced the excessive nonspecific binding of apoA-I(Δ1–59) and apoA-I(Δ1–59/Δ185–243) (data not shown). Furthermore, it has been shown that the amino-terminal deletion destabilizes apoA-I and leads to unfolding of the α-helices in the carboxyl-terminal domain which is responsible for specific interactions with ABCA1 (37, 38).

Finally, the deletion of a central domain in apoA-I(Δ144–165) interfered neither with specific binding nor specific transendothelial transport (Figs. 1 and 2). This mutant was previously found to behave like WT apoA-I in mediating ABCA1-dependent lipid efflux but to be defective in lecithin:cholesterol acyltransferase activation (22, 39, 40).

Taken together, our data further emphasize the importance of ABCA1 as a rate-limiting step for transendothelial apoA-I transport. Several authors have provided evidence for a physical interaction of apoA-I with ABCA1 (22, 41). The formation of a high affinity complex of apoA-I with ABCA1 is thought to play

an important regulatory first step in ABCA1-mediated lipid efflux by stabilizing ABCA1 in the plasma membrane and eliciting signaling events that enrich distinct plasma membranes with lipids for facilitated removal by apoA-I (39, 42, 3). However, the signaling events elicited by apoA-I/ABCA1 interaction have also been related to other cellular responses such as cell migration and endocytosis (44, 45). As a consequence, the defective transendothelial transport of apoA-I mutants with a missing or dysfunctional carboxyl-terminal ABCA1 interaction domain may be principally explained by disturbances in different downstream events. Our present results shed some light into these different scenarios.

By using gel filtration we here corroborated our previous finding that transendothelial transport leads to the secretion of a lipidated particle on the basolateral side (16). The apoA-I(L218A/L219A/V221A/L222A) mutant, which shows strongly reduced specific but normal nonspecific transendothelial transport (data not shown), was not recovered as a lipidated particle (Fig. 3). However, after prior cell-free lipidation the carboxyl-terminal apoA-I mutant was normally bound and transported by ECs (Fig. 6). This finding suggests that the transendothelial transport of apoA-I is initiated by ABCA1-mediated lipidation of apoA-I and followed by ABCA1-independent transport steps. These downstream pathways may be shared with the transport of HDL because knockdown of ABCG1 or SR-BI inhibited the specific transport of native HDL (15) as well as rHDL containing either WT apoA-I or apoA-I(L218A/L219A/V221A/L222A) (Fig. 8). In agreement with normal binding of rHDL containing apoA-I(L218A/L219A/V221A/L222A), ldlA-7 cells expressing SR-BI were previously found to bind rHDL containing apoA-I(Δ185–243) with affinity similar to that of rHDL with WT apoA-I (46). In general, our findings resemble similar findings and models on the interaction of ABCA1, ABCG1, and SR-BI in cholesterol efflux: ABCA1-mediated lipid efflux to initially lipid-free apoA-I generates particles which then interact with ABCG1 and SR-BI for enhanced cholesterol efflux (18–20).

Interestingly, the lipidation did not restore the abnormal binding and transport of apoA-I(Δ1–59) or apoA-I(Δ1–59/Δ185–243) (Fig. 7). Although less intense than in the lipid-free form, also in the prelipidated form these mutants showed strongly enhanced binding to ECs and not-recordable specific binding and transendothelial transport. This suggests that the amino-terminal domain is an important structural determinant for specific endothelial binding and transendothelial transport of HDL. Previously, rHDL containing apoA-I(Δ1–59/Δ185–243) were reported to be unable to compete for rHDL binding to ldlA-7 cells expressing the murine SR-BI receptor (27). Indirectly, this supports the importance of SR-BI as a rate-limiting factor for endothelial binding and transport of HDL. However, rHDL containing the apoA-I(Δ1–59) mutant, which in our hands is also defective in endothelial binding and transport, was reported to bind with normal affinity to SR-BI-overexpressing ldlA-7 cells (27, 46). The reason for this discrepancy remains unclear.

In summary, the distinct binding and transport defects of apoA-I mutants provide further support that transendothelial transport of apoA-I and HDL requires defined structural domains and hence involves specific protein/protein interactions rather than unspecific filtration. These experiments also support the importance of ABCA1 for the transport of lipid-free apoA-I and provided first hints on the underlying mechanisms. By lipidating apoA-I, ABCA1 helps to generate a particle that is then processed by ABCA1-independent mechanisms for transendothelial transport. Like the transport of mature HDL, the processing of these nascent HDL particles appears to involve ABCG1 and SR-BI.

Acknowledgment—We thank Silvija Radosavljevic for technical assistance.

REFERENCES

1. Miller, Y. I., Choi, S. H., Fang, L., and Tsimikas, S. (2010) *Subcell. Biochem.* **51,** 229–251
2. von Eckardstein, A. (2010) *Expert Rev. Cardiovasc. Ther.* **8,** 345–358
3. Tall, A. R., Yvan-Charvet, L., Terasaka, N., Pagler, T., and Wang, N. (2008) *Cell Metab.* **7,** 365–375
4. Thomas, M. J., Bhat, S., and Sorci-Thomas, M. G. (2008) *J. Lipid Res.* **49,** 1875–1883
5. Tanaka, M., Koyama, M., Dhanasekaran, P., Nguyen, D., Nickel, M., Lund-Katz, S., Saito, H., and Phillips, M. C. (2008) *Biochemistry* **47,** 2172–2180
6. Silva, R. A., Hilliard, G. M., Fang, J., Macha, S., and Davidson, W. S. (2005) *Biochemistry* **44,** 2759–2769
7. Li, L., Chen, J., Mishra, V. K., Kurtz, J. A., Cao, D., Klon, A. E., Harvey, S. C., Anantharamaiah, G. M., and Segrest, J. P. (2004) *J. Mol. Biol.* **343,** 1293–1311
8. Nolte, R. T., and Atkinson, D. (1992) *Biophys. J.* **63,** 1221–1239
9. Borhani, D. W., Engler, J. A., and Brouillette, C. G. (1999) *Acta Crystallogr. D Biol. Crystallogr.* **55,** 1578–1583
10. Segrest, J. P., Jones, M. K., Klon, A. E., Sheldahl, C. J., Hellinger, M., De Loof, H., and Harvey, S. C. (1999) *J. Biol. Chem.* **274,** 31755–31758
11. Natarajan, P., Ray, K. K., and Cannon, C. P. (2010) *J. Am. Coll. Cardiol.* **55,** 1283–1299
12. Curtiss, L. K., Valenta, D. T., Hime, N. J., and Rye, K. A. (2006) *Arterioscler. Thromb. Vasc. Biol.* **26,** 12–19
13. Minshall, R. D., and Malik, A. B. (2006) *Handb. Exp. Pharmacol.* **176,** 107–144
14. von Eckardstein, A., and Rohrer, L. (2009) *Curr. Opin. Lipidol.* **20,** 197–205
15. Rohrer, L., Ohnsorg, P. M., Lehner, M., Landolt, F., Rinninger, F., and von Eckardstein, A. (2009) *Circ. Res.* **104,** 1142–1150
16. Rohrer, L., Cavelier, C., Fuchs, S., Schlüter, M. A., Völker, W., and von Eckardstein, A. (2006) *Biochim. Biophys. Acta* **1761,** 186–194
17. Cavelier, C., Rohrer, L., and von Eckardstein, A. (2006) *Circ. Res.* **99,** 1060–1066
18. Lorenzi, I., von Eckardstein, A., Radosavljevic, S., and Rohrer, L. (2008) *Biochim. Biophys. Acta* **1781,** 306–313
19. Vaughan, A. M., and Oram, J. F. (2006) *J. Lipid Res.* **47,** 2433–2443
20. Jessup, W., Gelissen, I. C., Gaus, K., and Kritharides, L. (2006) *Curr. Opin. Lipidol.* **17,** 247–257
21. Zannis, V., *et al.* (eds) (2007) *High Density Lipoproteins*: *From Basic Biology to Clinical Aspects*, pp. 237–265, Wiley-VCH, Weinheim
22. Chroni, A., Liu, T., Gorshkova, I., Kan, H. Y., Uehara, Y., Von Eckardstein, A., and Zannis, V. I. (2003) *J. Biol. Chem.* **278,** 6719–6730
23. Gajdusek, C. M., and Schwartz, S. M. (1983) *In Vitro* **19,** 394–402
24. Havel, R. J., Eder, H. A., and Bragdon, J. H. (1955) *J. Clin. Invest.* **34,** 1345–1353
25. Brown, W. V., Levy, R. I., and Fredrickson, D. S. (1969) *J. Biol. Chem.* **244,** 5687–5694
26. Chroni, A., Koukos, G., Duka, A., and Zannis, V. I. (2007) *Biochemistry* **46,** 5697–5708
27. Liadaki, K. N., Liu, T., Xu, S., Ishida, B. Y., Duchateaux, P. N., Krieger, J. P., Kane, J., Krieger, M., and Zannis, V. I. (2000) *J. Biol. Chem.* **275,** 21262–21271

28. Liu, T., Krieger, M., Kan, H. Y., and Zannis, V. I. (2002) *J. Biol. Chem.* **277,** 21576–21584
29. Gorshkova, I. N., Liu, T., Zannis, V. I., and Atkinson, D. (2002) *Biochemistry* **41,** 10529–10539
30. Koukos, G., Chroni, A., Duka, A., Kardassis, D., and Zannis, V. I. (2007) *Biochem. J.* **406,** 167–174
31. Liu, L., Bortnick, A. E., Nickel, M., Dhanasekaran, P., Subbaiah, P. V., Lund-Katz, S., Rothblat, G. H., and Phillips, M. C. (2003) *J. Biol. Chem.* **278,** 42976–42984
32. Lorenzi, I., von Eckardstein, A., Cavelier, C., Radosavljevic, S., and Rohrer, L. (2008) *J Mol. Med.* **86,** 171–183
33. Reardon, C. A., Kan, H. Y., Cabana, V., Blachowicz, L., Lukens, J. R., Wu, Q., Liadaki, K., Getz, G. S., and Zannis, V. I. (2001) *Biochemistry* **40,** 13670–13680
34. Oram, J. F. (2003) *Arterioscler. Thromb. Vasc. Biol.* **23,** 720–727
35. Vedhachalam, C., Duong, P. T., Nickel, M., Nguyen, D., Dhanasekaran, P., Saito, H., Rothblat, G. H., Lund-Katz, S., and Phillips, M. C. (2007) *J. Biol. Chem.* **282,** 25123–25130
36. Le Goff, W., Peng, D. Q., Settle, M., Brubaker, G., Morton, R. E., and Smith, J. D. (2004) *Arterioscler. Thromb. Vasc. Biol.* **24,** 2155–2161
37. Tanaka, M., Saito, H., Dhanasekaran, P., Wehrli, S., Handa, T., Lund-Katz, S., and Phillips, M. C. (2005) *Biochemistry* **44,** 10689–10695
38. Tanaka, M., Dhanasekaran, P., Nguyen, D., Ohta, S., Lund-Katz, S., Phillips, M. C., and Saito, H. (2006) *Biochemistry* **45,** 10351–10358
39. Chroni, A., Liu, T., Fitzgerald, M. L., Freeman, M. W., and Zannis, V. I. (2004) *Biochemistry* **43,** 2126–2139
40. Chroni, A., Duka, A., Kan, H. Y., Liu, T., and Zannis, V. I. (2005) *Biochemistry* **44,** 14353–14366
41. Marcel, Y. L., and Kiss, R. S. (2003) *Curr. Opin. Lipidol.* **14,** 151–157
42. Fitzgerald, M. L., Morris, A. L., Chroni, A., Mendez, A. J., Zannis, V. I., and Freeman, M. W. (2004) *J. Lipid Res.* **45,** 287–294
43. Arakawa, R., and Yokoyama, S. (2002) *J. Biol. Chem.* **277,** 22426–22429
44. Sekine, Y., Demosky, S. J., Stonik, J. A., Furuya, Y., Koike, H., Suzuki, K., and Remaley, A. T. (2010) *Mol. Cancer Res.* **8,** 1284–1294
45. Azuma, Y., Takada, M., Shin, H. W., Kioka, N., Nakayama, K., and Ueda, K. (2009) *Genes Cells* **14,** 191–204
46. Zannis, V. I., Chroni, A., and Krieger, M. (2006) *J. Mol. Med.* **84,** 276–294

Original Article

Journal of INTERNAL MEDICINE

doi: 10.1111/j.1365-2796.2011.02381.x

Mutation in *APOA1* predicts increased risk of ischaemic heart disease and total mortality without low HDL cholesterol levels

C. L. Haase[1], R. Frikke-Schmidt[1], B. G. Nordestgaard[2,3], A. K. Kateifides[4,5], D. Kardassis[4], L. B. Nielsen[1,6], C. B. Andersen[7], L. Køber[8], A. H. Johnsen[1], P. Grande[8], V. I. Zannis[4,5] & A. Tybjærg-Hansen[1,3]

From the [1]Department of Clinical Biochemistry, Rigshospitalet, [2]Department of Clinical Biochemistry, Herlev Hospital, [3]The Copenhagen City Heart Study, Bispebjerg Hospital; Copenhagen University Hospitals and Faculty of Health Sciences, University of Copenhagen, Denmark, [4]Department of Biochemistry, University of Crete Medical School, Heraklion, Greece, [5]Department of Molecular Genetics, Whitaker Cardiovascular Institute, Boston University School of Medicine, Boston, MA, USA, [6]Departments of Biomedical Sciences, [7]Pathology, and [8]Cardiology, Rigshospitalet; Copenhagen University Hospitals and Faculty of Health Sciences, University of Copenhagen, Denmark

Abstract. Haase CL, Frikke-Schmidt R, Nordestgaard BG, Kateifides AK, Kardassis D, Nielsen LB, Andersen CB, Køber L, Johnsen AH, Grande P, Zannis VI, Tybjærg-Hansen A (Copenhagen University Hospitals and Faculty of Health Sciences, University of Copenhagen, Denmark; University of Crete Medical School, Heraklion, Greece; Whitaker Cardiovascular Institute, Boston University School of Medicine, Boston, MA, USA). Mutation in *APOA1* predicts increased risk of ischaemic heart disease and total mortality without low HDL cholesterol levels. *J Intern Med* 2011; doi: 10.1111/j.1365-2796.2011.02381.x.

Objectives. To determine whether mutations in *APOA1* affect levels of high-density lipoprotein (HDL) cholesterol and to predict risk of ischaemic heart disease (IHD) and total mortality in the general population.

Background. Epidemiologically, risk of IHD is inversely related to HDL cholesterol levels. Mutations in apolipoprotein (apo) A-I, the major protein constituent of HDL, might be associated with low HDL cholesterol and predispose to IHD and early death.

Design. We resequenced *APOA1* in 190 individuals and examined the effect of mutations on HDL cholesterol, risk of IHD, myocardial infarction (MI) and mortality in 10 440 individuals in the prospective Copenhagen City Heart Study followed for 31 years. Results were validated in an independent case–control study (n = 16 035). Additionally, we determined plasma ratios of mutant to wildtype (WT) apoA-I in human heterozygotes and functional effects of mutations in adenovirus-transfected mice.

Results. We identified a new mutation, A164S (1 : 500 in the general population), which predicted hazard ratios for IHD, MI and total mortality of 3.2 [95% confidence interval (CI): 1.6–6.5], 5.5 (95% CI: 2.6–11.7) and 2.5 (95% CI: 1.3–4.8), respectively, in heterozygotes compared with noncarriers. Mean reduction in survival time in heterozygotes was 10 years (P < 0.0001). Results for IHD and MI were confirmed in the case–control study. Furthermore, the ratio of mutant S164 to WT A164 apoA-I in plasma of heterozygotes was reduced. In addition, A164S heterozygotes had normal plasma lipid and lipoprotein levels, including HDL cholesterol and apoA-I, and this finding was confirmed in adenovirus-transfected mice.

Conclusions. A164S is the first mutation in *APOA1* to be described that predicts an increased risk of IHD, MI and total mortality without low HDL cholesterol levels.

Keywords: apolipoproteins, cardiovascular disease, genetics, lipoproteins, mortality.

Introduction

Epidemiological studies consistently demonstrate that a low plasma level of high-density lipoprotein (HDL) cholesterol is associated with increased risk of ischaemic heart disease (IHD) [1, 2]. However, whether HDL cholesterol is a primary causal factor in the pathogenesis of IHD is unclear [2–4].

Apolipoprotein (apo) A-I is the major protein component of the HDL particle and plays a crucial role in HDL particle formation, maturation and catabolism [5]. Structural mutations in *APOA1* might cause hereditary HDL deficiency syndromes often owing to lecithin:cholesterol acyltransferase (LCAT) deficiency [6, 7], but it remains to be determined what effect

structural mutations in *APOA1* have on the risk of developing IHD and on total mortality [5, 6].

To determine whether structural genetic variants in *APOA1* are associated with altered levels of HDL cholesterol and risk of IHD and total mortality, we resequenced the coding exons and exon–intron boundaries of *APOA1* in individuals from the general population with the lowest 1% and highest 1% apoA-I levels for age and gender [8]. Next, we genotyped 10 440 individuals from the Copenhagen City Heart Study (CCHS), a random sample of the Danish population followed for 31 years, for the genetic variants identified and determined the effect on HDL cholesterol and on risk of IHD and total mortality. Association with risk of IHD in the population study was retested in an independent case–control study (n = 16 035). These studies were complemented by adenovirus transfection of the mutations identified in apoA-I-deficient mice to determine the effects on lipid and lipoprotein levels, HDL subclass distribution, HDL morphology and LCAT activation. Finally, we determined the clinical characteristics and the relative levels of wildtype (WT) and mutant apoA-I in the plasma of individuals heterozygous for selected mutations.

Methods

Human studies

Subjects. Studies were approved by Copenhagen University Hospitals and Danish ethical committees (the Copenhagen and Frederiksberg committee and the Copenhagen County committee; KF-100. 2039/91, KF-01-144/01, H-KF-01-144/01) and conducted according to the Declaration of Helsinki. Written informed consent was obtained from participants. All participants were white and of Danish descent.

The Copenhagen City Heart Study (CCHS). The CCHS is a study of the Danish general population initiated between 1976 and 1978 with follow-up examinations during the periods 1981–1983, 1991–1994 and 2001–2003 [9]. Individuals were randomly selected based on the national Danish Civil Registration System to reflect the adult Danish general population aged 20 to 80+ years. We genotyped 10 440 individuals for all nonsynonymous mutations (V11X, L144R, A164S) identified by resequencing the coding region and exon–intron boundaries of *APOA1* in 190 individuals with the 1% highest and 1% lowest apoA-I levels for age and gender. All end-points were recorded in the follow-up period from 1976 until July 2007. Follow-up was 31 years (214 750 person-years) and was 100% complete.

Information on diagnoses of IHD (World Health Organization International Classification of Diseases: 8th edition, codes 410–414; 10th edition, codes I20–I25) was collected and verified by reviewing all hospital admissions and diagnoses included in the national Danish Patient Registry, all causes of death included in the national Danish Causes of Death Registry, and medical records from hospitals and general practitioners. IHD was defined as myocardial infarction (MI) or characteristic symptoms of stable angina pectoris [10]. A diagnosis of MI required the presence of at least two of the following criteria: characteristic chest pain, elevated cardiac enzymes and electrocardiographic changes indicative of MI.

Case–control study (verification sample). The cases were 2756 consecutive patients ≥60 years of age from the greater Copenhagen area referred for coronary angiography to Copenhagen University Hospital during the period between 2001 and 2004. (Results, see below, indicated that the effect of A164S heterozygosity on IHD and MI was mainly observed after age 60 years.) These patients had documented IHD based on characteristic symptoms of stable angina pectoris [10], plus at least one of the following: atherosclerosis on coronary angiography, a previous MI or a positive bicycle exercise electrocardiography test. The diagnosis of MI (n = 1467) was established with the same criteria as described above. Patients with IHD were compared with 13 279 controls ≥60 years of age without ischaemic cardiovascular events (IHD or ischaemic stroke) from the Copenhagen General Population Study, a cross-sectional study of the Danish general population initiated in 2003 and still recruiting [3]. Participants in the case–control study were genotyped for A164S.

See Data S1 including Tables S4 and S5, for detailed laboratory and statistical analyses of human studies as well as *in vitro*, cell and mice studies.

Results

Characteristics of participants and mutations in the coding region of APOA1

Characteristics of individuals with extremely high and low apoA-I levels and the corresponding nonsynonymous mutations (V11X, L144R, A164S) identified in the coding region of *APOA1* are shown in Tables S1 and S2.

Characteristics of subjects heterozygous for nonsynonymous mutations in APOA1 in the general population

In the CCHS (n = 10 440), 24, four and one unrelated individuals (carrier frequencies: 0.23%, 0.04% and 0.01%) were heterozygous for A164S, L144R and V11X, respectively (Table 1). No homozygotes were identified. These mutations were not in linkage disequilibrium with other previously reported genetic variants in *APOA1* identified by resequencing [8]. Lipid risk factors for IHD, including plasma levels of HDL cholesterol and apoA-I, did not differ between A164S heterozygotes and noncarriers (Table 1; Fig. 1, blue). By contrast, unadjusted plasma levels of HDL cholesterol and apoA-I were reduced by 0.7 mmol L^{-1} (47%) and 39 mg dL^{-1} (28%), respectively, in L144R heterozygotes compared with noncarriers (P = 0.001 and P = 0.006, Table 1). The age- and sex-adjusted mean percentile for HDL cholesterol in L144R heterozygotes was at the 2nd percentile [95% confidence interval (CI): 0 to 5th; P < 0.0001] and was reflected in the corresponding mean percentile for apoA-I (6th percentile; 95% CI: 0 to 19th; P = 0.0001) and total cholesterol (15th percentile; 95% CI: 1st to 28th; P = 0.03; Fig. 1a, pink). All four L144R heterozygotes had levels of HDL cholesterol at or below the 5th percentile for age and sex (Fig. 1b, pink). The only V11X heterozygote identified was a 70-year-old man with plasma levels of HDL cholesterol and apoA-I at or below the 5th percentile (Table 1; Fig. 1b, green).

Impact of APOA1 mutations on the biogenesis of HDL particles in apoA-I-deficient mice

To study the impact of the *APOA1* A164S and L144R mutations on the biogenesis of HDL particles, we generated recombinant adenoviruses expressing these mutants. Cell culture studies showed that when HTB-13 cells were infected with adenoviruses expressing the WT or the mutant apoA-I forms, in all cases apoA-I was secreted efficiently into the culture medium (Fig. S1). Adenovirus-mediated gene transfer in apoA-I-deficient mice showed that compared with mice that received the adenovirus expressing the WT apoA-I or apoA-I A164S, administration of the

Table 1 *Characteristics of subjects heterozygous for nonsynonymous mutations in* APOA1 *and 10 411 noncarriers in the Copenhagen City Heart Study*

		Heterozygotes		
	Noncarriers	V11X	L144R	A164S
No. of subjects (%)	10 411 (99.7)	1 (0.01)	4 (0.04)	24 (0.23)
Age (years)	58 (44–69)	70	46 (43–62)	53 (47–65)
Sex (F/M)	5784/4627	0/1	3/1	10/14
Total cholesterol (mmol L^{-1})	5.9 (5.1–6.9)	6.0	4.7 (4.2–5.4)*	5.9 (5.2–7.1)
Triglycerides (mmol L^{-1})	1.5 (1.1–2.2)	1.8	2.2 (1.2–3.0)	1.4 (1.1–2.2)
LDL cholesterol (mmol L^{-1})	3.6 (2.9–4.4)	4.4	3.2 (2.7–3.4)	3.7 (2.6–5.1)
HDL cholesterol (mmol L^{-1})	1.5 (1.2–1.8)	0.8	0.8 (0.7–0.9)†	1.4 (1.3–1.9)
ApoA-I (mg dL^{-1})	140 (122–161)	78	101 (84–118)‡	143 (121–154)
Body mass index (kg m^{-2})	25 (22–28)	31	27 (24–29)	26 (24–27)
Hypertension (%)	6217 (60)	1	3 (75)	14 (58)
Alcohol (g day^{-1})[a]	10 (2–22)	27	12 (7–127)	17 (5–29)
Physical inactivity (%)[b]	6582 (64)	1	3 (75)	16 (66)
Diabetes (%)	656 (6)	0	0 (0)	4 (17)§
Smoking (%)	7930 (76)	1	2 (50)	20 (83)

LDL, low-density lipoprotein; HDL, high-density lipoprotein. Values are median (interquartile range) or number (percentage). The risk factors, diabetes mellitus, smoking and hypertension were dichotomized and defined as 'ever-diabetics' (self-reported disease, use of insulin, use of oral hypoglycaemic drugs and/or nonfasting plasma glucose >11 mmol L^{-1}), 'ever-smokers' (ex-smoker or current smoker) and 'ever-hypertensives' (systolic blood pressure ≥140 mmHg or diastolic blood pressure ≥90 mmHg and/or use of antihypertensive drugs). LDL cholesterol levels were calculated using the Friedewald equation if triglycerides were <4 mmol L^{-1}, but measured directly at higher triglyceride levels (see Data S1). [a]12 g alcohol = 1 unit, equivalent to one glass of wine or one beer (33 cl). [b]Individuals who took part in <2–4 h per week of light leisure time physical activity. Heterozygotes were compared with noncarriers by Mann–Whitney U test or Pearson χ^2 test: *P = 0.03, †P = 0.001, ‡P = 0.006, §P = 0.04.

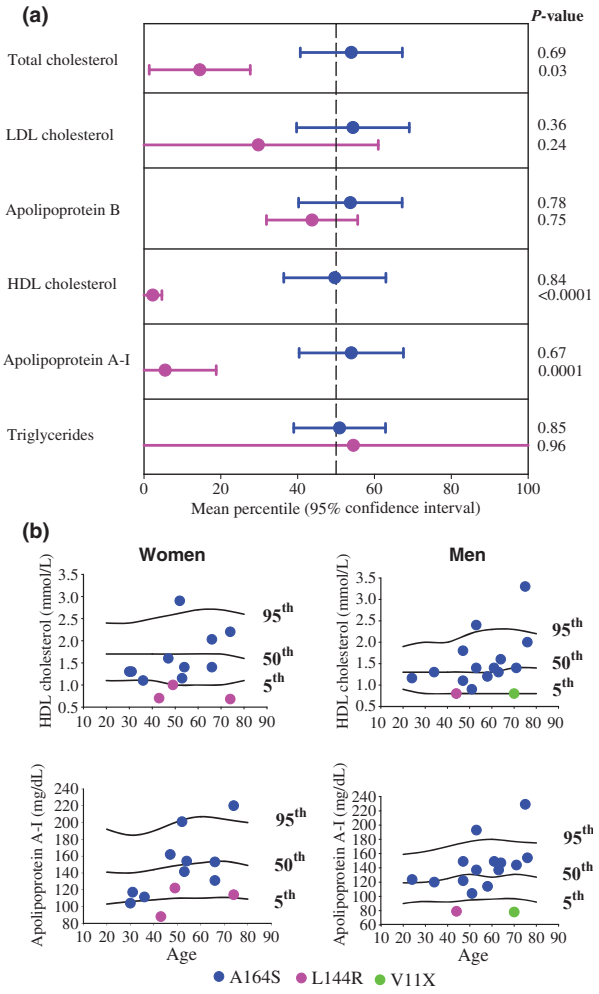

Fig. 1 *Plasma lipid, lipoprotein and apolipoprotein levels of APOA1 heterozygotes in the Copenhagen City Heart Study (CCHS). (a) Mean percentiles of plasma lipids, lipoproteins and apolipoproteins in A164S heterozygotes (blue) and L144R heterozygotes (red) in the CCHS relative to age- (in 10-year age groups) and sex-matched individuals in the CCHS as a whole (*n = *10 440). Heterozygotes were compared with the total CCHS cohort using the z-test. (b) Plasma high-density lipoprotein cholesterol and apolipoprotein A-I levels of A164S heterozygotes, L144R heterozygotes and the V11X heterozygote (green) in the CCHS. Values for each heterozygous individual are superimposed on the 5th, 50th and 95th percentiles for age and sex in the CCHS as a whole (*n = *10 440).*

adenovirus expressing apoA-I L144R resulted in very low total cholesterol levels and a decreased cholesteryl ester-to-total cholesterol ratio (CE/TC), the latter indicating reduced LCAT activity (Table S3). In normal WT apoA-I mice, virtually all the cholesterol is carried in the HDL fraction (Fig. 2a). Fast protein liquid chromatography fractionation of plasma showed that the mass of the HDL cholesterol fraction of mice expressing apoA-I L144R was very small and comparable with the HDL cholesterol fraction of apoA-I-deficient mice expressing the control protein, green fluorescent protein (GFP; Fig. 2a). Fractionation of plasma by density gradient ultracentrifugation showed that apoA-I in mice expressing apoA-I L144R was greatly reduced and was distributed mainly in the HDL-3 region (i.e. in lipid-poor HDL), compared with mice expressing the WT apoA-I or apoA-I A164S, in which apoA-I was also distributed in the HDL-2 region (i.e. in mature, lipid-rich HDL; Fig. 2b–d). Two-dimensional gel electrophoresis showed that the mutant apoA-I L144R promoted the formation of less mature, lipid-poor pre-β- and α4-HDL particles (Fig. 2f), whereas WT apoA-I and the mutant apoA-I A164S both promoted the formation of normal pre-β and αHDL subpopulations of different sizes (α1, α2, α3 and α4; Fig. 2e,g). Electron microscopy of the HDL fraction showed that apoA-I L144R promoted the formation of few discoidal particles as well as of small particles similar to those observed in mice expressing GFP (Fig. 2h,j). By contrast, WT apoA-I and apoA-I A164S promoted the formation of spherical HDL particles (Fig. 2i,k). Simultaneous treatment of mice with the adenovirus expressing apoA-I L144R and human LCAT normalized the total cholesterol level and the CE/TC (Table S3). LCAT treatment restored the mass of the HDL cholesterol peak (Fig. 3a). LCAT treatment also normalized the levels and the distribution of apoA-I in the HDL (Fig. 3b), restored normal pre-β- and α-HDL subpopulations (Fig. 3c) and promoted the formation of spherical HDL particles (Fig. 3d).

Impact of APOA1 mutations on risk of IHD and MI, total mortality and survival after diagnosis of IHD

Whether mutations in *APOA1* are associated with an increased risk of IHD in humans is highly controversial. We therefore determined whether mutations identified in *APOA1* predicted risk of IHD and MI, total mortality and survival after diagnosis of IHD in the CCHS. Surprisingly, the cumulative incidence of IHD and MI as a function of age was increased in A164S heterozygotes versus noncarriers ($P = 0.0004$ and $P < 0.0001$, respectively; Fig. 4a,b), despite the complete lack of effect of this mutation on plasma levels of HDL cholesterol and apoA-I. At the age of 80 years, the cumulative incidence of IHD and MI was 100% in

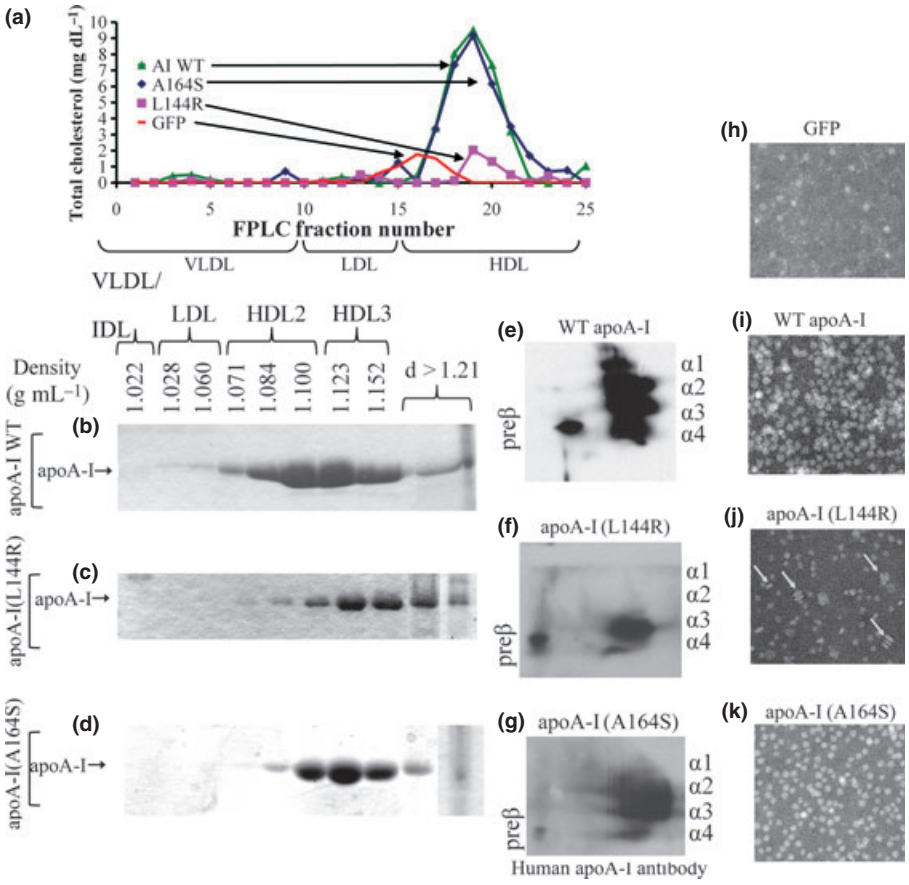

Fig. 2 *Fast protein liquid chromatography profiles, density gradient fractionation, two-dimensional gel electrophoresis and electron microscopy analyses of plasma of apoA-I-deficient mice expressing wildtype (WT) and mutant forms of apoA-I or green fluorescent protein (GFP). (a) Fast protein liquid chromatography profiles of total cholesterol of apoA-I-deficient mice infected with adenoviruses expressing WT apoA-I, apoA-I L144R, apoA-I A164S or the control protein GFP. (b–k) Analyses of plasma of apoA-I-deficient mice infected with adenoviruses expressing WT apoA-I (b,e,i), apoA-I L144R (c,f,j), apoA-I A164S (d,g,k) or GFP (h): by density gradient ultracentrifugation, followed by sodium dodecyl sulphate polyacrylamide gel electrophoresis (b–d), by two-dimensional gel electrophoresis and western blotting (e–g) and by electron microscopy of high-density lipoprotein fractions obtained by density gradient ultracentrifugation (h–k). The photomicrographs were taken at ×75 000 magnification and enlarged ×3. The arrows in panel j indicate discoidal particles.*

A164S heterozygotes and less than 30% in noncarriers. Longevity (i.e. the proportion surviving as a function of age) was reduced in A164S heterozygotes versus noncarriers ($P = 0.005$), and the median survival time in heterozygotes was reduced by 10 years ($P < 0.0001$; Fig. 4c,d). Hazard ratios for IHD, MI and total mortality were 3.2 (95% CI: 1.6–6.5; $P = 0.001$), 5.5 (95% CI: 2.6–11.7; $P < 0.001$) and 2.5 (95% CI: 1.3–4.8; $P = 0.007$), respectively, in A164S heterozygotes versus noncarriers (Table 2). During follow-up, eight of the 24 A164S heterozygotes developed IHD and seven of those were diagnosed with an MI. Nine heterozygotes died during follow-up: seven owing to cardiovascular disease, one from bladder cancer and one from unknown cause. (This individual had both diabetes and cardiovascular disease.)

The proportion surviving as a function of time after diagnosis of IHD was reduced in A164S heterozygotes versus noncarriers ($P = 0.08$), and the median survival time in heterozygotes was reduced by 5 years ($P < 0.0001$) (Fig. 5a,b). Hazard ratio for mortality after diagnosis was 2.2 (95% CI: 1.0–4.5; $P = 0.04$) in A164S heterozygotes versus noncarriers.

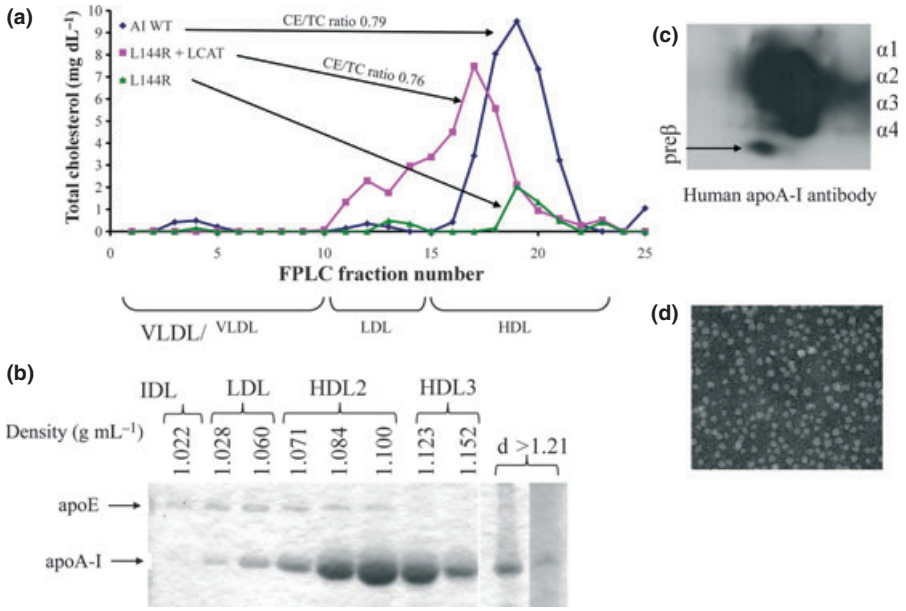

Fig. 3 *Fast protein liquid chromatography profiles, density gradient fractionation, two-dimensional gel electrophoresis and electron microscopy analyses of plasma of apoA-I-deficient mice expressing apoA-I L144R and lecithin:cholesterol acyltransferase (LCAT) in combination. (a) Fast protein liquid chromatography profiles of total cholesterol of apoA-I-deficient mice infected with adenoviruses expressing wildtype apoA-I, apoA-I L144R or a combination of apoA-I L144R and human LCAT. (b–d) Analyses of plasma from apoA-I-deficient mice infected with adenoviruses expressing apoA-I L144R and human LCAT: by density gradient ultracentrifugation followed by sodium dodecyl sulphate polyacrylamide gel electrophoresis (b), by two-dimensional gel electrophoresis and western blotting (c) and by electron microscopy of high-density lipoprotein fractions obtained by density gradient ultracentrifugation (d). The photomicrograph was taken at×75 000 magnification and enlarged×3.*

None of the four L144R heterozygotes had premature IHD; one woman developed IHD, but not MI, at 78 years of age. The only V11X heterozygote died at the age of 72 from an MI.

To validate the findings regarding A164S from the CCHS, we tested for an association between A164S and risk of IHD and MI in an independent case–control study (n = 16 035). We found that the odds ratios for IHD and MI were 2.7 (95% CI: 1.4–5.2; P = 0.003) and 2.9 (95% CI: 1.3–6.5; P = 0.008), respectively, confirming the results from the CCHS (Table 2).

Ratio of wildtype to mutant apoA-I in plasma of A164S heterozygotes

To examine whether the *APOA1* allele product of the WT A164-allele and the mutant S164-allele were present in the plasma of heterozygotes in similar concentrations, as would be expected if the production into and the removal from plasma of the two allele products were the same, we determined the ratio of apoA-I S164 to A164 in the plasma of heterozygotes by mass spectrometry. The mean ratio of mutant S164 to WT A164 apoA-I in plasma of A164S heterozygotes was 87%, corresponding to an average reduction of 13% of mutant S164 apoA-I in plasma (P < 0.0001; Fig. 6).

Clinical characteristics of APOA1 A164S heterozygotes

Additional clinical characteristics of A164S heterozygotes identified in the CCHS and in the case–control study are shown in Table S6. The 51 heterozygous individuals, who were still alive in October 2009, were invited for additional examination including echocardiography and electrocardiogram performed and evaluated by an experienced senior cardiologist, and subcutaneous abdominal fat tissue aspiration for the detection of systemic amyloidosis was performed as previously described [11]. Of these, 26 agreed to participate, six of whom had had an ischaemic event. Although about half of the 51 heterozygotes had other diagnoses suggestive of more generalized disease, of those who participated, only six had other diagnoses mainly related to the gastrointestinal tract and one had tarsal tunnel syndrome. Amyloid was not detected in any of the abdominal fat biopsies.

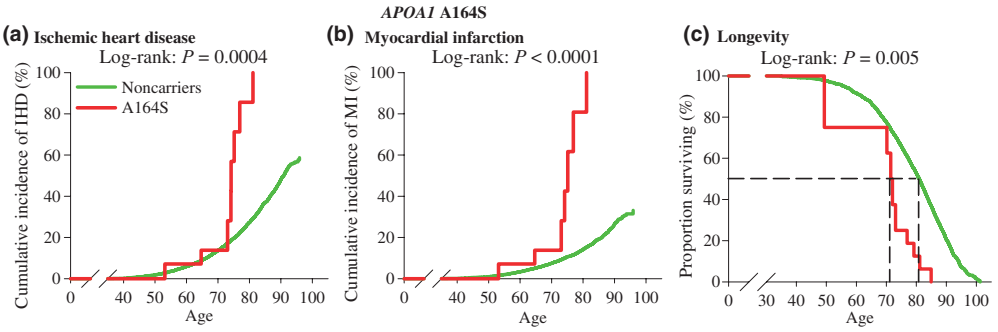

(d) **Median survival time in *APOA1* A164S heterozygotes and noncarriers in the Copenhagen City Heart Study.**

Genotype	*n*	Median survival (interquartile range) (years)	Change (years)	*P*-value
Noncarriers	10 416	81 (71–89)	–	
A164S heterozygotes	24	71 (49–73)	10	<0.0001

Fig. 4 *Risk of ischaemic heart disease (IHD), myocardial infarction, total mortality and median survival time in* APOA1 *A164S heterozygotes (red) and noncarriers (green) in the Copenhagen City Heart Study. (a) Cumulative incidence of IHD as a function of age. (b) Cumulative incidence of myocardial infarction as a function of age. (c) Proportion surviving as a function of age (longevity). Dashed lines indicate median survival time. All using left-truncated age.* P*-value by log-rank test. (d) Median survival time in* APOA1 *A164S heterozygotes compared with noncarriers.*

Table 2 *Risk of ischaemic heart disease (IHD), myocardial infarction (MI) and total mortality for* APOA1 *A164S heterozygotes versus noncarriers in the Copenhagen City Heart Study (CCHS) and in a case–control study*

	No. of noncarriers/A164S heterozygotes			Hazard/odds ratios (95% confidence interval)	
	Controls	Events	% With events	Age-adjusted	Age- and sex-adjusted
IHD					
CCHS	8608/16	1808/8	17/33	3.2 (1.6–6.5)	2.8 (1.4–5.7)
Case–control study	13 253/26[a]	2742/14	17/35	2.7 (1.4–5.2)	2.9 (1.5–5.6)
MI					
CCHS	9547/17	869/7	8/29	5.5 (2.6–11.7)	4.6 (2.2–9.8)
Case–control study	13 253/26[a]	1459/8	10/24	2.9 (1.3–6.5)	3.2 (1.4–7.2)
Total mortality					
CCHS	7363/15	3053/9	29/38	2.5 (1.3–4.8)	2.1 (1.1–4.0)

[a]Controls with cardiovascular events were excluded.

See Data S2, for additional clinical characteristics of A164S heterozygotes, the relative proportion of apoA-I only lipoprotein particles in heterozygotes and noncarriers and the predicted effect of A164S on apoA-I secondary structure.

Discussion

The major novel finding was that a new mutation in *APOA1*, A164S, was associated with increased risk of IHD and MI in two independent studies and with total mortality in the general population, despite a lack of effect on HDL cholesterol levels. Furthermore, median survival time in A164S heterozygotes overall and after diagnosis of IHD was reduced by 10 and 5 years, respectively.

As *APOA1* A164S is associated with normal LCAT activation and normal plasma levels of lipids and lipoproteins, including HDL cholesterol and apoA-I, as

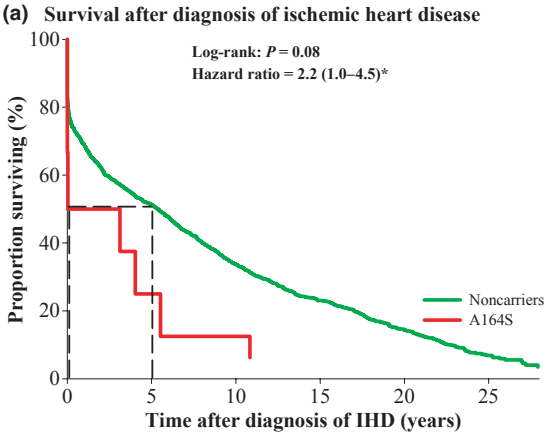

(b) Median survival time after diagnosis of ischemic heart disease in *APOA1* A164S heterozygotes and noncarriers in the Copenhagen City Heart Study.

Genotype	*n*	Median survival (interquartile range) (years)	Change (years)	*P*-value
Noncarriers	1969	5 (0–14)	–	
A164S heterozygotes	8	0 (0–4)	5	<0.0001

Fig. 5 *Survival and median survival time after diagnosis of ischaemic heart disease (IHD) in* APOA1 *A164S heterozygotes (red) and noncarriers (green) in the Copenhagen City Heart Study. (a) Proportion surviving after diagnosis of IHD as a function of time after diagnosis.* P*-value by log-rank test. Dashed lines indicate median survival time after diagnosis of IHD.* *P *= 0.04. (b) Median survival time after diagnosis of IHD in* APOA1 *A164S heterozygotes compared with noncarriers.*

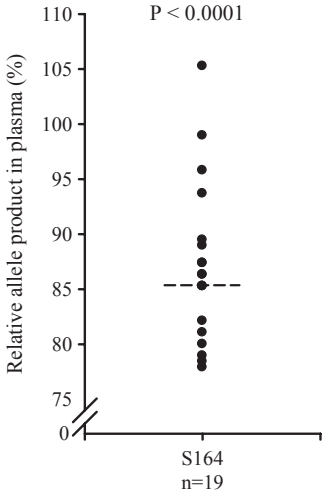

Fig. 6 *Ratio of mutant to wildtype apoA-I in plasma of A164S heterozygotes. The dashed line reflects the mean ratio. The allele product of apoA-I S164 relative to A164 in plasma of A164S heterozygotes was determined by mass spectrometry. Levels were adjusted for a minor difference in signal intensities.* P*-value by Mann–Whitney* U *test.*

demonstrated in both humans and mice in this study, we can rule out plasma levels of HDL cholesterol and other lipids and lipoproteins as causal factors for IHD in A164S heterozygotes. Furthermore, the increased risk of IHD despite normal HDL cholesterol levels could not be explained by a reduction in proposed cardioprotective LpA-I (apoA-I containing only high-density lipoprotein particles) particles with a simultaneous increase in LpA-I:A-II (apoA-I and apoA-II containing high-density lipoprotein particles)-containing particles such that HDL cholesterol levels remained normal, because neither LpA-I nor the ratio of LpA-I/total plasma apoA-I differed between A164S heterozygotes and noncarriers (Fig. S2).

The reduced concentration of the mutant S164 product relative to the WT A164 apoA-I in heterozygous carriers despite normal HDL cholesterol and apoA-I levels suggests that A164S is a less severe mutation. Other more severe apoA-I mutants, which were associated with more pronounced reductions in levels of mutant relative to WT apoA-I (e.g. R165P, R143P, R173C or R151C as well as several amyloidogenic apoA-I mutants), were also associated with low HDL cholesterol levels [6]. The relative decrease in mutant S164 product probably results from the enhanced catabolism of this protein. As most of the apoA-I resides on particles with several apoA-I molecules, the enhanced catabolism of the mutant apoA-I might even induce enhanced catabolism of the normal allele product as well. Thus, if the HDL cholesterol level is normal, this might be explained by counteracting effects of other mechanisms that either increase HDL production or decrease HDL catabolism. This raises the question of whether the mutant *APOA1* allele is in linkage disequilibrium with another gene defect that affects HDL production. *APOA1* A164S was not in linkage disequilibrium with other previously reported genetic variants in *APOA1* identified by resequencing and known to be associated with increased apoA-I levels [8]. However, we cannot exclude linkage disequilibrium with genetic variation in other nearby genes.

Other explanations for the increased risk of IHD, MI and total mortality associated with A164S without low HDL cholesterol could be as follows: (i) obstructive intramural coronary vascular amyloidosis presenting as symptomatic IHD, i.e. small-vessel

disease, as previously described in patients with primary amyloidosis [12–17]; (ii) atherosclerosis accelerated by amyloidosis; (iii) dysfunctional HDL particles caused by the loss of proposed anti-inflammatory and antioxidative properties of HDL [18, 19]; or (iv) other as yet unknown causes.

Structural mutations in *APOA1* might cause hereditary amyloidosis, a late-onset autosomal dominant disease that primarily affects the kidneys, liver, heart, vocal folds, arteries and/or nerves [6, 20, 21]. Amyloidosis of the heart might manifest as severe restrictive cardiomyopathy owing to massive amyloid infiltration of the organ, but might also manifest as IHD owing to obstructive vascular amyloidosis of the smaller intramural arteries [12, 13, 22]. Diagnosis of amyloidosis in such cases is extremely difficult unless an endomyocardial biopsy is performed, or involvement of other organs suggests the diagnosis [22]. Aspiration of subcutaneous abdominal fat tissue in A164S heterozygotes did not reveal deposition of amyloid. However, this does not preclude intramural coronary vascular amyloidosis, because high sensitivity of this method has only been shown for very severe systemic amyloidosis [11] and therefore is not necessarily representative of more modest amyloid deposition in intramural arteries of the heart.

Alternatively, *APOA1* A164S might accelerate the development of atherosclerosis owing to deposition of amyloid in pre-existing atherosclerotic plaques, or deposition of amyloid in the intima might accelerate plaque formation [23, 24].

A further possibility could be that *APOA1* A164S is associated with dysfunctional HDL particles caused by the loss of proposed anti-inflammatory and antioxidative properties of HDL. Recent data suggest that HDL might possess anti-inflammatory and antioxidative properties, which might be cardioprotective [19]. Shotgun proteomics has supported this by showing complement system proteins and antiproteolytic proteins in the HDL cargo [25].

Finally, *APOA1* V11X and L144R have been reported previously in, respectively, an Italian and a Spanish family with low HDL cholesterol and apoA-I levels, but without apparent increased risk of IHD in heterozygotes for either mutation [26, 27]. We have established that both mutations are rare and that the abnormal lipoprotein phenotype associated with *APOA1* L144R could be explained by reduced activation of LCAT.

In conclusion, this is the first report of a mutation in *APOA1*, A164S, which predicts an increased risk of IHD, MI and total mortality in the general population independent of HDL cholesterol levels.

Conflict of interest statement

No conflicts of interest to declare.

Acknowledgements

We thank Mette Refstrup, Karin Møller Hansen and Ragnhild Ånestad for their persistent attention to the details of resequencing and large-scale genotyping, Karen Rasmussen for the isolation of apoA-I from human plasma and Allan Kastrup for carrying out the mass spectrometry analyses. We are indebted to the staff and participants of the CCHS and the participants of the case–control study for their important contributions.

This work was supported by a Specific Targeted Research Project grant from the European Union, Sixth Framework Programme Priority (FP-2005-LIFESCI-HEALTH-6) contract 037631 (AT-H, RF-S, VIZ, DK), the Danish Medical Research Council, the Research Fund at Rigshospitalet, Copenhagen University Hospital, Chief Physician Johan Boserup and Lise Boserup's Fund, Copenhagen, Ingeborg and Leo Dannin's Grant, Copenhagen, Henry Hansen's and Wife's Grant, Copenhagen, and National Institutes of Health contract HL48739 (VIZ). AKK is a student of the graduate programme 'Molecular Basis of Human Disease of the University of Crete, Medical School'.

References

1 Gordon DJ, Probstfield JL, Garrison RJ *et al.* High-density lipoprotein cholesterol and cardiovascular disease. Four prospective American studies. *Circulation* 1989; **79:** 8–15.
2 Frikke-Schmidt R, Nordestgaard BG, Stene MCA *et al.* Association of loss-of-function mutations in the ABCA1 gene with high-density lipoprotein cholesterol levels and risk of ischemic heart disease. *JAMA* 2008; **299:** 2524–32.
3 Nordestgaard BG, Benn M, Schnohr P, Tybjærg-Hansen A. Nonfasting triglycerides and risk of myocardial infarction, ischemic heart disease, and death in men and women. *JAMA* 2007; **298:** 299–308.
4 Freiberg JJ, Tybjærg-Hansen A, Jensen JS, Nordestgaard BG. Nonfasting triglycerides and risk of ischemic stroke in the general population. *JAMA* 2008; **300:** 2142–52.
5 Tall AR, Breslow JL, Rubin EM. Genetic disorders affecting plasma high-density lipoproteins. In: Schriver CR, Beaudet AL, Sly WS, Valle D, eds. *The Metabolic and Molecular Bases of Inherited Diseases*. New York, NY: McGraw-Hill, 2001; 2915–36.

6 Sorci-Thomas MG, Thomas MJ. The effects of altered apolipoprotein A-I structure on plasma HDL concentration. *Trends Cardiovasc Med* 2002; **12:** 121–8.
7 Zannis VI, Koukos G, Drosatos K *et al.* Discrete roles of apoA-I and apoE in the biogenesis of HDL species: lessons learned from gene transfer studies in different mouse models. *Ann Med* 2008; **40:** 14–28.
8 Haase CL, Tybjærg-Hansen A, Grande P, Frikke-Schmidt R. Genetically elevated apolipoprotein A-I, high-density lipoprotein cholesterol levels, and risk of ischemic heart disease. *J Clin Endocrinol Metab* 2010; **95:** E500–10.
9 Schnohr P, Jensen JS, Scharling H, Nordestgaard BG. Coronary heart disease risk factors ranked by importance for the individual and community. A 21 year follow-up of 12000 men and women from The Copenhagen City Heart Study. *Eur Heart J* 2002; **23:** 620–6.
10 Julian DG, Bertrand ME, Hjalmarson Å, Fox K, Simoons ML. Management of stable angina pectoris: recommendations of the Task Force of the European Society of Cardiology. *Eur Heart J* 1997; **18:** 394–413.
11 van Gameren II, Hazenberg BPC, Bijzet J, van Rijswijk MH. Diagnostic accuracy of subcutaneous abdominal fat tissue aspiration for detecting systemic amyloidosis and its utility in clinical practice. *Arthritis Rheum* 2006; **54:** 2015–21.
12 Mueller PS, Edwards WD, Gertz MA. Symptomatic ischemic heart disease resulting from obstructive intramural coronary amyloidosis. *Am J Med* 2000; **109:** 181–8.
13 Neben-Wittich MA, Wittich CM, Mueller PS, Larson DR, Gertz MA, Edwards WD. Obstructive intramural coronary amyloidosis and myocardial ischemia are common in primary amyloidosis. *Am J Med* 2005; **118:** 1287e1–e7.
14 Wittich CM, Neben-Wittich MA, Mueller PS, Gertz MA, Edwards WD. Deposition of amyloid proteins in the epicardial coronary arteries of 58 patients with primary systemic amyloidosis. *Cardiovasc Pathol* 2007; **16:** 75–8.
15 Suwaidi JA, Velianou JL, Gertz MA *et al.* Systemic amyloidosis presenting with angina pectoris. *Ann Intern Med* 1999; **131:** 838–41.
16 Whitaker DC, Tungekar MF, Dussek JE. Angina with a normal coronary angiogram caused by amyloidosis. *Heart* 2004; **90:** e54.
17 Ishikawa Y, Ishii T, Masuda S *et al.* Myocardial ischemia due to vascular systemic amyloidosis: a quantitative analysis of autopsy findings on stenosis of the intramural coronary arteries. *Pathol Int* 1996; **46:** 189–94.
18 Navab M, Reddy S, van Lenten BJ, Anantharamaiah GM, Fogelman AM. The role of dysfunctional HDL in atherosclerosis. *J Lipid Res* 2009; **50(Suppl):** S145–9.
19 Barter PJ, Puranik R, Rye KA. New insights into the role of HDL as an anti-inflammatory agent in the prevention of cardiovascular disease. *Curr Cardiol Rep* 2007; **9:** 493–8.
20 Pepys MB. Amyloidosis. *Annu Rev Med* 2006; **57:** 223–41.
21 Benson MD. Ostertag revisited: the inherited systemic amyloidoses without neuropathy. *Amyloid* 2005; **12:** 75–87.
22 Falk RH, Dubrey SW. Amyloid heart disease. *Prog Cardiovasc Dis* 2001; **52:** 347–61.
23 Amarzguioui M, Mucchiano G, Häggqvist B *et al.* Extensive intimal apolipoprotein A1-derived amyloid deposits in a patient with an apolipoprotein A1 mutation. *Biochem Biophys Res Commun* 1998; **242:** 534–9.
24 Mucchiano GI, Häggqvist B, Sletten K, Westermark P. Apolipoprotein A-1-derived amyloid in atherosclerotic plaques of the human aorta. *J Pathol* 2001; **193:** 270–5.
25 Vaisar T, Pennathur S, Green PS *et al.* Shotgun proteomics implicates protease inhibition and complement activation in the antiinflammatory properties of HDL. *J Clin Invest* 2007; **117:** 746–56.
26 Miccoli R, Bertolotto A, Navalesi R *et al.* Compound heterozygosity for a structural apolipoprotein A-I variant, apo A-I(L141R) Pisa, and an apolipoprotein A-I null allele in patients with absence of HDL cholesterol, corneal opacifications, and coronary heart disease. *Circulation* 1996; **94:** 1622–8.
27 Recalde D, Velez-Carrasco W, Civeira F *et al.* Enhanced fractional catabolic rate of apo A-I and apo A-II in heterozygous subjects for apo A-I(Zaragoza) (L144R). *Atherosclerosis* 2001; **154:** 613–23.

Correspondence: Anne Tybjærg-Hansen, MD DMSc, Professor, Chief Physician, Department of Clinical Biochemistry KB 3011, Section for Molecular Genetics, Rigshospitalet, Copenhagen University Hospital, Blegdamsvej 9, DK-2100 Copenhagen Ø, Denmark.
(fax: +45 3545 4160; e-mail: at-h@rh.regionh.dk).

Supporting Information

Additional Supporting Information may be found in the online version of this article:

Data S1 Supplementary Methods.

Data S2 Supplementary Results.

Figure S1. ApoA-I synthesis and secretion following infection of HTB-13 cells with recombinant adenoviruses expressing wildtype and mutant apoA-I forms.

Figure S2. LpA-I levels and ratio of LpA-I over total plasma apoA-I in plasma of heterozygous carriers of *APOA1* A164S, L144R or R160L, and controls.

Table S1. Characteristics of individuals with the lowest 1% and highest 1% apoA-I levels among 10 440 participants in the Copenhagen City Heart Study.

Table S2. Genetic variation in the coding regions of the *APOA1* gene identified in individuals from the Copenhagen City Heart Study with extreme apoA-I levels.

Table S3. Hepatic apoA-I mRNA, total cholesterol, and cholesteryl esters-to-total cholesterol ratio of mice expressing wildtype and mutant apoA-I forms.

Table S4. PCR primers and fragment lengths for denaturing high performance liquid chromatography and sequencing of *APOA1* in the Copenhagen City Heart Study.

Table S5. Oligonucleotide sequence of primers used for the generation of adenovirus expressing wildtype and mutant apoA-I forms.

Table S6. Clinical characteristics of *APOA1* A164S heterozygotes in the Copenhagen City Heart Study and the case-control study.

Please note: Wiley-Blackwell are not responsible for the content or functionality of any supporting materials supplied by the authors. Any queries (other than missing material) should be directed to the corresponding author for the article.■